Recyclable and reprocessable elastomers relying on the vitrimer concept

Antoine Breuillac

PSL★
UNIVERSITÉ PARIS

THÈSE DE DOCTORAT
DE L'UNIVERSITÉ PSL
Préparée à l'ESPCI Paris

Elastomères recyclables et transformables reposant sur le concept des vitrimères

Recyclable and reprocessable elastomers relying on the vitrimer concept

Soutenue par
Antoine BREUILLAC
Le 19 décembre 2019

Ecole doctorale n° 397
Physique et chimie des matériaux

Spécialité
Chimie des matériaux

Composition du jury :

Mme Hélène, MONTES Professeur, ESPCI Paris	Présidente du jury
M. Luc, AVEROUS Professeur, ICPEES - Université de Strasbourg	Rapporteur
M. Yohann, GUILLANEUF Chargé de recherche, ICR - Université d'Aix-Marseille	Rapporteur
M. Philippe, CASSAGNAU Professeur, IMP - Université Claude Bernard Lyon 1	Examinateur
M. Renaud, NICOLAY Professeur, ESPCI Paris	Directeur de thèse

ESPCI ★ PARIS | PSL★

Remerciements

C'est fini !! Ce long et tumultueux travail de doctorat ne s'est pas effectué seul loin s'en faut. Je souhaite remercier ici tous ceux qui m'ont permis de mener à bien ma thèse.

Je te remercie Renaud Nicolaÿ pour m'avoir fait confiance et ce dès mon stage de fin d'études en janvier 2016, tu as cru en moi malgré mon parcours quelque peu atypique et mes lacunes en chimie. Tu as été l'initiateur et le soutien de tous mes projets lancés au cours de ces presque 4 années de travail commun. Tu as été toujours été là pour me redonner l'envie d'avancer en gardant une vision optimiste de tous mes résultats. Merci d'avoir créé un environnement qui me soit favorable pour que je puisse apprendre et développer les compétences utiles pour un chimiste des polymères.

Je remercie Ludwik Leibler avec qui j'ai eu la chance de pouvoir travailler durant la première partie de ma thèse. Merci pour toutes ces réflexions et discussions extrêmement riches qui m'ont permis de mieux cerner les subtilités de la matière molle. Merci également de m'avoir fait découvrir le monde fascinant des vitrimères.

Je tiens à remercier tous les membres permanents du laboratoire pour leur aide et les discussions que nous avons eues. Merci à Laurent Corté pour ses blagues réconfortantes, à François Tournilhac pour son aide précieuse concernant les réparations de l'extrudeuse DSM, à Nathan qui m'a donné un bon coup de main pour le greffage du polyisoprène. Je remercie également Michel Cloître, Sophie Norvez, Zorana Zeravcic et Corinne Soulié-Ziakovic (bonne adresse du médecin traitant !) pour vos propos constructifs en séminaire interne. Merci à Anne-Claire Dumanois et à Gaëlle Carré de Lusancay pour leur aide dans la gestion des stocks et des commandes de matériel. Merci à Marie-France Boucher et Aroul Radja pour leur aide concernant toutes les démarches et questions administratives. Un merci tout particulier à Isabelle Marlart pour ton aide précieuse en informatique qui m'a sauvé plus d'une fois ! Merci à Mickaël Pomes-Hadda pour m'avoir aidé à réparer la DMA et la DSC.

Je tiens à remercier mes stagiaires qui m'ont permis d'explorer de nouvelles pistes. Alexis Brastel, grâce à toi nous avons pu mener à bien l'étude modèle sur les échanges entre les dioxaborinanes. Tu as fait preuve d'une abnégation sans faille et tu as exploité mes remarques au maximum en te remettant en cause à chaque fois que cela s'avérait nécessaire. Tu as

apporté une lueur d'espoir dans cette thèse à un moment où je ne voyais pas trop d'issue. Ton sourire et ta bonne humeur m'ont aidé à garder le moral. Ton esprit de contradiction m'a toujours plu, garde-le mais reconnais que j'ai souvent raison aussi ! Rappelle-moi de ne plus JAMAIS courir avec toi car je n'ai jamais autant souffert de ma vie. Merci à Ombeline Taisne, tu as fait du super travail, grâce à toi j'ai pu écarter la voie de réticulation en deux étapes pour le polybutadiène de faible masse molaire, l'étude infra-rouge m'a été très utile par la suite ! J'ai apprécié ta curiosité et ton implication dans ton stage qui en ne durant qu'un mois m'a donné de belles réponses. Merci à Alexis Kassalias qui a su finir les caractérisations de recyclage des polybutadiènes. C'était vraiment 3 mois dont je me souviendrais, merci pour la soirée belge #WWT02, je me souviendrais encore longtemps de cette carbonade flamande ! Merci aux autres stagiaires Louise Breloy,Chloé Seyrig, Edolide Llusar, Maïka, Cyprien vous avez égayé cette année 2018 par votre spontanéité et votre bonne humeur inébranlable. Merci au bureau des « coucou » pour votre cadeau de fin stage ! Je vous cuisinerai les gâteaux dont vous m'avez donné les recettes. En prenant place dans l'ancien bureau du directeur, vous avez carrément changé l'ambiance du quatrième étage du labo, c'était devenu un peu le café du commerce !

Merci aux anciens qui m'ont fait découvrir le labo et m'ont accueilli alors que je n'étais qu'en stage de Master 2, Thibault Derouineau, Coralie Teulère, François Bargain, Raphaël Michel, Maddalena Mattiello. C'est vous qui avez donné le caractère familial à ce labo. Merci à Chirine Ben Osman et Hasina Ramanitra, vous m'avez rassuré quand je n'allais pas bien, votre gentillesse m'a beaucoup réconforté. Merci Mohamad Maaz pour nos discussions sur l'extrudeuse et sur les maléimides, ça a été un plaisir d'échanger avec toi. Bravo pour avoir arrêté de fumer durant ma thèse, chapeau bas ! Merci à toi Jaroslav Minar pour la soirée tchèque #WWT01, tu avais vu les choses en grand c'était génial, notamment la polka à la fin inoubliable ! Merci Maïssa !! C'est toi qui m'as accueilli le premier jour de mon stage de master 2 le lundi 1er février 2016, tu m'as tout de suite à l'aise. Voire un peu trop quand tu m'as recadré après ma blague sur les Libanais en soirée hahaha ! Grâce à toi j'ai su que faire des ventes privées ainsi que trouver les meilleures adresses de restaurants à Paris étaient compatibles ou plutôt faisaient partie intégrante du travail de thèse. Merci Rob van der Weegen pour m'avoir donné toutes les bases du chimiste que je suis devenu. C'était vraiment très chouette ces six de stage avec toi comme encadrant au quotidien. Je me souviendrai de ce moment où tu m'as fait quitter mon bureau et donc le live de Rolland Garros pour faire une précipitation, c'était magique ! J'ai aimé tes discussions animées sur le Brexit en 2016 et les

sujets politiques en général. Merci pour le travail collaboratif durant les six premiers mois de ma thèse. Merci à Max Röttger, qui m'a formé à la mythique GC et aux suivis cinétiques de folie. Ta thèse m'aura servi de socle pour la mienne, je n'ai jamais lu une thèse aussi profondément que la tienne ! Tu m'as appris l'implication qu'il fallait pour réussir ses projets. Merci à Nathan van Zee qui m'a aidé sur le greffage du polyisoprene, nos discussions m'ont permis de reconnaître que ce polymère était assez tempétueux. Un grand merci à Emeline Placet qui a passé du temps sur les dioxaborinanes ce qui m'a grandement dépanné alors que je devais rédiger mes autres chapitres. J'ai beaucoup aimé nos nombreuses discussions coutures, lombri-compost, MOOC zéro déchet, tu m'as compris alors qu'alors on me prenait pour un extrémiste vert. Je te souhaite plein de bonnes choses pour les EPDM ainsi que de quitter Paris prochainement.

Voici ceux sans qui cette thèse n'aurait pas été du tout la même, je veux dire Trystan Domenech et Florent Caffy. Trystan, tu as su me montrer qu'on pouvait bien bosser en arrivant décontracté le matin à 9h30 avec un croissant au beurre à la main. Ta force tranquille m'a souvent rassuré surtout lors des pics de stress que nous avons connus à l'occasion de la réponse à l'article. Ta sérénité m'a beaucoup aidé ! Ton expertise en mécanique des matériaux et en extrusion aussi ! Tu m'as montré la voie de l'extrusion réactive qui va sans doute me permettre de décrocher mon 2ème emploi (1er post thèse). Que de souvenirs partagés ; « Antoine est-ce que vous avez calculé les modules ? Est-ce que ça relaxe ? Mais Antoine vous avez eu une excellente idée ! » Je retiendrai nos interminables discussions autour de l'extrudeuse notamment sur la Socca et la pissaladière. J'ai pensé à toi lorsqu'avec Lucie, nous sommes arrivés à Nice après 22 jours de marche sur le GR 5 depuis Saint-Gingolph. Je n'oublierai pas les heures heureuses à essayer de comprendre les instructions données par RONDOL pour faire fonctionner leur extrudeuse bi-vis en continu et leur presse à injecter et les longs dialogues de sourds qui en résultaient : « Il est blanc de PE là », « bon d'accord il est gris mais vous chauffez trop le PE là », et surtout le mythique « je vous contacte à propos de notre PE hydrosoluble dans l'eau »… C'était bien d'avoir créé une roue des services pour décider qui allait cuisiner le prochain gâteau du vendredi sucrerie, dommage qu'elle fût entachée de soupçon de trucage haha. Je suis sûr que tu vas trouver le poste de chercheur qui te convient. Florent, tu as éclairé ma thèse quand tu es arrivé au laboratoire fin 2016. Tu as initié et porté de bout en bout le projet azoture, ce qui m'a permis d'écrire un chapitre de thèse, bravo tu auras fait deux thèses grâce à moi hahaha. Tu m'as fait découvrir le vrai monde de chimie organique, ainsi que l'existence du triphosgène qui m'a donné pas mal de

sueurs froides, mais heureusement j'en suis sorti vivant. Ton expertise sécurité m'a rassuré aussi surtout quand une stagiaire s'est prise de l'anhydride maléique dans les yeux, tu as magnifiquement géré la situation en gardant ton sang froid. A la suite de quoi je suis devenu Sauveteur Secouriste du Travail. Tes innombrables qualités ont laissé un grand vide quand tu nous as quittés. A tel point qu'un extérieur t'a pris pour le directeur du laboratoire, je dirai que, sauf pour le titre, c'était vrai. Merci pour avoir mis en mémoire les fréquences de mes stations radios, que sont nostalgie et Chante France ! Surtout je me souviendrais longtemps de ce rituel de l'écoute de France inter de 14h à 15h pour la Tête au carré puis de 15h à 16h pour Affaires sensibles par Fabrice Drouelle. C'était magique notamment lorsque je me suis rendu compte qu'on écoutait la même émission alors que j'étais en D422 et que tu extrudais en C053 ! Bravo tu as réussi à rejoindre le monde de l'industrie désormais. J'espère que je ne t'ai pas trop fatigué vu qu'on partageait le même laboratoire et le bureau ! Je souhaitais de dire Bravo également car c'est avec toi qu'on a réussi à faire tourner correctement l'extrudeuse RONDOL en juin 2018 après 2 ans d'efforts continus, ce n'était pas gagné !

Merci Marta Abellan-Flos pour ton sourire que tu gardes en toute circonstance et qui a bien éclairé nos journées de doctorants en détresse. Je te souhaite tout le meilleur pour ton retour en Espagne à Valence, que tu puisses te rapprocher encore plus de ton chéri et de ta famille. C'était un réel plaisir de partager du temps avec toi. Un immense merci pour avoir organisé la soirée espagnole #WWT05. Merci à Phuong Anh Dang, toujours souriante et dynamique, tu es la reine des pâtissiers et pâtissières du labo, je me souviens encore de ton Paris-Brest qui était à mourir ! Bravo pour la soirée #WWT06 sur le Vietnam et les nems !! Sélène Chappuis, tu as illuminé le labo en arrivant. Ton autodérision est géniale et garde ta hauteur de vue. J'ai beaucoup apprécié nos pérégrinations mentales à la DSC ou dans ton bureau sur moult sujets dont le féminisme, grâce à toi j'ai découvert les podcasts des Couilles sur la table ! Merci Larissa Hammer d'avoir discuté avec moi sur nos malheurs avec les esters boroniques et les imines, tu m'as bien conseillé pour mon cadeau de 25 ans à Lucie, grâce à toi j'ai découvert *Freiburg und die Schwarzwälder Kirschtorte*, profite bien de ta thèse à Paris et des croissants au beurre ! Mille merci pour la soirée allemande de feu #WWT05 que tu as préparée, entrejeux interactifs sur la culture allemande, les bières Paulaner, les mets faits maison, ton Dirndl, et les chansons et danses de la fête de la bière, tu avais tout compris du principe du WWT !! On s'est cru de l'autre côté du Rhin le temps d'une soirée, même si tu habites du même côté que nous je sais haha. On se retrouvera tous ensemble à la Frühlingsfest ou l'Oktoberfest selon le bon vouloir du Coronavirus ! Maeva Balima, je ne t'ai croisée que

quelques jours après ma thèse, mais c'était assez pour te dire que tu es quelqu'un bien quoique tu ne connaisses pas encore le kéfir, Qwant, ProtonMail et les joies de l'achat en vrac au Biocoop, hahaha. Merci à Thomas Vialon pour ton implication dans le projet azoture qui a connu bien des rebondissements ! Bon vol chez Air France ! Maxime Beaugendre tu as de la ressource, bon courage pour les synthèses à grandes échelles, je suis sûr que tu vas y arriver. Julien Crozzolo, nous sommes arrivés le même jour au laboratoire en février 2016, c'était chouette de passer quatre années ensemble à échanger sur nos misères de doctorants en détresse. Maïlie Roquart, merci pour ta bonne humeur et tes conseils écolos frappés au coin du bon sens, tu as su te montrer large d'esprit en déménageant du 19ème au 6ème arrondissement au cours de ta thèse. Merci pour la soirée Vietnamienne super bien organisée !! Henrique Trevisan tu es très enthousiaste c'était top de parler avec toi, j'espère que tu pourras faire la soirée brésilienne #WWT07, je compte sur toi ! Merci Jakob Langenbach, tu as la patate et ça c'est chouette, ça redonne le moral ! Grâce à tes conseils j'ai gagné le jeu de Larissa lors de la soirée allemande et ça n'a pas de prix. Je passerai te faire coucou à Passau quand je ferai véloroute, Eurovélo 6, qui longe le Danube jusqu'à son embouchure. Merci à toi Sarah Goujard, on a passé ces trois ans ensembles au labo c'était chouette de partager nos questions et nos galères de thésards, notamment au moment de la rédaction du manuscrit. Tes nombreux potins m'ont permis de bien décompresser durant cette thèse, tu es vraiment une experte en renseignements, n'hésite pas à postuler à la DGSI ! Je passerai te voir à Dijon ! Stephania Traettino c'était chouette que tu sois parmi, merci pour la soirée italienne #WWT03 j'ai bien aimé faire mon masque de Carnaval ! Merci à toi Quentin Nozet, tu as été le premier à me parler de Pierre Rabhi, Jean-Baptiste Fressoz et bien d'autres, j'ai bien apprécié nos discussions dignes des milieux alternatifs berlinois des années 80. Un énorme merci pour le montage de la vidéo de fin de thèse, bon courage pour la dernière année ça va le faire tranquillement. Bruno Flavio je n'ai pas eu le temps de faire ta connaissance mais bonne chance pour la suite, Léo Gury profite bien de ces derniers mois de post-docs après c'est le chômage comme pour bibi ! Alexi Riba-Bremerch, Imed Ben-Tarcha, Deyo Maeztu-Redin vous avez été super avec moi, vos projets sont bien lancés que ce soit pour le PP à cristallisation rapide, les réservoirs d'hélicoptère auto réparant ou les textiles de Laurent. Amusez-vous bien durant vos thèses. Olivia Kool je te souhaite le meilleur pour ton doctorat, ne lâche rien même si c'est parfois dur, passe au 3ème et 4ème à chaque fois que tu déprimes !

Merci à mes ami.e.s et ma famille pour avoir écouté mes problèmes de thésard durant mes trois années au laboratoire ainsi que pour avoir été présents à ma soutenance. Je remercie en

Abbreviations and Variables

AIBN	Azobisisobutyronitrile
BR	Butadiene rubber
CR	Chloroprene rubber
DA	Diels-Alder
DCM	Dichloromethane
DMA	Dynamic mechanical analysis
DMSO	Dimethyl sulfoxide
DSC	Differential scanning calorimetry
ENR	Epoxidized natural rubber
EPDM	Ethylene-propylene-diene monomer
Eq	Equivalent
Et_2O	Diethyl ether
FID	Flame ionization detector
FT-IR	Fourier-transform infrared
GC	Gas chromatography
GPC	Gel permeation chromatography
GRG	General rubber goods
HPLC	High-performance liquid chromatography
IIR	Isobutylene isoprene rubber
IR	Isoprene rubber
IS	Internal standard
MA	Maleic anhydride
MeOH	Methanol
NBR	Nitrile butadiene rubber
NMR	Nuclear magnetic resonance
NR	Natural rubber
PDMS	Polydimethylsiloxanes
PEG	Polyethylene glycol
PPG	Propylene glycol
PPh_3	Triphenylphosphine
ppm	Parts per million
PB	Polybutadiene
PI	Polyisoprene
PIB	Polyisobutylene

pTSA	*p*-Toluenesulfonic acid
PU	Polyurethane
RAFT	Reversible addition-fragmentation chain transfer
RT	Room temperature
SBR	Styrene butadiene rubber
SEC	Size-exclusion chromatography
t_{eq}	Time of equilibrium
TEMPO	2,2,6,6-Tetramethyl-1-piperidinyloxy
TGA	Thermo-gravimetric analysis
THF	Tetrahydrofurane
T_g	Glass transition temperature
T_{inj}, T_{col}, T_{det}	Injection, column, detection temperatures
T_m	Melting temperature
T_v	Vitrimeric transition temperature
TPE	Thermoplastic elastomers
UPy	Ureidopyrimidinone
UV	Ultraviolet
XNBR	Carboxylated nitrile butadiene rubber
A	Frequency factor
c	Concentration (mol/L)
Da	Dalton
$Đ$	Dispersity
DP_n	Number-average degree of polymerization
E	Young's modulus
E'	Storage modulus
E"	Loss modulus
E_a	Activation energy
η	Viscosity (Pa.s)
$η_0$	Zero-shear viscosity (Pa.s)
F	Force
f	Functionalization degree
G	Shear modulus
G'	Shear storage modulus
G"	Shear loss modulus
γ	Deformation (%)
$\dot{γ}$	Shear rate (s^{-1})
J_{eq}	Steady state compliance

k_{ass}	Association rate constant
k_{diss}	Dissociation rate constant
K_{eq}	Equilibrium constant
l, w, t	Length, width, thickness (m, mm, cm,… etc)
m	Mass (Kg, g, mg, … etc)
M_n	Number-average molar mass (Da)
M_w	Mass-average molar mass (Da)
M_e	Mass between entanglements
M	Molecular mass (g/mol)
n	Molarity (mol)
ω	Angular frequency
ρ	Density (g/mL)
rpm	Rounds per minute
σ	Stress (Pa)
T	Temperature
τ	Relaxation time (s)
V	Volume (L)

Table of Contents

General Introduction

General Introduction

With more than 27 million tons produced per year, conventional vulcanised elastomers raise important environmental issues because of their non-recyclability. Polydiene (co)polymers account for more than 80% of the global rubber market. Transforming these elastomers into vitrimers would impart to them recyclability, welding ability and potentially self-healing properties. In this PhD thesis, the approach selected to prepare vitrimers was based on the cross-linking of commercially available thermoplastic precursors. This strategy is particularly attractive from an application and industrial point of view, as it does not require to change existing syntheses.

Vitrimers are polymer networks that are able to change their topology through dynamic covalent exchange reactions. As a result, vitrimers behave like elastic solids when the topology of the network is frozen, and like viscoelastic liquids when exchange reactions are operating. Therefore, ideal exchange reactions for elastomers are those with a large activation energy, as the life time of the dynamic links would be extremely long at room temperature, to prevent creep, and very short at high temperature, to provide good processability. The degenerate nature of the exchange reactions ensures that the number of chemical bonds remains constant regardless of the temperature. Beside the criterion on the activation energy, the dynamic covalent bonds have to be stable at processing temperatures (100 – 150 °C) and not prone to side reactions that would lead to static irreversible cross-links. The incorporation of these dynamic covalent bonds into the polydiene matrices requires to use grafting chemistries that are selective towards the elastomeric precursors, compatible with the dynamic bonds and stable at reprocessing temperatures.

The first section of chapter one presents a literature review on reversible interactions used in elastomeric materials, paying particular attention to dynamic covalent bonds that exchange through associative mechanisms. In the second part, several grafting chemistries used to functionalise polydienic elastomers are presented.

Chapter two describes the functionalisation and the dynamic cross-linking of a polybutadiene with dioxaborolanes, using thiol-ene chemistry. Comparison with static cross-linking and the impact of the dioxaborolane modification is investigated. The ability of the resulting networks

to be reprocessed by industrial techniques was tested. A dual network with both static and dynamic bonds was designed to improve creep resistance while keeping the recyclability of the material.

Chapter three presents a model study on previously described reactions involving boronic esters as well as a new exchange reaction between dioxaborinanes. The influence of parameters such as the nature of the solvent, atmospheric moisture, presence of bulky substituents is investigated.

Using the same polybutadiene precursor and thiol-ene grafting chemistry as described in chapter two, chapter four presents our effort to synthesise a dioxaborinane based vitrimer and to study the impact of the exchange reaction on the macroscopic properties of the vitrimer. The recyclability and the mechanical properties of the obtained vitrimer were analysed.

Chapter five is focusing on the modification of polyisoprene via another grafting chemistry, namely nitrene chemistry. Azide compounds containing dioxaborolane moieties were synthesised and used to transform this polymer into vitrimer via reactive processing. The impact of the functionalisation was studied in the first part, and then two different strategies to generate vitrimers were compared.

Chapter 1

Design of Recyclable Elastomers Thanks to Dynamic Covalent Chemistry

Table of Contents

Chapter 1 - Design of Recyclable Elastomers Thanks to Dynamic Covalent Chemistry

1.1 Introduction to elastomers

1.1.1 Introduction

1.1.1.1 Plastics: the new paradigm

Nowadays, polymers are everywhere in our daily life, from the cup of coffee to the airplane, construction, electronics, vehicles, packaging and energy. Beginning in the late XIXth century with the Bakelite, produced through the condensation of phenol and formaldehyde, polymers are now involved in a wide range of applications and sectors thanks to their impressive versatility and innovation capacity. If huge progresses were made possible by polymers, however they are now facing great concerns because of their very long lifetime, leaching of potentially toxic monomers or additives over time, and dumping into landfills, rivers, and oceans, especially taking into account their exponential production. The world plastics production rose from 1.5 million of tons in 1950 to 250 million in 2009 and reached 348 million in 2017. It increased of 39% within less than ten years (**Figure 1.1**).
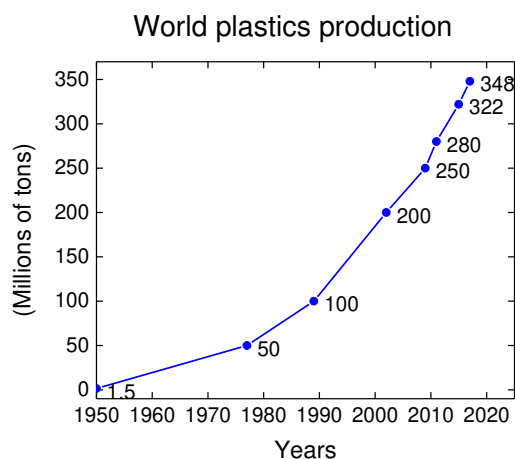

Figure 1.1. World plastics production in millions of tons from 1950 to 2017. [1]

1.1.1.2 Two categories: thermoplastic and thermosets

The origin of the term "plastic" comes from the Greek "plastikos" and was reused in Latin as "plasticus" to describe something able to be molded. Polymers are usually divided in two

categories, thermoplastics and thermosets, depending on the presence or not of chemical cross-links. Thermoplastics are long, entangled polymeric chains. The absence of chemical cross-links between the chains allows the material to be fully malleable. By increasing the temperature, the molecular mobility increases and the chains are able to diffuse by reptation.[2] This diffusion process at high temperature, *i.e.* above their main thermal transition temperature, glass transition temperature (T_g) and/or melting temperature (T_m), enables a drastic drop of their viscosity and consequently their easy processing and shaping by injection, blow or extrusion moulding. These very fast production methods are perfectly adapted for industrial production, explaining their dominating position on the plastic market, with more than 90 % of the overall plastic production. In theory, all thermoplastics are fully reprocessable an infinite number of times through melting/cooling processes. On the contrary, thermosets possess chemical cross-links between polymer chains preventing them to diffuse and rearrange even at high temperatures. These chemical bonds offer nonetheless deep interest. They provide thermosets with dimensional stability as they do not deform even at high temperatures. For instance, cured elastomers possess excellent mechanical properties, such as high elasticity above their T_g. Furthermore, thermosets stay insoluble in any solvent at all the temperatures. As a consequence, they cannot be recycled by conventional thermo-mechanical methods, that is why they are considered as non recyclable polymers.

1.1.1.3 Elastomer issues

Among the 348 million of tons of polymer that were produced in 2017, 28.6 million concerned rubber.[3]

Elastomers belong to thermoset materials, and are a subcategory presenting additional properties such as elasticity and resilience at room temperature. Widely used in the industry thanks to their very high flexibility, they are perfectly suitable to make seals, gaskets, tyres, or damping materials. One of the most challenging issues with rubbers is their recycling, which is not possible as they are a kind of thermoset. The presence of static covalent bonds between polymer chains prevents them from flowing and being reprocessed. Two problems have to be faced for elastomers. The direct consequence of their non recyclability is their end-of-life landfill disposal or incineration, as no global reuse is available except for scarce applications, such as fillers for instance. Morever, the growing elastomer demand induces a pressure on natural resources, which leads to deforestation followed by mono agricultural surface and loss

of biodiversity in the case of polyisoprene latex. For these two main reasons, it is essential to find out efficient methods to extend the cycle of life of elastomers.

If the landfill disposal is no longer an option in Europe, since the European Union banned it in 1999, the energy recovery is not a sustainable approach because of the green houses gazes, *e.g.* SO_2 and CO_2, produced during the incineration. Recycling remains the only way to manage end-of-life rubbers. However, it remains a very challenging problem because conventional recycling leads to a drastic loss of mechanical properties. As elastomers have been used for many decades, an interesting approach is to use the same polymer matrix but modified the way of cross-linking. The strategy is to impart the processability of thermoplastics at high temperature and to keep their high elasticity and advantages of thermosets at service temperature. Both physical and chemical cross-linking were investigated as will be discussed in the second part of this chapter. A novel kind of elastomers, called thermoplastic elastomers (TPE) is presented first. Already produced industrially their phase separation is used as cross-links but they are prone to dissolve in good solvent of the polymer matrix and their viscosity drops abruptly above their thermal transition temperature, so their heat resistance is not sufficient for demanding applications. Dynamic covalent chemistry offers new opportunities to design recyclable elastomers.

1.1.2 History, definition, structures and properties of rubbers

1.1.2.1 History

Rubbers can be prepared from latex of several plants, as more than 2000 different plants produce latex; Hevea brasiliensis, guayule (partenium argentatum), Russian dandelion (taraxacum kok-saghyz), castilla elastica, ficus elastica and funtumia elastica. Hevea brasiliensis, which is the most important source of natural latex, belongs to the family of Euphorbiacea, native of the Amazon rainforest. Guayule may also provide rubber in decent quantities in the Mediterranean region, but with a yield of 2/3 compared to that of Hevea and with the need to grind the Guayule plant to extract the latex.[4,5] That is why Hevea is the most used tree for latex production. If the original rubber tree Hevea brasiliensis was cultivated in Central and South America, people began to develop Heveas plantations in Asia and Africa. Nowadays, Thaïland, Indonesia and Vietnam share 2/3 of the world natural rubber production, while Brazil produces less than 2%.

Natural latex production is the result of a protection mechanism of trees against external aggressions. The latex is harvested by incision of the Hevea, flows out of the tree and then coagulates on exposure to air. To prevent raw latex from coagulating, if the colloidal suspensions are to be preserved for long periods of time, solutions of ammonia are added. After latex coagulation and drying, rubber bales are obtained that need to be further cured in order to impart heat resistance. Indeed, before the XIXth century, uncured natural rubber was already used for sealing or waterproofing, but their properties were very much temperature dependent. During winter, the material was brittle, while during summer or when exposed to sun, the material became sticky and viscous. In 1839, Charles Goodyear found out that if raw natural rubber is mixed with sulphur at high temperatures, the material does not flow any more when exposed to heat or sun. He patented the sulphur curing process, so called vulcanisation, in 1844.[6] Ten years later, Hiram Hutchinson bought the patents from Charles Goodyear, produced boots made out of rubber and opened the first French factory for rubber production. Sulphur vulcanisation has been widely studied and used in the industry since then. The process creates thioether and polysulphides bridges between rubber chains, which improve the mechanical properties and thermal resistance of the material.

1.1.2.2 Definition

The term "rubber" is now applied to any material that shows similar mechanical properties to those of natural rubber, regardless of its chemical composition.

Rubbers are special polymers that possess high elasticity. The intermolecular forces between the polymer chains are rather weak and let the chains take all the variety of statistical conformations. To form a three dimensional network, rubbers need to be slightly cross-linked. The cross-links suppress flow, but the chains are still very flexible at room temperature, which is above their glass transition temperature, thus small forces lead to large deformations. As a consequence, rubbers have a low Young's modulus and very high elongations at break, when compared with other polymers. "Elastomer" is a more recent term that has the same meaning than rubber, and no difference will be made between these two words in this work.

Elastomers can be classified into two broad categories, which reflect the presence or not of carbon-carbon double bonds in the polymer backbone. Dienic elastomers are often polymerized from monomers containing at least two double bonds. This category includes

polyisoprene (IR), polybutadiene (BR) and styrene butadiene rubber (SBR), which account for 82% of the world consumption, as well as nitrile butadiene rubber (NBR), chloroprene rubber (CR), ethylene-propylene-diene monomer (EPDM) and isobutylene isoprene rubber (IIR), which account for 12% of world consumption) (**Figure 1.2**). Non-diene elastomers include chlorinated or chlorosulfonated polyethylene, silicone rubber, polyurethane, hydrogenated acrylonitrile butadiene rubber and fluoro-elastomers. They represent 6% of the global demand. Non-diene elastomers do not have double bonds in their backbone, and thus, cross-linking requires different methods than vulcanisation, such as addition of trifunctional monomers (condensation polymers), or addition of divinyl monomers (free radical polymerization), or copolymerization with diene monomers like isoprene or butadiene.
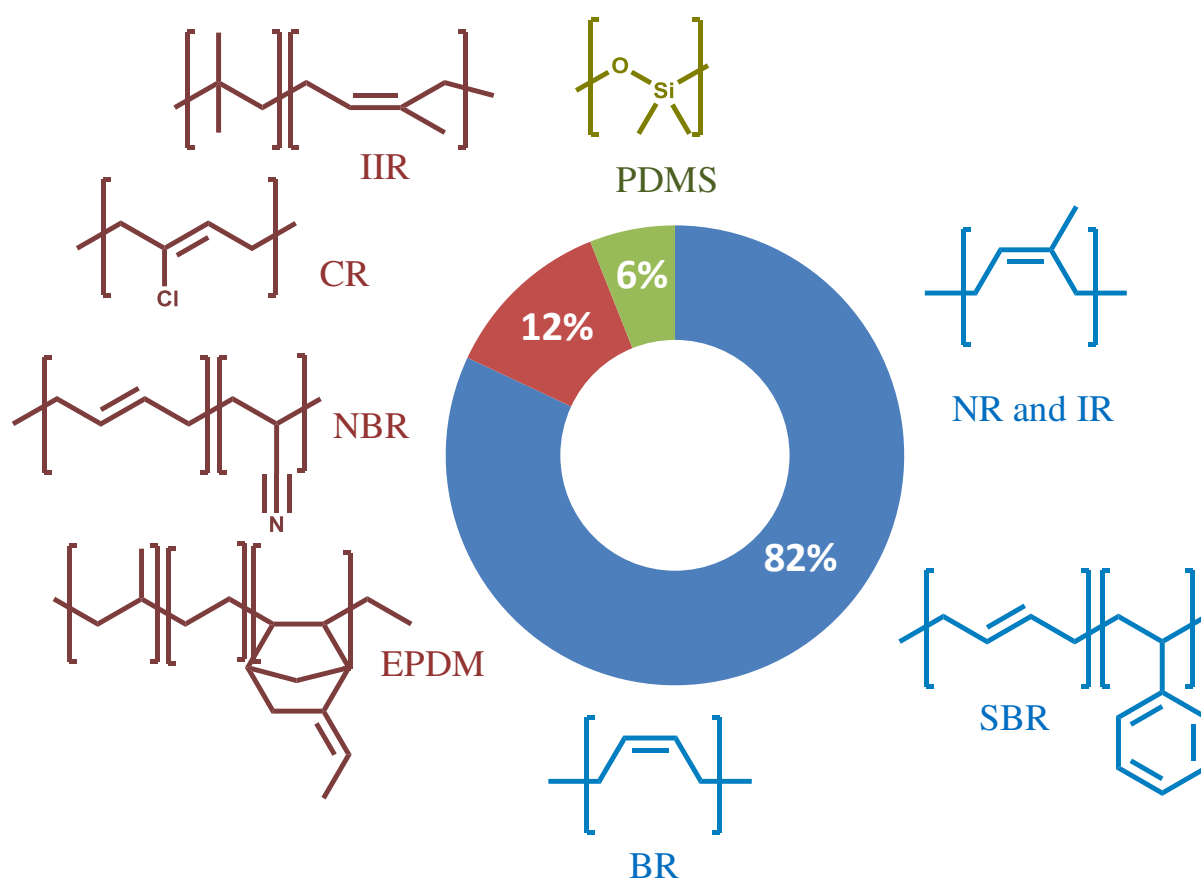
Figure 1.2. Distribution of the global consumption of elastomers.

1.1.2.3 Structures and properties

As shown in **Table 1.1**, depending on their chemical composition and structure, rubbers have special properties like ozone, oil, heat, heat, abrasion resistance, strength and gas permeability.

Table 1.1. Properties of the main dienic elastomers. Green : excellent; blue : good or medium; and red : fair or poor.

Elastomer	Strength	Abrasion resistance	Gas permeability	Ozone resistance	Oil resistance	Heat resistance
Natural rubber and Isoprene rubber	green	red	red	red	red	red
Polybutadiene	blue	green	blue	red	red	red
Styrene butadiene rubber	blue	green	blue	red	red	red
Nitrile butadiene rubber	blue	blue	blue	red	green	red
Chloroprene rubber	blue	blue	blue	blue	blue	green
Butyl rubber	blue	red	green	blue	red	blue
Ethylene-propylene-diene monomer	blue	blue	red	green	red	green

Natural rubbers

    Cis-1,4-polyisoprene

Natural rubber (NR) is made of cis-1,4-polyisoprene with a very high stereoregularity (>99%) (**Scheme 1.1**), but also contains non-rubber components (6 wt%), such as phospholipids and proteins in varying amounts depending on the source.[7] Natural rubber has unique properties, especially the capacity to crystallise upon straining. In the absence of tensile stress, the polymer chains are disordered so the polymer state is amorphous. Upon stretching, the chains start to align, and eventually reach a more ordered crystalline state. This crystallinity leads to a material with high strength, that's why natural rubber is considered to be self-reinforcing. This ability to crystallise upon deformation is due to the exceptional stereoregularity of the polyisoprene and to the presence of the non-rubber components. Even before cross-linking,

natural rubber contains a gel fraction of around 50-70 wt% caused by two types of bonding: hydrogen bonds between the proteins and covalent bonds between phospholipids. Indeed, the addition of ethanol in toluene breaks the former bonds, while transesterification breaks the latter cross-linking points.[8] Others non-rubber components play an important role on the exceptional properties of natural rubber. For instance, linked and free fatty acids contained in NR have nucleating effect on NR crystallisation.

Cis-1,4
for NR

Trans-1,4
for Gutta Percha

Mixture for synthetic isoprene rubber (IR)
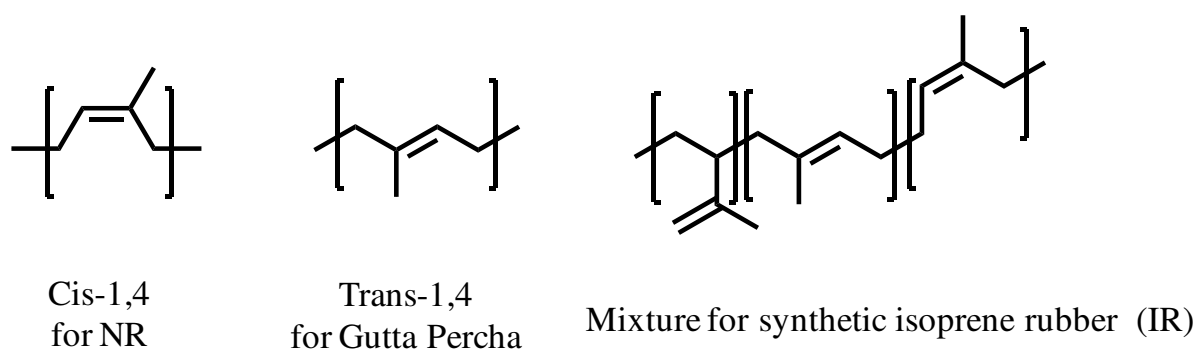
Scheme 1.1. Structure of polyisoprene depending on its origin.

Natural rubber exhibits good fatigue and abrasion resistance, low compression set and high tensile strength. However, it has poor solvent and heat resistance, and is prone to be attacked by ozone due to the presence of double bonds in the polymer backbone. Indeed, these insaturation are sensitive to thermal and oxidative degradation. The degradation generally occurs through chain scission and leads to a drastic drop of the mechanical properties. Thanks to its outstanding properties, natural rubber is the preferred polymer for many engineering applications. Typical uses include anti-vibration mounts, drive couplings, tyres, springs, bearings, rubber bands, and adhesives.

Trans-1,4-polyisoprene

Trans-1,4-polyisoprene can be harvested from two species, gutta-percha and balata, which produce latex similarly to hevea brasiliensis. Nonetheless, this polyisoprene isomer is highly crystalline at rest, unlike cis-1,4-polyisoprene. The material is hard and tough at room temperature, but is used for golf balls or waterproofing.

Synthetic rubbers

The vast majority of synthetic elastomers comes from petroleum, except silicon rubbers which are made from silica. If their chemical composition can be very different from an elastomer to another, most commercial rubbers contain carbon-carbon double bonds.

12

Isoprene rubber (IR), the synthetic counterpart of natural rubber, is produced through the polymerization of isoprene, which is obtained by thermal cracking of the naphtha fraction of petroleum. The polymerization is conducted in solution, either via a coordination mechanism, using Ziegler-Natta catalysts, or via an anionic mechanism. The resulting polymers can present a stereoregularity as high as 98 mol% of cis-1,4-isoprene reapeating unit, which is still slightly less than NR. As a consequence, and also because of the absence of non-rubber parts (phospholipids, fatty acids, *etc.*) isoprene rubber does not crystallise as well as NR. Indeed, even if the two materials appear to crystallise in a similar way, IR crystallises two to three times less than NR over a wide range of strains.[9] Tensile strength and crack growth resistance, in fatigue and in static conditions, are higher for NR than for IR.
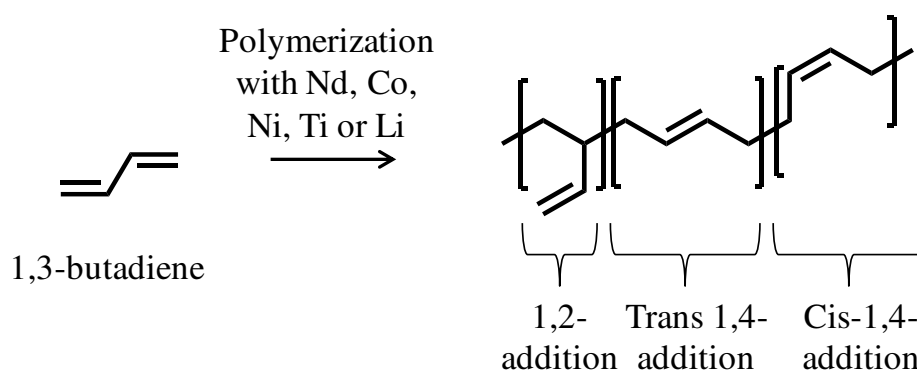
Scheme 1.2. Polymerization of 1,3-butadiene to obtain polybutadiene.

Polybutadiene (PB) is prepared by Ziegler-Natta polymerization of 1,3-butadiene. The nature of the catalysts greatly influences the stereochemistry of PB, through 1,2-addition, trans-1,4-addition or cis-1,4-addition (**Scheme 1.2**). For instance, neodymium catalysts lead to the formation of 98% of cis configuration, while alkyllithium catalysts favour medium to low yield of cis units (10-30%).

PB has moderate fatigue resistance and low temperature properties as compared to natural rubber, while its heat-ageing properties and abrasion resistance are better. Like natural rubber, PB is sensitive to thermal and oxidative degradation, also due to the presence of double bonds in the polymer backbone. In contrast with NR, degradation generally occurs through cross-linking.

Isobutylene isoprene rubber (IIR), chloroprene rubber (CR), acrylonitrile rubber (NBR) and ethylene propylene diene monomer rubber (EPDM) exhibit excellent but different properties, such as gas impermeability, oil, abrasion, ozone or heat resistance (**Table 1.1**).

1.1.3 Conventional recycling issues

Natural cis-1,4-polyisoprene is greatly affected by temperature; it becomes tacky and starts to flow if heated, and crystallises at low temperatures. It possesses a low hydrocarbon oil resistance and reacts with oxygen and ozone from the atmosphere, which can result in polymer chains scission and lead to the softening of the material. Therefore, cross-linking is mandatory to create a network and obtain the pre-cited elastomeric properties. The conventional method uses elemental sulphur, S_8, with activator, precursors etc, or peroxides to create static and dynamic covalent bonds between polymer chains. Once the permanent network is obtained, recycling is no longer possible.

In 2018, the world production of rubbers reached 29.1 million of tons. 48% of the production came from natural rubber and 52% from synthetic rubber. In 2016, about 65% of the global rubber production, natural and synthetic combined, was used to produce tyres, which often leads to summarise the elastomer recycling to the recycling of tyres. The other category is named as general rubber goods (GRG).

Despite many efforts to improve the recycling processes, only 8 to 10% of recycled rubber is used to make new tyres.

In the ideal case, the recycling process should break only the chemical cross-links. This process is known as devulcanisation. However, such a perfect method does not exist up to now, and existing processes lead to main chain scission. All the reclaiming processes give two parts, a soluble one composed of linear molecules with lower molar masses than the initial elastomer precursor, and an insoluble cross-linked part. The decrease of molar masses after recycling leads to inferior mechanical properties compared to the original ones, when new materials are prepared from these polymers. The way the rubber is recycled relies then on its incorporation into a virgin matrix. In order to increase its compatibility and miscibility with the new matrix, rubber is degraded into smaller chains through physical, chemical, physico-chemical and microbial techniques.[10,11]

Beside landill disposal, which is banned by the European Union since 1999, and the recycling through blending with pure matrix, rubber can be burned to recover energy. However, this solution generates greenhouse gases. End-of-life rubbers can also be degraded at 400 to 800 °C in the absence of oxygen. This process, called pyrolysis, produces hydrocarbons that can be used as fuel or gas, depending on their structure. However, pyrolysis costs lots of energy.

If static cross-links cannot be selectively cleaved, preventing the elastomer to be recycled, bonds involved in the cross-linking need to rearrange themselves under external stimuli, such as light, temperature, pH, etc… Such bonds are called dynamic bonds.

1.2. New ways to recycle rubber: from thermoplastic elastomers to dynamic covalent chemistry

Tremendous efforts have been made to impart recyclability and self-healability to thermosets, while preserving their good mechanical properties. Using dynamic interactions and/or bonds appears as the most widespread approach these last decades. Depending on the nature of the dynamic interactions, such materials can be divided in two groups: those relying on dynamic physical interactions and those relying on dynamic covalent bonds.

1.2.1 Physically cross-linked elastomer

Elastomers relying on physical interactions include elastomers based on phase separaration, as well as networks incorporating physical bonds, such as hydrogen bonds, ionics bonds, coordination bonds, π-π stacking, host-guest interactions. These interactions are weaker than chemical bonds, but this can be used as an advantage. They can easily be cleaved by an external stimulus, such as temperature. Furthermore, because of their weaker strength, they are prone to break before the chemical bonds constituting the main chain of the elastomer. Acting as sacrificial bonds, they dissipate energy preventing the cracks to propagate and preserving the integrity of the network. Nevertheless, physically cross-linked networks show poor heat, oil and solvent resistance. Despite these shortcomings, elastomers relying on phase separation and physical bonds have attracted a lot of attention.

1.2.1.1 Thermoplastic Elastomers

Thermoplastic elastomers (TPE) are a very interesting class of polymers that combined the rubbery properties of vulcanized elastomers with the processability of thermoplastics, which make them suitable for melt extrusion, injection moulding and blow moulding processing for example.

TPE are divided in two categories; the microphase separated block copolymers and the microphase separated multi-segmented copolymers, which include polyurethanes (TPE-U), copolyesters (TPE-E) or polyamides (TPE-A). The chemistry and architecture of these two families of TPE are different. Indeed, block copolymers have a discrete number of blocks, typically between 2 and 3. They possess two types of blocks, a soft one (meaning with a low T_g, such as polybutadiene, polysiloxane or polyether) and a rigid one (meaning with a high T_g or T_m, such as polystyrene or poly(methyl methacrylate)). If the two blocks are incompatible enough, the copolymers phase separate and exhibit thermo-mechanical properties of both materials. Thanks to their low dispersity and number of blocks, they can self-arrange into highly ordered structures. They possess a phase separated morphology that was established by Cooper and Tobolsky in 1966.[12] In 1980, Leibler developed a statistical theory of phase equilibria for A-B type block copolymers.[13] According to Leibler's theory, only two quantities are relevant parameters for the characterization of phase equilibria in a block copolymer melt: the product χN and the composition f. With these two parameters only, all the different equilibrium morphologies, *e.g.* spheres, cylinders, bicontinuous channels or lamellae, can be predicted (**Figure 1.3**).
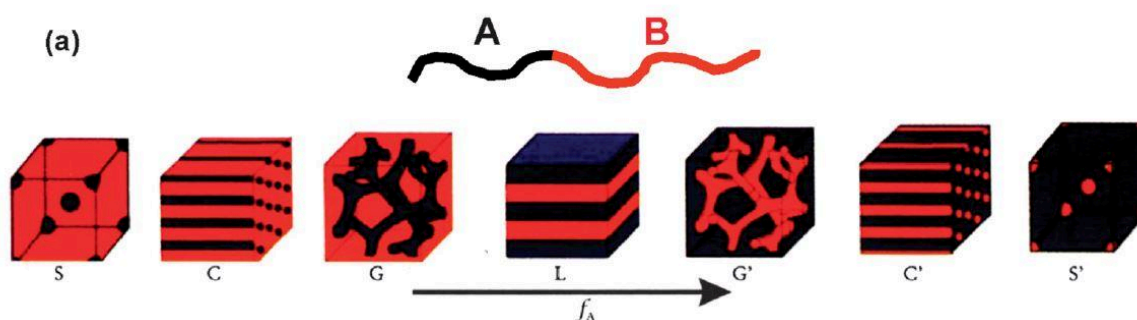
Figure 1.3. Equilibrium morphologies of AB diblock copolymers in bulk: S : body-centered-cubic spheres, C := hexagonally packed cylinders, G : bicontinuous gyroids, and L :lamellae.[14]

Because of their higher molecular dispersity and more complex molecular architectures, segmented copolymers microphase separate into less ordered nanostructured elements than block copolymers.

Polyurethane segmented thermoplastic elastomers are versatile materials that have found a wide variety of industrial applications, ranging from textile fibers, automobile, footwear, cell phones, packaging, building, adhesives, foams, coatings and biomaterials.[15–17] Their synthesis is based on addition reactions between a polyol (*e.g.* an aliphatic linear polyether terminated

by hydroxyl functions at both ends) with a number average molar mass (M_n) of 1000 to 3000 g/mol, typically, and a diisocyanate (ususally aromatic molecules, like methylene diphenyl diisocyanate) to form a prepolymer (**Scheme 1.3**). This prepolymer is further reacted with a chain extender (usually diols or diamines resulting in urethane or urea bonds) or a chain capper (mono-functional species). When the chain extenders are tri-functional, they are called cross-linkers. However, in this case, the resulting material is no longer a TPE, but a thermoset. Industrially, the syntheses are carried out in bulk, requiring a full control of viscosity to avoid premature aggregation or crystallisation. The synthesis conditions have an influence on the phase segregation behaviour, and thus on the properties of the final material, making them an important subject of study.[18–20]
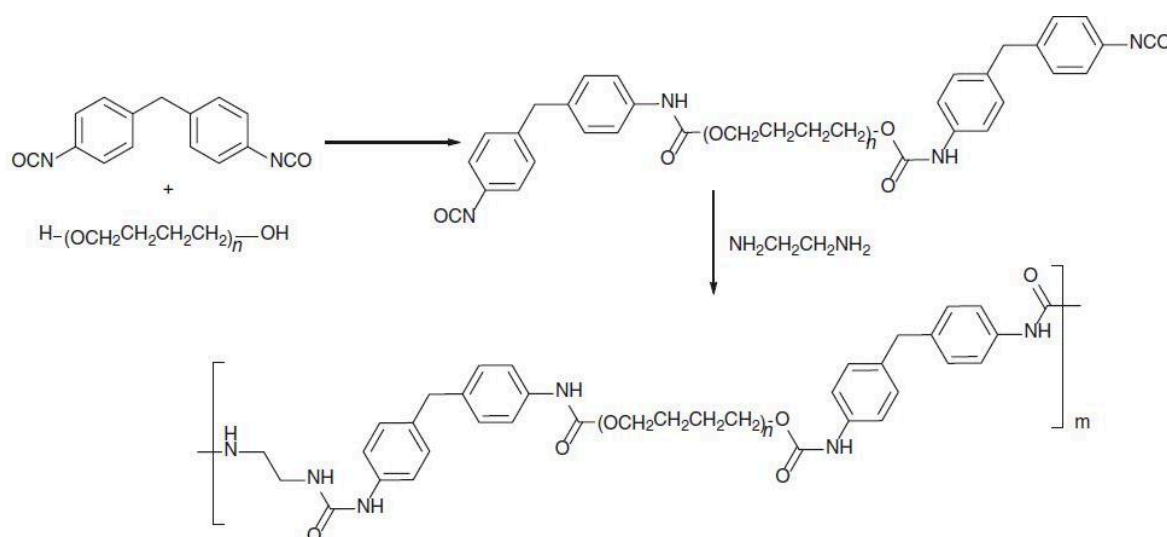
Scheme 1.3. Synthesis of Spandex polyurethane via a one-pot two-step reaction.[21]

This step-growth polyaddition results in alternating hard and soft domains. The polyols constitute the soft blocks. They are low T_g oligomers and bring flexibility and ductility to the final material. The aromatic diisocyanates, potentially linked with small chain extenders, are more rigid portions which play the role of hard segments. The incompatibility between the soft and hard segments leads to a microphase separation. The hard segments self-assemble and crystallise, acting as physical cross-links.

As previously mentioned, TPEs are reprocessable and healable with temperature. Such trigger can be an advantage but also a disadvantage because the healing does not occur without heating. The incorporation of hydrogen bonds in the soft segments of conventional TPEs was proposed to solve this issue.[22] A brush-like architecture was first designed with a hard polystyrene backbone grafted with soft polyacrylate amide. A modified styrene block

copolymer was also synthesized by introducing of a quadruple hydrogen bonding moiety inside the soft block chain.[23] The resulting supramolecular TPE exhibited good mechanical and self-healing properties at room temperature. Another strategy focused on the incorporation of hydrogen bonds in the hard phase of TPEs, but it did not result in any self-healing properties.[24]

Sustainable TPE-Us were synthesised with plant oil derived long chain diisocyanates and diols.[25] The long-chain aliphatic polyurethane segments provide physical cross-linking via hydrogen bonding, resulting in thermoplastic materials with melting points as high as 116 °C and an elastomeric behaviour. This strategy is very interesting since the obtained recyclable materials are partially bio-sourced.

1.2.1.2 Ionomers

Ionomers are a special kind of polymers containing low amount of ionic groups (up to 15 mol%) neutralized with a multivalent metal ion or counter ion, which acts as dynamic cross-links. [26,27] These polymers exhibit unique physical properties, such as transparency, toughness, flexibility and oil resistance and even quite high melt viscosity because of the presence of strong and numerous intermolecular ionic bonds. The ionomers properties depend on the kind of polymer backbone, ionic content, degree of neutralization and the types of cation and anion.

These ionic sites tend to form clusters, which leads to microphase separation between ion pair rich and poor regions (**Figure 1.4**). These ionic cross-links are temperature sensitive. They can gain some mobility with temperature, thereby allowing the polymer chains to rearrange and eventually to flow if the melt viscosity is sufficiently low. Elastomeric ionomers represent a new class of thermoplastic elastomers that can be processed using thermoplastics processing techniques, just like thermoplastic elastomers.
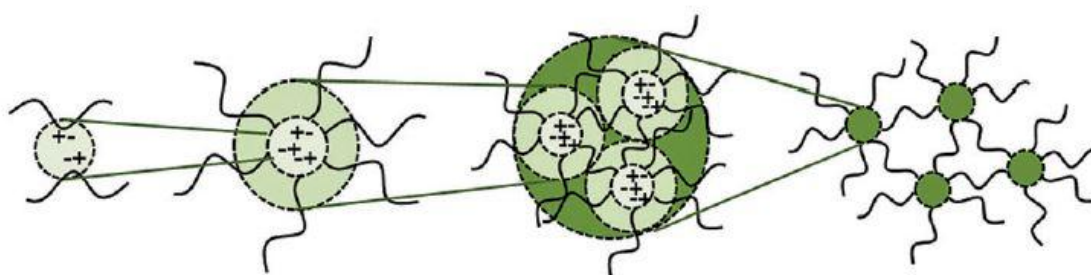

Figure 1.4. Hierarchical structure formatioin in ionomers: ion pair, multiplet, ionic cluster network with regions of restricted polymer mobility. [28]

Lundberg *et al.* studied the rheological behaviour of carboxylated and sulphonated polystyrene, using polymers presenting the same molecular weight, ion content and counter ion.[29] They showed that the ionic association is stronger in sulphonated ionomers than in their carboxylated counterpart. Thus, the melt viscosity was far higher for sulfonated ionomers, making their melt processing more difficult.

To decrease their melt viscosity and improve their processability, plasticizers can be incorporated into ionomers. The two phase morphology and the large difference of polarity of the hydrocarbon and ionic phases give two ways for the plasticization of ionomers: either the plasticization of the hydrocarbon phase or the plasticization of the ionic clusters.

Bazuin and Eisenberg[30] investigated the effects of polar (glycerol) and nonpolar (ethylbenzene) plasticizers on the dynamic mechanical properties of styrene/methacrylic acid ionomers.[31] The addition of 5 wt% of glycerol as a plasticizer in this ionomer reduces the melt viscosity by a factor of 1000 at elevated temperatures. To get the same viscosity, 40 wt% of dioctylphthalate is required. This major difference is attributed to the preferential plasticization of metal sulfonate groups by the polar glycerol, whereas dioctylphthalate plasticizes the polystyrene backbone.

The influence of the metal ions used to neutralize ionomers was investigated by Ibarra *et al.* on the properties of carboxylated nitrile rubber (XNBR).[32,33] It was reported that magnesium oxide cross-linking agents led to better physical properties than other oxides, like calcium oxide. An excess of calcium oxide tends to form agglomerates, which constitute weak points, while an increase of magnesium oxide improved the hardness and tear strength. In the latter case, two transitions were observed in dynamic mechanical analysis (DMA), the glass transition around 0 °C, and a transition above 150 °C, associated to the formation of ionic structures.

It was confirmed by Van der Mee *et al.* that the nature of the neutralizing cation affects the structure and properties of ionomers.[34] Using potassium (K^+) instead of zinc (Zn^{2+}) on hydrolyzed maleated EPM rubber, resulted in a material with higher mechanical properties thanks to a better phase separation. Hohlbein *et al.* also showed that Co^{2+} and Zn^{2+} gave improved physical and self-healing properties.[28] The Co^{2+} based ionomers were shown to be

the best materials based on their tensile strength, recovery of mechanical properties and short healing times. The aggregate size of ionic multiplets ranged from 7 Å to 45 Å.

Chatterjee *et al.* compared ZnO and ZnO$_2$ as cross-linking agent.[35] They reported that in the latter case, both ionic and covalent cross-links were formed in the XNBR, while ZnO only form ionic cross-links. Thus ZnO$_2$ cross-linked ionomers are superior to ZnO ones but, their impact on the recyclability was not reported.

1.2.1.3 Hydrogen bonds

Hydrogen bonds count among the weakest interactions, with bond energy typically ranging from 10 to 40 kJ/mol, but they possess intrinsic advantages, such as their directionality and the capacity to break and reform easily. The most common approach to incorporate hydrogen bonds in rubber relies on grafting hydrogen bonding molecules onto elastomeric polymer chains.

Hydrogens bonding could be introduced into elastomers though partially bio sourced blocks. The use of lignin, which is the second most abundant terrestrial polymer obtained from woody biomass, was investigated to prepare elastomers.[36] Lignin oligomers (hard phase) were reacted with diglycidyl polyethylene glycol (soft phase) to obtain a tough but also self-healing material. The presence of hydrogen bonds and the coexistence of hard and soft phases endow the polymer with this interesting combination of properties.

Wu *et al.* employed another strategy.[37] They incorporated weak and strong dynamic bonds to impart self-healing ability, high stretchability and robustness. Hydrogen bonds were introduced through the polycondensation of bis(3-aminopropyl) terminated polydimethylsiloxane (PDMS) with 2,2-toluene diisocyanate, whereas strong bonds were metal coordination bonds with Al(III) ions. Guo, Liu and coworkers presented a natural rubber based dual network with hydrogen bonds and dynamic covalent bonds.[38] Commercially available epoxidized natural rubber (ENR) was dynamically cross-linked with a diacid (sebacid acid) and also grafted with *N*-acetylglycine, which provided the hydrogen bonds. The latter are prone to break prior to the covalent network and can dissipate energy, thereby improving the strength and extensibility of the material. The dynamic covalent cross-linked network can also rearrange under thermal treatment via transesterification, which is facilitated by the presence of a catalyst. Other combination of hydrogen bonds and dynamic covalent bonds were also reported.[39] ENR was cross-linked into a dual network based on disulfifde metathesis and thermo reversible hydrogen bonds. This dual material exhibited high

strength (9 MPa), high self-healing capacity (up to 98%), good recyclability and fatigue resistance.
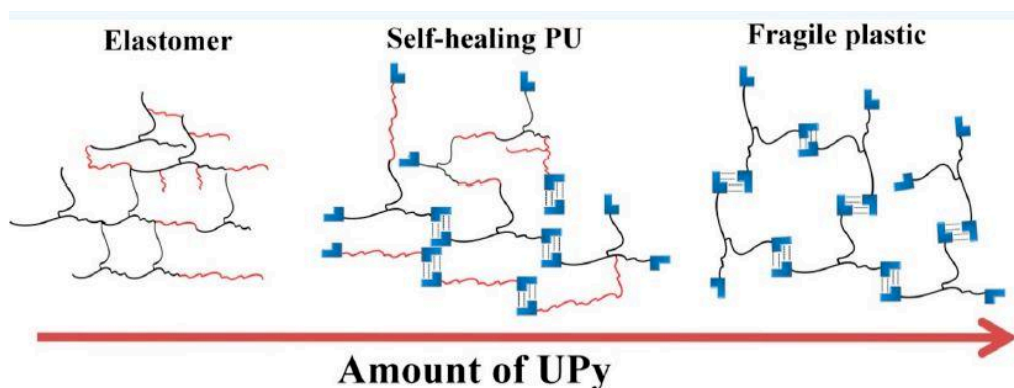
Figure 1.5. Elastomeric and self-healing properties depending on the amount of UPy.[40]

A self-healing polyurethane was designed by incorporating hydrogen bonds with ureidopyrimidinone (UPy) motifs at the chain ends of polyethylene glycol (PEG) and propylene glycol (PPG) block copolymers (**Figure 1.5**).[40] Indeed, UPy motifs can self-assemble via lateral hydrogen bonding interactions (**Figure 1.6**).[41] Increasing the amount of UPy units resulted in increasing both Young's modulus and elongation at break, as compared to the control system free of UPy. However, if the percentage of these hydrogen bonding units was too high, the material became fragile and brittle, loosing its elastomeric properties.
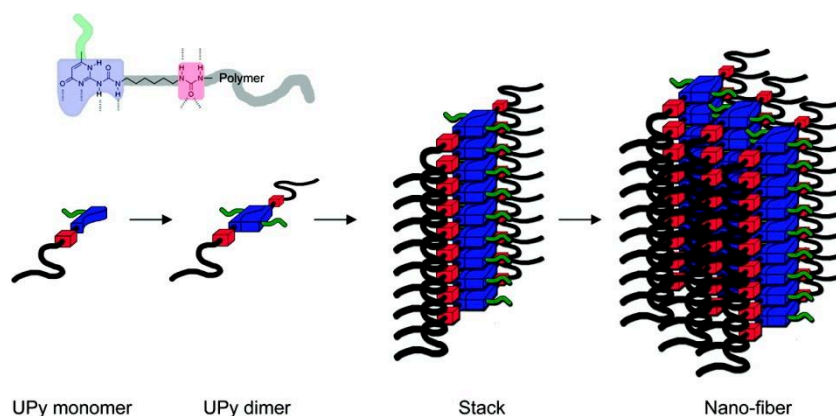
Figure 1.6. Organization of dimerized UPys units with lateral hydrogen bonding urea and urethane groups into fibers.[41]

Another approach was employed by Leibler *et al.* to obtain dynamic elastomers with hydrogen bonds (**Figure 1.7**).[42] A major issue in supramolecular network is crystallisation, which was prevented in this system by using a wide diversity of fatty trimer and dimer acids from vegetable oils. As their composition is a mixture of different species, these molecules

21

are liquid at room temperature and do not crystallise but just become glassy at low temperature, unlike other classical diacids. In addition, entropy of mixing and directional interactions contributed to hamper phase separation in this system. Through a two-step pathway a supramolecular polymer bearing functional groups able to strongly associate via hydrogen bonds was synthesized. Yet, the resulting material had a too high T_g (28 °C) to be considered an elastomer. The T_g could be decreased down to 8 °C by the addition of 11 wt % of dodecane plasticizer. This way, a rubber with excellent elongations at break and small residual strains was obtained. More interestingly, the elastomer could be reprocessed at high temperatures, above 160 °C, through extrusion modling and compression moulding, and exhibited good self-healing properties.

Figure 1.7. Design of a self-healing supramolecular rubber made from fatty acids and other small molecules.[42]

However, it was shown that the self-healing efficiency of the supramolecular elastomer decreases with the time elapsed before putting pieces in contact again, up to a point where the materials is no longer able to self-heal if the waiting time is too long. During this time, some free hydrogen bonding groups find partners within the broken pieces and recombined to reach a novel equilibriums state.[43]

2.1.4 Others interactions

π-π stacking is another weak interaction. Dynamic polymers were designed thanks to aromatic π-π stacking. Burattini and coworkers reported a self-healable elastomer made from blending chain-folding polyimide and polyurethane end-capped with pyrenemethylurea groups (**Figure 1.8**).[44,45] A triple π -stack was proposed as possible structure of the cross-link leading to the good macroscopic properties of the material. The obtained material exhibited a higher tensile modulus than the hydrogen bonded system reported by Leibler and *al.,* thanks to the combination of both kinds of interactions. The healing capacity was tested after 4 hours of annealing at 100 °C. A recovery of 77% to 95% of the initial mechanical properties was obtained.
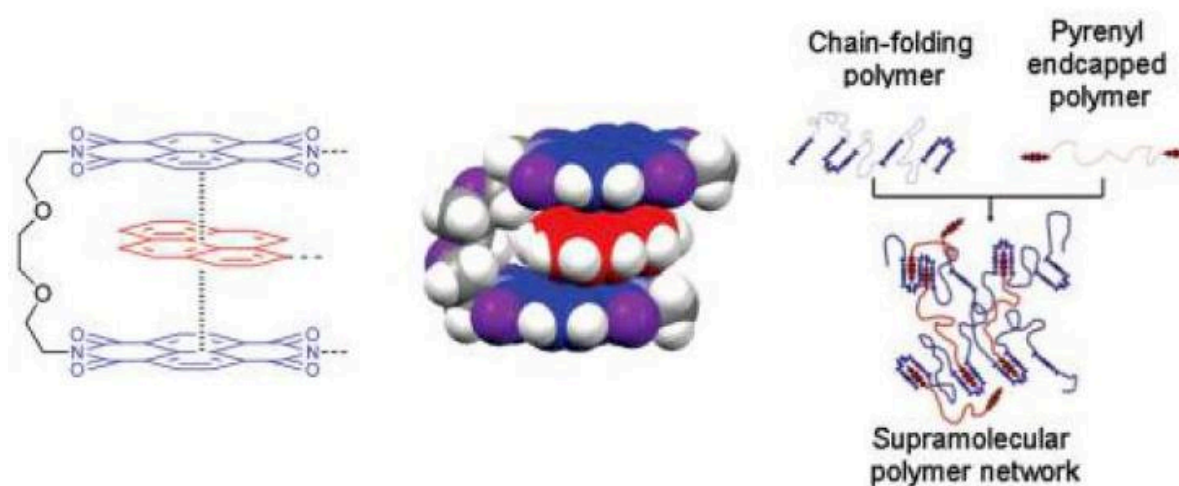
Figure 1.8. Left: Structure for the π-π stacking interactions between a bis(diimide) chain fold in polyimide and a pyrenyl residue. Right: Schematic of formed supramolecular network.[44]

Host-guest interactions

Host-guest interactions were also employed to synthesize dynamic hydrogels.[46,47] One of the most common host guest molecules are adamantane and β-cyclodextrin, which possess a high selective complementarity (**Figure 1.9**). Elastomer with excellent self-healing properties and recyclability were reported using this complementary couple.[48,49] This supramolecular interaction also allowed to change the miscibility of two incompatible polymers to create an interpenetrating double network.[48,49]
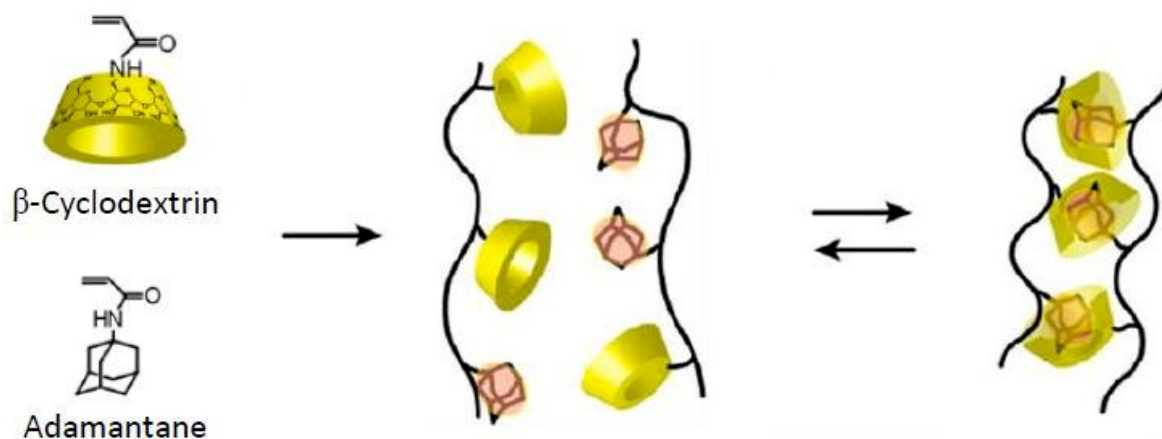
Figure 1.9. Chemical structures of the host and guest monomers and the reversible gelation through host-guest interactions.[47]

Metallophilic interactions

Coordination bonds are among the highest energy non-covalent bonds. For NBR, the nitrile groups can be used as ligand when they are in contact with a suitable metal. Very interestingly, this dynamic chemistry does not necessarily require a pre-functionalization to incorporate the dynamic cross-linker. For instance, a non sulphur cured network was prepared using these coordination cross-links with anhydrous copper sulfate ($CuSO_4$).[50] As this study focused on the cross-linking of carboxylated nitrile rubber, both ionic links, via the carboxylic groups (-COOH), and coordination links, via the nitrile (-CN) groups, were involved in the dynamic curing. The former increased abrasion resistance and thermo-mechanical properties, whereas the latter improved compression set. The combination of these two kinds of links resulted in a highly resistant and potentially reprocessable elastomer.

Others metal-ligand couples may be considered to cross-link elastomers. Indeed, Fe^{3+}-catechol groups were incorporated in nitrile rubber.[51] To this aim, epoxidized NBR was reacted with dopamines to graft catechol moieties on the polymer backbone. $FeCl_3$ was added and the solid products were dried and moulded at 170 °C for 10 minutes. This kind of bonds imparts good mechanical properties and excellent recyclability to NBR.
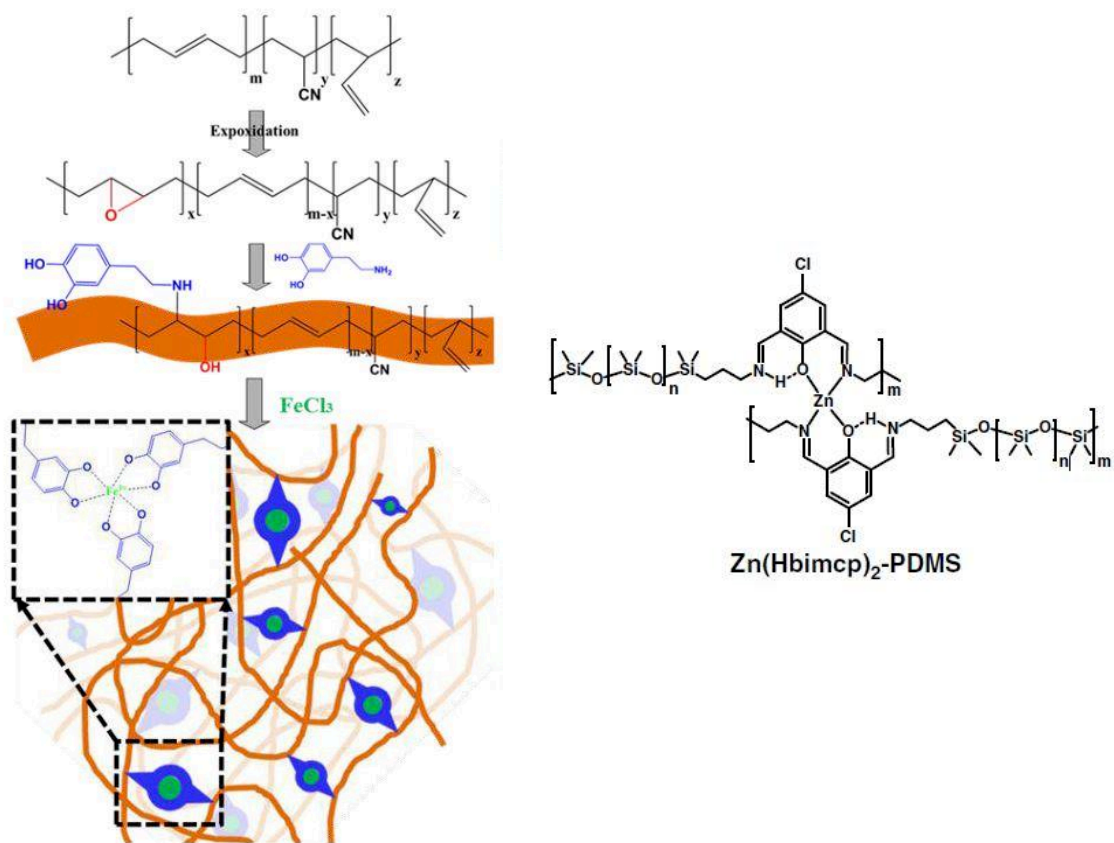
Figure 1.10. Left : scheme of cross-linking NBR with dopamine and FeCl$_3$.[51] Right : Dynamic Zn-Hbimcp coordination bonds applied to PDMS.[52]

Other polymers have been cross-linked thanks to coordination bonding.[53] PDMS with pending pyridine was synthesised and cross-linked with cobalt chloride (CoCl$_2$) to generate a self-healing elastomer that could recover 91% of its properties after 24h at room temperature. For a comparison, the NBR elastomer cross-linked through Fe^{3+}- catechol interaction required to be heated above 100 °C to be healed. PDMS was also transformed into a dynamic network thanks to Zn-Hbimcp (2,6-bis((imino)methyl)-4-chlorophenol) complexation (**Figure 1.10**). This interactions is characterised by a very high association constant (2.2 x 10^{11}) and a fast dynamic, which give access to tough materials that present self-healing ability at room temperature.[52]

1.2.2 Dynamic covalent chemistry

Covalent bonds are stronger than most physical interactions, giving the elastomer better mechanical properties and chemical resistance. But to impart recyclability these bonds need to be dynamic, meaning that they can break and reform under the action of an external stimulus. Based on the mechanism of bond exchange, two main categories can be established in the domain of cross-linked polymers using dynamic covalent bonds: the dissociative mechanism, where de-cross-linking occurs before re-cross-linking, and the associative mechanism in which de-cross-linking and re-cross-linking happen at the same time (**Scheme 1.4**). In the latter case, and if the cross-linking density is not altered by side reactions, the network is called a "vitrimer", which is a new class of polymeric materials beside thermoplastics and thermosets.
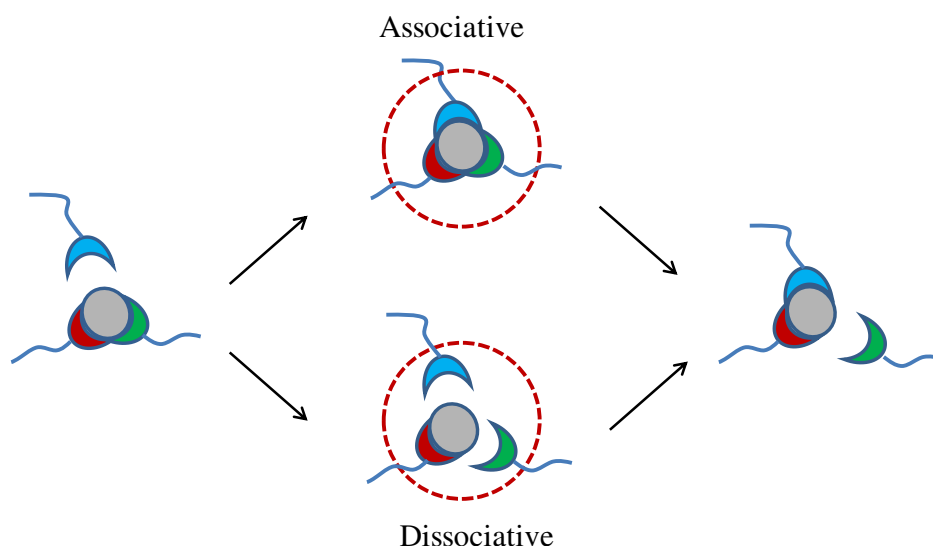
Scheme 1.4. Top: Associative mechanism; a bond opens after the new bond formation via a transition state with three chains connected at the same time. Bottom: Dissociative mechanism; a bond opens before the new bond formation leading to a temporally debonded system.

1.2.2.1 Dissociative systems

Diels-Alder

A lot of different materials based on association-dissociation of dynamic covalent bonds were reported with different dynamic chemistries. One of the most popular reactions is the Diels-Alder (DA) cycloaddition discovered by Diels and Alder in 1928.[54] It is a [4+2] cyloaddition between a conjugated diene and a dienophile (for instance an alkene or an alkyne) to give a product named the Diels-Alder adduct. The formation of σ-bonds from π-bonds is the (enthalpic) driving force of the reaction, whereas the dissociation of the adduct, called retro-

Diels-Alder reaction, is entropically favoured. As a consequence, the reaction is reversible under certain conditions. For instance, the adduct formation between furan and maleimide is favoured below 60 °C and the dissociation above 100 °C. Interestingly, this reversible addition does not form any by-product, such as water in the case of a condensation, which could migrate out or be evaporated during processing or lead to side reactions affecting the reversible reaction.
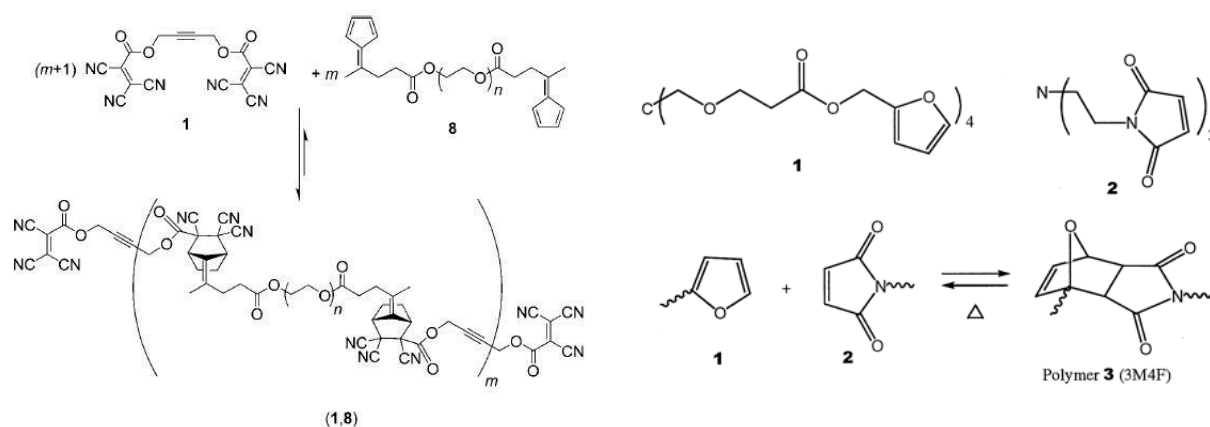
Scheme 1.5. Diels-Alder reactions imparting recyclability to the polymer network.[55,56]

Liu and *al.* showed that the Diels-Alder reaction between a bismaleimide and furfuryl alcohol has an activation energy of 41.6 kJ/mol.[57] The same reaction with a polyurethane prepolymer end-capped with furan rings was followed by ^{1}H NMR spectroscopy in DMSO-d$_6$. Assuming the retro Diels-Alder reaction was negligible up to 70 °C, the Diels-Alder reaction was observed to follow a second-order kinetic, giving activation energy of 47 kJ/mol. The final equilibrium state was reached after more than 300 minutes at 70 °C, whereas the retro-Diels Alder reaction could achieve equilibrium within 20 minutes at 130 °C. In another study,[58] an activation energy of around 67 kJ/mol was found for the Diels-Alder reaction between a tri functional furan and a bis-maleimide, which illustrates the impact of the network topology and functionality on the dynamics of the reversible interactions and/or reactions. The retro Diels-Alder reaction had an activation energy as high as 156.7 kJ/mol.[59] Boutelle and Northrop studied the effect of the substituents on the formation of Diels-Alder adducts and showed that electron-donating groups on the furan lead to a decrease in both free energy and transition state energy, whereas electron withdrawing groups yield the opposite trend.[60] Authors pointed out that using too electron-rich furans could stop the exchange reaction as the products are too stable to react in the backward reaction. The reactivity was not really affected by the maleimide substitution, no matter the N-alkyl, N-allyl or N-phenyl substituent. If the

backward reaction always needs high temperatures to occur as shown previously, Lehn and *al.* reported a dynamic exchange at room temperature between two specific species: an fulvene as diene and an diethyldicyanofurmarate as a dienophile.[61] The equilibrium was reached only within seconds after mixing the two reactants. Once grafted onto polyethylene glycol, a flexible dynamic elastomer could be synthesized showing self-healing properties at room temperature (**Scheme 1.5**). As an inherent drawback, the material was also prone to creep under these conditions.[55] Gheneim and *al.* reported the DA-cross-linking of poly(hexyl acrylate) and PDMS at the same time.[62] The highly flexible cross-linker and its low amount (3-5%) guarantee the low T_g of the cross-linked elastomers, -60°C and -111 °C respectively. ^{1}H NMR and GPC analysis of the de-cross-linked polymers proved that linear polymers were identical to the original samples, showing the absence of sides reactions over the process. Nevertheless, mechanical testing was missing for this reference. Sun and coworkers reported a linear polyurethane containing maleimide groups cross-linked with bis-furan.[63] If the polymer exhibits excellent recyclability, up to 100% of the elongation at break and 93% for the stress at break, after dissolution at 130 °C in dimethylacetamide followed by evaporation of the solvent, the mechanical properties dropped from 300% to 225% for the elongation at break and from 45 MPa to 30 MPa for the stress at break, when the material is reprocessed by hot compression moulding. Wudl and *al.* decided to start from multifunctional monomers to achieve a thermally re-mendable polymer that can be repaired at elevated temperatures after fracture and whose properties equals those of commercial epoxy resins at room temperature (**Scheme 1.5**).[56,64] The degree of de-cross-linking was estimated to be 30% at 120 °C, according to solid-state NMR spectroscopy. Upon cooling to 80 °C, a full recovery of the initial cross-linking degree was observed. More recently, Deng and coworkers designed an elastomeric material made from three monomers, including a furan, and cross-linked with a bis-maleimide.[65] With a T_g lower than -35 °C, the polymer showed better mechanical properties (tensile strength 13.1 MPa, elongation at break of 455-520% and Young's modulus around 2.0 MPa) than the traditional vulcanized counterpart, and very good recyclability once remolded at 155 °C over two hours. Another strategy was employed by Zhao and *al.*[66] They polymerized an amine functionalized PDMS with a triisocyanate and diol containing a Diels-Alder adduct. The poly(siloxane-urethane) elastomer showed good self-healing and reprocessing abilities at 140 °C. Enhanced tensile properties, biocompatibility and shape memory were provided by the introduction of semi crystalline polycaprolactone segments. In order to suppress property losses at high temperature, Fuhrmann *et al.* designed a photoswitchable cross-linker that can be reversibly transformed into its inactive state to

inhibit decross-linking. When the network is locked in the cross-linked state and heated up to 130 °C, it maintains its elastic solid behaviour, characteristic of static networks. On the contrary, the unlocked system becomes dynamic above 100 °C, like traditional Diels-Alder polymers.[67]

Sulphur chemistries

Dynamic sulphur chemistries are commonly used to transform traditional vulcanized rubber into their recyclable counterparts. Vulcanisation involving sulphur based compounds is the most popular method used to cross-link rubber and make tyres. In 1946, Stern and Tobolsky observed that polyisobutylene and butadiene-acrylonitrile rubbers show stress relaxation and creep between 35 °C and 120 °C.[68] The tetradisulfides based elastomers relax faster than disulfides ones but they possess the same activation energy of viscous flow. The authors proposed two mechanisms: one could consist in breaking and reforming of interchain bonds and another could involve a direct metathesis between disulfide bridges. Later, Tobolsky and *al.* showed that stress relaxation occurs through homolytic scission of polysulphides bonds and fast recombination.[69] It was further confirmed by Matxain and *al.* through density functional theory and quantum molecular dynamics calculations.[70] They did not find any evidence for the existence of a transition state for the metathesis mechanism, while the radical mediated process was calculated to have a reaction barrier of *ca.* 42 kJ/mol. Thiuram aromatic and dendralene disulfides were found to have low bond dissociation energies, which makes them suitable to design self-healing materials.

Disulfides can be transformed reversibly into thiols through redox reactions as shown by Tesoro and Sastri in an epoxy resin.[71,72] Matyjaszewski and *al.* reported functionalized star with the same redox responsive thiol-disulfide bonds as reversible cross-linker (**Scheme 1.6**).[73,74] But as mentioned above, disulfides can break and reform easily. To do so, aliphatic disulfides need to be activated by an external stimulus, such as heat, UV light or a catalyst. For instance, Goosen, Klumperman and *al.* reported a cross-linked elastomer (with a T_g of -35 °C) that can be healed at 60 °C and creep at low shear rate (100 Pa).[75] Made by the addition reaction of a tetra functional thiol onto a difunctional epoxy containing disulfide links, the material shows a rubbery plateau between 0 and 100 °C, and starts to flow at higher temperature. At this point, the cross-linking degree decreases due to disulfides cleavage, the chains have then enough mobility to diffuse, leading to a macroscopic flow. Otsuka and *al.* mixed two disulfide-containing polyesters with different molecular weights and

photoirradiated the mixture during 60 minutes. The GPC traces of the reaction mixture change from a bimodal distribution to a monomodal distribution, proving the dynamic exchange at 30 °C under UV.[76] Rowan and *al.* designed a polymer combining both shape memory and healable properties. When scratched and exposed to UV light for 5 minutes, the material recovers fully its mechanical properties.[77] Xiang and *al.* cross-linked a polybutadiene through thiol-ene chemistry. They used UV irradiation for 3h to recycle the elastomer, but were confronted to a drastic decrease of transmittance with the times of recycling as well as with a degradation of the tensile strength.[78] The use of a catalyst may also provide self-healing properties at room temperature without the need for UV irradiation.[79] Xiang demonstrated the ability of $CuCl_2$ to catalyze the reshuffling of sulphur vulcanised polybutadiene.[80] A strong influence of solvent polarity was pointed out as the activation energy in acetonitrile was calculated to be 22 kJ/mol, while in heptanes it was 172 kJ/mol. If the model reaction showed that the equilibrium state was reached after 60 min at 25 °C with 0.5 mol% of catalyst, it required 12 hours at 110 °C to exhibit a healing efficiency of 75% in the elastomer. The authors claim that the healing mechanism is different from tributyl phosphine or UV-light one as no radicals seem to play a role. To overcome the incompatibility of the catalyst with the rubber matrix, and enhance its dispersion, $CuCl_2$ was replaced by an organic methacrylate copper (II) complex, resulting in better recyclability of the rubber. More recently, Takahashi and *al.* designed a recyclable poly(hexyl methacrylate) thanks to a disulfide linked to nitrogen moieties.[81] Although the authors claim that this specific disulfide possess a lower bond dissociation energy (110-130 kJ/mol) as compared to alkyl disulfides (250-290 kJ/mol), the material needed to be process at 120 °C for 12 hours to obtain clear samples after recycling. Wu presented a PDMS based polyurethane containing disulfide bonds showing high self-healing efficiency at 120 °C but with weak tensile stress.[82] Thiol-Michael adducts were also used by Konkolewicz *et al.* to design a thermoreversible network.[83] At high temperature, 90 °C, retro-Michael reaction is promoted releasing free thiol and acrylates that can react again between each others.
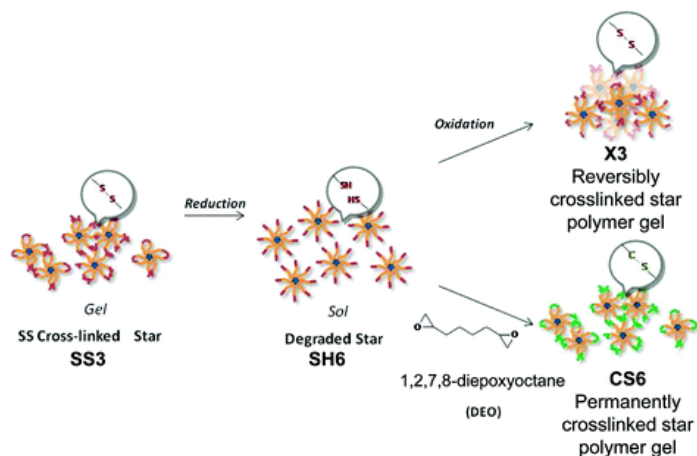
Scheme 1.6. Reduction of disulfide bonds functionalized star polymers into thiols and back oxidation. Synthesis of permanently cross-linked star polymers as control.[73]

Beside these materials that require external stimuli, Rekondo and *al*. reported a polyurethane elastomer that is able to self-heal at room temperature without any catalyst.[84] Thanks to aromatic disulfides bonds and hydrogen bonds between ureas present in the monomer, the elastomer could achieve a healing efficiency of 62% after 1h of contact at room temperature and up to 97% after 24h. Nevertheless, the mechanism was not investigated but the hydrogen bonding effect was calculated to contribute to the half of the self-healing properties. Matyjaszewski and *al*. presented a polyurethane elastomer (with a T_g of -50 °C) containing thiuram disulfides bonds capabale of self-healing under ambient conditions, *i.e.* in air, at room temperature and in the absence of solvent or specific UV irradiation.[85]

Imine bonds

Schiff's base chemistry is widely used to design cross-linked and self-healing polymers thanks to imine, acylhydrazone or oxime formation. Taking advantage of the reversible acylhydrazone bond, Deng and *al.* reported a self-healing hydrogel which can be turned back into its monomer under acidic conditions.[86] This sol-gel transition can be repeated over many cycles without side reaction. Self-healing could occur autonomously without any external trigger if acetic acid (15% v/v) was added prior to the experiment. Chen and *al*. designed another hydrogel but dynamic over a large range of pH, from pH 3 to 9.[87] The idea was to use two orthogonal chemistries, first the acylhydrazone formation, dynamic at low pH, and the thiol-disulfide exchange, which is dynamic under basic conditions. Furthermore, the disulfides could be reduced into thiols by adding dithiothreitol, leading to the depolymerization of the network; and oxidized back with H_2O_2 to re-form a gel. At neutral pH, all the exchange reactions were kinetically blocked but catalytic amounts of aniline

31

allowed the gel to be dynamic again. Schubert and *al.* synthesised in bulk a polymeric network using a methacrylate cross-linker containing an acylhydrazone group and hydroxyethyl methacrylate as one of the comonomers.[88] Cracks could be healed at 100 °C, which can be explained by two mechanisms. On one hand, water can cleave the acylhydrazone bonds leading o free aldehydes and hydrazides, which can react with each other again. However, according to solid state NMR and FT-IR measurements, no change could be observed in the molecular structure of the polymer network at high temperatures. On the other hand, a direct metathesis reaction between acylhydrazones bonds may also explain the observed results.

Liu and *al.* reported an oxime-based polyurethane, which was synthesized at room temperature from multifunctional isocyanates and oximes (**Figure 1.11**).[89] The elastomer is reprocessable at 120 °C for 30 minutes, and recovers almost entirely its tensile properties, whereas conventional polyurethanes need to reach 220 °C to do so, or the presence of a catalyst. In comparison with alcohols, oximes lead to more dynamic systems. Indeed, the presence of the nitrogen atom assists the intramolecular hydrogen transfer, weakening the C(O)-O bond. The relaxation process involves a dissociative transcarbamoylation, in which urethane bond dissociates and re associates.

Zhang and *al.* reported a self-healing PDMS elastomer using a amino functionalized PDMS and a triformylbenzene as a dynamic cross-linker.[90] The network has the same healing efficiency when immersed in water as in air, showing that atmospheric moisture is sufficient to drive the dynamic reaction.
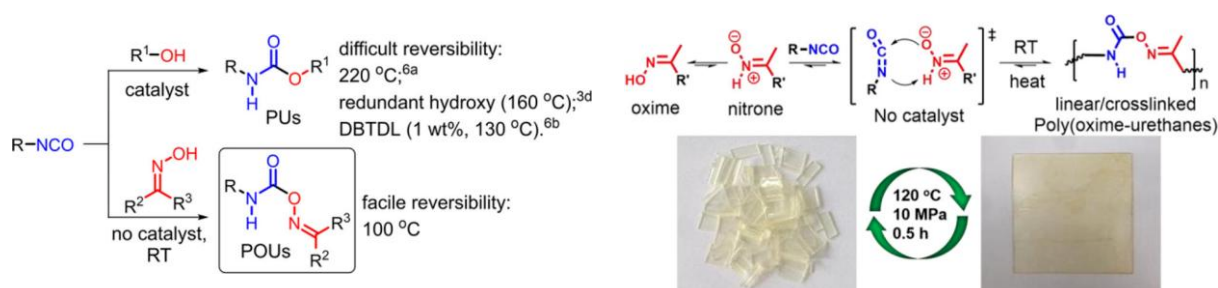
**Figure 1.11.** Left: Synthesis and dynamic nature of conventional polyurethane (PU) and oxime based PU. Right: Mechanism of dynamic reaction between oxime and an isocyanate leading to the reprocessability of the network.[89]

Taynton and *al.* formed a network using a difunctional aldehyde, di- and trivalent amines, which were simply mixed in an organic solvent that was evaporated after the completion of

the reaction.[91] Imine formation and consumption of the aldehydes were confirmed by FT-IR. The T_g and Young's modulus at room temperature were estimated to be around 56 °C and 1 GPa. Thermo-mechanical properties were studied, the material could relax faster when temperature increased, for instance 90% of stresses were relaxed within 30 min at 80 °C, while it would take 480 days at 25 °C. As a consequence, the polyamines network could be reprocessed at 80 °C for 45 min, transforming a yellow powder into a rigid orange disc. In comparison, the reshaping at 25 °C was not possible. Interestingly, when water was added, the network became recyclable even at room temperature. Tensile properties were quite identical before and after recycling for hot processed samples. The presence of water accelerated the relaxation process in such a way that it was faster at room temperature than in dry conditions at 127 °C. Even though the reprocessing was harder without water, it could still be achieved at high temperatures. The exchange reaction can occur through two distinct and potentially simultaneous mechanisms. On one hand, the easier processing with water reflects the partial hydrolysis of imines to generate free amines and aldehydes that can subsequently react again with other partners. On the other hand, the polymer is still dynamic at high temperatures without added water, thanks to transimination of imines in the presence of free amines. Looking into the same exchange reaction, Lei and *al*. paid attention to the exchange between two aromatic imines (benzylideneaniline and N-(4-methylbenzey-lidene)-3-chloroaniline) thanks to high-performance liquid chromatography.[92] After 5 min of reaction at room temperature, the two exchange products could be clearly observed and equilibrium was reached after 8h. An aldehyde-functionalized polyacrylate was then cross-linked with an aromatic bisamine. The material could completely relax stresses at 25 °C, as confirmed by stress relaxation experiments and the crossover of G' and G'' around 0.01 rad/s. After 24h of compression moulding at room temperature, the polymer showed a good healing efficiency of 92%. The authors did not demonstrate the absence of residual water or free amines in their system, which could lead to other exchange mechanisms, compared to the above mentioned article. Furthermore, aromatic imines seem to have a different reactivity than aliphatic ones, which allows the exchange reaction to occur at room temperature. Interestingly, similar behaviours were observed for the aromatic disulfides compounds.

More recently, Zheng and *al*. reported a highly stretchable and reprocessable PDMS elastomer formed by a dual network of disulfide and imines bonds.[93] The latter acts like a semi-permament network, while the former is a sacrificial network. At room temperature, the system could be reshaped after 4 hours under press and showed good recyclability and high

energy dissipation, even though the hysteresis decreased by a factor 2 after a recycling cycle. If the material was degraded by the addition of an acid, an aldehyde or a strong nucleophile, the mechanism of the exchange reactions was not investigated.

Boron based moieties

The boron-oxygen bond is a very versatile bond that permits exchange reactions. Boronic acids can condense with diols to yield boronic esters whose stability depends on the structure of the boronic acid and of the diols. Summerlin and *al.* synthesized a boronic ester based network through photoinitated thiol-ene coupling.[94] The polymer whose T_g was below room temperature, showed a consequent water uptake, 9% over two months, further demonstrated by the decrease of water contact angle measurements over time. Self-healing between two dry pieces at high temperature did not occur at all, while adding few drops of water before putting the cut surfaces in contact resulted in merging almost completely the pieces into a new one after four days. The wetting led to hydrolysis of boronic esters present at the surface. The diols and boronic hence formed can then recombine with each other forming new bridges and finally achieving self-healing at room temperature. This highly dynamic system was prone to creep when exposed to wet conditions, preventing further applications. Zuo and *al.* demonstrated on a similar system that the self-healing could be obtained after 30 minutes without any addition of water.[95] They claimed that the atmospheric humidity was sufficient to hydrolyse boronic ester bonds, promoting reconnections between free boronic acids and diols. With small amounts of water added prior to self-healing, the pieces could be merged within only 10 min. Nevertheless, the mechanical properties were too low for the considered applications. To overcome this issue, a permanent cross-linker and 10 wt% of nanosilica were incorporated. Material crept less while keeping its self-healing property.

Another way to play with B-O bonds is to form boroxine through direct condensation of boronic acids. Lai and coworkers prepared a polymer via amidification between 4-carboxyphenyl boronic acid and telechelic amines from PDMS (H_2N-PDMS-NH_2).[96] After removal of the water, the boroxine network was formed at high temperature, resulting in a stiff and strong polymer, with a Young's modulus of *ca.* 182 MPa and a low elongation at break (less than 10%). These characteristics reflect a limited molecular segment mobility, which also prevents the network to self-heal. Water addition was required to achieve such property. Even so the material stays quite nonhygroscopic and stable under moist conditions. The healing mechanism was not investigated, on contrary to Guan and Ogden's work

(**Figure 1.12**).[97] Models studies on boroxines were conducted first, an activation energy of 82 kJ/mol was measured for these model reactions. A stiff material was then obtained from bis-boronic acid by heating at 80 °C for 12h under high vacuum. Stress relaxation experiments gave relaxation times which followed Arrhenius law with an activation energy of 80 kJ/mol, comparable to the model reaction. The amount of remaining boronic acid was quantified from methanolysis, which generates different quantity of water whether it is a boronic acid (two molecules of water are released) or boroxine (only one is released then). Methanolysis indicated that the network contained more than 89% of boroxines. The residual water and boronic acid promoted the exchange reaction, allowing recycling by compression moulding at 80 °C. Depolymerization in boiling water was achieved to reach the initial monomer as clean as originally according to ^{1}H NMR.
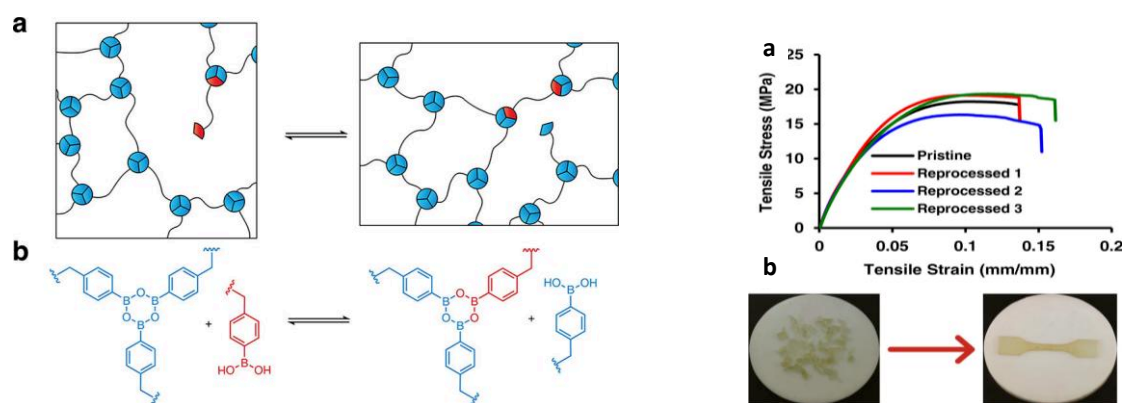
Figure 1.12. Left: (a) Malleable boroxine networks. (b) boroxine exchange mechanism. Right: (a) Tensile properties and reprocessability. (b) Images of cut and reprocessed samples.[97]

Dative bond between nitrogen and boron can be strong enough to obtain a dynamic network as reported by Brook[98] and Sun[99] with PDMS and PPG, respectively. In the first study, two complementary PDMS were used: one with a 5-membered boronic ester and another with pendant amines. Once mixed in bulk, a gel is formed without the need to use a solvent or a catalyst. This network exhibited good solvent resistance at room temperature. Decross-linking, and thus reprocessability, were achieved by heating at 60 °C, or by adding an excess of butylamine as a competing monofunctional Lewis base. However, the mechanical properties were not reported because they were too weak for an elastomer.

Alkoxyamine exchange

Yuan and coworkers designed a thermally reversible polyurethane network using alkoxyamine cross-linkers (**Figure 1.13**).[100] A material that could be cross-linked and

uncross-linked at 80 °C was obtained by mixing PEG, triisocyanate and a diol containing an alkoxyamine moiety. To avoid oxidation, the reprocessing had to be conducted under argon atmosphere. Yet, even under these conditions the self-healing efficiency was not higher than 70%, whereas stress and elongation at break decreased over the recycling cycles. To overcome this shortcoming, an alkoxyamine bearing a nitrile group was synthesized in order to reduce the homolysis temperature and make the elastomer ($T_g = 12$ °C) oxygen insensitive at the same time. As a consequence, the material was healed successfully at 25 °C in air.[101]
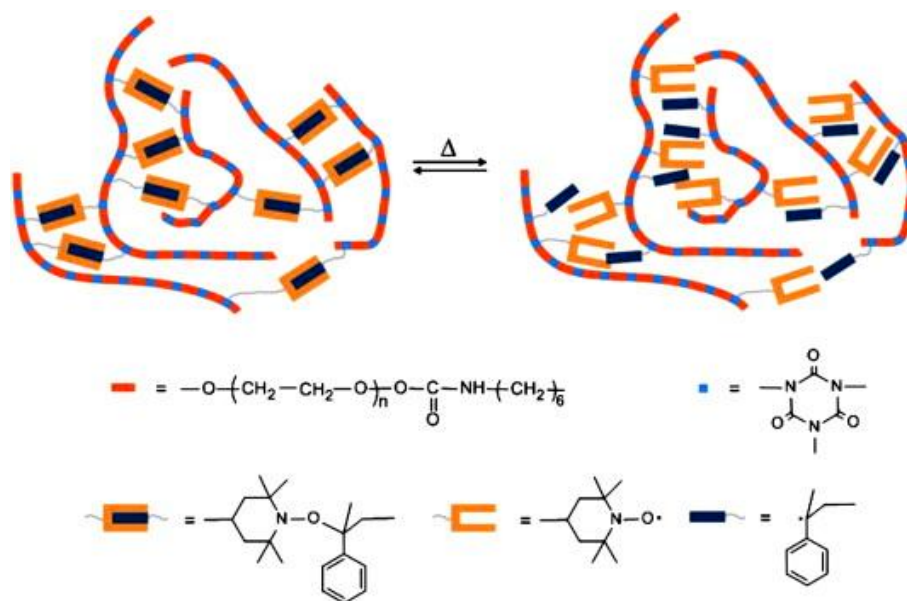
Figure 1.13. Healing mechanism of polyurethane corsslinked by alkoxyamines.[100]

C-C cleavage

Using the homolytic cleavage of C-C bond of diarylbenzofuranone, Otsuka and *al*.[102] reported a self-healing polyurethane (**Scheme 1.7**). The diarylbenzofuranone C-C bond was dynamic enough to allow rearrangement of the network at room temperature and fast self-healing at 50 °C via partial de-cross-linking permit. As a consequence, the material was prone to creep at 25 °C, limiting the potential applications. Brook and *al*.[103] reported stimuli responsive polysiloxanes, modified with coumarin groups, which can generate both physical cross-links, by polar interactions, and covalent cross-links, via a [2+2] cycloaddition under UV light. The material could be partially de-cross-link through the retro-cycloaddition, allowing the fine tuning of the elastic modulus.
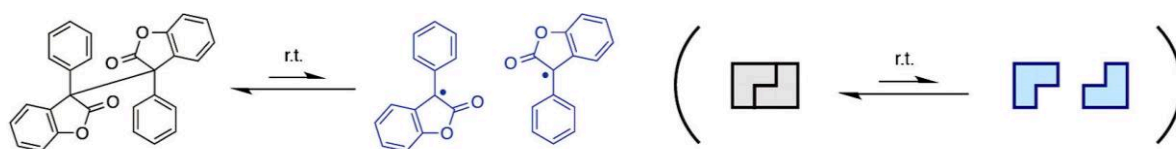
Scheme 1.7. Equilibrium between diarylbibenzofuranone and the corresponding radicals at room temperature.[102]

Reversible urea bonds

Urea bonds can be reversible at high temperature.[104] Fu and *al*. took advantage of this property to design a healable poly(oxime-urethane) elastomer.[105] Above 80 °C, the oxime carbamate bond was able to dissociate to reform the starting isocyanate and oxime monomers. The material exhibited excellent healing efficiencies, around 100%, after 2h at 100 °C or 30 min at 110 °C. Due to the displacement of the thermodynamic equilibrium, the material flowed like a viscous liquid when the healing time was too long. Thanks to the quantitative healing, the high stresses at break (12 MPa) and elongation at break (800%) were totally recovered after recycling. The major drawback of this system is the need for a thermal treatment after healing. Indeed, the material had to be annealed at 60 °C for 24 hours after healing in order to reform the polymer netywork. Cheng and *al*. reported a catalyst free polyurethane with autonomous repairing at moderated temperatures.[106] Incorporating a hindered amine made the urea bond reversible even at room temperature. However, this material needed to be cured at 37°C for 12 hours to reach good self-healing efficiency (ca. 87%).

Numerous dissociative links are suitable to design self-healing and reprocessable cross-linked materials. Nonetheless, these systems face some limitations. They either creep at service temperature or need external trigger, such as heat, UV irradiation or addition of small molecules, to become reversible. Moreover, the decrease of the cross-linking degree results in an uncontrolled flow which requires the use of moulds in order to repare the systems. Finally, the decrease of the cross-linking density at high tempertaure, for example, leads to a decrease of the sovent resistance of such systems. A solution to address these shortcomings is to design networks incorporating dynamic links operating via an associative mechanism.

1.2.2.2 Associative systems

In associative systems, the nature of the bonds involved in the reaction does not change during the exchange reaction. For instance, during a transesterification, products and reactants are both composed of an ester and an alcohol. As a consequence, the thermodynamic equilibrium of such reaction equals one at any temperature and the rate constant of the forward and backward reactions are identical. Therefore, varying the temperature only increases the dynamics of the systems but does not affect the connectivity of the system nor its chemical composition.

Siloxane exchange reactions

Reconsidering a prediction made in 1954 by Grubb and *al*.[107,108] McCarthy and *al*. reported a dynamic polysiloxane network relying on siloxane anionic equilibration (**Figure 1.14**).[109] The network contained reactive tetramethylammonium dimethylsilanolates end groups that can react with cross-links via an associative mechanism, or form cyclic oligomers. As a consequence, the material could be healed or even remolded into different shapes by heating at 90 °C for 24 hours. The dynamic of this system can be turned off by heating at 150 °C, which liberates triethylamine and desactivates the anionic end groups. The addition of basic or acid catalysts could potentially convert silicone elastomers into dynamic recyclable materials. Yet, the formation of volatile cyclic monomers during network rearrangements could limit the applicability of such systems.
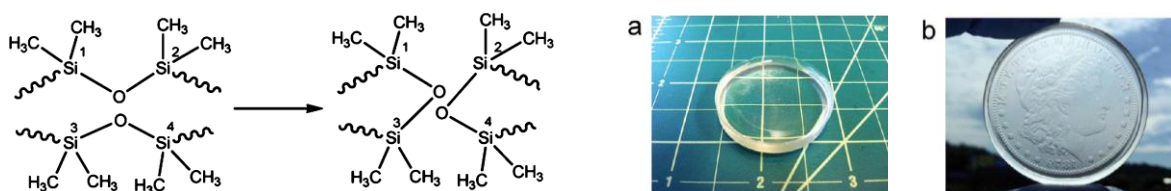
Figure 1.14. Left: Siloxane exchange. Right: (a) Disc-shape sample and (b) remolded with a silver dollar. [109]

Back to sulphur based bonds

Bowman and *al*. synthesized a photo cross-linkable elastomer, with a T_g around -25 °C, through the ring opening polymerization of a cyclic allyl sulfide monomer.[110] After the polymerization, the residual photoinitiator could be used to generate radicals (upon exposure to light) that would react onto the vinyl bonds through reversible addition-fragmentation chain transfer. The associative mechanism does not change the chemistry of the system nor the

cross-linking degree while allowing stress relaxation and so multiple changes of shape. Even so the reshuffling of this network is limited by the initial amount of photoiniator, and by the termination reactions that decrease the quantity of radicals over time and generate permanent static cross-links. Following a conceptually similar approach, Matyjaszewski and *al.* copolymerized methyl methacrylate and *n*-butyl acrylate with a trithiocarbonate based cross-linker.[111,112] Upon UV light exposure, specific C-S bonds could be cleaved homolytically and the resulting radicals involved in a reversible addition-fragmentation chain transfer. Self-healing was proved to occur both in solution and in bulk, but nitrogen atmosphere was required. Klumperman, Goossens and *al.* reported a self-healing network based on the disulfide-thiol exchange reaction.[113] The polymer could be repaired after one day at room temperature, but oxygen was pointed out to increase the cross-linking density through the coupling of free thiols into disulfides (thereby decreasing the number of exchangeable thiol groups). Oxidation of free thiols is an important drawback of this chemistry.

Imbernon and *al.* introduced disulfide bonds into epoxidized natural rubber (**Figure 1.15**).[114] Cross-linking was achieved via epoxy ring opening with a dicarboxylic acid containing a disulfide. The elastomer was creep resistant until 100 °C. At 180 °C, the material could creep enough to be reshaped by compression moulding for 40 min. The mechanical properties were affected by the process. After a single recycling step, only 50% and 80% of the stress and strain at break were recovered, respectively. Side reactions prevented the elastomer to fully relax stresses. Creep experiments showed an increase of viscosity from 150 °C to 180 °C, due to the appearance of static cross-links. Nevertheless, pieces of rubber could be welded together showing good adhesion compared to model systems that did not contain disulfide bonds.
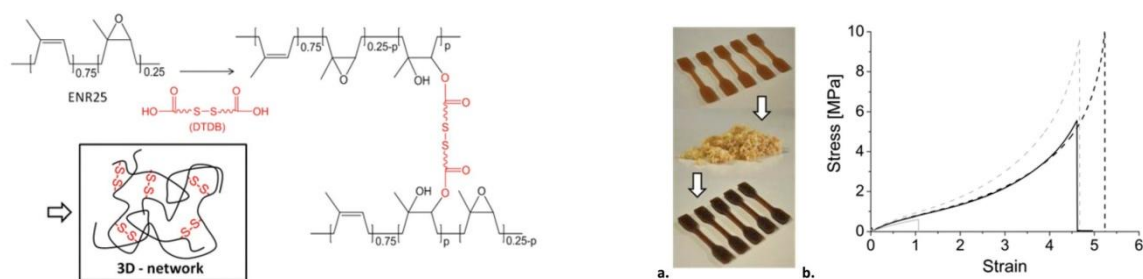

Figure 1.15. Left side: Cross-linking of epoxidized natural rubber by dicarboxylic acid containing disulfide bonds. Right side: Reprocessing of materials by compression moulding at 180 °C. Black: dynamic material, dashed lines: before re-processing, solid line: after re-processing, Grey: control material.[114]

Imines

Debnath and *al*. used exchangeable hydrazide Michael adduct to create a self-healable and recyclable network at room temperature.[115] Because of the high glass transition temperature (67 °C), the polymer had to be softened in THF/H$_2$O before being reprocessed by compression moulding for 48h at room temperature. The exchange reaction is the trans-hydrazide Michael addition, which occurs at room temperature and has an activation energy of 86 kJ/mol for model compounds. A higher activation energy, 109.5 kJ/mol, was obtained from stress relaxations experiment conducted on the network. The high polarity of these groups make them incompatible with non-polar materials. The low thermal stability of this network, degradation starts as from 170 °C, caused by the sensitive beta-keto esters is a considerable drawback.

Brook and *al*. made a dynamic PDMS-based network using terephthalaldehyde and PDMS carrying amino pendant groups.[116] The material exhibited good self-healing properties after 24 hours at room temperature, as stress and elongation at break were fully recovered. Investigating the mechanism of the exchange reaction by size exclusion chromatography (SEC), they concluded that aldehyde would cleave randomly the polymer resulting in a progressive decrease of the molecular weight. Adding amines leaded to a chain depolymerization process. For hydrolysis, it was observed that if the silicone content was sufficiently high, this reaction could be avoided even at 120 °C in pressurized water. The role of water is still unclear especially for the aldehyde-imine exchange. Is a direct exchange between these two species possible or is water mandatory to allow this exchange to occur ? It remains an open question.

Feng and *al*. reported also a PDMS based on the imine exchange reaction (**Figure 1.16**), but a low activation energy was found, 23.5 kJ/mol, as compared to others values reported in literature.[117] This may be explained by traces of water or amines.
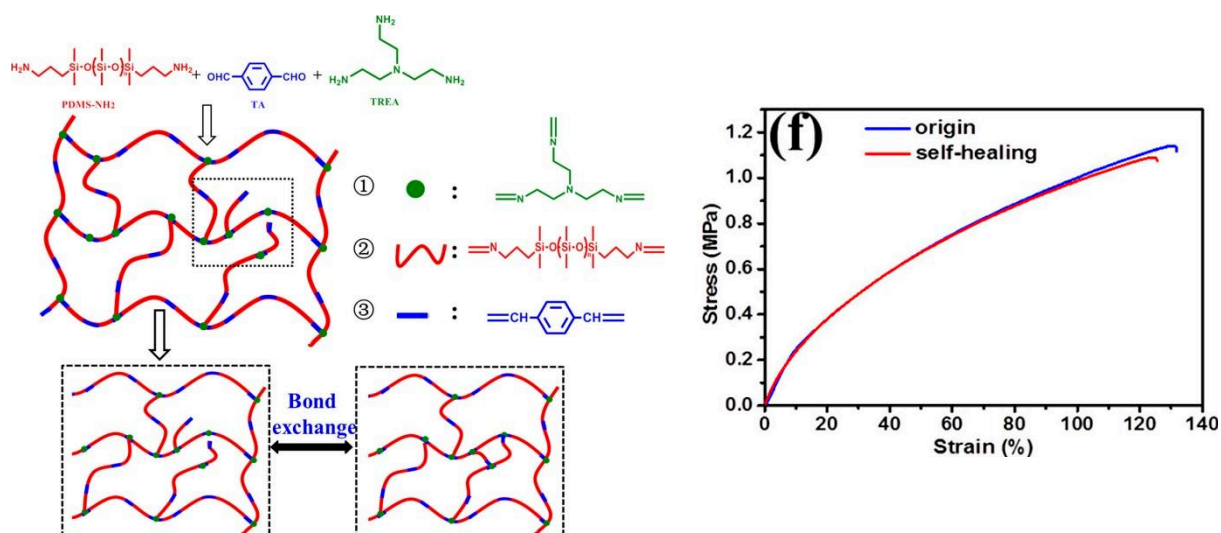
Figure 1.16. Left: Synthetic protocol and mechanism of the dynamic cross-linked PDMS network. Right: Tensile test before and after healing test. [117]

Boronic esters

Guan and coworkers reported a malleable and self-healing material obtained from a polymer carrying diols moieties and a diboronic ester cross-linker (**Figure 1.17**).[118] Tuning the design of the cross-linker resulted in different speeds of exchange reactions. Tertiary amine substituted arylboronic ester exchanged five orders of magnitude faster than the un-substituted arylboronic ester. According to the authors, the nitrogen atom of the aminomethyl group could act as a base to facilitate the proton transfer during the transesterification. A diol containing polymer was synthesized through ring-opening metathesis polymerization then cross-linked in toluene with a difunctional boronic ester. From frequency sweeps, the gel with the aminobased cross-linker was observed to relax two orders of magnitude faster than it amino free counterpart, which is consistent with the model reaction study. The two materials were dried and shaped by compression moulding to investigate their self-healing properties. The fast exchangeable boronic ester showed good healability, while the slow network exhibited minimal healing, very close to the control non dynamic material. After multiple recycling at 80 °C, the samples maintained their mechanical properties. One issue with this chemistry could be the hydrolytic stability of boronic ester linkages. However, after one night of immersion in water, no mass change nor mechanical degradation were observed on the elastomers. No additional experiments were conducted to further investigate the water

stability of these networks. The ability of this elastomer to complexy relax stress was not tested. Stress relaxation experiments were stopped after 20 min, before complete relaxation.
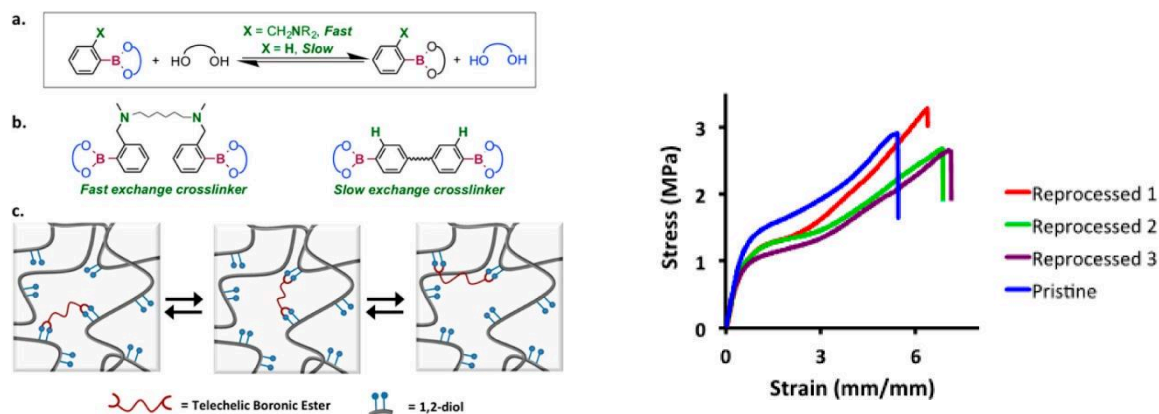

Figure 1.17. Top left: Chemical structure of boronic esters used as cross-linkers. Bottom left: Schematic view of dynamic exchange of borornic esters through transesterification. Right: Tensile properties of pristine material and reprocessed up to three times. [118]

1.2.2.3 Vitrimers

Thermosets possess excellent stability against solvents and temperature making them irreplaceable for highly demanding applications. Yet, thermosets are not healable and recyclable. Vitrimers are a novel class of cross-linked polymers. Vitrimers are cross-linked with dynamic bonds that exchange via an associative mechanism, which provides them with a constant number of links at any temperatures. As a consequence, the material exhibits insolubility and glass-like behaviour at elevated temperatures. Thermoplastics show a sharp decrease of viscosity above their thermal transition temperature, which is useful for injection or blow moulding, but makes it challenging to weld without mold or assemble high complex structures. On the contrary, the viscosity of vitrimers follows an Arrhenius dependence with temperature, resulting in a fully malleable material over a wide range of temperature. Leibler and coworkers introduced the concept of vitrimers in 2011, using the well-known transesterification reaction to transform epoxy/acid and epoxy/anhydride networks into vitrimers (**Figure 1.18**).[119] A material that did not flow or creep at room temperature but could be reshaped via compression moulding within three mintutes at 240 °C without affecting its mechanical properties was reported for example. This processability is made possible by the transesterification occuring between β-hydroxy esters, which allows a fast

topological rearrangement of the cross-links at high temperature. Similar to the glass transition, the material is frozen below its typical thermal transition, called T_v. Above this temperature, the material may flow following an Arrhenius-like dependance, as seen from creep-recovery and stress relaxation experiments.
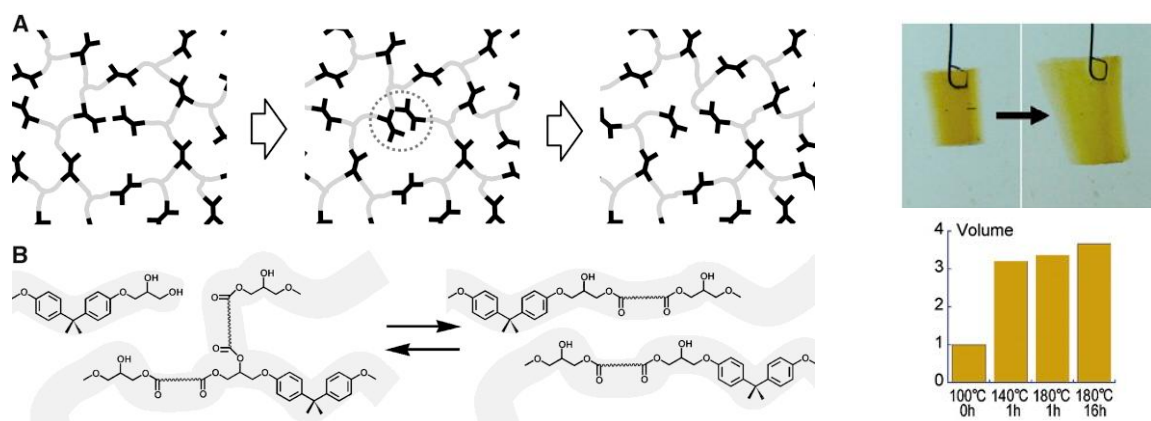
Figure 1.18. Left: Topological rearrangement via transesterification reactions keeping the number of cross-links constant at any temperature and any time. Right: Swelling behaviour in trichlorobenzene at different times and temperatures of β-hydroxy esters vitrimers.[119]

A typical feature of vitrimers is their ability to entirely relax stress above both T_v and T_g, proving that absence of permanent static cross-links that could prevent recycling. The material is easily malleable juste like silica. Changing the amount and the nature of the catalyst, is a way to tune the topological transition temperature of epoxy-based vitrimers opening new possibilities for practical applications.[120] For instance, with 10 mol% of zinc acetate, the system exhibited a T_v of 75 °C. As a consequence, this system did not creep at 70 °C over two hours, while it flowed at 150 °C (**Figure 1.19**). As the amount of catalyst increased the T_v decreased. Using the same reaction of transesterification, a polylactide vitrimer was synthesized with a different catalyst, $Sn(Oct)_2$.[121] It exhibited very short relaxation times, such as 50 s at 140 °C, and recovered most of its mechanical properties after compression moulding.
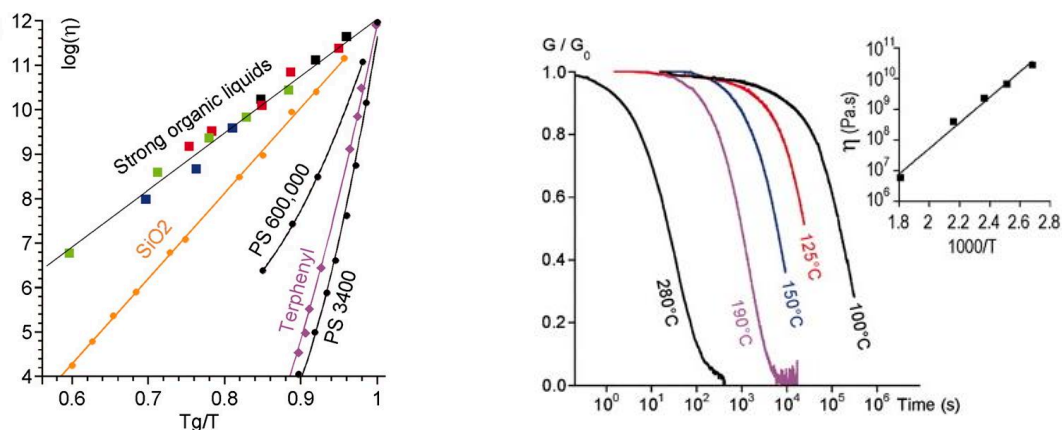
Figure 1.19. Left: Angell fragility plot showing viscosity as a function of inverse temperature normalized by the glass transition temperature. Right: Normalized stress relaxation and the corresponding zero-shear viscosities of β-hydroxy esters vitrimers at different temperatures.[119]

In order to extend the scope of application of vitrimers, different dynamic exchange chemistries have been used. Cis-1,4-polybutadiene was cross-linked with 1 mol% of benzoyl peroxide and then transformed into a vitrimer via the incorporation of Grubbs' second generation Ru catalyst (**Figure 1.20**).[122] The material was dissolved in DCM with 1 mol% of benzyl peroxide and dried at room temperature. The mixture was heated at 100 °C to obtain a cross-linked network. Afterwards, the polybutadiene was swollen in a solution of Grubbs' catalyst and the solvent was evaporated. To get a control sample, the incorporated catalyst was desactivated by adding an excess of vinyl ether and then washed out with DCM. The presence of Grubbs'catalyst enables the topological rearrangement of the cross-links via olefin metathesis and thus the relaxation of stresses. As a consequence, the elastomer could creep over time, in contrast with the control sample, and creep was faster as the amount of catalyst increased. The dynamic network showed swelling ratios and insoluble factions closed to the control samples proving its cross-linked nature. However, the fact that the material creeps at 25 °C, the cost and stability of the catalyst over ageing, limit the potential applications of this strategy.
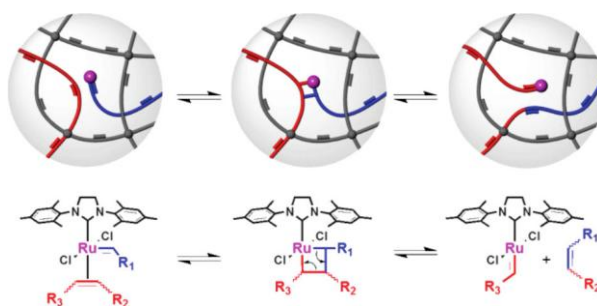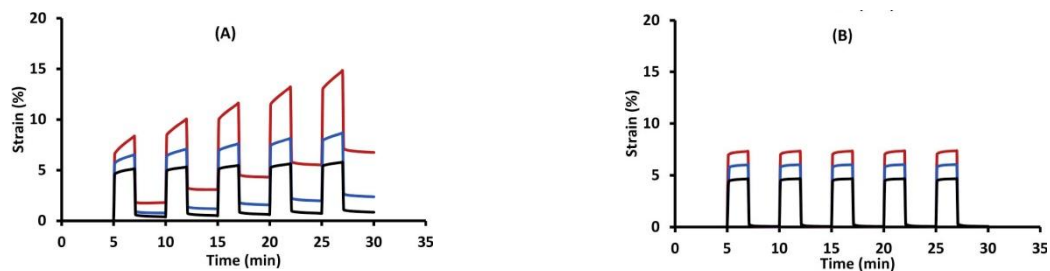
Figure 1.20. Top: Schematic of Grubbs' catalyst mediated olefin-exchange in polybutadiene matrix. Bottom left: Increasing creep of vitrimers with catalyst loading. Bottom right: Control networks.[122]

Drockenmuller and *al*. showed that dynamic covalent C-N bonds can be used to form ion-conducting and recyclable vitrimers.[123,124] After mixing the two azide-alkyne and dibromohexane monomers, the mixture was cured at 110 °C for 48 hours, using a solvent and catalyst free approach. The ionic network exhibited a glass transition temperature of -11 °C, a rubbery plateau at 10 MPa, and a T_v of 98 °C. Below this transition, the material behaves as a conventional elastomer, while at higher temperature it completely relaxes stresses and can be reprocessed. This large difference between the high viscosities at service temperature and the low ones at processing temperature is due to the high activation energy of the exchange reaction, around 140 kJ/mol. Interestingly, the authors suggested two different mechanisms for this dynamic reaction: one is a concerted nucleophilic substitution and the other assumes that the *N*-alkylation of 1,2,3-triazole is a dissociative reaction. If a plateau regime is observed in DMA between 50 and 170 °C, the storage modulus drastically dropped above 170 °C, leading to think that the second mechanism is involved. However, the polymer still followed Arrhenius-like behaviour below 170 °C. As a conclusion, the authors thought that the viscoelastic characteristics of vitrimers may be reached with non strictly associative exchange reactions.[125]

Du Prez, Winne and *al*. developed a similar strategy with the transalkylation of trialkylsulfonium salts.[126] A kinetic study between model compounds was conducted and allowed determining an activation energy of 108 kJ/mol by ^{13}C NMR. The network was formed between multifunctional thiols, dienes and alkylating agent through a thiol-ene radical photopolymerization, and then cured at 140 °C for 90 min. Stress relaxation experiments gave an activation energy very close to the one extracted from the model reactions, and a T_v around 65 °C, while T_g remained below room temperature. The material could be reprocessed many times with identical macroscopic properties.

Du Prez, Winne and *al.* prepared a catalyst free vitrimer (**Figure 1.21**).[127] As amides are more stable than esters, they are less reactive than esters for dynamic reactions, which typically require highly active catalysts. To overcome this problem, amides can be converted into vinylogous amides or urethanes. Kinetic studies on model vinylogous urethane molecules showed a fast exchange and the stability of the products. The reaction had an activation energy of 60 kJ/mol, which is 20 kJ/mol lower than the transesterification reaction catalyzed by $Zn(OAc)_2$ or $Sn(Oct)_2$.[119,121] The network was obtained in bulk from commercially available products, but required more than 24 hours at 90 °C to reach a complete monomers conversion. DMA analysis confirmed the elastic behaviour of the network. Indeed, above its relatively high T_g, 87 °C, a 10 MPa plateau could be observed. The network could rearrange its topology at high temperatures, with relaxation times as short as 85 s at 170 °C, thanks to the fast dynamic of the transamination of vinylogous urethanes. The same activation energy of 60 kJ/mol was calculated from stress relaxation experiments as for the model compounds. No change of the material properties, such as T_g, E', tan δ or soluble fractions, was observed after recycling by grinding and compression moulding, further proving the stability and the dynamic nature of the material. The necessary presence of free amines in this system may be an issue. Their high nucleophilicity can lead to side reactions that can for example generate permanent static cross-links. This work was further applied to composites by pre impregnating fibers with a solution of monomers and curing the mixture.[128] Thermoforming, good thermal fusion of multiple layers as well as depolymerization of the network were successfully conducted.
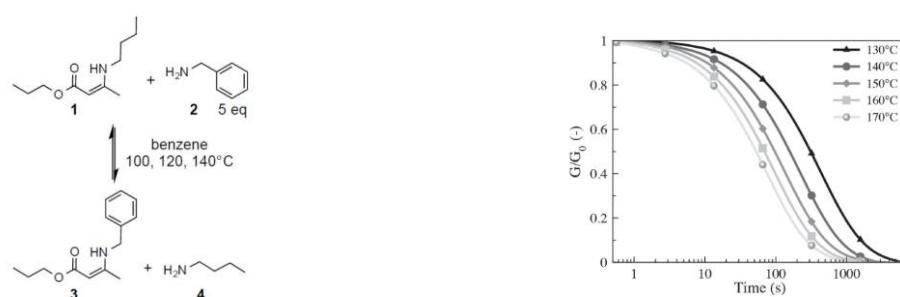
Figure 1.21. Left: Exchange reaction of model compounds for kinetic studies. Right: Normalized stress relaxation at different temperatures.[127]

Polydimethylsiloxanes were also transformed into vitrimers thanks to the amine-vinylogous urethane exchange reaction.[129] PDMS copolymers with amino side groups were dissolved in THF with a bis-vinylogous urethane, leading after 16h at 100 °C to polymer networks. The material could be reshaped at 90 °C for 3h, with compression data similar before and after recycling. It could relax 99% of stress within 10^4 s, but a remaining stress was observed due

to static cross-links. Inherent cross-linking of the crude material containing pendant amine was observed at 100 °C, even in the absence of any other chemicals. Free amines were thought to be involved in this process, further illustrating the propention of this group to generate side reactions.

Nicolaÿ, Leibler and coworkers found out a novel exchange reaction, the direct metathesis between two dioxaborolanes, that once implemented in polystyrene, polymethylmetacrylate or polyethylene transformed these materials into vitrimers (**Figure 1.22**).[130] Thanks to the high rate of exchange of the reaction at 170 °C or 200 °C, usual industrial processing techniques, such as extrusion or injection moulding, were used for the synthesis or processing of the vitrimers. Insoluble materials with creep and stress cracking resistance greatly improved as compared to their thermoplastic counterparts were prepared this way.
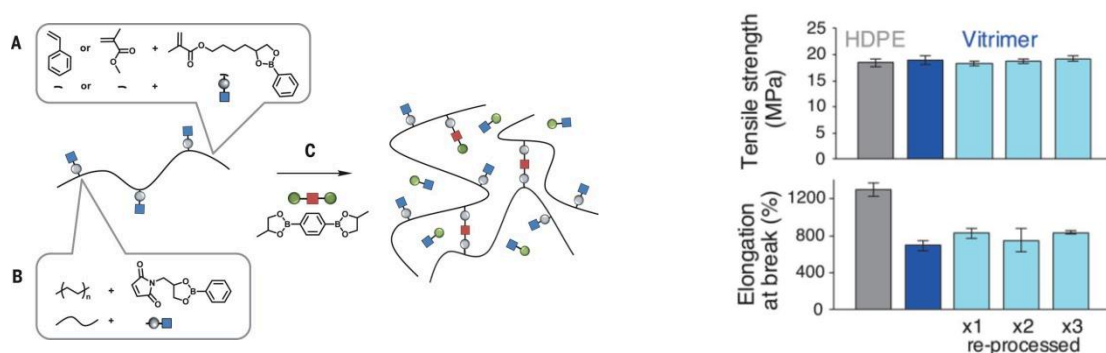
Figure 1.22. Left: Synthesis of vitrimers from thermoplastics. Right: Tensile properties of HDPE (gray), HDPE vitrimer (blue) and recycled HDPE vitrimer.[130]

Dichtel and *al*. reported reprocessable polyhydroxyurethanes (PHU) using the disulfide exchange reaction.[131] The material could be reshaped after 30 min at 150 °C, while showing identical rubbery storage modulus and same tan δ curve after recycling. Nevertheless, tensile strength could not be fully recovered with only 65% of the initial measurement.

Inspired by reversible reaction between an amine and a thiol,[132] Ishibashi and Kalow [133] aim to convert silicone elastomers into vitrimers thanks to addition of thiols onto a Meldrum's acid (**Scheme 1.8**). This reaction does not require any catalyst. Nevertheless, Meldrum's acid can decompose and permanently cross-link the material. After 16h at 100 °C, a 5% change is observed in the integration of S-CH$_3$ protons versus an internal standard, showing the potential stability issues of this system.
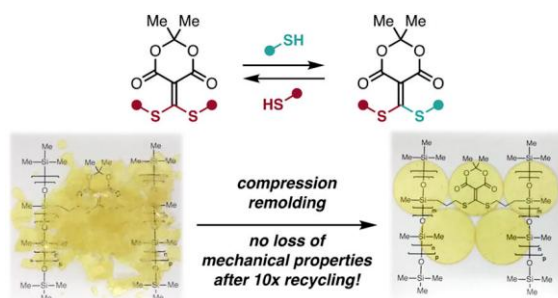
Scheme 1.8. Reversible addition of alkyl thiols enables vitrimer synthesis.[133]

Interestingly, it was observed that if more than 5 mol% of the cross-linker is added, the elastomer becomes brittle at room temperature, meaning that the glass transition is above 20 °C. With 2 mol% of cross-linker, the T_g of the elastomer remained below – 100 °C. A major drawback of this method is the experimental set up: cross-linker and PDMS are stirred 30 min in xylenes at 120 °C, then cured 14h at 120 °C and finally the solvent is evaporated under vacuum for 2h. It is a too long process for any possible applications. Furthermore, dangerous and extremely ill-smelling methanethiols are degassed during the process. Unfortunately, dissolution tests are not reported, not probing the stability of the network in good solvents. HPLC experiments on model small molecules gave access to the activation energy of the exchange reaction, *ca.* 90 kJ/mol, which is quite high compared to others. According to stress relaxation experiments, the stresses are not relaxed at 25 °C but are at 120 °C. A deep creep investigation should confirm this behaviour. Moreover, final relaxation is not shown, as the experiments were stopped when G/G_0 equals to 1/e. Therefore, it is not possible to affirm that the elastomeric material entirely relaxes stress, proving that side reaction generating permanent cross-links did not occur during the synthesis. DMA and stress-strain experiments after 10 recycle cycles show the reprocessability of the PDMS vitrimer, even if the strain at break (10%) is extremely low for an elastomer. Fortunately, the activation energy is high enough to prevent the PDMS to creep at room temperature.

More recently, Averous and coworkers made a worth reported contribution with the synthesis of a fully bio-based vitrimer.[134] 2,5-Furandicarboxaldehyde and di- or trimeric amines, all bio-based monomers, were mixed at room temperature, then solvent casted and cured 1h at 120 °C to obtain a dark elastomeric network. An activation energy of 64 kJ/mol was determined from stress relaxation experiments, which is consistent with literature data on polyimines. However, as the exchange reaction is still activate at room temperature, the system creeps at service temperature, preventing its use in common applications.

1.3 Different pathways to graft onto rubbers

In order to prepare elastomers, it is necessary to find a chemistry that allows cross-linking of the low T_g thermoplastic precursors while modifying as little as possible their properties, such as their high molecular weight, very low glass transition temperature, the strain induced crystallisation, etc. As presented in the introduction, elastomers are mostly composed of dienes, *e.g.* polyisoprene and polybutadiene, which are difficult to functionalize. In the frame of vitrimer synthesis, the chemical modification has to be highly efficient, to permit the grafting of the exchangeable part of the cross-linker, and compatible with the dynamic chemistry responsible for the specific properties of vitrimers. Therefore, efficiency and selectivity are two important characteristics for the grafting chemistry of vitrimers.

This subchapter will only present the grafting onto natural and synthetic polyisoprene, rubber, and on polybutadiene and its copolymers, like styrene butadiene rubber (**Scheme 1.9**).
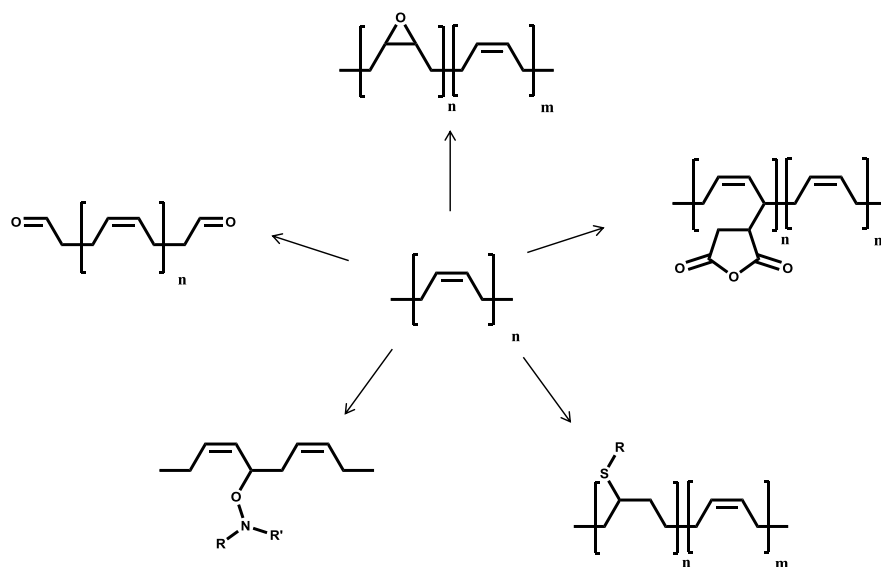
Scheme 1.9. Main routes to functionalization of polybutadienes and copolymers.

1.3.1 Epoxidation

Polydienes possess carbon-carbon double bonds that can be epoxidized by reaction with peracids, such as peroxybenzoic or peracetic acids. [135,136] The reaction is prone to induce side reactions, such as epoxyde ring opening through the attack of carboxylic acids. To prevent these undesired reactions, the epoxidation must be carried out carefully, with a precise control of the temperature and concentration of peracids. [137–139] Usually, the peracid is formed in situ by adding hydrogen peroxide and carboxylic acid. This method allows all degrees of epoxidation to be reached.

Epoxidation is a random process, as proved by Davey and Loadman through combination of titration methods with infrared spectroscopy and DSC analysis. [140] ^{13}C NMR confirmed this result showing that epoxidation reaction has a random distribution, regarless of the process; in homogeneous solution or in latex particles. [141] Performic acid can also be used as oxidizing agent. However, due to its high acidity, the formed oxiranes can be ring-opened to yield glycol, which can lead to cross-linking through ester linkages. [142]
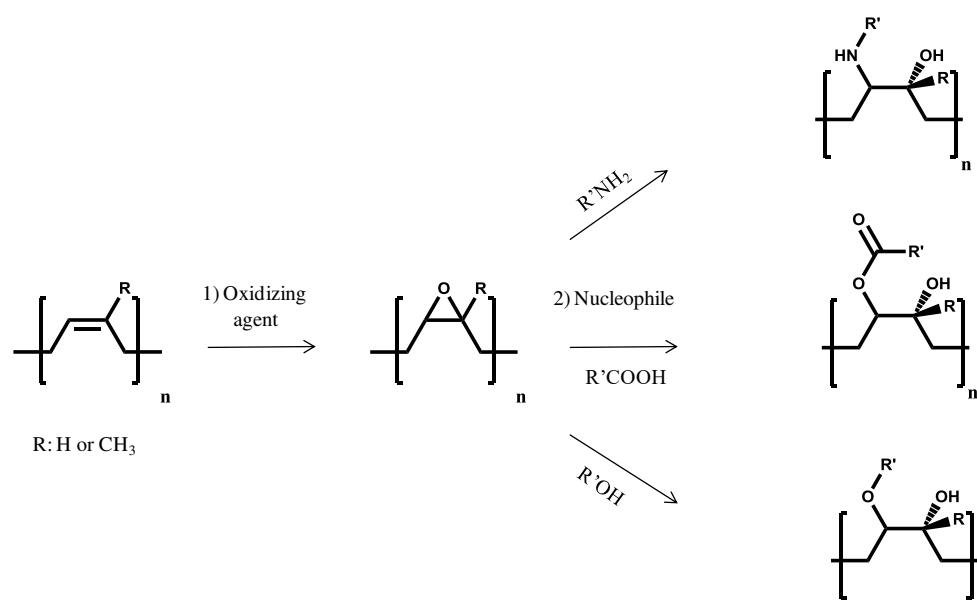
Scheme 1.10. Epoxidation followed by further functionalization of polydienes.

Interestingly, selective conversion of polyutadiene double bonds in copolymers can be done with *t*-BuOOH and metal systems, but this method is very sensitive to oxygen and humidity. [143] Bates and *al*. presented a new method to selectively epoxidize isoprene units, while the vinyl units from butadiene monomer do not react, and only half of the 1,4-butadiene units are epoxidized. [144] Instead of peroxyacid, a dimethyldioxirane is formed in situ from

acetone and potassium monopersulfate at 0 °C. The reaction is let heat up to room temperature and stirred for 18h, before extraction and precipitation in methanol. Lucki and *al*. reported the oxidation of 1,2-polybutadienes by molecular oxygen, singlet oxygen and ozone by UV and infrared spectroscopy. Cross-linking was observed in all cases. [145]

Zuchowska reported that the reactivity of polybutadienes towards epoxidation is very dependent on the microstructure of the polydiene.[146] In 1,2-polybutadiene, the trans units are more reactive than the cis ones, and vice-versa for the 1,4-polybutadiene. Furthermore, vinyl bonds are always less prone to epoxidation than double bonds from the main chain. All these differences may be due to different chain conformations. This was confirmed by Wang and *al*. who used H_2O_2 as oxidant and ammonium tungstate hydrate and phosphoric acid a co-catalysts, to prevent sides reactions and gelation at high epoxidation levels.[147]

Once the polydiene is epoxidized, the epoxy ring can be opened by common nucleophilic species, such as amines, acids or alcohols (**Scheme 1.10**).[148]

Cross-linking can occur with primary amines, which can react with two equivalents of epoxide, but cyclization products can be also obtained with high epoxy contents, as demonstrated by Perera.[149] In this study, it was confirmed that the conversion of opened epoxide, calculated from the intensity of the oxirane hydrogen peak, was higher than the nitrogen content at high conversion. This was further confirmed by gel content values around 20%.

Brosse and *al*. reported the modification of epoxidized polydienes through the study of model reactions with benzoic acid.[150] The influence of the temperature, concentration, solvent, carboxylic acids, and catalyst was investigated. It was showed that high concentrations combined with polar solvent and basic catalyst such as dimethylformamide and pyridine accelerate the reaction. At temperatures above 130 °C, the yield reached 70%. However, if dimethylformamide dissolve the model compounds, it is a bad solvent for polydienes, which prevents its use for this reaction.

Another strategy was used to functionalize epoxidized polybutadiene.[151] After the epoxidation with meta-chloroperoxybenzoic acid, epoxy ring were opened with HCl, and the obtained alcohols were further reacted with sulfonyl isocyanate. The overall process, which is composed of three successive reactions, gave a global yield superior to 90%, and all the reactions were conducted at room temperature and for less than four hours.

Pire and *al*. cross-linked epoxidized natural rubber with dodecanoic diacids (DA). Optimizing the ratio between DA and epoxy sites, very high strain (650%) and stress at break (5MPa) could be obtained.[152] A good compromise was reached because on the one hand, this cross-linking process creates covalent ester bonds that show a good stability, while on the other hand, the use of long diacids with 12 carbons provides flexibility and low steric hindrance. The resulting DA-cross-linked ENR showed good ageing resistance and fatigue properties. Very interestingly, the reaction was conducted in bulk with a pre-mixing step followed by the curing under press at 180 °C, simulating industrial conditions. Curing was completed within less than 30 minutes thanks to the addition of 1,2-dimethylimidazole.This base acts as an accelerator for the epoxy reaction through activation of DA by quantitative formation of the corresponding imidazolium salt. After the reaction, 1,2-dimethylimidazole is deprotonated by the alcoholate. This salt is soluble in ENR and ensures the good dispersion of the curing agent in the rubber matrix. The mechanism of the reaction was studied by solid-state NMR spectroscopy, confirming the formation of β-hydroxy esters along the chains.[153] The imidazolium dicarboxylate preferentially opens the epoxy at the less substituted side which is consistent with a mechanism associated to basic conditions. Furthermore, it could be shown that 1,2-dimethylimidazole-induced acceleration of the cross-linking process reduces secondary reactions that are otherwise favoured by long curing times. Thermal stability and fatigue experiments showed that this system offers a good compromise between the properties obtained with standard sulphur- or peroxide cross-linked samples, making this new vulcanisation process really competitive.[154]

Acrylic functions could also be grafted thanks to the reaction of acrylic acid onto epoxide rings.[155,156] The reaction was followed by infrared spectroscopy through the decrease of a band at 870 cm^{-1} associated to the epoxy group, while the methyl group of the isoprene unit was taken at the reference peak at 1357 cm^{-1}. The grafting was completed after 2 hours at 80 °C in toluene or 16 hours at 35 °C. Molecular weights were not affected by the grafting. However, the exact determination of the grafting yield was not reported, especially with NMR, because the disappearance of epoxy may also be caused by side reactions.

If carboxylic acids are commonly used to graft onto epoxidized polydienes,[157–160] sometimes even in combination with diamines,[39] others nucleophilic agents have been considered. Derouet and *al*. investigated the alcoholysis of epoxidized polyisoprene with model molecules and then studied directly on the polymer.[161,162] Mild conditions could be used, such as 25 °C

in chloroform or in bulk, but a catalyst, like cerium ammonium nitrate, is needed. After 72 hours, 88% of the epoxide groups were converted into alkoxylated units. The effect of alcohol substituent was studied and their reactivity was related to their structure. Indeed, electron withdrawing groups decreased the reactivity of the alcohol and thus favoured the rearrangement of epoxy to ketone and allylic alcohol units. A decrease of the number average molar mass, M_n, and an increase of the mass average molar mass, M_w, was observed resulting in an increase of the molecular weight distribution. This is probably a consequence of the combination of main chain cleavage and coupling processes.

Other nucleophiles were grafted onto an epoxidized styrene butadiene block copolymer, 2-mercaptobenzothiazole, 2-mercaptopyridine, *N*-methylpiperazine or acid chlorides in boiling THF, but grafting yields were not reported.[163] A broadening of the GPC peak was observed for all the nucleophiles, while the modification of epoxidized polymer by acid chlorides was free of side reactions.

1.3.2 Oxidative cleavage to yield telechelic oligomers

Another way to incorporate reactive groups is to cleave polymer chains. Photodegradation with hydrogen peroxide, chlorine, or benzophenone,[164,165] ozonolysis[166] and oxidative chemical degradation by periodic acid or cleavage of epoxidized polydienes[167] are suitable methods.

Gillier-Ritoit and *al.* investigated the H_5IO_6 oxidolysis of double bonds in polyisoprene.[168] Two methods were used: epoxidation with meta-chloroperoxybenzoic acid followed by H_5IO_6 cleavage, or the direct oxidation with two equivalents of periodic acid (**Scheme 1.11**). The comparison between these two procedures led the authors to propose a two-step mechanism for the second method. During the first step, one equivalent of periodic acid reacts with the double bond, resulting in an epoxide or alpha-glycol. Then, in the second step, the epoxide or alpha-glycol is cleaved into a ketone and an aldehyde by reacting with another equivalent of periodic acid. This last step is thought to be faster than the first one, because neither epoxide nor glycol could be detected during the course of the reaction.
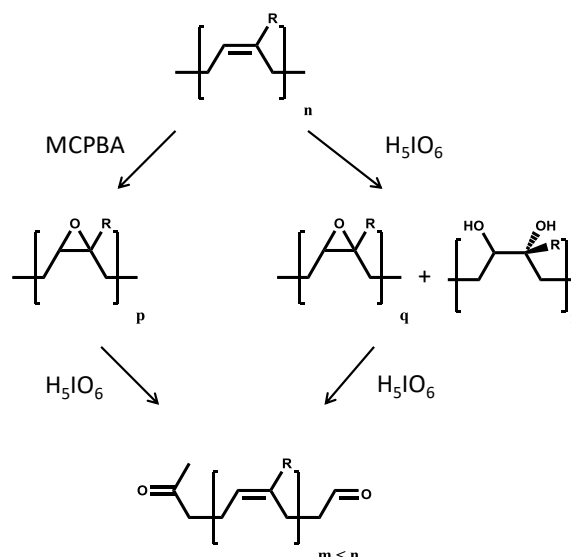
Scheme 1.11. Oxidative routes to obtain carbonyl telechelic polydienes in one pot. Left: Chain cleavage of epoxidized polydienes. Right: Chain cleavage by periodic acid only.

Peruch and *al*. demonstrated that the two step degradation of polybutadiene, *i.e.* epoxidation with meta-chloroperoxybenzoic acid followed by H_5IO_6 addition, gives more controlled molar mass (between 5 000 to 50 000 Da) with lower disperstity (around 1.5) than the direct oxidative cleavage with periodic acid alone.[169] In particular, the direct oxidation cleavage is not suitable to form small telechelic chains of polybutadienes. This is still true for polyisoprene, but to a lesser extent. The authors applied this method to transform cis-1,4-polybutadiene into thermoreversible elastomer through Diels-Alder chemistry.[170,171] The telechelic polybutadiene with aldehyde groups was further functionalized to introduce furan end-groups and cross-linked with a bis-maleimide. Mechanical properties were tuned by varying the amount of cross-linker and the telechelic chain length. In addition, the mechanical properties were fully preserved after five recycling cycles.

1.3.3 Grafting of maleic anhydride derivatives through ene or radical reactions

Polydienes are reactive towards maleic anhydride and its derivatives.[172] They were first used in the 50's to vulcanize unsaturated and saturated polymers.[173] Dimaleimides, such as *N-N'*-m-phenylenedimaledimide, was shown to cross-link natural rubber at 180 °C within 30 minutes in the absence of any other chemical.[174] But the high temperature used led to polymer

degradation and thus poor mechanical properties. The addition of a radical initiator, such as dicumyl peroxide (0.3wt%), to the dimaleimide allowed curing at lower temperature (155 °C), which provided a vulcanised rubber with better properties. Both aliphatic and aromatic dimaleimides gave highly cross-linked natural rubber when peroxides were added. Initiating free radicals abstract an allylic hydrogen from natural rubber to give a free radical on the polymer chain (**Scheme 1.12**). This radical can subsequently react with the carbon-carbon double bond of the dimaleimide. It bears now the free radical which can transfer to another polymer chain. The other carbon-carbon double bonds of the dimaleimide can then react following the same reaction scheme, yielding a cross-linked rubber.
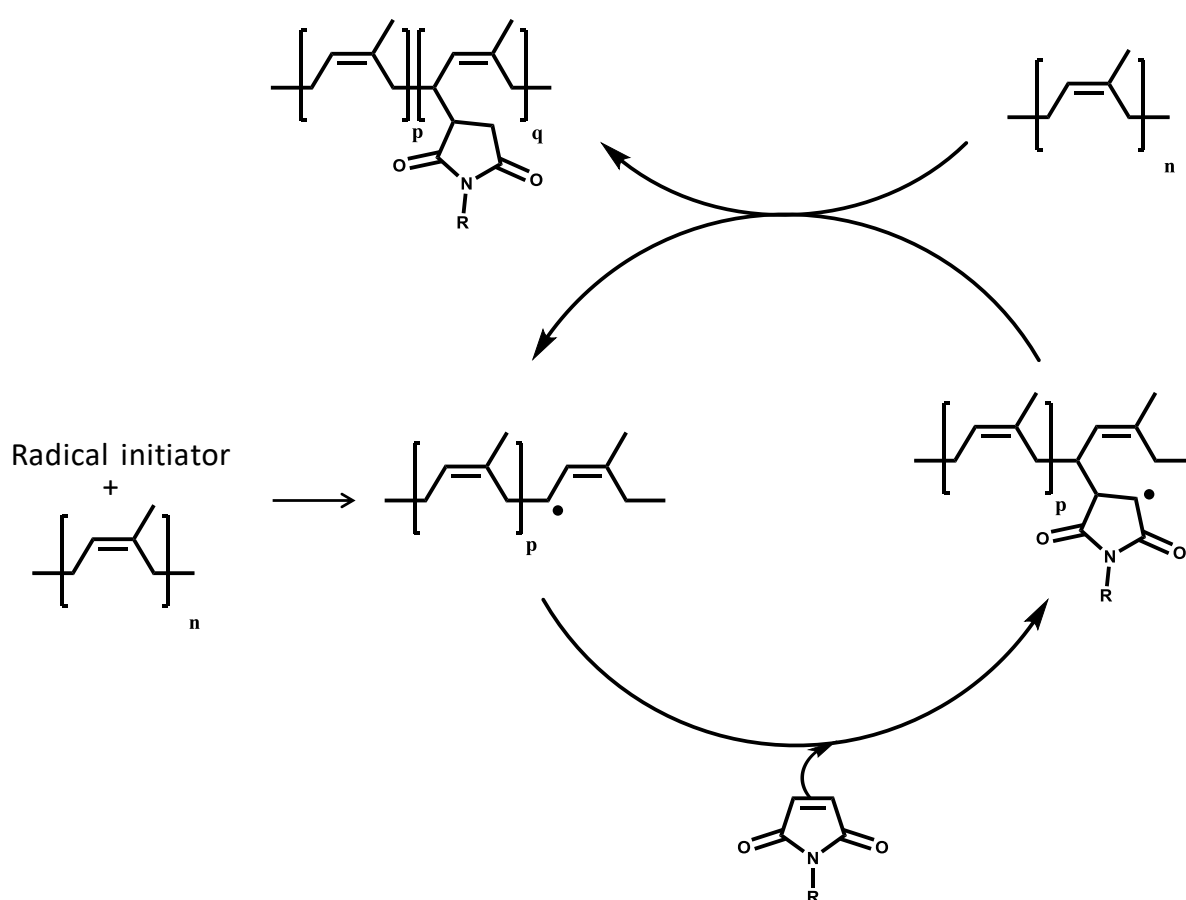
Scheme 1.12. Mechanism of maleimide grafting onto polyisoprene.

Very interestingly, the addition of a monomaleimide, namely *N*-phenylmaleimide, also led to the vulcanisation of natural rubber, but less efficiently. As the first mechanism mentioned above could not explain this result, a second mechanism was proposed. Once the radical is borne by the maleimide, instead of chain-transferring it can also react onto a double bond of the polymer chain or can undergo termination through combination with identical monomaleimide. In both cases, cross-links are produced.

The influence of various parameters on maleic anhydride grafting onto polybutadiene, such as the temperature, nature and concentration of radial initiator, was investigated in toluene.[175] The temperature of the reaction medium had to be kept below 70 °C to prevent cross-linking of polybutadiene. Benzoyl peroxide was observed to be two times more efficient than AIBN, but with a maximum grafting yield of 12%. Molecular weight distribution was not reported, nor the influence of the solvent. When temperatures were too elevated, reaction times too long or peroxide too concentrated, insoluble fractions were observed.[176] Aromatic diamines were added to prevent these cross-linking reactions but the grafting was then lower.[177] Addition of styrene could improve the grafting without affecting the insoluble fraction.[178] Finally dicumyl peroxide was even better than benzoyl peroxide and toluene was proved to be the best solvent to perform the grafting.[179]

Chino and Ashiura modified polyisoprene rubber into maleated polyisoprene through ene chemistry (**Scheme 1.13**).[180] Maleic anhydride was mixed in a kneader with an antioxidant, aromatic oil, xylenes and rubber at 210 °C for 60 min to yield a maximum 75% of grafting. Aromatic oil and xylene should act as activators while the antioxidant should prevent the rubber from being degradated but no information about molecular weight were provided. 3-Amino-1,2,4-triazole was then reacted with the grafted maleic anhydride to form a supramolecular network, tanks to pendant moieties that can be involved into six hydrogen bondings. The conversion of maleic anhydride was not calculated. However, the obtained mechanical properties were comparable to those of sulphur-vulcanized polyisoprene. Furthermore, the material could be reformed up to ten times. The mechanical data were not reported to confirm the good recyclability of this network. The low T_g, of around -61 °C, was conserved through the chemical modification, while a new endothermal peak appeared in DSC at 180 °C. It was attributed to the cleavage of hydrogen bonds, indicating that the recycling required higher temperatures to get a viscosity sufficiently low to enable the reprocessing. However, so elevated temperatures could damage irreversibly polyisoprene whose heat resistance is low.
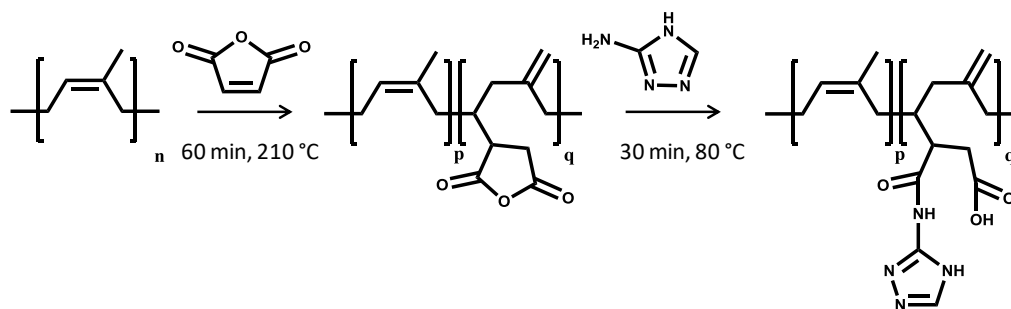
Scheme 1.13. Modification of polyisoprene to graft a hydrogen donor and acceptor moiety.[180]

This strategy was used to graft furan moieties further cross-linked with a dimaleimide,[181] or to create dual-networks with hydrogen bonds, coordination bonds and static covalent bonds in order to enhance cracking resistance through energy dissipation from sacrificial bonds.[182]

Maleic anhydride (MA) is a powerful molecule to functionalize polymers but is well-known to undergo homopolymerization at elevated temperatures. Roover and *al*. observed oligomers of maleic anhydride by SEC after reacting MA with polypropylene with and without peroxides.[183] Such side reactions may increase their local concentrations. They are not necessarily randomly dispersed along polymer chains but instead oligomers of maleic anhydrides are grafted onto the chains, which changes the topology of the modified rubber and could affect its dynamic properties.

1.3.4 Vinyl monomer and nitroxide grafting
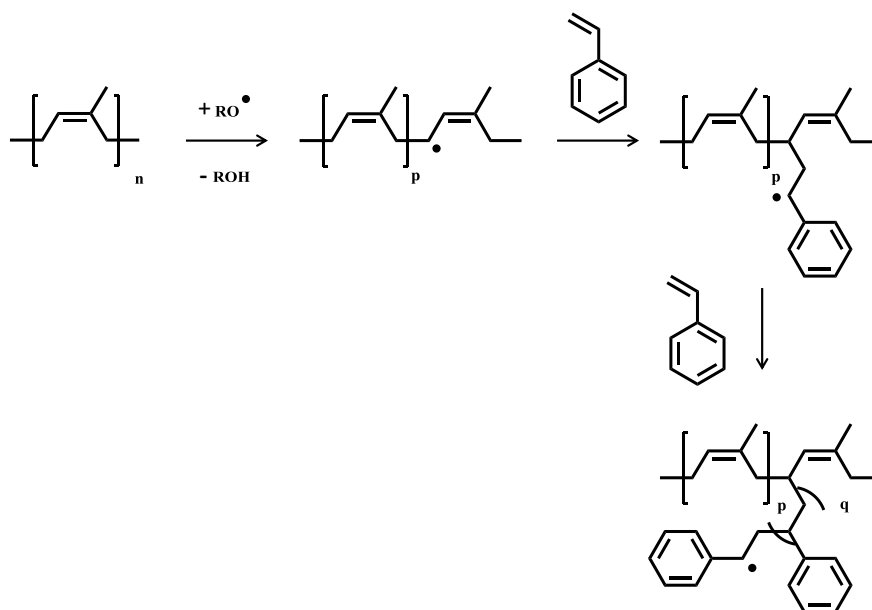
Scheme 1.14. Grafting of styrene on polyisoprene.

57

Many vinyl monomers can be polymerized from polydienes using the "grafting from" method through the abstraction of the allylic hydrogen with radical initiators.[184–189] Bloomfield and *al.* reported the graft polymerization of vinyl monomers onto natural rubber both in solution and in latex (**Scheme 1.14**).[190] Benzoyl peroxide gave better grafting yield than AIBN, for which only 5% of polymerized monomer gave short grafted poly(methyl methacrylate) ($DP_n = 20$) while the rest gave long free polymer chains ($DP_n = 2000$). However, the grafting of styrene improved the tensile strength and rubber grafted with methyl methacrylate presents excellent fatigue resistance. The amount of polystyrene incorporated was independent of the initiator concentration. Interestingly, the growing chain showed no tendency to react with rubber.[191,192] It means that polybutadiene rubber is grafted when attacked by reactive primary radicals formed by the decomposition of the initiator rather than by transfer with the less reactive radicals from growing chains. This was further confirmed by Brydon and *al.*, who also claimed that AIBN produced no graft copolymer at all on polybutadiene.[193] The grafting of side chains of polystyrene was predominant to monomer homopolymerization at lower temperatures (65-85 °C), at higher dilutions, and polymer/monomer ratios. [184,194] According to Kitayama and Vogl, the grafting of a styrene derivative depends on the structure of the polybutadiene.[195] The grafting efficiency reached 56% with 1,2-polybutadiene, while grafting was limited to 14%. with 1,4-polybutadiene
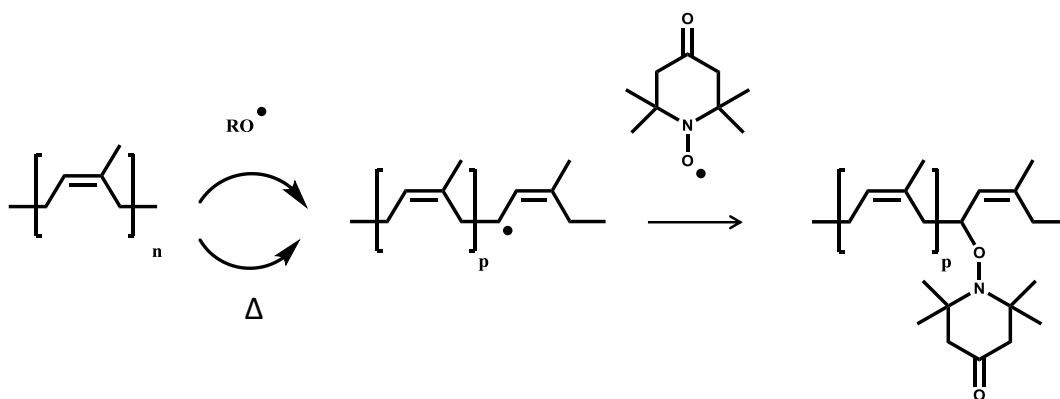
Scheme 1.15. Modification of polyisoprene via the incorporation of alkoxyamine moieties, initiated or not by peroxides or nitroxide itself.

More direct pathways were proposed by Bonilla-Cruz and *al.*[196] The first method used peroxides to generate radicals onto the polymer backbone, which are subsequently trapped by nitroxides to form alkoxyamine links (**Scheme 1.15**). The second approach consists in heating a mixture of nitroxide and polybutadiene, without peroxides. The first method gave a grafting yield of around 58%, while the second approach achieved efficiency between 60 and 70%.

The molecular weight was shifted to higher values matching with the incorporation of nitroxide moiety. In both cases, a shoulder at low elution volume was observed by SEC, which was attributed to branching and minor cross-linking. Light broadening towards lower molecular weight was also observed, which could indicate some chain cleavage because of *β*-scission. Once the alkoxyamine was present on the polybutadiene backbone, homopolymerization was conducted adding maleic anhydride or styrene.[197] The network could be cut into small pieces and reprocessed at 130 °C, or higher temperatures, by compression moulding followed by a cooling step to obtain a recycled material. Storage modulus decreased over recycling meaning the numbers of cross-linking point also dropped.[198]

1.3.5 Catalyst

Many reactions involving catalysts have been reported to functionalize polydienes, including hydroformylation, hydrocarboxylation, aminomethylation, hydrosilylation, oxidation, epoxidation and hydroboration (**Scheme 1.16**). They required expensive and rare catalysts such as rhodium, platinum and palladium.[199,200]
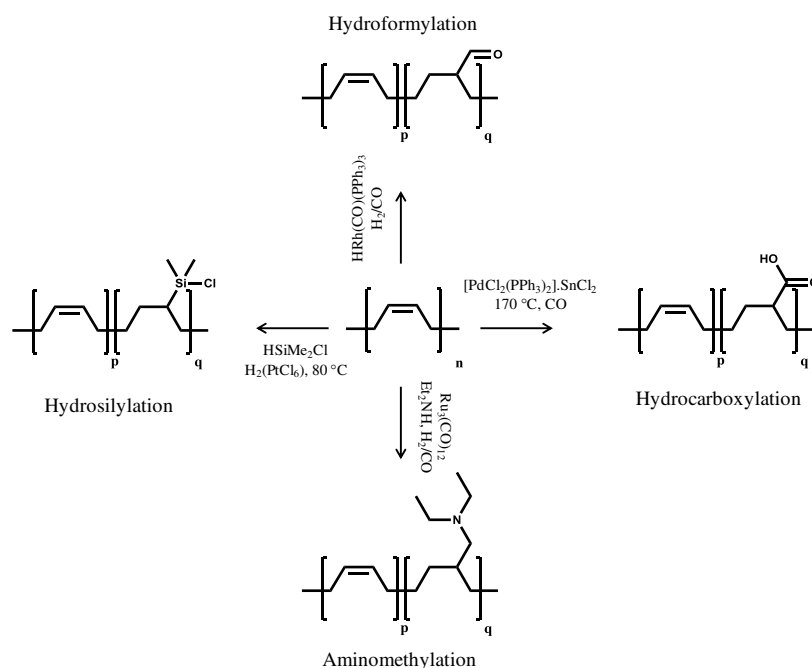
Scheme 1.16. Functionalization of polybutadiene by metal-mediated processes.

1.3.6 Thiol chemistry

One of the most promising chemical routes established to functionalize existing polymers is based on thiol−ene click chemistry,[201–203] which can precisely modify the physical, mechanical, optical, and other key properties of polymers. The reactions between multifunctional monomers and multifunctional thiols are part of attractive and versatile methods that can be used for the preparation of adhesives, sealants and coatings.

1.3.6.1 Thiol-ene click

Thiol-ene polymerizations are reactions between multifunctional thiol and ene (vinyl) monomers, which proceed via a step growth radical addition mechanism. Initiation is achieved through generation of radical centers, using thermal or photo initiators.[204] Thiol-ene addition reaction was discovered in 1905 by Posner, who investigated the kinetics of the reaction and monomer reactivities.[205]

Thiols can readily react with many functional groups, such as carbon-carbon doubles and triple bonds through radical reactions, or epoxides and isocyanates through nucleophilic reactions. Thiol-ene reactivity is well known since 1905.[205] However, thiol reactions have gained significant attention these recent years due to efficiency to functionalize polymers. Indeed, these reactions combined many advantages, including mild reaction conditions, high yields and rapid conversion. Thanks to these characteristics, thiol chemistry belongs to the "click chemistry".

1.3.6.2 Radical thiol-ene

Photopolymerizaion of thiols compounds with carbon-carbon double bonds is very attractive to cure thermosets, obtain homogenous networks, have narrow glass transition.[206–212]Applications range is very wide, from surfaces treatment,[213] lithography, [214] membranes, [215] hydrogels,[216] dental resins, [217]dendrimer synthesis,[214] and linear, branched or star copolymers.[214,218]

In some cases, thiol−ene chemistry has been employed [215,219,220] as an efficient avenue by which to impart additional chemical functionality. It has been remarkably successful in generating polymers with tunable bulk[221] or surface [222] functionalization, as well as

responsive polymers capable of switchable patterns.[223] This kind of post functionaliztion involves polymers with double bonds, especially vinyls one because of their higher reactivity.

Butadiene based polymers have been modified successfully with thiols. Serniuk was the first to report the grafting of alkyls thiols onto 1,2-PB.[224] Boutevin and *al.* reported the radical addition of fluorinated, hydroxylated or phosphorinated thiols onto telechelic polybutadienes.[225–227] A fraction of thiols was grafted on the 1,4 polybutadiene, even if vinyl bonds are more reactive than vinylenes. Schlaad and coworkers studied in details the modification of butadiene copolymers via thiol-ene chemistry.[228–230] Functionalization of hydrophobic copolymers with hydrophilic molecules is used widely for encapsulation. Modification of polymers bearing pendant double bonds away from each other prevent intramolecular cyclization. Hawker and *al.* synthesized styrene, methacrylate and caprolactone based copolymers with pendant vinyl bonds. These polymers were post-modified with thiols to reach high degrees of functionalization, around 99%.[231]
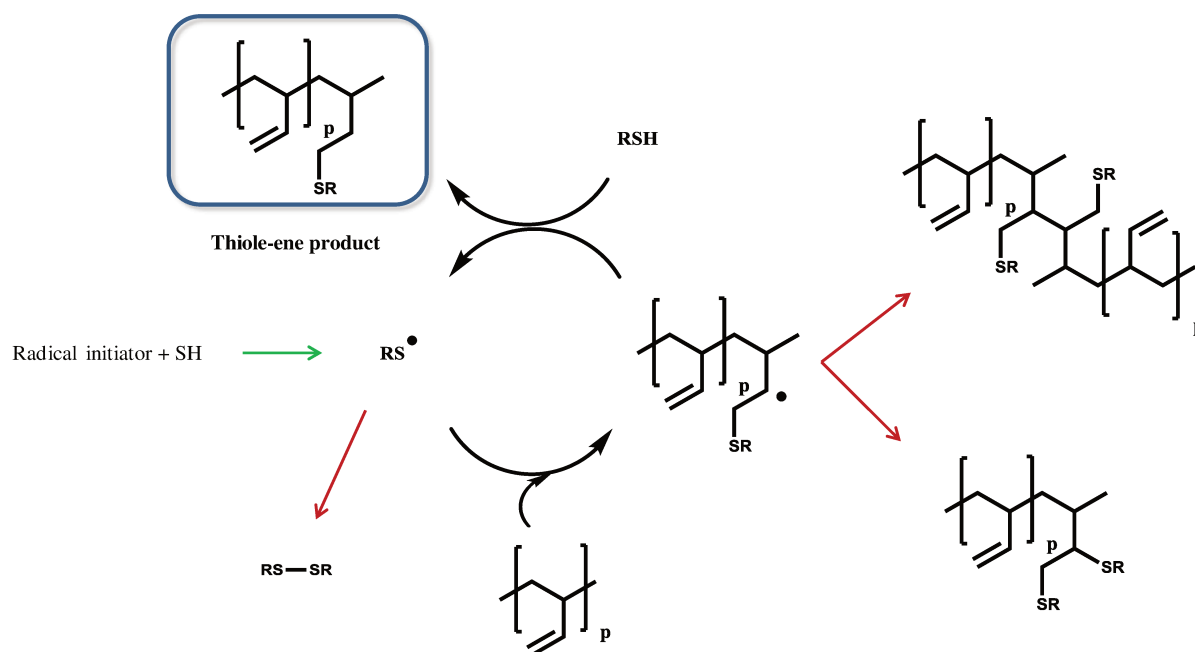
Scheme 1.17. Mechanism for the hydrothiolation of carbon-carbon double bonds of poly(1,2-butadiene) in the presence of a radical initiator. Green arrow: initiation, black arrows : propagation and red arrows : termination.

The general mechanism of thiol-ene chemistry was proposed by Kharasch and *al.*.[232,233] Once photo or thermal initiator is decomposed or excited, the initiator abstracts a hydrogen from a thiol generating a thiyl radical that can propagate, meaning it attacks the double bonds yielding carbon centrered radical (**Scheme 1.17**). This radical may then transfer to a free thiol

producing the copolymer and generating a new thiyl radical, which can propagate again. Radicals are also prone to terminate, by coupling of two thiyl radicals to yield disulphur compounds, by reaction between two carbon radicals, or by recombination involving a thiyl and a carbon radical.

Grafting reactions are often conducted on polybutadiene with high vinyl contents (superior to 80%) in solution using AIBN as a thermal initiator. Thiols are typicallly used in large excess,[234] with a molar ratio thiol/C=C varying between 5 and 40, which allows to functionalize 60 to 80% of the double bonds. Intermolecular cyclization prevents the reaction to reach higher yields.

Interestingly, thiol-ene polymerization can proceed readily even in the absence of initiator. A thiol (pentaerythritol tetrakis(3-mercaptopropionate) was shown to copolymerize with vinyl ether, allyl, acrylate, methacrylate and vinyl benzene monomers.[235] These thiol-ene polymerizations are photoinitiated without any photoinitiator at all. Thiol-vinyl and thiol-allyl polymerizations were shown to be true stoichiometric step-growth reactions, while thiol-acrylate, methacrylate and vinyl benzene polymerizations proceeded via a combination of step growth and vinyl homopolymerization reactions. Commercial SBR could be cross-linked using the thiol-ene click chemistry just by heating up the bulk mixture to 160 °C. [236] The temperature was high enough to generate radicals, leading to the grafting of the thiol.

The reactivity of the thiol-ene reaction depends on the structure of both alkenes and thiols. Vinyls bonds are more reactive than vinylenes bonds. The latter are prone to undergo cis-trans isomerisation and have often a steric hindrance more pronounced than vinyl groups.

Thiol-ene chemistry can be used to functionalize chain-ends to change their properties. Many polyolefins have terminal double bonds that can be used for thiol-ene modification. Polyisobutylene (PIB), polypropylene and polyethylene were modified with many different thiols.[237] Surface tension of PIB could be decreased thanks to the incorporation of a fluorinated thiol. Radical thiol-ene chemistry is widely used to functionalize polymers bearing vinyl double bonds. This versatile chemistry enables to graft many different groups onto these double bonds, very quickly and with high yields. Usually, small molecules are used because the grafting efficiency decreases with the size of the thiol.

1.3.6.3 Nucleophilic thiol-ene
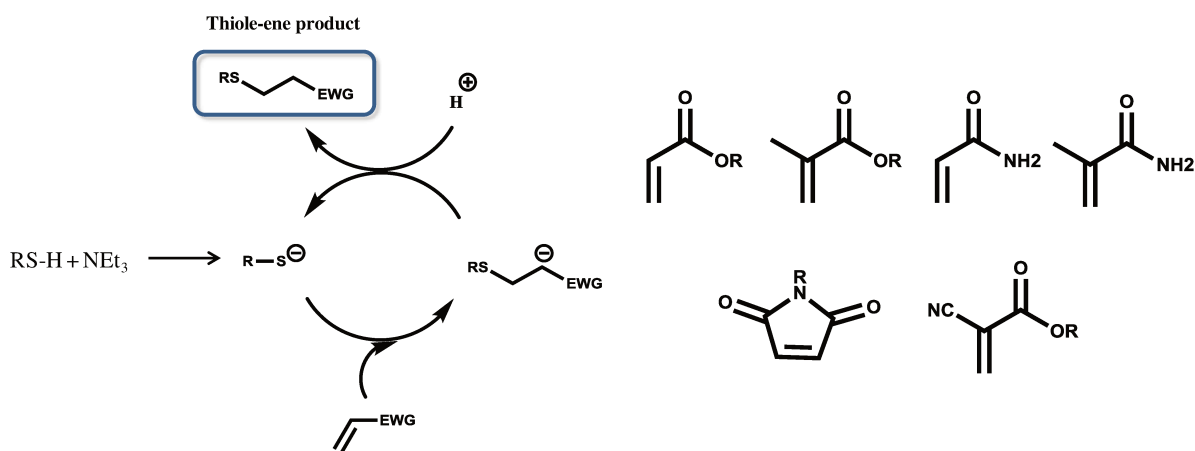
Scheme 1.18. Left: The proposed base-catalyzed mechanism for the hydrothiolation of an activated carbon carbon double bond. **Right:** Examples of activated substrates susceptible to hydrothiolation via a base/nucleophile-mediated process.

When the double bonds are electrophilic, such as (meth)acrylate derivatives, maleimides or fumaric esters, the thiol addition is a nucleophilic addition, known as thio Michael addition (**Scheme 1.18**). The reaction mechanism follows two steps, first thiolate ion is obtained thanks to a base, and then it reacts onto the double bond to yield enolate. Finally, the protonated base or another thiol gives up its labile proton to yield the desired thioester. Interestingly, the thiol deprotonation may be spontaneous when the solvent has dielectric constant high enough, no base is then required. Otherwise, bases such as benzyltrimethylammonium or triethylamine or sodium methoxide are usually employed. In some cases, the base can also attack the double bond to yield the enolate which generates the thiolate ion. Usually conducted at room temperature, the reaction yield depends on solvent polarity, pH, pKa of the base, thiol nucleophilicity and electrophilicity of the double bond.

Moreover, polymers, synthesised by RAFT (reversible addition-fragmentation chain-transfer) polymerization, have a thiocarbonylthio function readily convertible into thiols through aminolysis, for example. These polymers may react with acrylates or maleimides through the thio Michael addition.[238,239]

1.3.7 Others

Alder-ene reaction with triazoline diones

Triazoline diones (TAD) possess a chemical structure similar to maleimides.[240] However, triazoline diones react much faster and have a far higher thermodynamic driving force than maleimides. That is why they can react with much more substrates. The Alder-ene reaction involves an enophile with a carbon-carbon double bond and an ene reactant containing an allylic proton. First described by Alder and *al*. in 1943, this reaction is very similar to the Diels-Alder reaction.[241] Butler and *al*. used this reaction to graft hydrogen bonding moieties onto polydienes (**Scheme 1.19**).[242,243] Polymers and copolymers of 1,3-dienes, both butadiene and isoprene, were modified with triazoline diones. The polymers were dissolved in dry benzene or THF, and 4-phenyl-1,2,4-triazoline-3,5-dione or 4-methyl-1,2,4-triazoline-3,5-dione was added very quickly to the polymer solution at room temperature. The reaction was completed within less than 5 minutes for cis-1,4-polyisoprene, cis and trans polybutadiene and styrene-butadiene copolymers, while it required 1 to 6 hours to functionalize 1,2-polybutadiene and acrylonitrile-butadiene rubber.
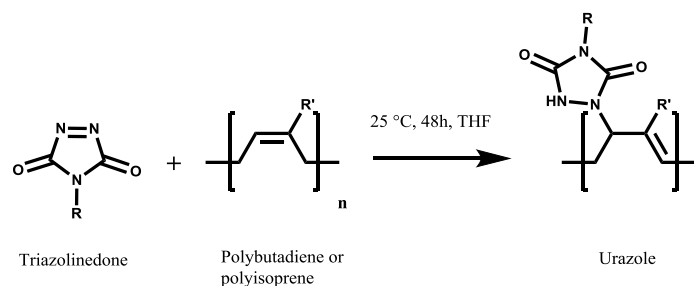
Scheme 1.19. Grafting reaction of triazoline dione onto polybutadiene or polyisoprene.

With feeding ratio of 1 mole of reactant for 1 mole of repeating unit, grafting yields as high as 78 to 93% were obtained after 48h of reaction as indicated by elemental analysis of the nitrogen content in the functionalized polymers. The amount of grafted urazole groups could be tuned at will, but too high incorporation resulted in very important changes of the physicochemical properties of the rubber. Above 10-20 mol% of functionalization, the copolymer started to precipitate out of the reaction medium. The hydrogen bonds formed between the urazole groups and their polarity limit the solubility of the functional polymers. The maximum modification allowed in order to retain thermoplasticity was found to be 7 mol% for cis polyisoprene, and 0.3 mol% for cis and trans polybutadiene. Glass transition was also drastically affected by the triazoline diones incorporation, with an increase of 20 °C with 10 mol% of urazoles for polyisoprene and 1,2-polybutadiene. The decrease of molar

mass observed in GPC in chloroform was attributed to intramolecular hydrogen bonds within polymer chains, through urazole pendant groups, leading to a decrease of the hydrodynamic volume in this non protic solvent and thus a higher retention volume.

As the urazole alone form weak complexes, they are easy to dissociate leading to permanent deformation of the polymer. To address this problem, Hilger and Stadler modified the urazole group attached to polybutadiene. They used an urazole groups that contained carboxylic acid function as a difunctional hydrogen donor and acceptor, in order to form linear supramolecular chains.[244,245] As a consequence, the grafted copolymer showed equivalent elastomeric properties to thermoplastic elastomers.

A different urazole, 5-urazoylisophtahalic acid, was grafted onto polybutadienes to obtain TPEs with melting temperatures ranging from 130 °C to 190 °C, depending on the functionalization degree..[246] Excellent mechanical properties were achieved, with stress at break between 2 and 6 MPa and strain at break around 1000%. However, for temperatures above 150 °C, irreversible cross-linking occurred, preventing the polymer from reprocessing.

Cross metathesis functionalization

Another interesting approach to functionalize rubber is to use the cross metathesis reaction. Ying and *al*. reacted cis-2-buten-1,4-diol based chain transfer agents containing –Si(OEt)$_3$ or –SiMe$_3$ functionalities with poly(cis-1,4-butadiene) to yield telechelic polybutadienes.[247] Because direct cross metathesis of polybutadiene with the targeted molecule is not efficient, the crude polybutadiene needed first to be activated by Grubbs 2nd generation catalyst in solution over 8 hours (**Scheme 1.20**). Dichloromethane was evaporated and the chain transfert agent was added in bulk to functionalize the polymer for 8h. The conversion was determined by weight differences before and after column chromatography on acidic silica gel and varied from 13.5% to 91.5%, depending on the concentration of catalyst and of the nature of the transfer agent.
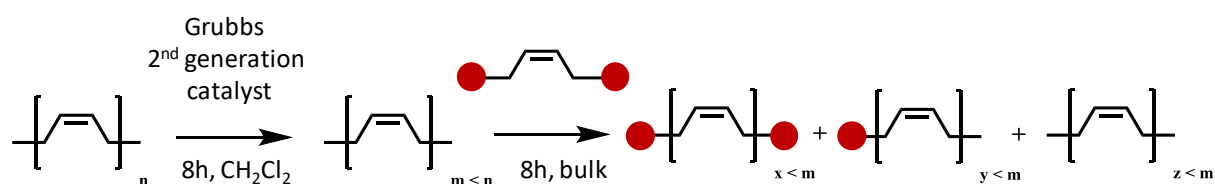

Scheme 1.20. Synthetic scheme for the end-functionalization of polybutadiene through cross metathesis.

This type of functionalization can only be used to attach new groups onto the chain-ends. The number of functions per chain cannot exceed two while to modulate the cross-link density of the future network it is preferable to be able to graft as many cross-links per chain as it is desired. Another limitation comes from the reaction itself. Indeed, cross metathesis leads to a decrease of the molecular weight of the polymer. In the present example, the M_n decreased from 200 000 Da to 28 000 when PB was mixed by Grubbs' catalyst and further decreased to 20 000-2000 Da during the functionalization step. As molecular weight significantly affects the properties of elastomers, such a drastic drop considerably alters the mechanical properties of the polymer. Last but not the least, the reaction requires an expensive catalyst, , which can favour side reactions, and can lead to phase separation, or be released over time. The highest conversation values were obtained for catalyst ratio of 2%, which is not negligible.

Multicomponent reactions

Multicomponent reactions have recently attracted the attention of polymer scientists. Barner-Kowollik and *al*. used a well-known electrophilic multicomponent reaction in order to functionalize a low molecular weight polybutadiene (M_n of 9 200 Da, 23% vinyl and 77% vinylene) with different kind of nucleophilic species (**Scheme 1.21**).[248] For instance, pentafluorobenzoic acid was dissolved in dry THF with polybutadiene and N-bromosuccinimide was added dropwise at 0°C and the reacton was let run during 22 hours. Yields varied a lot depending on the nature of the carboxylic acid.
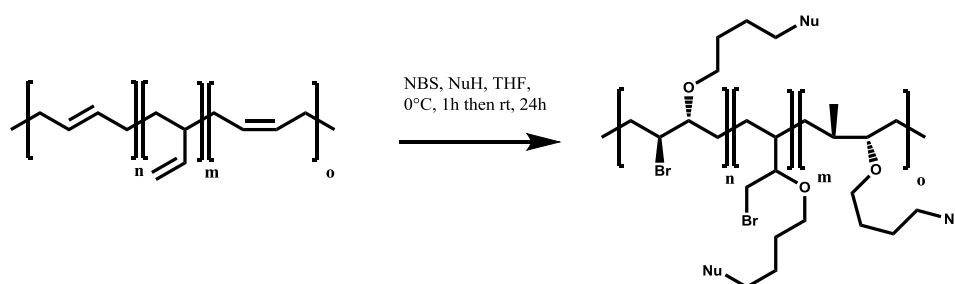
Scheme 1.21. The MCR modification of polybutadiene with a nucleophilic partner.

Even if the grafting yield could reach very high value (from 0 up to 99.5%), the only ratio used between the nucleophile and C=C repeating unit was 1 to 1. No lower targeted functionalization degrees were reported. Furthermore in every case, all the carbon-carbon double bonds disappeared during the reaction, meaning the grafting is not sufficiently selective and lots of side reactions occurred and consumed the dienes. Vinyl and vinylenes

were prone to react in the same manner according to the authors. The nucleophile partner had to be rather acidic; it is the reason why the authors only used carboxylic acids. This reaction led to the bromination of the polybutadiene, which could change the thermal or chemical stability of the material.

Onchoy and *al*. reported the direct electrophilic addition of N-bromosuccinimide onto natural rubber in latex at room temperature, with $FeCl_2$ as a catalyst.[249] The aim of this modification was to enhanced adhesion between rubber and silica filler thanks to hydrogen bonding and polar interactions. An incorporation degree of 2 mol% of bromine was determined according to ^{1}H NMR. However, many characterisations were missing as the molecular weight of the modified polymer, while the grafting yield remained unclear. Usually such reactions are prone to generate cross-linking as side reactions.

Nitrile N-oxides

Takate and *al*. designed a bifunctional nitrile *N*-oxide in order to cross-link natural rubber.[250] The reaction was carried out in toluene at 90 °C over one day. Low feed ratios were used, between 0.1 and 1.0 mol%, which corresponds to 10 and 100 cross-links per chain, respectively. ^{1}H NMR could not detect the signals from the protons of the *N*-oxide due to its very low content. The network with esters groups could be dissolved after immersion in a KOH suspension in $THF/MeOH/H_2O$ mixture. SEC measurements of this solution showed a decrease of the molecular weight by a factor two. No characterization was carried out with mono functional nitrile N-oxide to check the grafting yield and to study the kinetic of the reaction.

1.4. Conclusion

Increasing the part of recycled rubber is mandatory to reach a circular economy. Due to their sulphur or peroxide based cross-linking, elastomers are intrinsically very challenging to recycle regardless of the technique used: thermo-mechanical, microwaves, ultrasounds or chemical. Incineration cannot be considered as a sustainable approach due to the emission of green house gases and production of incinerator bottom ashes as side products, while pyrolysis is highly energy consuming.

Switching from static to dynamic cross-links may be a good solution to address this problem. Dynamic bonds rely on both physical and chemical bonds that possess different advantages and drawbacks. Thermoplastic elastomers are fully reprocessable but their heat resistance is too poor for demanding applications.

A very interesting solution could be to transform classical rubbers, such as polyisoprene and polybutadiene, into vitrimers. This method would keep the major characterics of rubber such as solvent resistance and elasticity, but impart recyclability to them. Many dynamic exchange reactions have been developed last decades, involving C-N, C=N, C-O or S-S dynamic bonds. All these reactions possess specific activation energies and rate constants. These parameters need to be well adapted to vitrimers, which require an associative covalent chemistry that is highly dynamic at processing temperature, while almost frozen at service temperature. Such a fine reaction is not easy to find. Futhermore, the dynamic moieties have to be stable at elevated temperature and not prone to side reactions that would generate static bonds. S-S bonds are already used in conventional curing of rubbers and do not lead to recyclable elastomers. C-N and C=N bonds may give free amines that are sensitive to oxidation and are highly reactive towards many functional groups. C-O bonds have the same problem with alcohols and require very elevated temperature and the presence of a catalyst to accelerate the exchang reaction. Boronic esters are thermally and chemically stables, while B-O bonds are highly dynamic in certain conditions. Therefore, boronic esters can be considered as interesting candidates to transform elastomers into vitrimers.

However, finding a dynamic reaction is not sufficient to reach this objective. Dynamic moieties have to be grafted onto the polydienes to cross-link elastomers as polyisoprene and polybutadiene. Epoxidation is a common way to functionalise polydienes but it requires two steps to introduce the dynamic part. Nitroxide and maleic anhydride derivatives may graft

onto rubbers but they are prone to generate side reactions. Many reactions led to an increase or decrease of the molar mass. Thiol-ene chemistry is an efficient and versatile tool that could be useful for the grafting onto vinyls bonds, but faced some limitations when expose to vinylenes.

Therefore, finding a combination of dynamic exchange reaction and grafting chemistry adapted to transform elastomers into vitrimers is highly challenging.

1.5 References

(1)   Home : PlasticsEurope https://www.plasticseurope.org/en (accessed Jun 11, 2019).

(2)   De Gennes, P.-G. *Scaling Concepts in Polymer Physics*; Cornell university press, 1979.

(3)   Http://Www.Mrepc.Com/Industry/World_production.Php.

(4)   Snoeck, D.; Chapuset, T.; García García, J.; Sfeir, N.; Palu, S. Feasibility of a Guayule Commodity Chain in the Mediterranean Region. *Ind. Crops Prod.* **2015**, *75*, 159–164. https://doi.org/10.1016/j.indcrop.2015.05.008.

(5)   Soratana, K.; Rasutis, D.; Azarabadi, H.; Eranki, P. L.; Landis, A. E. Guayule as an Alternative Source of Natural Rubber: A Comparative Life Cycle Assessment with Hevea and Synthetic Rubber. *J. Clean. Prod.* **2017**, *159*, 271–280. https://doi.org/10.1016/j.jclepro.2017.05.070.

(6)   Goodyear, C. Improvement in India-Rubber Fabrics. US3633A, June 15, 1844.

(7)   Tarachiwin, L.; Sakdapipanich, J.; Ute, K.; Kitayama, T.; Bamba, T.; Fukusaki, E.; Kobayashi, A.; Tanaka, Y. Structural Characterization of α-Terminal Group of Natural Rubber. 1. Decomposition of Branch-Points by Lipase and Phosphatase Treatments. *Biomacromolecules* **2005**, *6* (4), 1851–1857. https://doi.org/10.1021/bm058003x.

(8)   Tanaka, Y. Structural Characterization of Natural Polyisoprenes: Solve the Mystery of Natural Rubber Based on Structural Study. *Rubber Chem. Technol.* **2001**, *74* (3), 355–375. https://doi.org/10.5254/1.3547643.

(9)   Gent, A. N.; Kawahara, S.; Zhao, J. Crystallization and Strength of Natural Rubber and Synthetic Cis-1,4-Polyisoprene. *Rubber Chem. Technol.* **1998**, *71* (4), 668–678. https://doi.org/10.5254/1.3538496.

(10)   Adhikari, B.; De, D.; Maiti, S. Reclamation and Recycling of Waste Rubber. *Prog. Polym. Sci.* **2000**, *25* (7), 909–948. https://doi.org/10.1016/S0079-6700(00)00020-4.

(11)   Imbernon, L.; Norvez, S. From Landfilling to Vitrimer Chemistry in Rubber Life Cycle. *Eur. Polym. J.* **2016**, *82*, 347–376. https://doi.org/10.1016/j.eurpolymj.2016.03.016.

(12)   Cooper, S. L.; Tobolsky, A. V. Properties of Linear Elastomeric Polyurethanes. *J. Appl. Polym. Sci.* **1966**, *10* (12), 1837–1844. https://doi.org/10.1002/app.1966.070101204.

(13)   Leibler, L. Theory of Microphase Separation in Block Copolymers. *Macromolecules* **1980**, *13* (6), 1602–1617. https://doi.org/10.1021/ma60078a047.

(14)   Mai, Y.; Eisenberg, A. Self-Assembly of Block Copolymers. *Chem. Soc. Rev.* **2012**, *41* (18), 5969–5985. https://doi.org/10.1039/C2CS35115C.

(15)   Lelah, M. D.; Cooper, S. L. *Polyurethanes in Medicine*; 19860000.

(16)   Woods, G.; Imperial Chemical Industries, L. *The ICI Polyurethanes Book*; 19870000.

(17)   Drobny, J. G. *Handbook of Thermoplastic Elastomers*; Elsevier, 2014.

(18)   Sánchez–Adsuar, M. S.; Papon, E.; Villenave, J.-J. Influence of the Prepolymerization on the Properties of Thermoplastic Polyurethane Elastomers. Part II. Relationship between the Prepolymer and Polyurethane Properties. *J. Appl. Polym. Sci.* **2000**, *76* (10), 1602–1607. https://doi.org/10.1002/(SICI)1097-4628(20000606)76:10<1602::AID-APP16>3.0.CO;2-K.

(19)   Sánchez–Adsuar, M. S.; Papon, E.; Villenave, J.-J. Influence of the Prepolymerization on the Properties of Thermoplastic Polyurethane Elastomers. Part I. Prepolymer Characterization. *J. Appl. Polym. Sci.* **2000**, *76* (10), 1596–1601. https://doi.org/10.1002/(SICI)1097-4628(20000606)76:10<1596::AID-APP15>3.0.CO;2-U.

(20)   Rabani, G.; Rosair, G. M.; Kraft, A. Low-Temperature Route to Thermoplastic Polyamide Elastomers. *J. Polym. Sci. Part Polym. Chem.* **2004**, *42* (6), 1449–1460. https://doi.org/10.1002/pola.11098.

(21)   Houton, K. A.; Wilson, A. J. Hydrogen-Bonded Supramolecular Polyurethanes. *Polym. Int.* **2015**, *64* (2), 165–173. https://doi.org/10.1002/pi.4837.

(22)   Chen, Y.; Kushner, A. M.; Williams, G. A.; Guan, Z. Multiphase Design of Autonomic Self-Healing Thermoplastic Elastomers. *Nat. Chem.* **2012**, *4* (6), 467–472. https://doi.org/10.1038/nchem.1314.

(23) Hentschel, J.; Kushner, A. M.; Ziller, J.; Guan, Z. Self-Healing Supramolecular Block Copolymers. *Angew. Chem. Int. Ed.* **2012**, *51* (42), 10561–10565. https://doi.org/10.1002/anie.201204840.

(24) Gooch, A.; Nedolisa, C.; Houton, K. A.; Lindsay, C. I.; Saiani, A.; Wilson, A. J. Tunable Self-Assembled Elastomers Using Triply Hydrogen-Bonded Arrays. *Macromolecules* **2012**, *45* (11), 4723–4729. https://doi.org/10.1021/ma3001109.

(25) Schemmer, B.; Kronenbitter, C.; Mecking, S. Thermoplastic Polyurethane Elastomers with Aliphatic Hard Segments Based on Plant-Oil-Derived Long-Chain Diisocyanates. *Macromol. Mater. Eng.* **2018**, *303* (4), 1700416. https://doi.org/10.1002/mame.201700416.

(26) *Ionomers*; Tant, M. R., Mauritz, K. A., Wilkes, G. L., Eds.; Springer Netherlands: Dordrecht, 1997. https://doi.org/10.1007/978-94-009-1461-2.

(27) Antony, P.; De, S. K. Ionic Thermoplastic Elastomers: A Review. *J. Macromol. Sci. Part C* **2001**, *41* (1–2), 41–77. https://doi.org/10.1081/MC-100002055.

(28) Hohlbein, N.; Shaaban, A.; Bras, A. R.; Pyckhout-Hintzen, W.; Schmidt, A. M. Self-Healing Dynamic Bond-Based Rubbers: Understanding the Mechanisms in Ionomeric Elastomer Model Systems. *Phys. Chem. Chem. Phys.* **2015**, *17* (32), 21005–21017. https://doi.org/10.1039/C5CP00620A.

(29) Makowski, H.; Lundberg, R.; Westerman, L.; Bock, J. Ions in Polymers. *Adv. Chem. Ser.* **1980**, *187*, 37.

(30) Bazuin, C. G.; Eisenberg, A. Dynamic Mechanical Properties of Plasticized Polystyrene-Based Ionomers. I. Glassy to Rubbery Zones. *J. Polym. Sci. Part B Polym. Phys.* **1986**, *24* (5), 1137–1153. https://doi.org/10.1002/polb.1986.090240514.

(31) Lundberg, R.; Makowski, H.; Westerman, L. The Dual Plasticization of Sulfonated Polystyrene Ionomer. *Ions Polym.* **1980**, *187*, 67–76.

(32) Ibarra, L.; Alzorriz, M. Ionic Elastomers Based on Carboxylated Nitrile Rubber and Magnesium Oxide. *J. Appl. Polym. Sci.* **2007**, *103* (3), 1894–1899. https://doi.org/10.1002/app.25411.

(33) Ibarra, L.; Alzorriz, M. Ionic Elastomers Based on Carboxylated Nitrile Rubber and Calcium Oxide. *J. Appl. Polym. Sci.* **2003**, *87* (5), 805–813. https://doi.org/10.1002/app.11468.

(34) van der Mee, M. A. J.; l'Abee, R. M. A.; Portale, G.; Goossens, J. G. P.; van Duin, M. Synthesis, Structure, and Properties of Ionic Thermoplastic Elastomers Based on Maleated Ethylene/Propylene Copolymers. *Macromolecules* **2008**, *41* (14), 5493–5501. https://doi.org/10.1021/ma8007509.

(35) Chatterjee, T.; Hait, S.; Bhattacharya, A. B.; Das, A.; Wiessner, S.; Naskar, K. Zinc Salts Induced Ionomeric Thermoplastic Elastomers Based on XNBR and PA12. *Polym.-Plast. Technol. Mater.* **2019**, *0* (0), 1–13. https://doi.org/10.1080/25740881.2019.1625389.

(36) Cui, M.; Nguyen, N. A.; Bonnesen, P. V.; Uhrig, D.; Keum, J. K.; Naskar, A. K. Rigid Oligomer from Lignin in Designing of Tough, Self-Healing Elastomers. *ACS Macro Lett.* **2018**, *7* (11), 1328–1332. https://doi.org/10.1021/acsmacrolett.8b00600.

(37) Wu, X.; Wang, J.; Huang, J.; Yang, S. Robust, Stretchable and Self-Healable Supramolecular Elastomers Synergistically Crosslinked by Hydrogen Bonds and Coordination Bonds. *ACS Appl. Mater. Interfaces* **2019**. https://doi.org/10.1021/acsami.8b20303.

(38) Liu, Y.; Tang, Z.; Wu, S.; Guo, B. Integrating Sacrificial Bonds into Dynamic Covalent Networks toward Mechanically Robust and Malleable Elastomers. *ACS Macro Lett.* **2019**, *8* (2), 193–199. https://doi.org/10.1021/acsmacrolett.9b00012.

(39) Cheng, B.; Lu, X.; Zhou, J.; Qin, R.; Yang, Y. Dual Cross-Linked Self-Healing and Recyclable Epoxidized Natural Rubber Based on Multiple Reversible Effects. *ACS Sustain. Chem. Eng.* **2019**. https://doi.org/10.1021/acssuschemeng.8b06437.

(40) Pan, Y.; Hu, J.; Yang, Z.; Tan, L. From Fragile Plastic to Room-Temperature Self-Healing Elastomer: Tuning Quadruple Hydrogen Bonding Interaction through One-Pot Synthesis. *ACS Appl. Polym. Mater.* **2019**. https://doi.org/10.1021/acsapm.8b00153.

(41) Appel, W. P. J.; Portale, G.; Wisse, E.; Dankers, P. Y. W.; Meijer, E. W. Aggregation of Ureido-Pyrimidinone Supramolecular Thermoplastic Elastomers into Nanofibers: A Kinetic Analysis. *Macromolecules* **2011**, *44* (17), 6776–6784. https://doi.org/10.1021/ma201303s.

(42) Cordier, P.; Tournilhac, F.; Soulié-Ziakovic, C.; Leibler, L. Self-Healing and Thermoreversible Rubber from Supramolecular Assembly. *Nature* **2008**, *451* (7181), 977–980. https://doi.org/10.1038/nature06669.

(43) Maes, F.; Montarnal, D.; Cantournet, S.; Tournilhac, F.; Corté, L.; Leibler, L. Activation and Deactivation of Self-Healing in Supramolecular Rubbers. *Soft Matter* **2012**, *8* (5), 1681–1687. https://doi.org/10.1039/C2SM06715C.

(44) Burattini, S.; Greenland, B. W.; Merino, D. H.; Weng, W.; Seppala, J.; Colquhoun, H. M.; Hayes, W.; Mackay, M. E.; Hamley, I. W.; Rowan, S. J. A Healable Supramolecular Polymer Blend Based on Aromatic Π−π Stacking and Hydrogen-Bonding Interactions. *J. Am. Chem. Soc.* **2010**, *132* (34), 12051–12058. https://doi.org/10.1021/ja104446r.

(45) Burattini, S.; Colquhoun, H. M.; Greenland, B. W.; Hayes, W. A Novel Self-Healing Supramolecular Polymer System. *Faraday Discuss.* **2009**, *143* (0), 251–264. https://doi.org/10.1039/B900859D.

(46) Nakahata, M.; Takashima, Y.; Yamaguchi, H.; Harada, A. Redox-Responsive Self-Healing Materials Formed from Host–Guest Polymers. *Nat. Commun.* **2011**, *2*, 511. https://doi.org/10.1038/ncomms1521.

(47) Kakuta, T.; Takashima, Y.; Harada, A. Highly Elastic Supramolecular Hydrogels Using Host–Guest Inclusion Complexes with Cyclodextrins. *Macromolecules* **2013**, *46* (11), 4575–4579. https://doi.org/10.1021/ma400695p.

(48) Hou, J.-B.; Zhang, X.-Q.; Wu, D.; Feng, J.-F.; Ke, D.; Li, B.-J.; Zhang, S. Tough Self-Healing Elastomer Based on Host-Guest Interaction of Poly-Cyclodextrin. *ACS Appl. Mater. Interfaces* **2019**. https://doi.org/10.1021/acsami.9b00626.

(49) Nomimura, S.; Osaki, M.; Park, J.; Ikura, R.; Takashima, Y.; Yamaguchi, H.; Harada, A. Self-Healing Alkyl Acrylate-Based Supramolecular Elastomers Cross-Linked via Host–Guest Interactions. *Macromolecules* **2019**. https://doi.org/10.1021/acs.macromol.9b00471.

(50) Ibarra, L.; Rodríguez, A.; Mora-Barrantes, I. Crosslinking of Carboxylated Nitrile Rubber (XNBR) Induced by Coordination with Anhydrous Copper Sulfate. *Polym. Int.* **2009**, *58* (2), 218–226. https://doi.org/10.1002/pi.2519.

(51) Cheng, Z.; Yan, M.; Cao, L.; Huang, J.; Yuan, D.; Chen, Y. Design of Nitrile Rubber with High Strength and Recycling Ability Based on Fe3+-Catechol Groups Coordination. *Ind. Eng. Chem. Res.* **2019**. https://doi.org/10.1021/acs.iecr.8b05993.

(52) Lai, J.-C.; Jia, X.-Y.; Wang, D.-P.; Deng, Y.-B.; Zheng, P.; Li, C.-H.; Zuo, J.-L.; Bao, Z. Thermodynamically Stable Whilst Kinetically Labile Coordination Bonds Lead to Strong and Tough Self-Healing Polymers. *Nat. Commun.* **2019**, *10* (1), 1164. https://doi.org/10.1038/s41467-019-09130-z.

(53) Liu, L.; Liang, S.; Huang, Y.; Hu, C.; Yang, J. A Stretchable Polysiloxane Elastomer with Self-Healing Capacity at Room Temperature and Solvatochromic Properties. *Chem. Commun.* **2017**, *53* (89), 12088–12091. https://doi.org/10.1039/C7CC06126A.

(54) Diels, O.; Alder, K. Synthesen in Der Hydroaromatischen Reihe. *Justus Liebigs Ann. Chem.* **1928**, *460* (1), 98–122. https://doi.org/10.1002/jlac.19284600106.

(55) Reutenauer, P.; Buhler, E.; Boul, P. J.; Candau, S. J.; Lehn, J.-M. Room Temperature Dynamic Polymers Based on Diels–Alder Chemistry. *Chem. – Eur. J.* **2009**, *15* (8), 1893–1900. https://doi.org/10.1002/chem.200802145.

(56) Chen, X.; Dam, M. A.; Ono, K.; Mal, A.; Shen, H.; Nutt, S. R.; Sheran, K.; Wudl, F. A Thermally Re-Mendable Cross-Linked Polymeric Material. *Science* **2002**, *295* (5560), 1698–1702. https://doi.org/10.1126/science.1065879.

(57) Liu, X.; Du, P.; Liu, L.; Zheng, Z.; Wang, X.; Joncheray, T.; Zhang, Y. Kinetic Study of Diels–Alder Reaction Involving in Maleimide–Furan Compounds and Linear Polyurethane. *Polym. Bull.* **2013**, *70* (8), 2319–2335. https://doi.org/10.1007/s00289-013-0954-8.

(58) Liu, Y.-L.; Hsieh, C.-Y. Crosslinked Epoxy Materials Exhibiting Thermal Remendablility and Removability from Multifunctional Maleimide and Furan Compounds. *J. Polym. Sci. Part Polym. Chem.* **2006**, *44* (2), 905–913. https://doi.org/10.1002/pola.21184.

(59) Froidevaux, V.; Borne, M.; Laborbe, E.; Auvergne, R.; Gandini, A.; Boutevin, B. Study of the Diels–Alder and Retro-Diels–Alder Reaction between Furan Derivatives and Maleimide for the

Creation of New Materials. *RSC Adv.* **2015**, *5* (47), 37742–37754. https://doi.org/10.1039/C5RA01185J.

(60) Boutelle, R. C.; Northrop, B. H. Substituent Effects on the Reversibility of Furan–Maleimide Cycloadditions. *J. Org. Chem.* **2011**, *76* (19), 7994–8002. https://doi.org/10.1021/jo201606z.

(61) Boul, P. J.; Reutenauer, P.; Lehn, J.-M. Reversible Diels−Alder Reactions for the Generation of Dynamic Combinatorial Libraries. *Org. Lett.* **2005**, *7* (1), 15–18. https://doi.org/10.1021/ol048065k.

(62) Gheneim, R.; Perez-Berumen, C.; Gandini, A. Diels−Alder Reactions with Novel Polymeric Dienes and Dienophiles: Synthesis of Reversibly Cross-Linked Elastomers. *Macromolecules* **2002**, *35* (19), 7246–7253. https://doi.org/10.1021/ma020343c.

(63) Yu, S.; Zhang, R.; Wu, Q.; Chen, T.; Sun, P. Bio-Inspired High-Performance and Recyclable Cross-Linked Polymers. *Adv. Mater.* **2013**, *25* (35), 4912–4917. https://doi.org/10.1002/adma.201301513.

(64) Chen, X.; Wudl, F.; Mal, A. K.; Shen, H.; Nutt, S. R. New Thermally Remendable Highly Cross-Linked Polymeric Materials. *Macromolecules* **2003**, *36* (6), 1802–1807. https://doi.org/10.1021/ma0210675.

(65) Deng, M.; Guo, F.; Liao, D.; Hou, Z.; Li, Y. Aluminium-Catalyzed Terpolymerization of Furfuryl Glycidyl Ether with Epichlorohydrin and Ethylene Oxide: Synthesis of Thermoreversible Polyepichlorohydrin Elastomers with Furan/Maleimide Covalent Crosslinks. *Polym. Chem.* **2017**, *9* (1), 98–107. https://doi.org/10.1039/C7PY01516J.

(66) Zhao, J.; Xu, R.; Luo, G.; Wu, J.; Xia, H. Self-Healing Poly(Siloxane-Urethane) Elastomers with Remoldability, Shape Memory and Biocompatibility. *Polym. Chem.* **2016**, *7* (47), 7278–7286. https://doi.org/10.1039/C6PY01499B.

(67) Fuhrmann, A.; Göstl, R.; Wendt, R.; Kötteritzsch, J.; Hager, M. D.; Schubert, U. S.; Brademann-Jock, K.; Thünemann, A. F.; Nöchel, U.; Behl, M.; et al. Conditional Repair by Locally Switching the Thermal Healing Capability of Dynamic Covalent Polymers with Light. *Nat. Commun.* **2016**, *7*, 13623. https://doi.org/10.1038/ncomms13623.

(68) Stern, M. D.; Tobolsky, A. V. Stress-Time-Temperature Relations in Polysulfide Rubbers. *J. Chem. Phys.* **1946**, *14* (2), 93–100. https://doi.org/10.1063/1.1724110.

(69) Tobolsky, A. V.; MacKnight, W. J.; Takahashi, M. Relaxation of Disulfide and Tetrasulfide Polymers. *J. Phys. Chem.* **1964**, *68* (4), 787–790. https://doi.org/10.1021/j100786a013.

(70) Matxain, J. M.; Asua, J. M.; Ruipérez, F. Design of New Disulfide-Based Organic Compounds for the Improvement of Self-Healing Materials. *Phys. Chem. Chem. Phys.* **2016**, *18* (3), 1758–1770. https://doi.org/10.1039/C5CP06660C.

(71) Tesoro, G. C.; Sastri, V. Reversible Crosslinking in Epoxy Resins. I. Feasibility Studies. *J. Appl. Polym. Sci.* **1990**, *39* (7), 1425–1437. https://doi.org/10.1002/app.1990.070390702.

(72) Sastri, V. R.; Tesoro, G. C. Reversible Crosslinking in Epoxy Resins. II. New Approaches. *J. Appl. Polym. Sci.* **1990**, *39* (7), 1439–1457. https://doi.org/10.1002/app.1990.070390703.

(73) Yoon, J. A.; Kamada, J.; Koynov, K.; Mohin, J.; Nicolaÿ, R.; Zhang, Y.; Balazs, A. C.; Kowalewski, T.; Matyjaszewski, K. Self-Healing Polymer Films Based on Thiol–Disulfide Exchange Reactions and Self-Healing Kinetics Measured Using Atomic Force Microscopy. *Macromolecules* **2012**, *45* (1), 142–149. https://doi.org/10.1021/ma2015134.

(74) Kamada, J.; Koynov, K.; Corten, C.; Juhari, A.; Yoon, J. A.; Urban, M. W.; Balazs, A. C.; Matyjaszewski, K. Redox Responsive Behavior of Thiol/Disulfide-Functionalized Star Polymers Synthesized via Atom Transfer Radical Polymerization. *Macromolecules* **2010**, *43* (9), 4133–4139. https://doi.org/10.1021/ma100365n.

(75) Canadell, J.; Goossens, H.; Klumperman, B. Self-Healing Materials Based on Disulfide Links. *Macromolecules* **2011**, *44* (8), 2536–2541. https://doi.org/10.1021/ma2001492.

(76) Otsuka, H.; Nagano, S.; Kobashi, Y.; Maeda, T.; Takahara, A. A Dynamic Covalent Polymer Driven by Disulfide Metathesis under Photoirradiation. *Chem. Commun.* **2010**, *46* (7), 1150–1152. https://doi.org/10.1039/B916128G.

(77) Michal, B. T.; Jaye, C. A.; Spencer, E. J.; Rowan, S. J. Inherently Photohealable and Thermal Shape-Memory Polydisulfide Networks. *ACS Macro Lett.* **2013**, *2* (8), 694–699. https://doi.org/10.1021/mz400318m.

(78) Xiang, H.; Yin, J.; Lin, G.; Liu, X.; Rong, M.; Zhang, M. Photo-Crosslinkable, Self-Healable and Reprocessable Rubbers. *Chem. Eng. J.* **2019**, *358*, 878–890. https://doi.org/10.1016/j.cej.2018.10.103.

(79) Caraballo, R.; Rahm, M.; Vongvilai, P.; Brinck, T.; Ramström, O. Phosphine-Catalyzed Disulfide Metathesis. *Chem. Commun.* **2008**, *0* (48), 6603–6605. https://doi.org/10.1039/B815710C.

(80) Xiang, H. P.; Qian, H. J.; Lu, Z. Y.; Rong, M. Z.; Zhang, M. Q. Crack Healing and Reclaiming of Vulcanized Rubber by Triggering the Rearrangement of Inherent Sulfur Crosslinked Networks. *Green Chem.* **2015**, *17* (8), 4315–4325. https://doi.org/10.1039/C5GC00754B.

(81) Takahashi, A.; Goseki, R.; Ito, K.; Otsuka, H. Thermally Healable and Reprocessable Bis(Hindered Amino)Disulfide-Cross-Linked Polymethacrylate Networks. *ACS Macro Lett.* **2017**, *6* (11), 1280–1284. https://doi.org/10.1021/acsmacrolett.7b00762.

(82) Wu, X.; Li, J.; Li, G.; Ling, L.; Zhang, G.; Sun, R.; Wong, C.-P. Heat-Triggered Poly(Siloxane-Urethane)s Based on Disulfide Bonds for Self-Healing Application. *J. Appl. Polym. Sci.* **2018**, *135* (31), 46532. https://doi.org/10.1002/app.46532.

(83) Zhang, B.; Digby, Z. A.; Flum, J. A.; Chakma, P.; Saul, J. M.; Sparks, J. L.; Konkolewicz, D. Dynamic Thiol–Michael Chemistry for Thermoresponsive Rehealable and Malleable Networks. *Macromolecules* **2016**, *49* (18), 6871–6878. https://doi.org/10.1021/acs.macromol.6b01061.

(84) Rekondo, A.; Martin, R.; Luzuriaga, A. R. de; Cabañero, G.; J. Grande, H.; Odriozola, I. Catalyst-Free Room-Temperature Self-Healing Elastomers Based on Aromatic Disulfide Metathesis. *Mater. Horiz.* **2014**, *1* (2), 237–240. https://doi.org/10.1039/C3MH00061C.

(85) Amamoto, Y.; Otsuka, H.; Takahara, A.; Matyjaszewski, K. Self-Healing of Covalently Cross-Linked Polymers by Reshuffling Thiuram Disulfide Moieties in Air under Visible Light. *Adv. Mater.* **2012**, *24* (29), 3975–3980. https://doi.org/10.1002/adma.201201928.

(86) Deng, G.; Tang, C.; Li, F.; Jiang, H.; Chen, Y. Covalent Cross-Linked Polymer Gels with Reversible Sol−Gel Transition and Self-Healing Properties. *Macromolecules* **2010**, *43* (3), 1191–1194. https://doi.org/10.1021/ma9022197.

(87) Deng, G.; Li, F.; Yu, H.; Liu, F.; Liu, C.; Sun, W.; Jiang, H.; Chen, Y. Dynamic Hydrogels with an Environmental Adaptive Self-Healing Ability and Dual Responsive Sol–Gel Transitions. *ACS Macro Lett.* **2012**, *1* (2), 275–279. https://doi.org/10.1021/mz200195n.

(88) Kuhl, N.; Bode, S.; Bose, R. K.; Vitz, J.; Seifert, A.; Hoeppener, S.; Garcia, S. J.; Spange, S.; Zwaag, S. van der; Hager, M. D.; et al. Acylhydrazones as Reversible Covalent Crosslinkers for Self-Healing Polymers. *Adv. Funct. Mater.* **2015**, *25* (22), 3295–3301. https://doi.org/10.1002/adfm.201501117.

(89) Liu, W.-X.; Zhang, C.; Zhang, H.; Zhao, N.; Yu, Z.-X.; Xu, J. Oxime-Based and Catalyst-Free Dynamic Covalent Polyurethanes. *J. Am. Chem. Soc.* **2017**, *139* (25), 8678–8684. https://doi.org/10.1021/jacs.7b03967.

(90) Zhang, B.; Zhang, P.; Zhang, H.; Yan, C.; Zheng, Z.; Wu, B.; Yu, Y. A Transparent, Highly Stretchable, Autonomous Self-Healing Poly(Dimethyl Siloxane) Elastomer. *Macromol. Rapid Commun.* **2013**, *35* (15), 2017. https://doi.org/10.1002/marc.201700110.

(91) Taynton, P.; Yu, K.; Shoemaker, R. K.; Jin, Y.; Qi, H. J.; Zhang, W. Heat- or Water-Driven Malleability in a Highly Recyclable Covalent Network Polymer. *Adv. Mater.* **2014**, *26* (23), 3938–3942. https://doi.org/10.1002/adma.201400317.

(92) Lei, Z. Q.; Xie, P.; Rong, M. Z.; Zhang, M. Q. Catalyst-Free Dynamic Exchange of Aromatic Schiff Base Bonds and Its Application to Self-Healing and Remolding of Crosslinked Polymers. *J. Mater. Chem. A* **2015**, *3* (39), 19662–19668. https://doi.org/10.1039/C5TA05788D.

(93) Lv, C.; Zhao, K.; Zheng, J. A Highly Stretchable Self-Healing Poly(Dimethylsiloxane) Elastomer with Reprocessability and Degradability. *Macromol. Rapid Commun.* **2018**, *39* (8), 1700686. https://doi.org/10.1002/marc.201700686.

(94) Cash, J. J.; Kubo, T.; Bapat, A. P.; Sumerlin, B. S. Room-Temperature Self-Healing Polymers Based on Dynamic-Covalent Boronic Esters. *Macromolecules* **2015**, *48* (7), 2098–2106. https://doi.org/10.1021/acs.macromol.5b00210.

(95) Zuo, Y.; Gou, Z.; Zhang, C.; Feng, S. Polysiloxane-Based Autonomic Self-Healing Elastomers Obtained through Dynamic Boronic Ester Bonds Prepared by Thiol-Ene "Click" Chemistry. *Macromol. Rapid Commun.* **2016**, *37* (13), 1052–1059. https://doi.org/10.1002/marc.201600155.

(96)   Lai, J.-C.; Mei, J.-F.; Jia, X.-Y.; Li, C.-H.; You, X.-Z.; Bao, Z. A Stiff and Healable Polymer Based on Dynamic-Covalent Boroxine Bonds. *Adv. Mater.* **2016**, *28* (37), 8277–8282. https://doi.org/10.1002/adma.201602332.

(97)   Ogden, W. A.; Guan, Z. Recyclable, Strong, and Highly Malleable Thermosets Based on Boroxine Networks. *J. Am. Chem. Soc.* **2018**, *140* (20), 6217–6220. https://doi.org/10.1021/jacs.8b03257.

(98)   Dodge, L.; Chen, Y.; Brook, M. A. Silicone Boronates Reversibly Crosslink Using Lewis Acid–Lewis Base Amine Complexes. *Chem. – Eur. J.* **2014**, *20* (30), 9349–9356. https://doi.org/10.1002/chem.201402877.

(99)   Bao, C.; Jiang, Y.-J.; Zhang, H.; Lu, X.; Sun, J. Room-Temperature Self-Healing and Recyclable Tough Polymer Composites Using Nitrogen-Coordinated Boroxines. *Adv. Funct. Mater.* **2018**, *28* (23), 1800560. https://doi.org/10.1002/adfm.201800560.

(100)   Yuan, C.; Rong, M. Z.; Zhang, M. Q. Self-Healing Polyurethane Elastomer with Thermally Reversible Alkoxyamines as Crosslinkages. *Polymer* **2014**, *55* (7), 1782–1791. https://doi.org/10.1016/j.polymer.2014.02.033.

(101)   Zhang, Z. P.; Rong, M. Z.; Zhang, M. Q. Room Temperature Self-Healable Epoxy Elastomer with Reversible Alkoxyamines as Crosslinkages. *Polymer* **2014**, *55* (16), 3936–3943. https://doi.org/10.1016/j.polymer.2014.06.064.

(102)   Imato, K.; Takahara, A.; Otsuka, H. Self-Healing of a Cross-Linked Polymer with Dynamic Covalent Linkages at Mild Temperature and Evaluation at Macroscopic and Molecular Levels. *Macromolecules* **2015**, *48* (16), 5632–5639. https://doi.org/10.1021/acs.macromol.5b00809.

(103)   Fawcett, A. S.; Hughes, T. C.; Zepeda-Velazquez, L.; Brook, M. A. Phototunable Cross-Linked Polysiloxanes. *Macromolecules* **2015**, *48* (18), 6499–6507. https://doi.org/10.1021/acs.macromol.5b01085.

(104)   Delebecq, E.; Pascault, J.-P.; Boutevin, B.; Ganachaud, F. On the Versatility of Urethane/Urea Bonds: Reversibility, Blocked Isocyanate, and Non-Isocyanate Polyurethane. *Chem. Rev.* **2013**, *113* (1), 80–118. https://doi.org/10.1021/cr300195n.

(105)   Fu, D.; Pu, W.; Wang, Z.; Lu, X.; Sun, S.; Yu, C.; Xia, H. A Facile Dynamic Crosslinked Healable Poly(Oxime-Urethane) Elastomer with High Elastic Recovery and Recyclability. *J. Mater. Chem. A* **2018**, *6* (37), 18154–18164. https://doi.org/10.1039/C8TA06059B.

(106)   Ying, H.; Zhang, Y.; Cheng, J. Dynamic Urea Bond for the Design of Reversible and Self-Healing Polymers. *Nat. Commun.* **2014**, *5* (1), 3218. https://doi.org/10.1038/ncomms4218.

(107)   Kantor, S. W.; Grubb, W. T.; Osthoff, R. C. The Mechanism of the Acid- and Base-Catalyzed Equilibration of Siloxanes. *J. Am. Chem. Soc.* **1954**, *76* (20), 5190–5197. https://doi.org/10.1021/ja01649a076.

(108)   Osthoff, R. C.; Bueche, A. M.; Grubb, W. T. Chemical Stress-Relaxation of Polydimethylsiloxane Elastomers1. *J. Am. Chem. Soc.* **1954**, *76* (18), 4659–4663. https://doi.org/10.1021/ja01647a052.

(109)   Zheng, P.; McCarthy, T. J. A Surprise from 1954: Siloxane Equilibration Is a Simple, Robust, and Obvious Polymer Self-Healing Mechanism. *J. Am. Chem. Soc.* **2012**, *134* (4), 2024–2027. https://doi.org/10.1021/ja2113257.

(110)   Scott, T. F.; Schneider, A. D.; Cook, W. D.; Bowman, C. N. Photoinduced Plasticity in Cross-Linked Polymers. *Science* **2005**, *308* (5728), 1615–1617. https://doi.org/10.1126/science.1110505.

(111)   Nicolaÿ, R.; Kamada, J.; Van Wassen, A.; Matyjaszewski, K. Responsive Gels Based on a Dynamic Covalent Trithiocarbonate Cross-Linker. *Macromolecules* **2010**, *43* (9), 4355–4361. https://doi.org/10.1021/ma100378r.

(112)   Amamoto, Y.; Kamada, J.; Otsuka, H.; Takahara, A.; Matyjaszewski, K. Repeatable Photoinduced Self-Healing of Covalently Cross-Linked Polymers through Reshuffling of Trithiocarbonate Units. *Angew. Chem.* **2011**, *123* (7), 1698–1701. https://doi.org/10.1002/ange.201003888.

(113)   Pepels, M.; Filot, I.; Klumperman, B.; Goossens, H. Self-Healing Systems Based on Disulfide–Thiol Exchange Reactions. *Polym. Chem.* **2013**, *4* (18), 4955–4965. https://doi.org/10.1039/C3PY00087G.

(114) Imbernon, L.; Oikonomou, E. K.; Norvez, S.; Leibler, L. Chemically Crosslinked yet Reprocessable Epoxidized Natural Rubber via Thermo-Activated Disulfide Rearrangements. *Polym. Chem.* **2015**, *6* (23), 4271–4278. https://doi.org/10.1039/C5PY00459D.

(115) Debnath, S.; Ujjwal, R. R.; Ojha, U. Self-Healable and Recyclable Dynamic Covalent Networks Based on Room Temperature Exchangeable Hydrazide Michael Adduct Linkages. *Macromolecules* **2018**, *51* (23), 9961–9973. https://doi.org/10.1021/acs.macromol.8b01827.

(116) Bui, R.; Brook, M. A. Dynamic Covalent Schiff-Base Silicone Polymers and Elastomers. *Polymer* **2019**, *160*, 282–290. https://doi.org/10.1016/j.polymer.2018.11.043.

(117) Feng, Z.; Yu, B.; Hu, J.; Zuo, H.; Li, J.; Sun, H.; Ning, N.; Tian, M.; Zhang, L. Multifunctional Vitrimer-Like Polydimethylsiloxane (PDMS): Recyclable, Self-Healable, and Water-Driven Malleable Covalent Networks Based on Dynamic Imine Bond. *Ind. Eng. Chem. Res.* **2019**. https://doi.org/10.1021/acs.iecr.8b05309.

(118) Cromwell, O. R.; Chung, J.; Guan, Z. Malleable and Self-Healing Covalent Polymer Networks through Tunable Dynamic Boronic Ester Bonds. *J. Am. Chem. Soc.* **2015**, *137* (20), 6492–6495. https://doi.org/10.1021/jacs.5b03551.

(119) Montarnal, D.; Capelot, M.; Tournilhac, F.; Leibler, L. Silica-Like Malleable Materials from Permanent Organic Networks. *Science* **2011**, *334* (6058), 965–968. https://doi.org/10.1126/science.1212648.

(120) Capelot, M.; Unterlass, M. M.; Tournilhac, F.; Leibler, L. Catalytic Control of the Vitrimer Glass Transition. *ACS Macro Lett.* **2012**, *1* (7), 789–792. https://doi.org/10.1021/mz300239f.

(121) Brutman, J. P.; Delgado, P. A.; Hillmyer, M. A. Polylactide Vitrimers. *ACS Macro Lett.* **2014**, *3* (7), 607–610. https://doi.org/10.1021/mz500269w.

(122) Lu, Y.-X.; Tournilhac, F.; Leibler, L.; Guan, Z. Making Insoluble Polymer Networks Malleable via Olefin Metathesis. *J. Am. Chem. Soc.* **2012**, *134* (20), 8424–8427. https://doi.org/10.1021/ja303356z.

(123) Obadia, M. M.; Mudraboyina, B. P.; Serghei, A.; Montarnal, D.; Drockenmuller, E. Reprocessing and Recycling of Highly Cross-Linked Ion-Conducting Networks through Transalkylation Exchanges of C–N Bonds. *J. Am. Chem. Soc.* **2015**, *137* (18), 6078–6083. https://doi.org/10.1021/jacs.5b02653.

(124) Obadia, M. M.; Drockenmuller, E. Poly(1,2,3-Triazolium)s: A New Class of Functional Polymer Electrolytes. *Chem. Commun.* **2016**, *52* (12), 2433–2450. https://doi.org/10.1039/C5CC09861K.

(125) Obadia, M. M.; Jourdain, A.; Cassagnau, P.; Montarnal, D.; Drockenmuller, E. Tuning the Viscosity Profile of Ionic Vitrimers Incorporating 1,2,3-Triazolium Cross-Links. *Adv. Funct. Mater. 27* (45), 1703258. https://doi.org/10.1002/adfm.201703258.

(126) Hendriks, B.; Waelkens, J.; Winne, J. M.; Du Prez, F. E. Poly(Thioether) Vitrimers via Transalkylation of Trialkylsulfonium Salts. *ACS Macro Lett.* **2017**, *6* (9), 930–934. https://doi.org/10.1021/acsmacrolett.7b00494.

(127) Denissen, W.; Rivero, G.; Nicolaÿ, R.; Leibler, L.; Winne, J. M.; Du Prez, F. E. Vinylogous Urethane Vitrimers. *Adv. Funct. Mater.* **2015**, *25* (16), 2451–2457. https://doi.org/10.1002/adfm.201404553.

(128) Denissen, W.; De Baere, I.; Van Paepegem, W.; Leibler, L.; Winne, J.; Du Prez, F. E. Vinylogous Urea Vitrimers and Their Application in Fiber Reinforced Composites. *Macromolecules* **2018**, *51* (5), 2054–2064. https://doi.org/10.1021/acs.macromol.7b02407.

(129) Stukenbroeker, T.; Wang, W.; Winne, J. M.; Prez, F. E. D.; Nicolaÿ, R.; Leibler, L. Polydimethylsiloxane Quenchable Vitrimers. *Polym. Chem.* **2017**, *8* (43), 6590–6593. https://doi.org/10.1039/C7PY01488K.

(130) Röttger, M.; Domenech, T.; Weegen, R. van der; Breuillac, A.; Nicolaÿ, R.; Leibler, L. High-Performance Vitrimers from Commodity Thermoplastics through Dioxaborolane Metathesis. *Science* **2017**, *356* (6333), 62–65. https://doi.org/10.1126/science.aah5281.

(131) Fortman, D. J.; Snyder, R. L.; Sheppard, D. T.; Dichtel, W. R. Rapidly Reprocessable Cross-Linked Polyhydroxyurethanes Based on Disulfide Exchange. *ACS Macro Lett.* **2018**, 1226–1231. https://doi.org/10.1021/acsmacrolett.8b00667.

(132) Diehl, K. L.; Kolesnichenko, I. V.; Robotham, S. A.; Bachman, J. L.; Zhong, Y.; Brodbelt, J. S.; Anslyn, E. V. Click and Chemically Triggered Declick Reactions through Reversible Amine

and Thiol Coupling via a Conjugate Acceptor. *Nat. Chem.* **2016**, *8* (10), 968–973. https://doi.org/10.1038/nchem.2601.

(133) Ishibashi, J. S. A.; Kalow, J. A. Vitrimeric Silicone Elastomers Enabled by Dynamic Meldrum's Acid-Derived Cross-Links. *ACS Macro Lett.* **2018**, *7* (4), 482–486. https://doi.org/10.1021/acsmacrolett.8b00166.

(134) Dhers, S.; Vantomme, G.; Avérous, L. Fully Bio-Based Polyimine Vitrimer Derived from Fructose. *Green Chem.* **2019**. https://doi.org/10.1039/C9GC00540D.

(135) Gelling, I. R. Modification of Natural Rubber Latex with Peracetic Acid. *Rubber Chem. Technol.* **1985**, *58* (1), 86–96. https://doi.org/10.5254/1.3536060.

(136) Gan, S.-N.; Hamid, Z. A. Partial Conversion of Epoxide Groups to Diols in Epoxidized Natural Rubber. *Polymer* **1997**, *38* (8), 1953–1956. https://doi.org/10.1016/S0032-3861(96)00710-0.

(137) Burfield, D. R.; Lim, K.-L.; Law, K.-S. Epoxidation of Natural Rubber Latices: Methods of Preparation and Properties of Modified Rubbers. *J. Appl. Polym. Sci.* **1984**, *29* (5), 1661–1673. https://doi.org/10.1002/app.1984.070290520.

(138) Baker, C. S. L.; Gelling, I. R.; Newell, R. Epoxidized Natural Rubber. *Rubber Chem. Technol.* **1985**, *58* (1), 67–85. https://doi.org/10.5254/1.3536059.

(139) Wheelock, C. Epoxidation of Liquid Polybutadiene. *Ind. Eng. Chem.* **1958**, *50* (3), 299–304. https://doi.org/10.1021/ie50579a022.

(140) Davey, J. E.; Loadman, M. J. R. A Chemical Demonstration of the Randomness of Epoxidation of Natural Rubber. *Br. Polym. J.* **1984**, *16* (3), 134–138. https://doi.org/10.1002/pi.4980160305.

(141) Bradbury, J. H.; Perera, M. C. S. Epoxidation of Natural Rubber Studied by Nmr Spectroscopy. *J. Appl. Polym. Sci.* **1985**, *30* (8), 3347–3364. https://doi.org/10.1002/app.1985.070300817.

(142) Ng, S.-C.; Gan, L.-H. Reaction of Natural Rubber Latex with Performic Acid. *Eur. Polym. J.* **1981**, *17* (10), 1073–1077. https://doi.org/10.1016/0014-3057(81)90030-6.

(143) Nicol, M.; Cole-hamilton, D. J. The Synthesis of Polyepoxides from Unsaturated Polymers and Their Attempted Isomerisation to Polyketones. *J. Mater. Chem.* **1998**, *8* (7), 1511–1515. https://doi.org/10.1039/A800899J.

(144) Grubbs, R. B.; Broz, M. E.; Dean, J. M.; Bates, F. S. Selectively Epoxidized Polyisoprene−Polybutadiene Block Copolymers. *Macromolecules* **2000**, *33* (7), 2308–2310. https://doi.org/10.1021/ma992049z.

(145) Lucki, J.; Rånby, B.; Rabek, J. F. Comparative Studies of Reactions of Commercial Polymers with Molecular Oxygen, Singlet Oxygen, Atomic Oxygen and Ozone—II. Reactions with 1,2-Polybutadiene. *Eur. Polym. J.* **1979**, *15* (12), 1101–1110. https://doi.org/10.1016/0014-3057(79)90043-0.

(146) Zuchowska, D. Polybutadiene Modified by Epoxidation. 1. Effect of Polybutadiene Microstructure on the Reactivity of Double Bonds. *Polymer* **1980**, *21* (5), 514–520. https://doi.org/10.1016/0032-3861(80)90217-7.

(147) Wang, Q.; Zhang, X.; Wang, L.; Mi, Z. Kinetics of Epoxidation of Hydroxyl-Terminated Polybutadiene with Hydrogen Peroxide under Phase Transfer Catalysis. *Ind. Eng. Chem. Res.* **2009**, *48* (3), 1364–1371. https://doi.org/10.1021/ie800875h.

(148) Kirpichev, V. P.; Yakubchik, A. I.; Maglysh, G. N. Modification of CIS-1,4-Polybutadiene with β-Naphthylamine. *Rubber Chem. Technol.* **1970**, *43* (5), 1225–1229. https://doi.org/10.5254/1.3547320.

(149) Perera, M. C. S. Reaction of Aromatic Amines with Epoxidized Natural Rubber Latex. *J. Appl. Polym. Sci.* **1990**, *39* (3), 749–758. https://doi.org/10.1002/app.1990.070390323.

(150) Brosse, J.-C.; Soutif, J.-C.; Pinazzi, C. Modification Au Deuxième Degré de Polymères Époxydés, 1. Etude Sur Molécules Modèles Des Polyalcadiènes. *Makromol. Chem.* **1979**, *180* (9), 2109–2121. https://doi.org/10.1002/macp.1979.021800906.

(151) Peng, C.-C.; Abetz, V. A Simple Pathway toward Quantitative Modification of Polybutadiene: A New Approach to Thermoreversible Cross-Linking Rubber Comprising Supramolecular Hydrogen-Bonding Networks. *Macromolecules* **2005**, *38* (13), 5575–5580. https://doi.org/10.1021/ma050419f.

(152)   Pire, M.; Oikonomou, E. K.; Imbernon, L.; Lorthioir, C.; Iliopoulos, I.; Norvez, S. Crosslinking of Epoxidized Natural Rubber by Dicarboxylic Acids: An Alternative to Standard Vulcanization. *Macromol. Symp.* **2013**, *331–332* (1), 89–96. https://doi.org/10.1002/masy.201300053.

(153)   Pire, M.; Lorthioir, C.; Oikonomou, E. K.; Norvez, S.; Iliopoulos, I.; Rossignol, B. L.; Leibler, L. Imidazole-Accelerated Crosslinking of Epoxidized Natural Rubber by Dicarboxylic Acids: A Mechanistic Investigation Using NMR Spectroscopy. *Polym. Chem.* **2012**, *3* (4), 946–953. https://doi.org/10.1039/C2PY00591C.

(154)   Pire, M.; Norvez, S.; Iliopoulos, I.; Rossignol, B. L.; Leibler, L. Dicarboxylic Acids May Compete with Standard Vulcanisation Processes for Crosslinking Epoxidised Natural Rubber. *Compos. Interfaces* **2014**, *21* (1), 45–50. https://doi.org/10.1080/15685543.2013.830527.

(155)   Xuan, H. L.; Decker, C. Photocrosslinking of Acrylated Natural Rubber. *J. Polym. Sci. Part Polym. Chem.* **1993**, *31* (3), 769–780. https://doi.org/10.1002/pola.1993.080310323.

(156)   Phinyocheep, P.; Duangthong, S. Ultraviolet-Curable Liquid Natural Rubber. *J. Appl. Polym. Sci.* **2000**, *78* (8), 1478–1485. https://doi.org/10.1002/1097-4628(20001121)78:8<1478::AID-APP30>3.0.CO;2-K.

(157)   Tang, Z.; Liu, Y.; Guo, B.; Zhang, L. Malleable, Mechanically Strong, and Adaptive Elastomers Enabled by Interfacial Exchangeable Bonds. *Macromolecules* **2017**, *50* (19), 7584–7592. https://doi.org/10.1021/acs.macromol.7b01261.

(158)   Qiu, M.; Wu, S.; Fang, S.; Tang, Z.; Guo, B. Sustainable, Recyclable and Robust Elastomers Enabled by Exchangeable Interfacial Cross-Linking. *J. Mater. Chem. A* **2018**, *6* (28), 13607–13612. https://doi.org/10.1039/C8TA04173C.

(159)   Feng, Z.; Hu, J.; Zuo, H.; Ning, N.; Zhang, L.; Yu, B.; Tian, M. Photothermal-Induced Self-Healable and Reconfigurable Shape Memory Bio-Based Elastomer with Recyclable Ability. *ACS Appl. Mater. Interfaces* **2019**, *11* (1), 1469–1479. https://doi.org/10.1021/acsami.8b18002.

(160)   Cao, L.; Fan, J.; Huang, J.; Chen, Y. A Robust and Stretchable Cross-Linked Rubber Network with Recyclable and Self-Healable Capabilities Based on Dynamic Covalent Bonds. *J. Mater. Chem. A* **2019**, *7* (9), 4922–4933. https://doi.org/10.1039/C8TA11587G.

(161)   Derouet, D.; Brosse, J.-C.; Challioui, A. Alcoholysis of Epoxidized Polyisoprenes by Direct Opening of Oxirane Rings with Alcohol Derivatives 1. Modelization of the Reaction. *Eur. Polym. J.* **2001**, *37* (7), 1315–1326. https://doi.org/10.1016/S0014-3057(00)00266-4.

(162)   Derouet, D.; Brosse, J.-C.; Challioui, A. Alcoholysis of Epoxidized Polyisoprenes by Direct Opening of Oxirane Rings with Alcohol Derivatives 2. Study on Epoxidized 1,4-Polyisoprene. *Eur. Polym. J.* **2001**, *37* (7), 1327–1337. https://doi.org/10.1016/S0014-3057(00)00267-6.

(163)   Antonietti, M.; Förster, S.; Hartmann, J.; Oestreich, S. Novel Amphiphilic Block Copolymers by Polymer Reactions and Their Use for Solubilization of Metal Salts and Metal Colloids. *Macromolecules* **1996**, *29* (11), 3800–3806. https://doi.org/10.1021/ma951446g.

(164)   Nor, H. M.; Ebdon, J. R. Telechelic Liquid Natural Rubber: A Review. *Prog. Polym. Sci.* **1998**, *23* (2), 143–177. https://doi.org/10.1016/S0079-6700(97)00028-2.

(165)   Ravindran, T.; Nayar, M. R. G.; Francis, D. J. Production of Hydroxyl-Terminated Liquid Natural Rubber—Mechanism of Photochemical Depolymerization and Hydroxylation. *J. Appl. Polym. Sci.* **1988**, *35* (5), 1227–1239. https://doi.org/10.1002/app.1988.070350509.

(166)   Nor, H. M.; Ebdon, J. R. Ozonolysis of Natural Rubber in Chloroform SolutionPart 1. A Study by GPC and FTIR Spectroscopy. *Polymer* **2000**, *41* (7), 2359–2365. https://doi.org/10.1016/S0032-3861(99)00417-6.

(167)   Zhou, Q.; Jie, S.; Li, B.-G. Preparation of Hydroxyl-Terminated Polybutadiene with High Cis-1,4 Content. *Ind. Eng. Chem. Res.* **2014**, *53* (46), 17884–17893. https://doi.org/10.1021/ie503652g.

(168)   Gillier-Ritoit, S.; Reyx, D.; Campistron, I.; Laguerre, A.; Singh, R. P. Telechelic Cis-1,4-Oligoisoprenes through the Selective Oxidolysis of Epoxidized Monomer Units and Polyisoprenic Monomer Units in Cis-1,4-Polyisoprenes. *J. Appl. Polym. Sci.* **2003**, *87* (1), 42–46. https://doi.org/10.1002/app.11661.

(169)   Berto, P.; Grelier, S.; Peruch, F. Controlled Degradation of Polyisoprene and Polybutadiene: A Comparative Study of Two Methods. *Polym. Degrad. Stab.* **2018**, *154*, 295–303. https://doi.org/10.1016/j.polymdegradstab.2018.06.019.

(170)   Berto, P.; Pointet, A.; Le Coz, C.; Grelier, S.; Peruch, F. Recyclable Telechelic Cross-Linked Polybutadiene Based on Reversible Diels–Alder Chemistry. *Macromolecules* **2018**, *51* (3), 651–659. https://doi.org/10.1021/acs.macromol.7b02220.

(171)   Berto, P.; Grelier, S.; Peruch, F. Telechelic Polybutadienes or Polyisoprenes Precursors for Recyclable Elastomeric Networks. *Macromol. Rapid Commun.* **2017**, *38* (22), n/a-n/a. https://doi.org/10.1002/marc.201700475.

(172)   Crouch, W. W.; Shotton, J. A. Liquid Polybutadiene. *Ind. Eng. Chem.* **1955**, *47* (10), 2091–2095. https://doi.org/10.1021/ie50550a023.

(173)   Kovacic, P.; Hein, R. W. Cross-Linking of Polymers with Dimaleimides1. *J. Am. Chem. Soc.* **1959**, *81* (5), 1187–1190. https://doi.org/10.1021/ja01514a043.

(174)   Kovacic, P.; Hein, R. W. Cross-Linking of Unsaturated Polymers with Dimaleimides1. *J. Am. Chem. Soc.* **1959**, *81* (5), 1190–1194. https://doi.org/10.1021/ja01514a044.

(175)   Sheng, J.; Lu, X. L.; Yao, K. D. Investigation of Graft Polymerization of Maleic Anhydride Onto Polybutadiene Rubber. *J. Macromol. Sci. Part - Chem.* **1990**, *27* (2), 167–178. https://doi.org/10.1080/00222339009351494.

(176)   Nakason, C.; Kaesaman, A.; Supasanthitikul, P. The Grafting of Maleic Anhydride onto Natural Rubber. *Polym. Test.* **2004**, *23* (1), 35–41. https://doi.org/10.1016/S0142-9418(03)00059-X.

(177)   Wilhelm, H. M.; Felisberti, M. I. Bulk Modification of Styrene–Butadiene–Styrene Triblock Copolymer with Maleic Anhydride. *J. Appl. Polym. Sci.* **2002**, *83* (13), 2953–2960. https://doi.org/10.1002/app.10355.

(178)   Saelao, J.; Phinyocheep, P. Influence of Styrene on Grafting Efficiency of Maleic Anhydride onto Natural Rubber. *J. Appl. Polym. Sci.* **2005**, *95* (1), 28–38. https://doi.org/10.1002/app.20810.

(179)   Qi, R.; Yu, Q.; Shen, Y.; Liu, Q.; Zhou, C. Grafting Copolymerization of Maleic Anhydride onto Styrene-Butadiene-Styrene Block Copolymer through Solvothermal Process. *J. Appl. Polym. Sci.* **2006**, *102* (6), 5274–5279. https://doi.org/10.1002/app.24780.

(180)   Chino, K.; Ashiura, M. Themoreversible Cross-Linking Rubber Using Supramolecular Hydrogen-Bonding Networks. *Macromolecules* **2001**, *34* (26), 9201–9204. https://doi.org/10.1021/ma011253v.

(181)   Tanasi, P.; Santana, M. H.; Carretero-González, J.; Verdejo, R.; López-Manchado, M. A. Thermo-Reversible Crosslinked Natural Rubber: A Diels-Alder Route for Reuse and Self-Healing Properties in Elastomers. *Polymer* **2019**. https://doi.org/10.1016/j.polymer.2019.04.059.

(182)   Liu, J.; Wang, S.; Tang, Z.; Huang, J.; Guo, B.; Huang, G. Bioinspired Engineering of Two Different Types of Sacrificial Bonds into Chemically Cross-Linked cis-1,4-Polyisoprene toward a High-Performance Elastomer http://pubs.acs.org/doi/full/10.1021/acs.macromol.6b01576 (accessed May 5, 2017).

(183)   Roover, B. D.; Devaux, J.; Legras, R. Maleic Anhydride Homopolymerization during Melt Functionalization of Isotactic Polypropylene. *J. Polym. Sci. Part Polym. Chem.* **1996**, *34* (7), 1195–1202. https://doi.org/10.1002/(SICI)1099-0518(199605)34:7<1195::AID-POLA5>3.0.CO;2-2.

(184)   Liaw, D.-J.; Lin, L.-L. Studies on Graft Copolymerization of Cyclohexyl Methacrylate onto 1,2-Polybutadiene. *J. Appl. Polym. Sci.* **1989**, *37* (7), 1993–2006. https://doi.org/10.1002/app.1989.070370719.

(185)   Geuskens, G.; Kanda, M. N. Surface Modification of Polymers—I. Grafting Initiated by Photo-Generated Hydroperoxides. *Eur. Polym. J.* **1991**, *27* (9), 877–879. https://doi.org/10.1016/0014-3057(91)90026-K.

(186)   Pham, B. T. T.; Tonge, M. P.; Monteiro, M. J.; Gilbert, R. G. Grafting Kinetics of Vinyl Neodecanoate onto Polybutadiene. *Macromolecules* **2000**, *33* (7), 2383–2390. https://doi.org/10.1021/ma990604r.

(187)   El-Wakil, A. A. Synthesis, Characterization, and Evaluation of Natural Rubber-Graft-N-(4-Aminodiphenyl Methane) Acrylamide as an Antioxidant. *J. Appl. Polym. Sci.* **2006**, *101* (2), 843–849. https://doi.org/10.1002/app.23279.

(188)   Vikram, T.; Nando, G. B. Synthesis and Characterization of Cardanol-Grafted Natural Rubber—The Solution Technique. *J. Appl. Polym. Sci.* **2007**, *105* (3), 1280–1288. https://doi.org/10.1002/app.24714.

(189)   Juntuek, P.; Ruksakulpiwat, C.; Chumsamrong, P.; Ruksakulpiwat, Y. Glycidyl Methacrylate Grafted Natural Rubber: Synthesis, Characterization, and Mechanical Property. *J. Appl. Polym. Sci.* **2011**, *122* (5), 3152–3159. https://doi.org/10.1002/app.34324.

(190)   Bloomfield, G. F.; Merrett, F. M.; Popham, F. J.; Swift, P. M. L. Graft Polymers Derived from Natural Rubber. *Rubber Chem. Technol.* **1956**, *29* (1), 99–105. https://doi.org/10.5254/1.3542530.

(191)   Gesner, B. D. Graft Copolymerization : On the Structure of the Graft Phase and the Mechanism of Grafting Polybutadiene Rubber. *Rubber Chem. Technol.* **1965**, *38* (3), 655–656. https://doi.org/10.5254/1.3535684.

(192)   Cameron, G. G.; Qureshi, M. Y. Free Radical Grafting of Monomers to Polydienes. III. Kinetics and Mechanism of Styrene Grafting to Polyisoprene. *J. Polym. Sci. Polym. Chem. Ed.* **1980**, *18* (7), 2143–2153. https://doi.org/10.1002/pol.1980.170180710.

(193)   Brydon, A.; Burnett, G. M.; Cameron, G. G. Free-Radical Grafting of Monomers to Polydienes. I. Effect of Reaction Conditions on Grafting of Styrene to Polybutadiene. *J. Polym. Sci. Polym. Chem. Ed.* **1973**, *11* (12), 3255–3269. https://doi.org/10.1002/pol.1973.170111218.

(194)   Gasperowicz, A.; Łaskawski, W. Grafting of Styrene onto Low Molecular Weight Polymers and Copolymers of Butadiene. *J. Polym. Sci. Polym. Chem. Ed.* **1976**, *14* (12), 2875–2886. https://doi.org/10.1002/pol.1976.170141204.

(195)   Kitayama, M.; Vogl, O. Functional Polymers. XVIII. Radical Grafting of 2-(2-Hydroxy-5-Vinylphenyl)-2H-Benzotriazole onto Polybutadienes. *Polym. J.* **1982**, *14* (7), 537–543. https://doi.org/10.1295/polymj.14.537.

(196)   Bonilla-Cruz, J.; Saldívar-Guerra, E.; Torres-Lubián, J. R.; Guerrero-Santos, R.; López-Carpy, B.; Luna-Bárcenas, G. Controlled Grafting-From of Polystyrene on Polybutadiene: Mechanism and Spectroscopic Evidence of the Functionalization of Polybutadiene with 4-Oxo-TEMPO. *Macromol. Chem. Phys.* **2008**, *209* (21), 2268–2283. https://doi.org/10.1002/macp.200800367.

(197)   Bonilla-Cruz, J.; Guerrero-Sánchez, C.; Schubert, U. S.; Saldívar-Guerra, E. Controlled "Grafting-from" of Poly[Styrene-Co-Maleic Anhydride] onto Polydienes Using Nitroxide Chemistry. *Eur. Polym. J.* **2010**, *46* (2), 298–312. https://doi.org/10.1016/j.eurpolymj.2009.10.009.

(198)   Jin, K.; Li, L.; Torkelson, J. M. Recyclable Crosslinked Polymer Networks via One-Step Controlled Radical Polymerization. *Adv. Mater.* **2016**, *28* (31), 6746–6750. https://doi.org/10.1002/adma.201600871.

(199)   McGrath, M. P.; Sall, E. D.; Tremont, S. J. Functionalization of Polymers by Metal-Mediated Processes. *Chem. Rev.* **1995**, *95* (2), 381–398.

(200)   Marciniec, B.; Lewandowski, M.; Pietraszuk, C.; Foltynowicz, Z. Functionalization of 1,2-Polybutadiene by Ruthenium Complex Catalysed Coupling with Vinylsilanes. *Polymer* **1997**, *38* (20), 5169–5172. https://doi.org/10.1016/S0032-3861(97)00034-7.

(201)   Hoyle, C. E.; Bowman, C. N. Thiol–Ene Click Chemistry. *Angew. Chem. Int. Ed.* **2010**, *49* (9), 1540–1573. https://doi.org/10.1002/anie.200903924.

(202)   B. Lowe, A. Thiol-Ene "Click" Reactions and Recent Applications in Polymer and Materials Synthesis. *Polym. Chem.* **2010**, *1* (1), 17–36. https://doi.org/10.1039/B9PY00216B.

(203)   Kade, M. J.; Burke, D. J.; Hawker, C. J. The Power of Thiol-Ene Chemistry. *J. Polym. Sci. Part Polym. Chem.* **2010**, *48* (4), 743–750. https://doi.org/10.1002/pola.23824.

(204)   Mishra, M.; Yagci, Y. *Handbook of Vinyl Polymers: Radical Polymerization, Process, and Technology, Second Edition*; CRC Press, 2016.

(205)   Posner, T. *Ber Dtsch Chem Ges* **1905**, *38*, 646–657.

(206)   Schlögl, S.; Trutschel, M.-L.; Chassé, W.; Letofsky-Papst, I.; Schaller, R.; Holzner, A.; Riess, G.; Kern, W.; Saalwächter, K. Photo-Vulcanization Using Thiol-Ene Chemistry: Film Formation, Morphology and Network Characteristics of UV Crosslinked Rubber Latices. *Polymer* **2014**, *55* (22), 5584–5595. https://doi.org/10.1016/j.polymer.2014.06.007.

(207)   Trovatti, E.; Lacerda, T. M.; Carvalho, A. J. F.; Gandini, A. Recycling Tires? Reversible Crosslinking of Poly(Butadiene). *Adv. Mater.* **2015**, *27* (13), 2242–2245. https://doi.org/10.1002/adma.201405801.

(208)   Bai, J.; Li, H.; Shi, Z.; Yin, J. An Eco-Friendly Scheme for the Cross-Linked Polybutadiene Elastomer via Thiol–Ene and Diels–Alder Click Chemistry. *Macromolecules* **2015**, *48* (11), 3539–3546. https://doi.org/10.1021/acs.macromol.5b00389.

(209)   Wang, D.; Guo, J.; Zhang, H.; Cheng, B.; Shen, H.; Zhao, N.; Xu, J. Intelligent Rubber with Tailored Properties for Self-Healing and Shape Memory. *J. Mater. Chem. A* **2015**, *3* (24), 12864–12872. https://doi.org/10.1039/C5TA01915J.

(210)   Li, L.; Li, S.; Cui, D. Highly Cis-1,4-Selective Living Polymerization of 3-Methylenehepta-1,6-Diene and Its Subsequent Thiol–Ene Reaction: An Efficient Approach to Functionalized Diene-Based Elastomer. *Macromolecules* **2016**, *49* (4), 1242–1251. https://doi.org/10.1021/acs.macromol.5b02654.

(211)   Wang, D.; Zhang, H.; Cheng, B.; Qian, Z.; Liu, W.; Zhao, N.; Xu, J. Dynamic Cross-Links to Facilitate Recyclable Polybutadiene Elastomer with Excellent Toughness and Stretchability. *J. Polym. Sci. Part Polym. Chem.* **2016**, *54* (10), 1357–1366. https://doi.org/10.1002/pola.27983.

(212)   Zhang, H.; Wang, D.; Liu, W.; Li, P.; Liu, J.; Liu, C.; Zhang, J.; Zhao, N.; Xu, J. Recyclable Polybutadiene Elastomer Based on Dynamic Imine Bond. *J. Polym. Sci. Part Polym. Chem.* **2017**, n/a-n/a. https://doi.org/10.1002/pola.28577.

(213)   Khire, V. S.; Lee, T. Y.; Bowman, C. N. Surface Modification Using Thiol−Acrylate Conjugate Addition Reactions. *Macromolecules* **2007**, *40* (16), 5669–5677. https://doi.org/10.1021/ma070146j.

(214)   Killops, K. L.; Campos, L. M.; Hawker, C. J. Robust, Efficient, and Orthogonal Synthesis of Dendrimers via Thiol-Ene "Click" Chemistry. *J. Am. Chem. Soc.* **2008**, *130* (15), 5062–5064. https://doi.org/10.1021/ja8006325.

(215)   Sutisna, B.; Polymeropoulos, G.; Musteata, V.; Sougrat, R.; Smilgies, D.-M.; Peinemann, K.-V.; Hadjichristidis, N.; Nunes, S. P. Functionalized Nanochannels from Self-Assembled and Photomodified Poly(Styrene-b-Butadiene-b-Styrene). *Small* **2018**, *14* (18), 1701885. https://doi.org/10.1002/smll.201701885.

(216)   Rydholm, A. E.; Bowman, C. N.; Anseth, K. S. Degradable Thiol-Acrylate Photopolymers: Polymerization and Degradation Behavior of an in Situ Forming Biomaterial. *Biomaterials* **2005**, *26* (22), 4495–4506. https://doi.org/10.1016/j.biomaterials.2004.11.046.

(217)   Carioscia, J. A.; Lu, H.; Stanbury, J. W.; Bowman, C. N. Thiol-Ene Oligomers as Dental Restorative Materials. *Dent. Mater.* **2005**, *21* (12), 1137–1143. https://doi.org/10.1016/j.dental.2005.04.002.

(218)   Shin, J.; Matsushima, H.; Chan, J. W.; Hoyle, C. E. Segmented Polythiourethane Elastomers through Sequential Thiol−Ene and Thiol−Isocyanate Reactions. *Macromolecules* **2009**, *42* (9), 3294–3301. https://doi.org/10.1021/ma8026386.

(219)   Silverstein, J. S.; Casey, B. J.; Natoli, M. E.; Dair, B. J.; Kofinas, P. Rapid Modular Synthesis and Processing of Thiol–Ene Functionalized Styrene–Butadiene Block Copolymers. *Macromolecules* **2012**, *45* (7), 3161–3167. https://doi.org/10.1021/ma300304h.

(220)   Sun, H.; Jiang, C.; Ning, N.; Zhang, L.; Tian, M.; Yuan, S. Homogeneous Dielectric Elastomers with Dramatically Improved Actuated Strain by Grafting Dipoles onto SBS Using Thiol–Ene Click Chemistry. *Polym. Chem.* **2016**, *7* (24), 4072–4080. https://doi.org/10.1039/C6PY00581K.

(221)   Cole, M. A.; Jankousky, K. C.; Bowman, C. N. Redox Initiation of Bulk Thiol–Ene Polymerizations. *Polym. Chem.* **2013**, *4* (4), 1167–1175. https://doi.org/10.1039/C2PY20843A.

(222)   Nguyen, L.-T. T.; Devroede, J.; Plasschaert, K.; Jonckheere, L.; Haucourt, N.; Prez, F. E. D. Providing Polyurethane Foams with Functionality: A Kinetic Comparison of Different "Click" and Coupling Reaction Pathways. *Polym. Chem.* **2013**, *4* (5), 1546–1556. https://doi.org/10.1039/C2PY20970E.

(223)   Radl, S. V.; Schipfer, C.; Kaiser, S.; Moser, A.; Kaynak, B.; Kern, W.; Schlögl, S. Photo-Responsive Thiol–Ene Networks for the Design of Switchable Polymer Patterns. *Polym. Chem.* **2017**, *8* (9), 1562–1572. https://doi.org/10.1039/C7PY00055C.

(224)   Serniuk, G. E.; Banes, F. W.; Swaney, M. W. Study of the Reaction of Buna Rubbers with Aliphatic Mercaptans1. *J. Am. Chem. Soc.* **1948**, *70* (5), 1804–1808. https://doi.org/10.1021/ja01185a046.

(225)   Ameduri, B.; Boutevin, B.; Nouiri, M. Synthesis and Properties of Fluorinated Telechelic Macromolecular Diols Prepared by Radical Grafting of Fluorinated Thiols onto Hydroxyl-Terminated Polybutadienes. *J. Polym. Sci. Part Polym. Chem.* **1993**, *31* (8), 2069–2080. https://doi.org/10.1002/pola.1993.080310813.

(226)   Boutevin, G.; Ameduri, B.; Boutevin, B.; Joubert, J.-P. Synthesis and Use of Hydroxyl Telechelic Polybutadienes Grafted by 2-Mercaptoethanol for Polyurethane Resins. *J. Appl. Polym. Sci.* **2000**, *75* (13), 1655–1666. https://doi.org/10.1002/(SICI)1097-4628(20000328)75:13<1655::AID-APP11>3.0.CO;2-A.

(227)   Boutevin, B.; Hervaud, Y.; Moulédous, G. Grafting Phosphonated Thiol on Hydroxy Telechelic Polybutadiene. *Polym. Bull.* **1998**, *41* (2), 145–151. https://doi.org/10.1007/s002890050345.

(228)   Justynska, J.; Hordyjewicz, Z.; Schlaad, H. Toward a Toolbox of Functional Block Copolymers via Free-Radical Addition of Mercaptans. *Polymer* **2005**, *46* (26), 12057–12064. https://doi.org/10.1016/j.polymer.2005.10.104.

(229)   Koňák, Č.; Šubr, V.; Kostka, L.; Štěpánek, P.; Ulbrich, K.; Schlaad, H. Coating of Vesicles with Hydrophilic Reactive Polymers. *Langmuir* **2008**, *24* (14), 7092–7098. https://doi.org/10.1021/la800119w.

(230)   Justynska, J.; Hordyjewicz, Z.; Schlaad, H. New Functional Diblock Copolymers Through Radical Addition of Mercaptans. *Macromol. Symp.* **2006**, *240* (1), 41–46. https://doi.org/10.1002/masy.200650806.

(231)   Campos, L. M.; Killops, K. L.; Sakai, R.; Paulusse, J. M. J.; Damiron, D.; Drockenmuller, E.; Messmore, B. W.; Hawker, C. J. Development of Thermal and Photochemical Strategies for Thiol−Ene Click Polymer Functionalization. *Macromolecules* **2008**, *41* (19), 7063–7070. https://doi.org/10.1021/ma801630n.

(232)   Kharasch, M.; Read, A. T.; Mayo, F. The Peroxide Effect in the Addition of Reagents to Unsaturated Compounds. XVI. The Addition of Thioglycolic Acid to Styrene and Isobutylene. *Chem Ind* **1938**, *57*, 752.

(233)   Kharasch, M. S.; Nudenberg, W.; Mantell, G. J. Reactions of Atoms and Free Radicals in Solution. XXV. The Reactions of Olefins with Mercaptans in the Presence of Oxygen. *J. Org. Chem.* **1951**, *16* (4), 524–532. https://doi.org/10.1021/jo01144a005.

(234)   Justynska, J.; Schlaad, H. Modular Synthesis of Functional Block Copolymers. *Macromol. Rapid Commun.* **2004**, *25* (16), 1478–1481. https://doi.org/10.1002/marc.200400228.

(235)   Cramer, N. B.; Scott, J. P.; Bowman, C. N. Photopolymerizations of Thiol−Ene Polymers without Photoinitiators. *Macromolecules* **2002**, *35* (14), 5361–5365. https://doi.org/10.1021/ma0200672.

(236)   Chen, Y.; Tang, Z.; Zhang, X.; Liu, Y.; Wu, S.; Guo, B. Covalently Cross-Linked Elastomers with Self-Healing and Malleable Abilities Enabled by Boronic Ester Bonds. *ACS Appl. Mater. Interfaces* **2018**, *10* (28), 24224–24231. https://doi.org/10.1021/acsami.8b09863.

(237)   Boileau, S.; Mazeaud-Henri, B.; Blackborow, R. Reaction of Functionalised Thiols with Oligoisobutenes via Free-Radical Addition.: Some New Routes to Thermoplastic Crosslinkable Polymers. *Eur. Polym. J.* **2003**, *39* (7), 1395–1404. https://doi.org/10.1016/S0014-3057(02)00388-9.

(238)   Boyer, C.; Granville, A.; Davis, T. P.; Bulmus, V. Modification of RAFT-Polymers via Thiol-Ene Reactions: A General Route to Functional Polymers and New Architectures. *J. Polym. Sci. Part Polym. Chem.* **2009**, *47* (15), 3773–3794. https://doi.org/10.1002/pola.23433.

(239)   Yu, B.; Chan, J. W.; Hoyle, C. E.; Lowe, A. B. Sequential Thiol-Ene/Thiol-Ene and Thiol-Ene/Thiol-Yne Reactions as a Route to Well-Defined Mono and Bis End-Functionalized Poly(N-Isopropylacrylamide). *J. Polym. Sci. Part Polym. Chem.* **2009**, *47* (14), 3544–3557. https://doi.org/10.1002/pola.23436.

(240)   De Bruycker, K.; Billiet, S.; Houck, H. A.; Chattopadhyay, S.; Winne, J. M.; Du Prez, F. E. Triazolinediones as Highly Enabling Synthetic Tools. *Chem. Rev.* **2016**, *116* (6), 3919–3974. https://doi.org/10.1021/acs.chemrev.5b00599.

(241)   Alder, K.; Pascher, F.; Schmitz, A. Über Die Anlagerung von Maleinsäure-Anhydrid Und Azodicarbonsäure-Ester an Einfach Ungesättigte Koh an Einfach Ungesättigte Kohlenwasserstoffe. Zur Kenntnis von Substitutionsvorgängen in Der Allyl-Stellung. *Berichte Dtsch. Chem. Ges. B Ser.* **1943**, *76* (1–2), 27–53. https://doi.org/10.1002/cber.19430760105.

(242)   Butler, G. B.; Williams, A. G. Low-Temperature Modification of Dienic Polymers via the "Ene" Reaction with 4-Substituted-1,2,4-Triazoline-3,5-Diones. *J. Polym. Sci. Polym. Chem. Ed.* **1979**, *17* (4), 1117–1128. https://doi.org/10.1002/pol.1979.170170416.

(243)   Leong, K.-W.; Butler, G. B. Chemical Reactions on Polymers. II. Modification of Diene Polymers with Triazolinediones via the Ene Reaction. *J. Macromol. Sci. Part - Chem.* **1980**, *14* (3), 287–319. https://doi.org/10.1080/00222338008056715.

(244)   Hilger, C.; Stadler, R. New Multiphase Thermoplastic Elastomers by Combination of Covalent and Association-Chain Structures. *Makromol. Chem.* **1990**, *191* (6), 1347–1361. https://doi.org/10.1002/macp.1990.021910614.

(245)   Hilger, C.; Stadler, R. Cooperative Structure Formation by Directed Noncovalent Interactions in an Unpolar Polymer Matrix. 7. Differential Scanning Calorimetry and Small-Angle x-Ray Scattering. *Macromolecules* **1992**, *25* (24), 6670–6680. https://doi.org/10.1021/ma00050a042.

(246)   Hellmann, J.; Hilger, C.; Stadler, R. Cooperative Self-Assembling in Statistical Copolymers: A New Approach to High-Temperature Thermoplastic Elastomers. *Polym. Adv. Technol.* **1994**, *5* (12), 763–774. https://doi.org/10.1002/pat.1994.220051202.

(247)   Ying, W.; Pan, W.; Gan, Q.; Jia, X.; Grassi, A.; Gong, D. Preparation and Property Investigation of Chain End Functionalized Cis-1,4 Polybutadienes via de-Polymerization and Cross Metathesis of Cis-1,4 Polybutadienes. *Polym. Chem.* **2019**. https://doi.org/10.1039/C9PY00485H.

(248)   Geiselhart, C. M.; Offenloch, J. T.; Mutlu, H.; Barner-Kowollik, C. Polybutadiene Functionalization via an Efficient Avenue. *ACS Macro Lett.* **2016**, *5* (10), 1146–1151. https://doi.org/10.1021/acsmacrolett.6b00679.

(249)   Onchoy, N.; Phinyocheep, P. Preparation and Characterization of Brominated Natural Rubber Applied in Silica-Filled Natural Rubber Vulcanizates. *Rubber Chem. Technol.* **2016**, *89* (3), 406–418. https://doi.org/10.5254/rct.16.84833.

(250)   Sogawa, H.; Monjiyama, S.; Wang, C.-G.; Tsutsuba, T.; Takata, T. New Synthetic Entry to OH-Functionalized Nitrile N-Oxide and Polyfunctional Nitrile N-Oxides For Click Crosslinking and Decrosslinking of Natural Rubber. *Polym Chem* **2018**. https://doi.org/10.1039/C8PY00904J.

Chapter 2

Polybutadiene Vitrimers Based on Dioxaborolane Chemistry and Dual Networks with Static and Dynamic Cross-links

Table of Contents

Chapter 2 - Polybutadiene Vitrimers Based on Dioxaborolane Chemistry and Dual Networks with Static and Dynamic Cross-links

2.1 Introduction

Vitrimers are polymer networks that are able to change their topology through degenerate exchange reactions.[1–4] As a result, vitrimers behave like elastic solids when the topology of the network is frozen and like viscoelastic liquids when exchange reactions are operating. The degenerate nature of the exchange reactions ensures that the number of chemical bonds remains constant regardless of the temperature. Vitrimers present a unique combination of properties, which can include recyclability, creep resistance, enhanced adhesion, adjustable solid-to-liquid transition, environmental stress-cracking resistance, shape memory, and self-healing ability.[3–9]

Most vitrimers have been prepared so far through a step growth process,[2,4,5,10–17] yet examples of vitrimers prepared by a chain-growth polymerization or from thermoplastic precursors have been reported recently.[3,7,18–23] The latter approach is particularly attractive from an application and industrial point of view, as it allows transforming thermoplastics into vitrimers without changing existing syntheses. With more than 27 million tons produced per year, conventional vulcanized elastomers raise important environmental issues because of their non-recyclability. Polydiene (co)polymers account for more than 80% of the global rubber market. Transforming these elastomers into vitrimers would endow them with recyclability, welding ability and potentially self-healing properties.[24–30] For instance, Tang, Guo *et al.* reported the synthesis of recyclable and self-reparable styrene-butadiene rubbers incorporating dioxaborolane cross-links.[28] However, while creep resistance at service temperatures in high glass transition temperature (T_g) and semi-crystalline vitrimers is ensured by the absence of motion of polymer molecules, the situation is drastically different for elastomeric vitrimers. For such materials, creep resistance is solely provided by the chemical cross-links, which translates for vitrimers into the ability to quench the exchange reaction.[5,19,31,32] In that context, ideal exchange reactions are those with a large activation energy, as the life time of the dynamic links would be extremely long at room temperature, to

prevent creep, and very short at high temperature, to provide good processability.[33] On the other hand, exchange reactions that are highly dynamic but present a low activation energy, such as dioxaborolane metathesis,[7] appear as poor candidates to design elastomers with good creep resistance. Yet, dioxaborolanes are very interesting dynamic links to prepare vitrimers thanks to their compatibility with a large number of chemical functions and their very high bond dissociation energy.[7,34–36] Therefore, we were interested to investigate the possibility to prepare creep resistant vitrimers relying on dioxaborolane cross-links. To conduct this model study, we decided to use a low molar mass unentangled polybutadiene (PB) as a vitrimer precursor, in order to emphasize the effect of the dynamic cross-links onto creep resistance. Using a bis-thiol dioxaborolane cross-linker, vitrimers with various cross-linking degrees are obtained in a single-step and used to perform a comprehensive study of the impact of the cross-linking density onto the physicochemical and thermomechanical properties of these materials. In order to develop reprocessable and recyclable elastomers with improved creep resistance, dual networks incorporating various fractions of dynamic and static cross-links were also prepared and compared to networks containing solely static or dynamic cross-links.
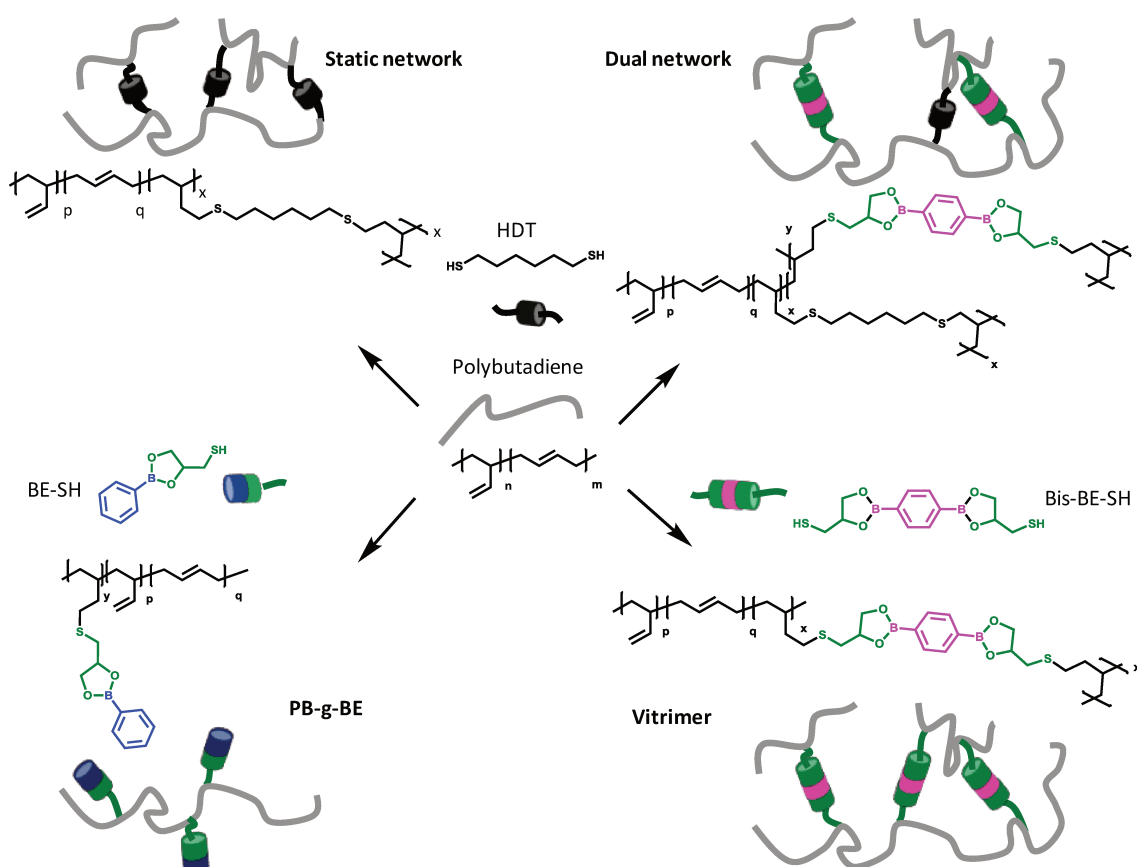

Figure 2.1. Synthesis of: polybutadiene grafted with dioxaborolanes (bottom left), polybutadiene vitrimers (bottom right), polybutadiene dual (top right) and static (top left) networks.

2.2 Experimental section

2.2.1 Materials

Polybutadiene (PB) (vinyl content = 84 mol %, M_n = 3.9 kg/mol, Đ = 1.48), 1-thioglycerol (98%), 1,6-hexanedithiol (96%), benzene-1,4-diboronic acid (98%), phenylboronic acid (97%), 1,2-propanediol (98%), 2,2'-azobis(2-methylpropionitrile) (AIBN) and magnesium sulfate ($MgSO_4$) were purchased from Sigma-Aldrich. Toluene, anisole, tetrahydrofuran (THF) and methanol were obtained from Carlos Erba and $CDCl_3$ from Eurisotop. Unless otherwise noted, reagents were used without further purification. Solvents (including deuterated solvents) were dried over activated 3Å molecular sieves under an inert atmosphere for at least 72 hours prior to use. Glassware used for dioxaborolane and vitrimer syntheses was oven-dried and then heated with a heat gun while being purged with dry argon (< 0.5 ppm H_2O). AIBN was recrystallised from methanol. Diols were dried over $MgSO_4$ and filtered before use.

2.2.2 Characterisation

Size exclusion chromatography (SEC). SEC was performed on a Viscotek GPCmax/VE2001 connected to a triple detection array (TDA 305) from Malvern. Molecular weights were determined based on conventional calibration with monodisperse polystyrene (PS) standards.

Fourier-transform infrared (FT-IR) spectroscopy. FT-IR spectroscopy was conducted on a Tensor 37 spectrometer from Bruker in solid state and recorded in attenuated total reflectance (ATR) mode and converted to absorbance spectra.

Nuclear magnetic resonance (NMR) spectroscopy. ^{1}H and ^{13}C NMR spectra were recorded at 297 K on a Bruker AVANCE 400 spectrometer at 400 MHz and 100 MHz, respectively, and referenced to the residual solvent peaks (^{1}H, δ 7.26 for $CDCl_3$; ^{13}C, δ 77.16 for $CDCl_3$).

Rheological characterizations. Viscoelastic properties of polybutadiene samples were determined using a TA Instruments ARES G2 rotational rheometer equipped with parallel plate geometry (25 mm in diameter) in a convection oven under air.

Step stress-creep recovery experiments. Creep-recovery tests were carried out between 25 °C and 120 °C by imposing a constant stress over time (creep) and releasing it for a certain period of time (recovery) while measuring the strain. The linear part of variation of the strain versus time of the creep-recovery plots was fitted using linear regression. The shear creep compliance J_{eq} was determined from the intercept of the linear fit. The strain rate $\dot{\gamma}$ was determined from the slope of the linear fit. The viscosity η and the relaxation time τ were calculated from equations 1 and 2:

Equation 2.1.
$$\eta = \frac{\sigma}{\dot{\gamma}}$$

Equation 2.2.
$$\tau = \eta J_{eq}$$

Stress relaxation experiments. Stress relaxation measurements on polybutadiene samples were conducted between 60 °C and 160 °C by applying a constant shear strain of 1%. The zero-shear viscosity η_0 and the relaxation time τ were calculated from stress relaxation experiments using equations 3 and 4, respectively:

Equation 2.3.
$$\eta_0 = \int_0^\infty G(t)dt$$

Equation 2.4.
$$\tau = \frac{\int_0^\infty t\,G(t)dt}{\int_0^\infty G(t)dt}$$

Differential scanning calorimetry (DSC). Glass transitions of materials were determined by DSC. Sequences of temperature ramps (heating, cooling, heating) in the −50 °C to 60 °C range were performed at 10 °C/min using a TA Instruments Q1000 equipped with a liquid nitrogen cooling accessory and calibrated using sapphire and high purity indium metal. All samples were prepared in hermetically sealed pans (5−10 mg/sample) and were referenced to an empty pan. The reported T_g values are from the second heating cycle.

Thermogravimetric analysis (TGA). TGA analyses were conducted on a TG 209 F1 Libra from Netzsch under nitrogen flow. The samples were heated at a constant rate of 10 °C/min from 25 to 500 °C.

Dynamic mechanical analysis (DMA). DMA analyses were conducted on a TA Instruments Q800 in tension mode. Heating ramps were performed from -75 °C to 120, 150 or 250 °C at a constant rate of 3 °C/min with a maximum strain amplitude of 1% at a fixed frequency of 1 Hz.

Tensile tests and recycling. Uniaxial tensile tests were performed on dumbell-shaped specimens (gauge length 10 mm) using an Instron 5564 tensile machine mounted with a 100 N cell. Specimens were tested in quintuplicates at a fixed crosshead speed of 10 mm/min. Testing was carried out at room temperature for all materials. Engineering stress-strain curves were obtained through measurements of the tensile force F and crosshead displacement Δl by defining the engineering stress as $\sigma = F/S_0$ and the strain as $\gamma = \Delta l/l_0$, where S_0 and l_0 are the initial cross-section and gauge length of the specimens, respectively. The Young's modulus was determined as the initial slope of the engineering stress-strain curves. Following tensile testing, the vitrimer specimens were cut down to small fragments and reshaped via compression moulding for 10 min at 150 °C under a load of 3 tons in order to test their recyclability over several reprocessing cycles. Tensile tests were repeated at room temperature for each generation.

Adhesion measurements between dual networks. Double networks were molded under press at 150 °C for 10 min into rectangular shape of 25 mm in length, 5 mm in width and 1.5 mm in thickness. The samples still in their molds were overlapped with a length of 15 mm and were pressed at 150 °C for 2 min under a pressure of 10 kPa. Lap joints were left to slowly cool down to room temperature and de-molded. Lap-shear tests were performed with a speed of 10 mm/min using an Instron 5564 tensile machine mounted with a 100 N cell.

Swelling tests and cleavage by diolysis of boronic ester vitrimers, static and dual networks. The samples (typically, with an initial mass og 200 mg) were immersed in dried THF (typically 15 mL) at room temperature and weighed after 24h (mass of the swollen sample). Then, the samples were dried under vacuum at 120 °C until complete dryness and weighed again (mass of the dried sample). All tests were performed in triplicate. The swelling ratio and the insoluble fraction were calculated according to the following equations:

Equation 2.5.
$$Insoluble\ fraction = \frac{Mass\ dried}{Initial\ Mass}$$

Equation 2.6. $$Swelling\ ratio = \frac{Mass\ swollen - Mass\ dried}{Mass\ dried}$$

The samples (initial mass: 50-250 mg of polymer, *n* equivalents of dioxaborolane functions) were put in THF at room temperature and 1,2-propanediol ($50-150 \times n$ equivalents for vitrimers and dual networks while 25 wt % was used for the static networks) was added. After 24 h of immersion, the samples were removed from the solution (THF + diols) and dried under vacuum at 120 °C until complete dryness and weighed again (mass of the dried sample). All tests were performed in triplicate. The insoluble fraction was calculated according to **equation 2.5**.

2.2.3 Syntheses
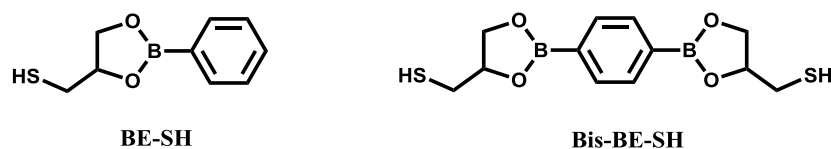
Scheme 2.1. Thio-dioxaborolanes used in this study.

Synthesis of 4-thioethyl-2-phenyl-1,3,2-dioxaborolane (BE-SH): The synthesis of **Bis-BE-SH** was adapted from the literature.[28] In a typical experiment, thioglycerol (1.0 eq) and phenylboronic acid (1.05 eq) were mixed in THF (2 mL/1 mmol boronic acid) at room temperature and stirred until complete dissolution of all compounds. $MgSO_4$ (3.0 eq) was added stepwise and the mixture was stirred at room temperature for 5 hours, filtered and concentrated under reduced pressure. The purified thio-functionalized dioxaborolane (**BE-SH**) was transferred directly to a dried and purged Schlenk flask and stored under an inert atmosphere (88%). ^{1}H NMR (400 MHz, CDCl$_3$): δ 7.81 p.p.m. (d, J = 5.6 Hz, 2H), 7.49 (m, 1H), 7.39 (m, 2H), 4.73 (q, J = 6.3 Hz, 1H), 4.48 (m, 1H), 4.15 (m, 1H), 2.81 (m, 2H), 1.49 (t, J = 8.8 HZ, 1H). ^{13}C NMR (100 MHz, CDCl3): δ 135.0, 131.8, 128.0, 77.6, 69.9, 29.8. Carbon adjacent to boron not detected. Purity: no diol detected by ^{1}H NMR.

Synthesis of 2,2'-(1,4-phenylene)-bis[4-thioethyl-1,3,2-dioxaborolane] (Bis-BE-SH): In a typical experiment, thioglycerol (2.0 eq) and benzene-1,4-diboronic acid (1.05 eq) were mixed in THF (2 mL/1 mmol boronic acid) at room temperature and stirred until complete dissolution of all compounds. $MgSO_4$ (6 eq.) was added stepwise and the mixture was stirred at room temperature for 5 hours, filtered and concentrated under reduced pressure. The

purified bis-thiol dioxaborolane cross-linker (**Bis-BE-SH**) was transferred directly to a dried and purged Schlenk flask and stored under an inert atmosphere (92%). ^{1}H NMR (400 MHz, CDCl$_3$): δ 7.81 (s, 4H), 4.74 (q, J = 6.2 Hz, 2H), 4.50 (m, 2H), 4.17 (m, 2H), 2.81 (m, 4H), 1.48 (t, J = 8.6 HZ, 2H). ^{13}C NMR (100 MHz, CDCl$_3$): δ 134.3, 77.7, 70.0, 29.8. Carbon adjacent to boron not detected. Purity: no diol detected by ^{1}H NMR.

Grafting procedure of BE-SH onto polybutadiene: In a typical experiment, polybutadiene (PB) (1.00 g, 15.5 mmol of vinyl groups) was dissolved in anhydrous anisole (20 wt%), followed by **BE-SH** (0.284 g, 1.46 mmol). Then, AIBN (1.2 mg, 0.008 mmol) was dissolved in anisole (0.5 mL) in another vial and added to the solution of polybutadiene and **BE-SH**. The mixture was bubbled with argon for 30 min. Then, argon flow was stopped and the mixture was heated at 100°C for 60 min (9 × $\tau_{1/2}$). Finally, the polymer was precipitated in 20 mL of anhydrous methanol. The isolated residue was dried under high vacuum overnight at 100 °C.

Vitrimers syntheses: In a typical experiment, PB (1.00 g, 15.5 mmol of vinyl groups) was dissolved in anhydrous anisole (20 wt%), followed by **Bis-BE-SH** (0.275 g, 0.89 mmol). Then, AIBN (0.73 mg, 0.004 mmol) was dissolved in anisole (0.5 mL) in another vial and added to the solution of polybutadiene and **Bis-BE-SH**. The mixture was bubbled with argon for 30 min. Then, argon flow was stopped and the mixture was heated at 100°C for 60 min (9 × $\tau_{1/2}$). The obtained gel was dried under high vacuum overnight at 100 °C.

Dual networks syntheses: Dual networks were obtained following the same procedure as described above, but replacing **Bis-BE-SH** by a mixture of **Bis-BE-SH** and 1,6-hexanedithiol.

Static networks syntheses: In a typical experiment, PB (3.00 g, 46.6 mmol of vinyl groups) was dissolved in anhydrous THF (67 wt%), followed by 1,6-hexanedithiol (0.333 g, 2.2 mmol). Then, a solution of DMPA (5.7 mg, 0.02 mmol) in THF (0.5 mL) was added to the mixture of polybutadiene and 1,6-hexanedithiol. The resulting solution was poured into a mold and cured for 5 min in a UV chamber from UWAVE at a wavelength of 365 nm and a power of 142 mW/cm^2. The obtained gel was dried under high vacuum overnight at 100 °C.

2.3 PB grafting with a thio-functionalized dioxaborolane

The functionalization of PB was first studied with **BE-SH** in order to quantify the grafting efficiency as a function of the targeted functionalization degree, as well as the impact of this chemical modification onto the physicochemical properties of PB (**Figure 2.1**). The grafting of PB was performed in anisole, keeping a constant ratio [AIBN]/[**BE-SH**] of 0.01, and varying the [**BE-SH**]/[C=C] ratio to tune the functionalization degree.
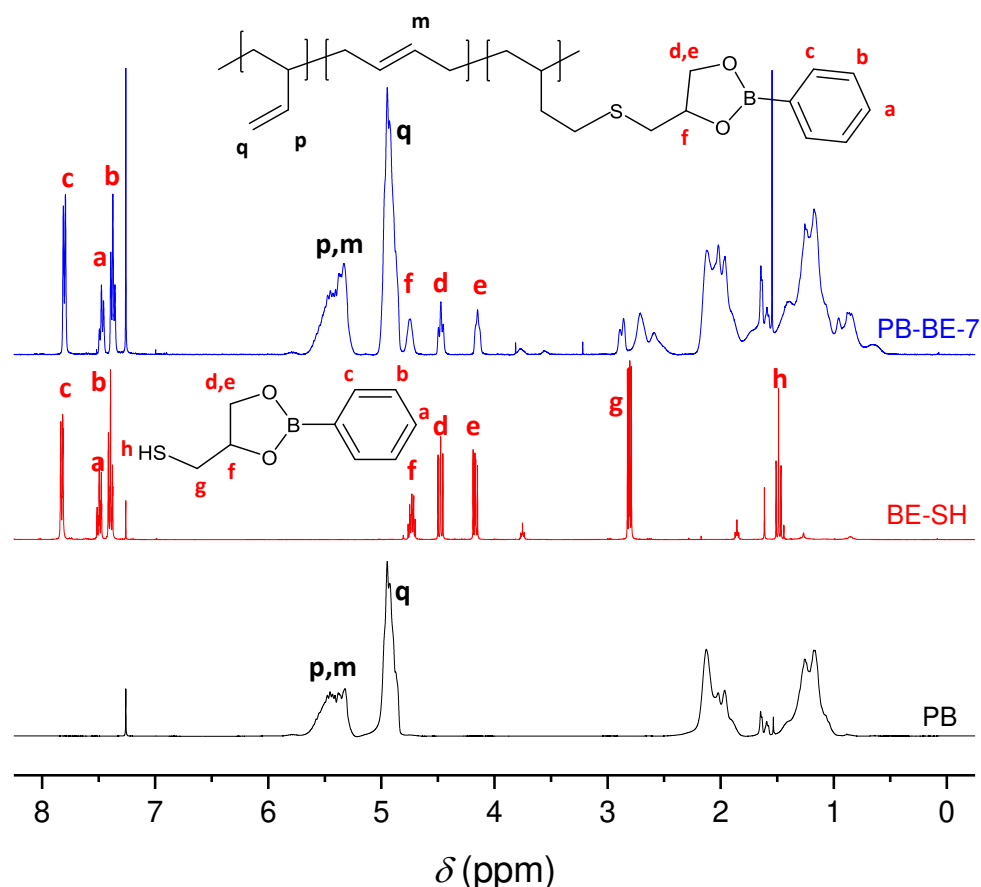
Figure 2.2. ^{1}H-NMR spectra in CDCl$_3$ of **PB-BE-7** after purification by precipitation into anhydrous methanol (grafting yield = 89%, f = 9%) (top, blue), **BE-SH** (middle, red), and the starting neat PB (bottom, black).

2.3.1 ^{1}H-NMR analysis

The efficiency of **BE-SH** grafting onto PB was quantified by performing ^{1}H NMR analysis of grafted PBs before and after purification by precipitation into anhydrous methanol. A typical spectrum of an isolated **BE-SH**-grafted PB after purification by precipitation into anhydrous methanol is displayed in **Figure 2.2**. Peaks at 7.79, 7.48 and 7.38 ppm, characteristic of the phenyl group of the phenylboronic ester, as well as peaks corresponding

to the proton of the dioxaborolane ring (-OCH2- and –CH-C), *e.g.* 4.75, 4.48 and 4.15 ppm, confirmed the grafting of **BE-SH** onto PB. The functionalization degree, which corresponds to the number of repeating unit carrying a pendant dioxaborolane, and the grafting yields are reported in **Table 2.1**. They were calculated according to the following equations:

Equation 2.7.
$$f(\%) = \frac{Integration\ proton\ d}{(Integration\ all\ protons - 11\ x\ Integration\ proton\ d\ )/6}$$

Equations 2.8.
$$Grafting\ yield\ (\%) = \frac{Integration\ proton\ d\ after\ precipitation}{Integration\ proton\ d\ before\ precipitation}$$

Grafting yields were high regardless of the targeted functionalization degree. Yet, they slightly increased with the molar ratio [**BE-SH**]/[C=C], going from 85% to 92% with functionalization degrees increasing from 4 to 13%.

Table 2.1. Characterization of polybutadiene grafted with **BE-SH**.

Sample	f (%) measured	Grafting yield (%)	Vinyl (%)[a]	Vinylene (%)[b]	f measured + vinyl + vinylene (%)	$M_{n,th}$ (g/mol)[c]	$M_{n,exp}$ (g/mol)	$Đ$
PB	-	-	85	15	100	3900	3900	1.47
PB-BE-3	4	85 ± 2.5	70	13	87	4460	4170	1.39
PB-BE-5	6	81 ± 1.6	66	13	85	4740	4700	1.48
PB-BE-7	9	89 ± 1.5	60	12	81	5160	4950	1.44
PB-BE-9	13	92 ± 0.9	55	12	80	5700	5300	1.45

[a] From equation 9; [b] From equation 10; [c] $M_{n,th} = 3900 + (3900/54) \times f$ measured $\times M_{BE-SH}$.

Following the sum (measured functionalization degree + vinyl + vinylene) as a function of the functionalization degree provides valuable information (**Table 2.1**). Indeed, in the absence of side reactions consuming carbon-carbon double bonds, this sum should remain equal to 100%, regardless of the functionalization degree. The greater the difference, the more side reactions are taking place. Going from a functionalization degree of 0 to 13%, the percentage of vinyl bonds decreased from 85 to 55%, while the percent of vinylene bonds only decreased from 15 to 12%. These values were calculated based on the following equations:

Equation 2.9. $\quad Vinyl\ (\%) = \dfrac{(Integration\ proton\ q)/2}{(Integration\ all\ protons-\ 11\ x\ Integration\ proton\ d\ )/6}$

Equation 2.10. $Vinylene\ (\%) = \dfrac{((Integration\ proton\ m+p)-\frac{Integration\ proton\ q}{2})/2}{(Integration\ all\ protons-\ 11\ x\ Integration\ proton\ d\ )/6}$

This observation reflects the well-known higher reactivity of pendant vinyl groups towards thiyl radicals, as compared to main-chain vinylene groups.[37] It also highlights the occurrence of intramolecular cyclizations involving mostly pendant vinyl groups, as the sum (measured functionalization degree + vinyl + vinylene) decreased from 100 to 80%.[37,38] These intramolecular cyclizations can occur between two adjacent vinyl bonds, two adjacent vinylene bonds, or between adjacent vinyl and vinylene bonds to yield cyclohexane and cyclopentane derivatives. Given the high vinyl content of the polybutadiene used in this study, and the higher reactivity of vinyl functions as compared to vinylene functions, the side-reactions mostly involved vinyl bonds here (**Table 2.1**). The NMR spectrum of **PB-BE-7** (**Figure 2.2**), which presents a functionalization degree of 9% (**Table 2.1**), displays strong peaks at 0.96 and 0.87 ppm corresponding to the methyl group of cyclopentane derivatives obtained by intramolecular cyclization of two adjacent vinyl groups.[39]

2.3.2 SEC and DSC measurements

As should be expected, the number average molar mass, M_n, increased with the grafting functionality. Good matches were obtained between theoretical and experimental M_n values (**Table 2.1, Figure 2.3**), indicating that minimal radical cross-linking and chain scission are taking place under these conditions. The low and constant dispersities of the various grafted PB samples further confirm the absence of undesirable non-dynamic cross-linking. These results are consistent with the low amount of AIBN used to perform **BE-SH** grafting.

The impact of the functionalization degree f on T_g of the PB was investigated by DSC. The T_g of the functionalized PB increases significantly with f, going from -29 °C for neat PB to 2 °C for $f = 13$ % (**Figure 2.3**). This increase of the T_g is a result of the introduction of 2-phenyl-1,3,2-dioxaborolane pendant groups capable of creating π-π interactions as well as coordinate covalent bonds. Therefore, the design of elastomeric vitrimers from low molecular

weight PB precursors will require a fine adjustment of the grafting density in order to have sufficient cross-links to ensure network formation while maintaining sub-ambient T_g values.
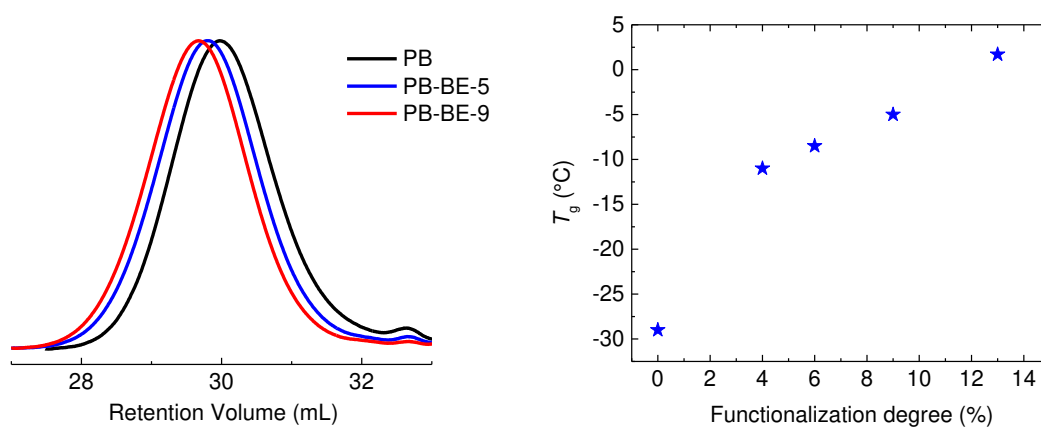

Figure 2.3. Left side: SEC chromatograms of neat PB (black), PB-BE-5 (blue) and PB-BE-9 (red). Right side: Glass transition temperature (T_g, °C) of PB grafted with **BE-SH** as a function of the functionalization degree f.

2.4 Vitrimer synthesis and characterisation

2.4.1 Vitrimer formation

The synthesis of PB vitrimers was achieved following the same procedure used for PB grafting, simply replacing **BE-SH** with **Bis-BE-SH** (**Figure 2.1**). This way, various cross-linking densities, *i.e.* **Bis-BE-SH** cross-linker per chain, can be obtained by simply adjusting the concentration of **Bis-BE-SH** in the reaction medium. Regardless of the amount of cross-linker per chain added, *e.g.* from 3 to 7, no macrophase separation was observed in the final material and colorless transparent polymers were always obtained. The grafting of **Bis-BE-SH** in vitrimers was confirmed by FT-IR, with the presence of stretching vibration bands characteristic of the dioxaborolane moiety (1220 cm^{-1} O-C, 1310 and 1360 cm^{-1} B-C), and the absence of a stretching vibration band associated to the S-H bond around 2560 cm^{-1}.

4.4.2 Dissolution of vitrimers

Swelling experiments were also conducted. Samples were immersed in dried THF at room temperature and weighed after 24h. While low molar mass PB cross-linked with 3 **Bis-BE-SH** per chain was soluble in THF, all other networks prepared with the **Bis-BE-SH** cross-linker were insoluble under these conditions, with insoluble fractions increasing from 75 to 93% with the content of **Bis-BE-SH** grafted increasing from 4 to 7 per chain. Static networks prepared with 1,6-hexanedithiol instead of **Bis-BE-SH** were all insoluble, even with as little as two cross-linkers per chain, and showed insoluble fractions higher than that of the corresponding vitrimers (**Figure 2.4**). As should be expected, swelling ratios decreased with the cross-linking degree, for both vitrimers and static networks. Interestingly, the swelling ratios of vitrimers were 1.5 to 2 times higher than the swelling ratios of the corresponding static networks (**Figure 2.4**). This observation is consistent with previous reports on vitrimers showing that vitrimer networks swell more than identical non-dynamic networks when exchange reactions between cross-links can take place during the swelling tests.[3]
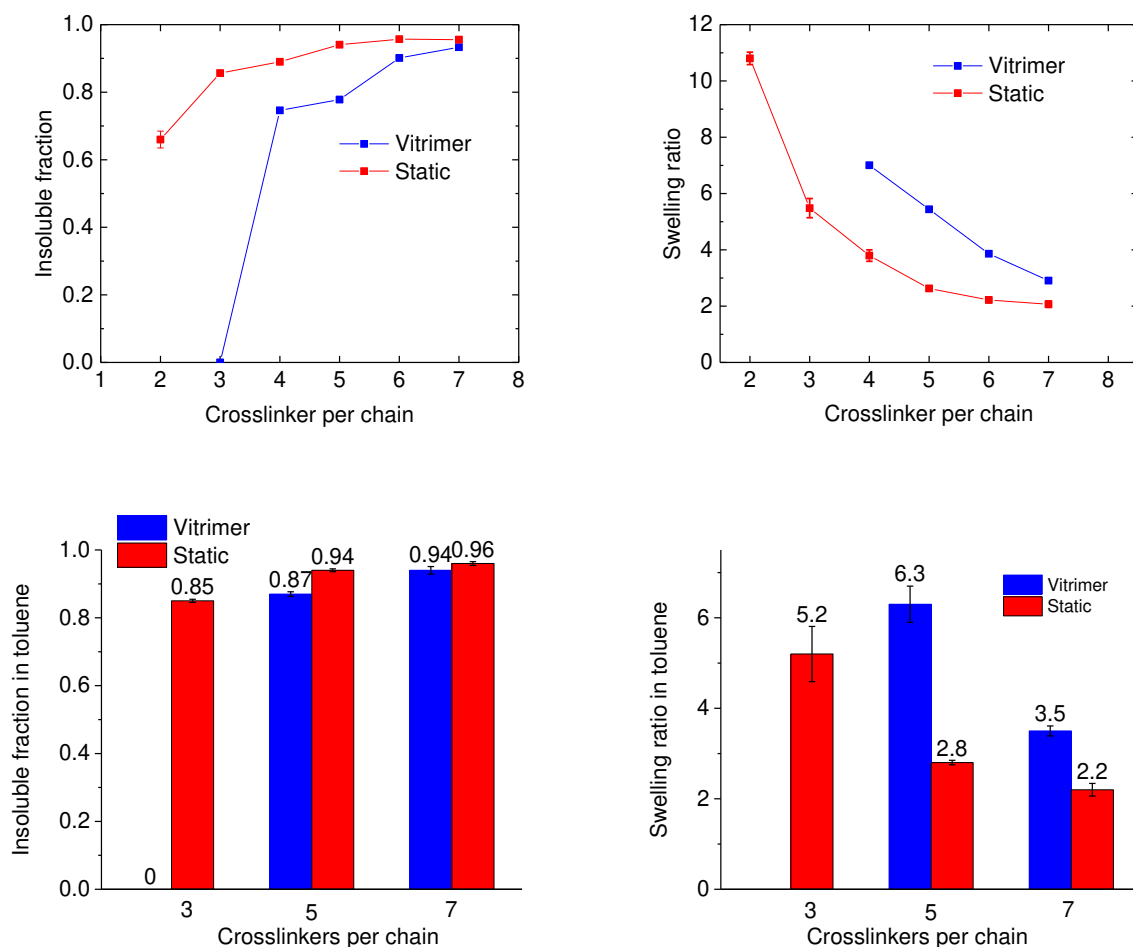
Figure 2.4. Insoluble fraction (left side) and swelling ratio (right side) of vitrimers (blue) and static networks (red) as a function of the number of cross-linker per chain under different solvents. Top: After 24h in THF at room temperature. Bottom: After 24 h in toluene at room temperature.

Depending on numerous parameters (*e.g.* the cross-link density, the M_n of the polymer chains constituting the network, the presence or not of exchangeable bonds within the backbone of the polymer chains, the ratio of pendant exchangeable groups to cross-links, the dynamics of exchange, the time of observation, the quality of the solvent) vitrimers can partially or completely dissolve during swelling tests.[3,40] This dissolution does not necessarily imply a decrease of the overall connectivity of the systems. Indeed, the formation of intramolecular loops during the reorganization of the gels can lead to soluble linear, cyclic and/or (hyper)branched polymers, in proportion that will depend on the parameters listed previously. Vitrimers prepared from low molecular weight polybutadienes, and which present a low number of cross-links per chain that are dynamic under the conditions of the swelling experiments (temperature and time), are particularly prone to undergoing such topological

98

rearrangements. Indeed, the vitrimer containing 5 **Bis-BE-SH** per chain, **PB-BE-V5**, became fully soluble in THF after 72 h, while the vitrimer containing 7 **Bis-BE-SH** per chain, **PB-BE-V7**, became fully soluble in THF after 120 h at room temperature. In toluene, the insoluble fraction of the vitrimer containing 5 **Bis-BE-SH** per chain, **PB-BE-V5**, was 87% and 69% after 24h and seven days of immersion at room temperature, respectively (**Figure 2.4**). This significant difference of insoluble fractions after prolonged immersion time in THF and toluene at room temperature reflects the faster dynamics of exchange of dioxaborolane cross-links in THF as compared to toluene. This finding indicates that solubility tests conducted under conditions where the cross-links are dynamic can lead to inaccurate assessment of the actual crossliking density of vitrimers. Such observation could apply for example to semi-crystalline polyolefin vitrimers containing few cross-links per chain and for which solubity tests are performed over prolonged time at high temperature.[7,22,23]
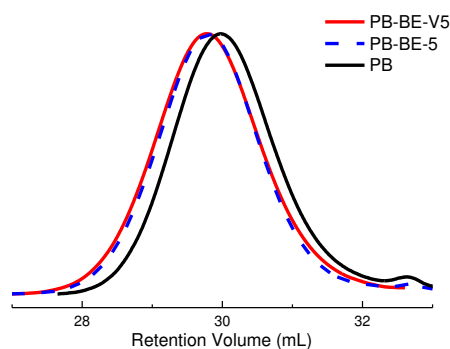

Figure 2.5. SEC chromatograms of **PB-BE-V5** after diolysis (red), **PB-BE-5** (blue, dashed) and PB (black).

As evidenced by the complete dissolution of vitrimers after prolonged immersion in THF, the network formation occurred with limited formation of static cross-links caused by radical recombination. To get more quantitative information, the vitrimers were swollen in THF and cleaved by selective diolysis of the boronic ester cross-links through transesterification with a large excess of 1,2-propanediol as compared to **Bis-BE-SH**. All vitrimers completely dissolved within few minutes under this treatment. The polymer recovered after diolysis of the vitrimer containing 5 **Bis-BE-SH** per chain, **PB-BE-V5**, was analyzed by SEC (**Figure 2.5**). The M_n (4400 g/mol) and $Đ$ (1.53) of the polymer were almost identical to that of the PB grafted with 5 **BE-SH** per chain (**PB-BE-5 Table 2.1**; M_n = 4700 g/mol and $Đ$ = 1.48). This result indicates that vitrimer synthesis via radical grafting of **Bis-BE-SH** onto PB occurred

with minimal radical cross-linking and chain scission. It also indicates that **BE-SH** and **Bis-BE-SH** have comparable reactivity for radical grafting onto PB.

2.4.3 Thermo-mechanical properties of vitrimers.

2.4.3.1 Dynamic mechanical analysis (DMA)

The cross-linked nature of PB vitrimers prepared by radical grafting of **Bis-BE-SH** was further confirmed by dynamic mechanical analysis (DMA). Whereas the low molar mass 1,2-polybutadiene does not present a rubbery plateau above its T_g, vitrimers show a plateau regime above their T_g, characteristic of cross-linked systems (**Figure 2.6**). The vitrimers exhibit increases to both the storage modulus of the rubbery plateau and the T_g as the cross-linking density is increased, which is to be expected for highly cross-linked elastomers.
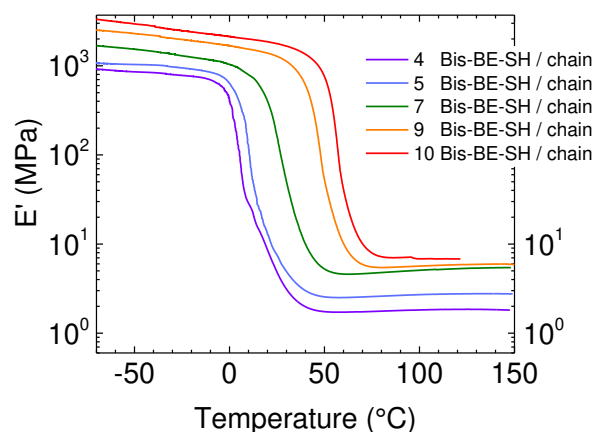

Figure 2.6. Evolution of the storage modulus of vitrimers as a function of temperature for various cross-linking densities.

2.4.3.2 Calorimetry

To quantify the respective impact of the cross-linking density and of the chemical nature of the cross-links onto the T_g of vitrimers, and to determine the maximal amount of **Bis-BE-SH** that can be introduced while keeping a sub-ambient T_g, the T_g values of vitrimers and model static networks were measured by DSC as a function of the cross-linking density (**Figure 2.7**). Starting from a T_g of −29 °C for neat polybutadiene, the T_g values of both networks progressively increase with the cross-linking density. Yet, the increase is much more pronounced for vitrimers than for static networks, with T_g values of 27 and 0 °C, respectively, for the vitrimer and the static network prepared with 8 cross-linkers per chain on average (**Figure 2.7**). This difference of T_g values between vitrimers and static networks is a consequence of the distinct chemical nature of their respective cross-links, with vitrimers

containing rigid dioxaborolane cross-links capable of creating physical (π-π) and chemical (coordinate covalent bonds) intermolecular interactions.[28,41] Vitrimers with 3, 5 and 7 **Bis-BE-SH** cross-linkers per chain displayed T_g values of −10, 2 and 14 °C, respectively, and can therefore be used to conduct model studies on elastomeric vitrimers. If we focused our effort in this study on synthesizing vitrimers from a low molecular weight PB precursor, it should be mentioned that the use of a high molecular weight PB precursors would allow introducing much less dioxaborolane cross-linkers to prepare vitrimers,[7,28] and therefore obtain materials with significantly lower T_g, if desired.
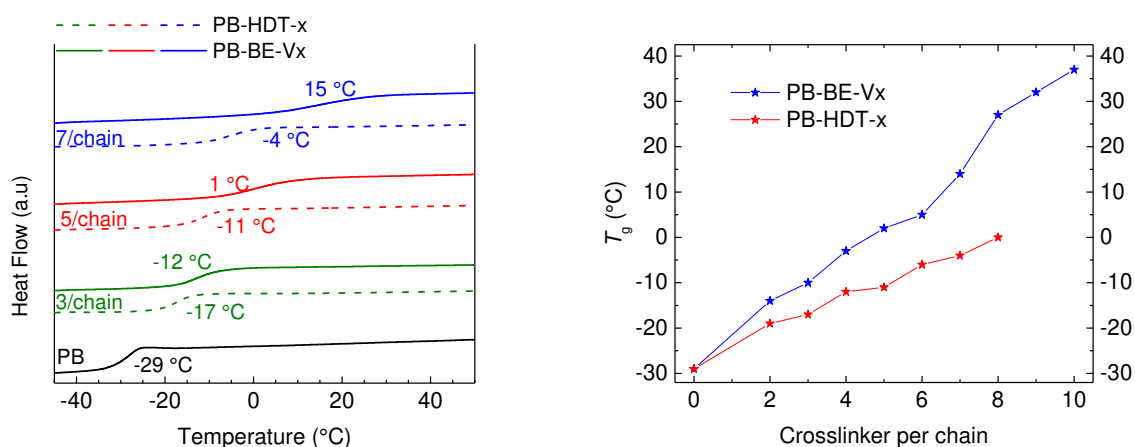

Figure 2.7. Left side: DSC curves of static networks (dashed lines) and vitrimers (solid lines) with various crosslinking densities, and of the polybutadiene precursor. Right side: Glass transition temperatures of vitrimers (blue) and static networks (red) as a function of the number of cross-links per chain.

2.4.3.3 Thermogravimetric analysis (TGA)

The thermal stability of vitrimers and model static networks were assessed by thermogravimetric analysis (TGA), performing heating ramps from 25 °C to 500 °C (**Figure 2.8**). All networks, vitrimer and static, showed excellent thermal stability (superior to neat PB) up to 375 °C. For example, regardless of the cross-linking density, all vitrimers showed weight loss lower than 1 wt % at 300 °C, whereas neat PB lost 2.6 wt % at this temperature. Nonetheless, the temperature at which 10 wt % is lost decreased with the cross-linking density, going from 418 °C for the neat polybutadiene to 409 °C for the 3 cross-linkers per chain and 395 °C for the 7 cross-linkers per chain (**Figure 2.8**). The static and the vitrimer networks showed very similar trends in term of thermal stability, further confirming the thermal stability of dioxaborolane.[7]
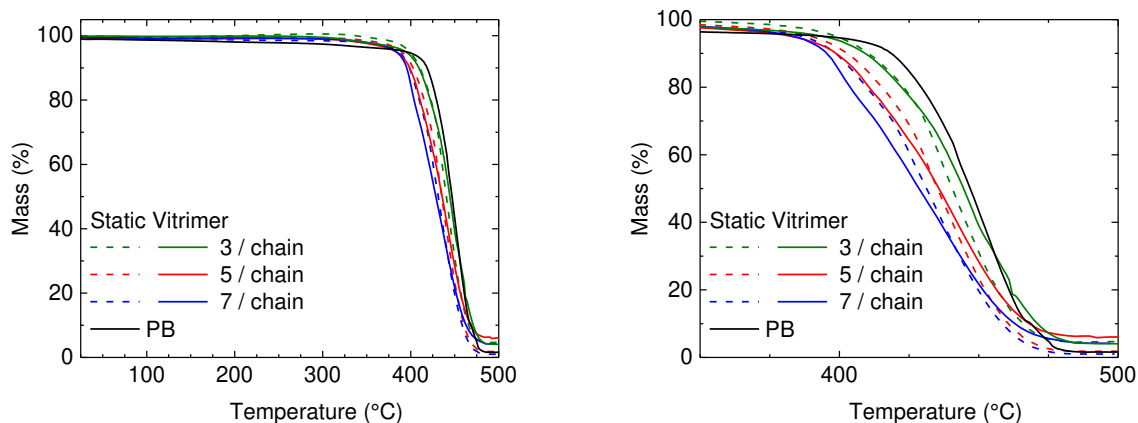
Figure 2.8. Thermogravimetric analysis of the polybutadiene precursor (black) and of vitrimers (solid line) and their static network counterparts (dashed line) with various cross-linking densities. Left: From 25 °C to 500 °C. Right: From 350 to 500 °C.

2.4.4 Flow properties of vitrimers

The aptitude of vitrimers to be processed and recycled while being permanently cross-linked reflects their ability to flow thanks to chemical exchange reactions taking place within the network. The dynamics of exchange within vitrimer networks depend on the rate constant of the chemical exchange reaction, the concentration, and the mobility of the chemical species involved in the exchange reaction. Therefore, for a given exchange reaction and a given thermoplastic precursor, the viscoelastic properties of vitrimers will depend on the cross-linking density, the concentration of pendant exchangeable groups (if present), and the temperature.
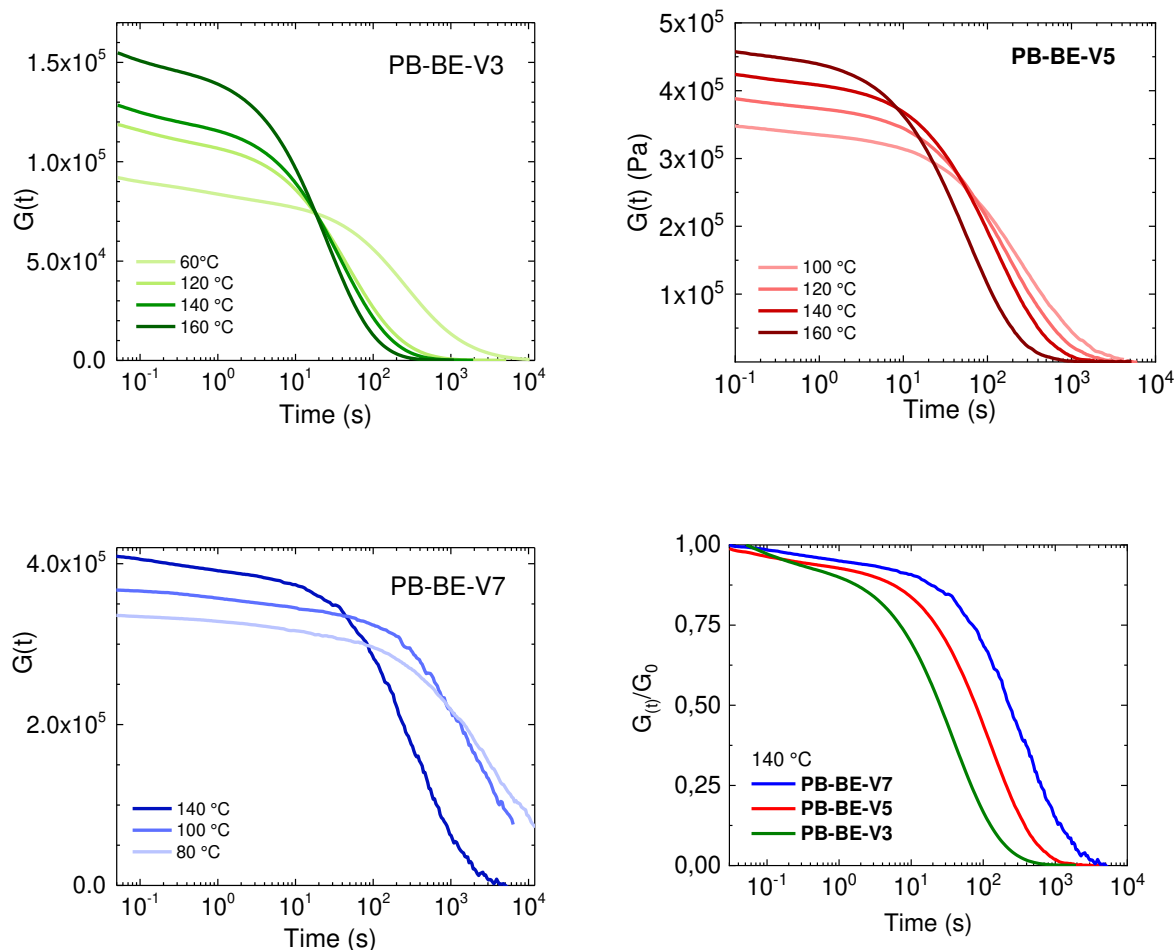
Figure 2.9. Stress relaxation of **PB-BE-V3** (top, left), **PB-BE-V5** (top, right) and **PB-BE-V7** (bottom, left) at different temperatures. Bottom, right: Normalized stress relaxation of **PB-BE-V3** (green), **PB-BE-V5** (red) and **PB-BE-V7** (blue) at 140 °C.

2.4.4.1 Stress relaxation

The dynamics of network reshuffling through dioxaborolane exchange reactions were measured by performing stress relaxation experiments at various temperatures on vitrimers containing 3 (**PB-BE-V3**), 5 (**PB-BE-V5**) and 7 (**PB-BE-V7**) **Bis-BE-SH** cross-linkers per chain (**Figures 2.9**). All of the vitrimers completely relaxed stress, further confirming that the radical grafting of **Bis-BE-SH** onto PB occurred with minimal radical cross-linking. The modulus at $t = 0.1$ s, G_0, increased with the cross-linking density and temperature, as predicted by the theory of rubber elasticity [42–45] and previously confirmed by the DMA measurements (**Figures 2.6 and 2.9**). The relaxation times increased with increasing the cross-link density, going from 128 s for **PB-BE-V3**, to 293 s for **PB-BE-V5** and 684 s for

PB-BE-V7 at 140 °C (**Figure 2.9** and **Table 2.2**). Vitrimers **PB-BE-V5** and **PB-BE-V3** relaxed via two modes, and especially the less cross-linked **PB-BE-V3**, whereas the more cross-linked vitrimer **PB-BE-V7** showed a more monomodal behaviour. The first relaxation process observed for **PB-BE-V3** and **PB-BE-V5** corresponds to the relaxation of dangling chains and chain segments between cross-links. The second relaxation process, which allows for a complete stress relaxation, occurs through covalent bond exchange between the dioxaborolane cross-links. Thanks to accelerated exchange reactions between cross-links, the relaxation is faster at higher temperatures, with relaxation times of 815 s and 142 s at 100 °C and 160 °C, respectively (**Figure 2.9** and **Table 2.2**). The relaxation times exhibited Arrhenius-like temperature dependence with a low activation energy of 38.9 kJ/mol for **PB-BE-V5**. Zero-shear viscosities for the different vitrimers were calculated from stress relaxation experiments (**Table 2.2**). As expected, they increased with the cross-linking density and a viscosity activation energy of 32.5 kJ/mol was measured for **PB-BE-V5**.

Table 2.2. Zero-shear viscosities and relaxation times of **PB-BE-V3**, **PB-BE-V5** and **PB-BE-V7**.

|	η_0 (Pa.s)			τ (s)		
T (°C)	V3	V5	V7	V3	V5	V7
100	-	2.91×10^8	-	-	815	-
120	2.67×10^7	2.13×10^8	-	364	533	-
140	8.72×10^6	1.29×10^8	2.01×10^8	128	293	684
160	5.47×10^6	6.76×10^7	-	72	142	-

2.4.4.2 Frequency sweep
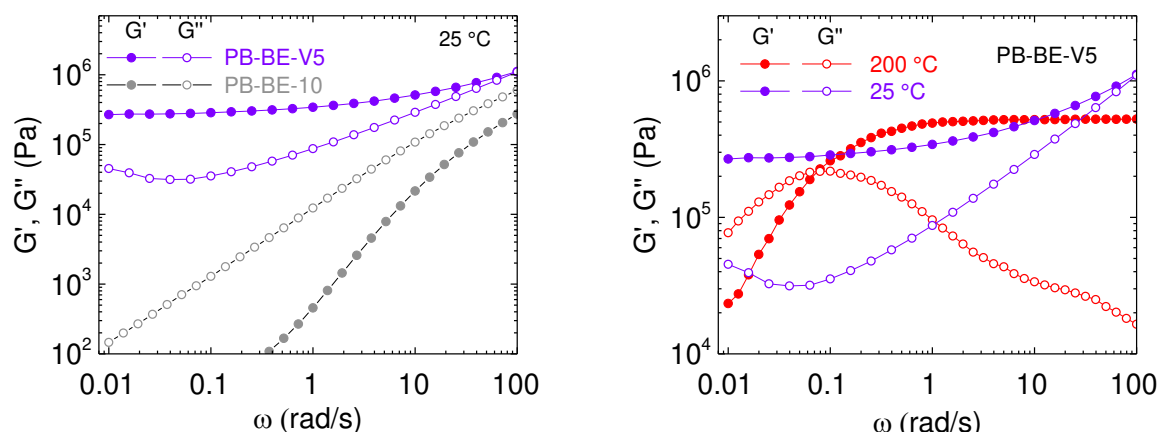
Figure 2.10. Left side: Comparison of frequency sweeps at 25 °C between the vitrimer **PB-BE-V5** (purple) and the linear polybutadiene functionalised with pending dioxaborolanes **PB-BE-10** (grey). Right side: Frequency sweeps of **PB-BE-V5** at 25 °C (purple) and 200 °C (red).

At 25 °C, the vitrimer **PB-BE-V5** was compared with a linear polybutadiene with pending dioxaborolanes **PB-BE-10.** Both G' and G'' were higher for the vitrimer at a given frequency confirming the network formation, moreover the linear polybutadiene did not present a rubbery plateau due to unentangled low molar mass chains. Consequently, **PB-BE-10** was already in its terminal relaxation region at 100 rad/s while the relaxation was shifted to lower frequencies by more than 4 orders of magnitude for the vitrimer.

Heating the vitrimer **PB-BE-V5** from 25 °C to 200 °C changed the viscoelastic properties, as shown in **Figure 2.10**. At high to moderate frequencies, *ie.* from 100 to 1 rad/s, the vitrimer exhibits a rubbery plateau because the network cannot relax the stresses within this range of time. At lower frequencies, G' started to decrease and finally crossed G'' at a frequency which corresponds to the longest relaxation time. At this point the system possesses a liquid-like behaviour because the material rearranges its topology faster than the characteristic time of the experiment; the vitrimer flows. When the temperatures increases, this cross-over point is shifted to higher frequencies, *ie.* shorter times, the system relaxes faster due to accelerated dioxaborolane exchange reactions between cross-links. **PB-BE-V5** has a characteristic relaxation time of 83 seconds at 200 °C, while at 25 °C the relaxation time was larger than 630 seconds and could not be observed in the frequency window used for the rheology experiments.

2.4.5 Tensile tests and recyclability of vitrimers

2.4.5.1 Tensile testing

   Thanks to their ability to flow, dioxaborolane based vitrimers should be recyclable. This ability was assessed by performing consecutive cycles of mechanical testing/reprocessing. After each set of tensile test, samples were cut down to small pieces, re-molded in a press for 10 min at 150 °C under a load of 3 tons, and re-tested for the tensile test. As expected, increasing the amount of cross-linker resulted in higher stresses at break and lower elongations at break (**Figure 2.11**). For all cross-linking densities tested, the elongation at break decreased with recycling cycles, with a decrease of 7%, 9% and 8% between the first and third recycling for vitrimers **PB-BE-V3**, **PB-BE-V5** and **PB-BE-V7**, respectively.

Whereas the elongation at break was affected by a factor of two approximately going from **PB-BE-V3** (113%) to **PB-BE-V7** (58%), the Young's modulus and stress at break varied to a much greater extent with the cross-linking density. The Young's modulus increased from 0.3 MPa to 56 MPa, and the stress at break from 0.2 to 4.3 MPa, when going from **PB-BE-V3** to **PB-BE-V7**, respectively. The Young's modulus remained rather constant through the recycling steps for vitrimers **PB-BE-V3** and **PB-BE-V5** and fluctuated for vitrimer **PB-BE-V7** (**Figure 2.11**). Stress at break decreased for **PB-BE-V3** and **PB-BE-V5** and increased for **PB-BE-V7** (**Figure 2.11**).
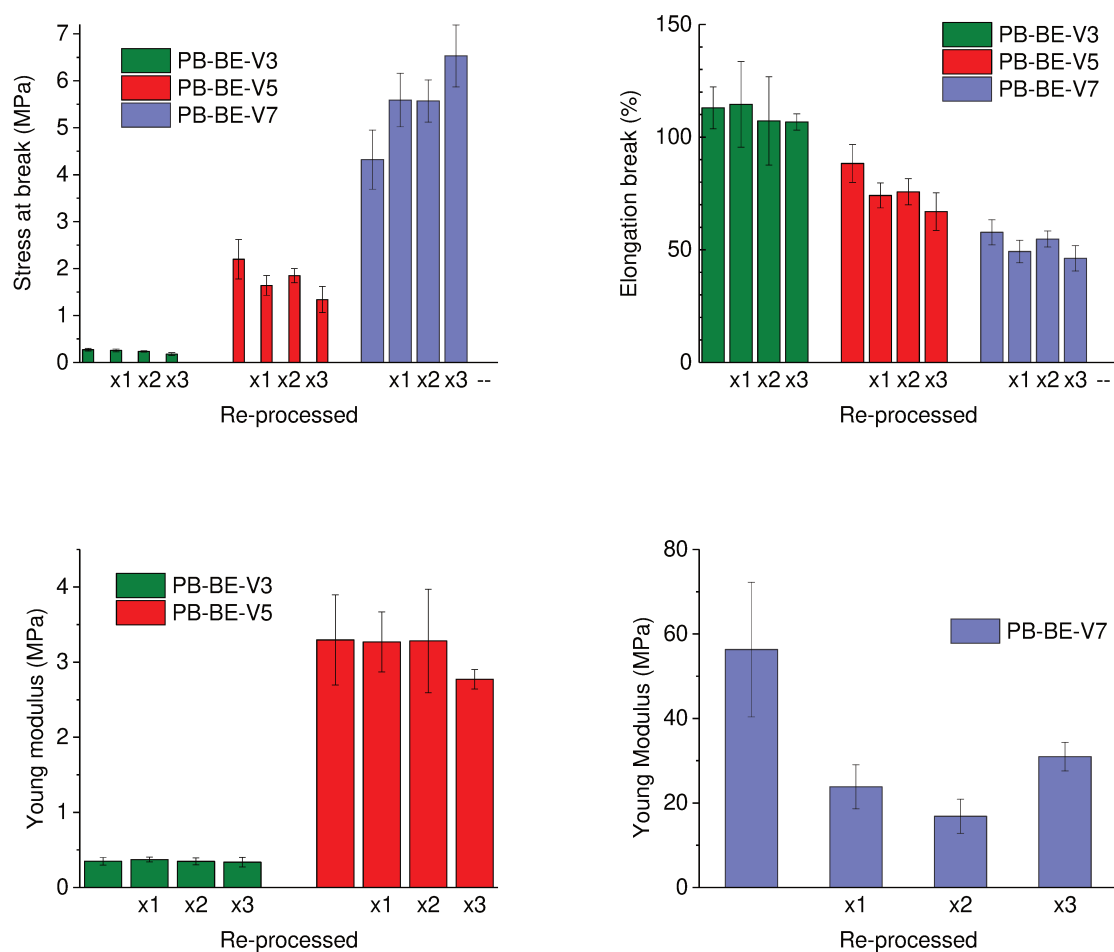
Figure 2.11. Stress at break (top, left), elongation at break (top, right) and Young's modulus (bottom) of vitrimers **PB-BE-V3** (green), **PB-BE-V5** (red) and **PB-BE-V7** (blue) as synthesized and after recycling up to 3 cycles.

2.4.5.2 DMA, DSC and TGA after recycling

   The impact of recycling on the physicochemical properties of PB vitrimers was evaluated by DMA and DSC analyses. The T_g and the storage modulus on the rubbery plateau of the different vitrimers were not impacted by consecutive cycles of mechanical testing and reprocessing, indicating minimal fluctuation of the cross-linking densities and chemical composition (**Figures 2.12**). Similarly, TGA indicated that the thermal stability of vitrimers was not affected at all by the successive mechanical testing and reprocessing cycles (**Figure 2.12**).
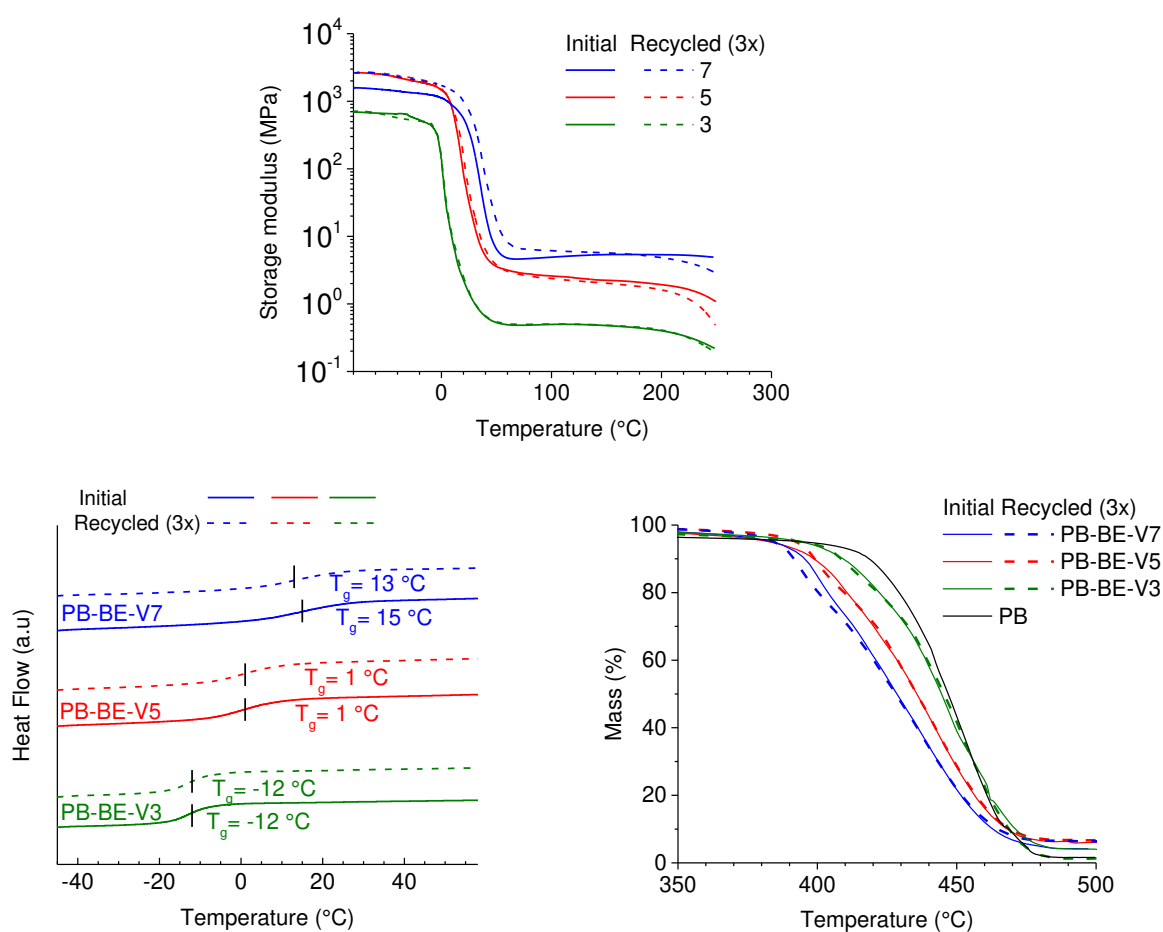
Figure 2.12. DMA (top), DSC analysis (bottom, left) TGA (bottom, right) of vitrimers **PB-BE-V3** (green), **PB-BE-V5** (red) and **PB-BE-V7** (blue) as synthesized and after 3 recycling cycles, and of the polybutadiene precursor (black).

2.4.5.3 Polymer recycling via selective de-cross-linking

Table 2.3. M_n and $Đ$ of polymers recovered after diolysis of vitrimers before and after recycling obtained by SEC and based on polystyrene standards.

	M_n (g/mol)	$Đ$
PB-BE-V3 as synthesized	4150	1.69
PB-BE-V3 recycled 3 times	4100	1.70
PB-BE-V5 as synthesized	4360	1.53
PB-BE-V5 recycled 3 times	4280	1.58
PB-BE-V7 as synthesized	4530	1.53
PB-BE-V7 recycled 3 times	4540	1.55

The impact of recycling on the structure of the polymer chains constituting the vitrimers was also investigated by performing SEC analyses. As synthesized vitrimers, and vitrimers that underwent 3 cycles of mechanical testing and reprocessing were immersed in THF at room temperature and diolyzed in the presence of a large excess of 1,2-propanediol as compared to **Bis-BE-SH** cross-links. All samples completely dissolved under these conditions and polymers from as synthesized networks and recycled networks essentially had identical M_n and $Đ$ (**Table 2.3, Figure 2.13**). Therefore, no scission, branching or static irreversible cross-linking could be detected by SEC on polymer chains of vitrimers processed and tested multiple times.
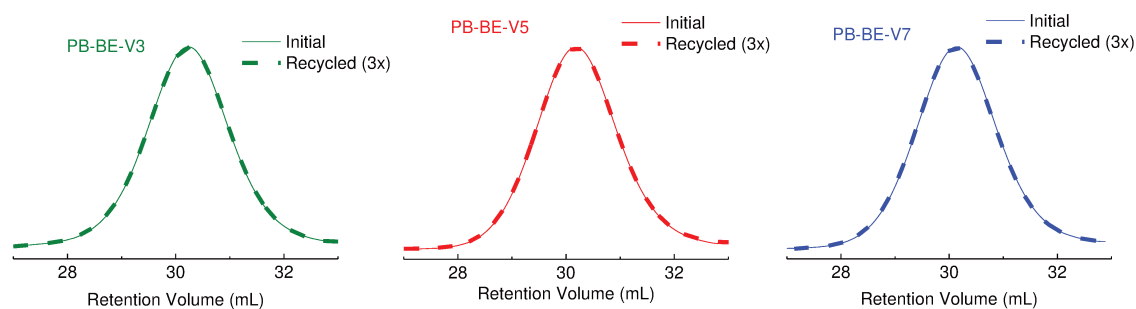

Figure 2.13. SEC chromatograms before (solid lines) and after three recycling (dashed lines) of PB-BE-V3 (green), PB-BE-V5 (red) and PB-BE-V7 (blue) vitrimers. After diolysis for all specimens.

The results collected with these different analytical techniques (DMA, DSC, TGA, SEC) clearly indicate that the dioxaborolane cross-links and the polymer chains constituting the vitrimer networks are stable under the processing and testing conditions. Thus, the

fluctuations of the elongation and stress at break observed over successive mechanical testing and reprocessing cycles likely originate from the processing of the samples by compression moulding.

2.4.6 Creep resistance

Cross-linking provides dimensional stability and solid properties to elastomers. However, because of the dynamic nature of the cross-links, these properties can be affected or even lost in vitrimers. In the present case, the low activation energy of dioxaborolane metathesis, *i.e.* 16 kJ/mol,[7] combined with the low M_n of the PB precursor, lead to poor creep resistance of the vitrimers. Consecutive creep-recovery cycles were performed on **PB-BE-V3**, **PB-BE-V5** and **PB-BE-V7** at different temperatures under a constant load of 0.1 MPa for **PB-BE-V5** and **PB-BE-V7** and of 0.01 MPa for **PB-BE-V3** (**Figure 2.14**). After an initial annealing cycle, the successive creep cycles became identical, providing reproducible viscosities for a given vitrimer at a given temperature. Viscosities and residual deformations were calculated on the fifth cycle, which we consider to be representative for each material's behaviour (**Figures 2.14, Table 2.4**)
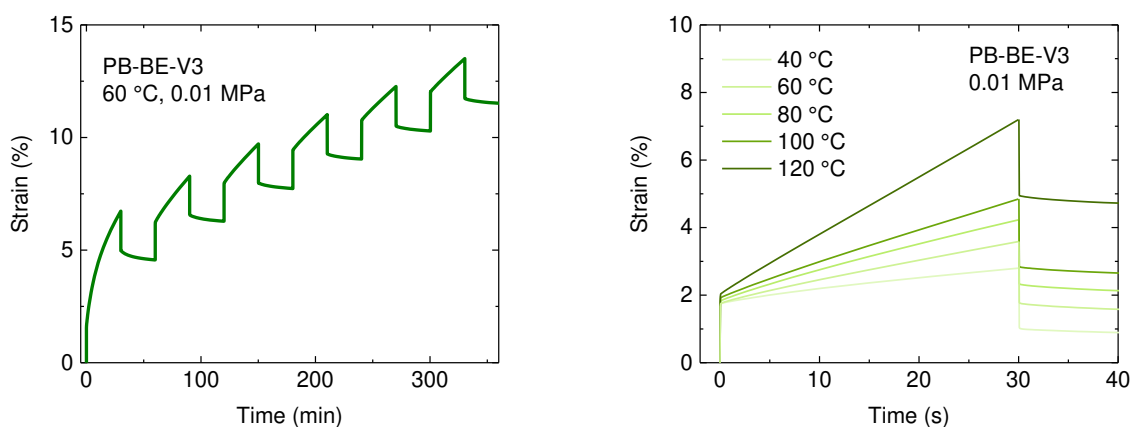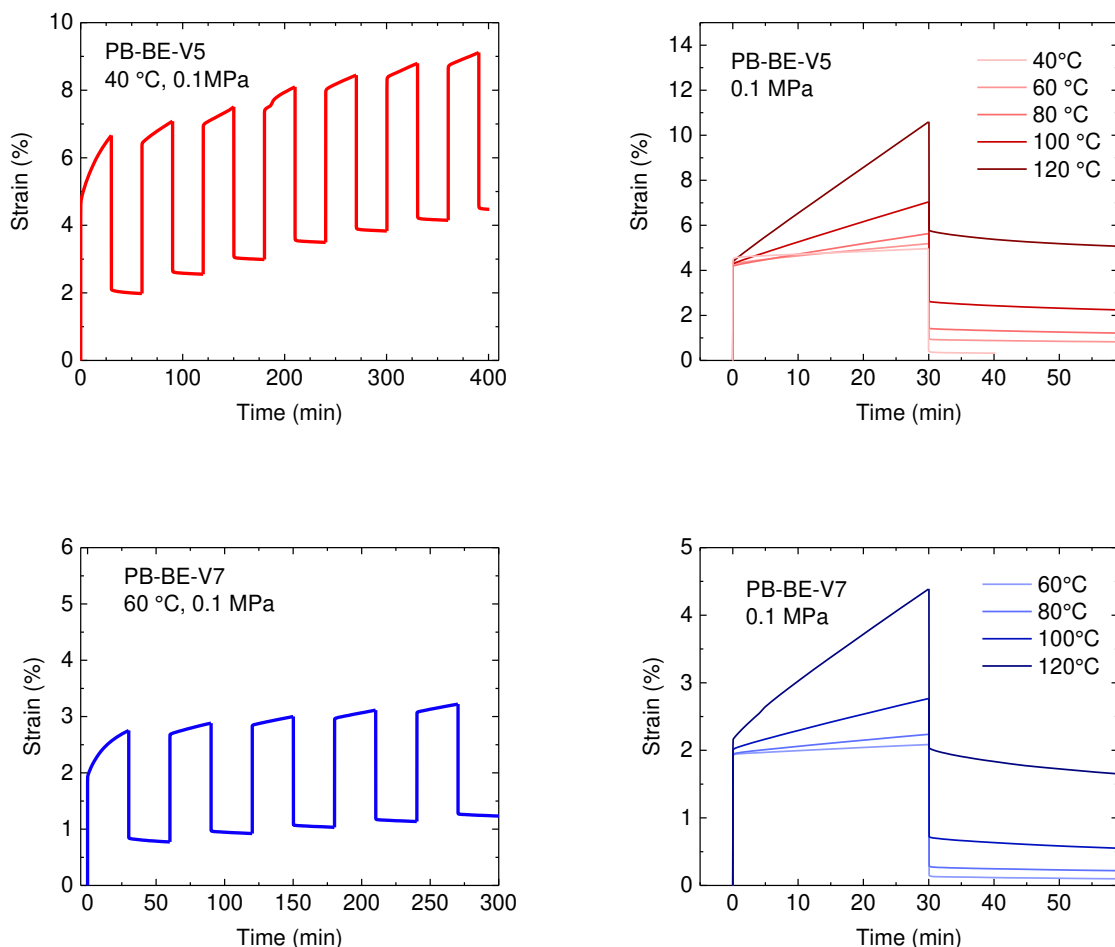
Figure 2.14. Left: Step-stress elongational creep-recovery (5 consecutive cycles of 30 min of creep under a load of 0.1 MPa followed by 30 min of recovery; 5th cycle presented) at different temperatures for vitrimers **PB-BE-V3** (top, green), **PB-BE-V5** (middle, blue) and **PB-BE-V7** (bottom, red) at a given temperature. 5th cycle of step-stress elongational creeps-recovery for vitrimers **PB-BE-V3** (top, green), **PB-BE-V5** (middle, blue) and **PB-BE-V7** (bottom, red) at different temperatures.

Upon application of an axial stress of 0.1 MPa at 100 °C, **PB-BE-V5** and **PB-BE-V7** deformed of 4.1% and 2%, respectively, which correspond to an elastic modulus of 2.44 MPa and 5 MPa, (**Figure 2.14**) and agree with the moduli measured by DMA (**Figure 2.12**). After release of the stress, only the elastic deformation was recovered proving that the exchange reaction actually allowed the vitrimer to flow and that the network reached a new equilibrium topology. The actual creep was determined once the deformation stabilized after stress release. As expected, and already confirmed by stress-relaxation experiments, the creep resistance increases with the cross-linking density. For example, after 30 min under 0.1 MPa stress at 80 °C, **PB-BE-V5** and **PB-BE-V7** retained a permanent deformation of 1.2% and 0.35%, respectively, after recovery of the elastic deformation. The viscous flow activation energy was found to be dependent on the cross-linking density, increasing from 20.5 kJ/mol,

to 36 kJ/mol and eventually 49.3 kJ/mol, for **PB-BE-V3**, **PB-BE-V5** and **PB-BE-V7**, respectively (**Figure 2.15, Table 2.5**).
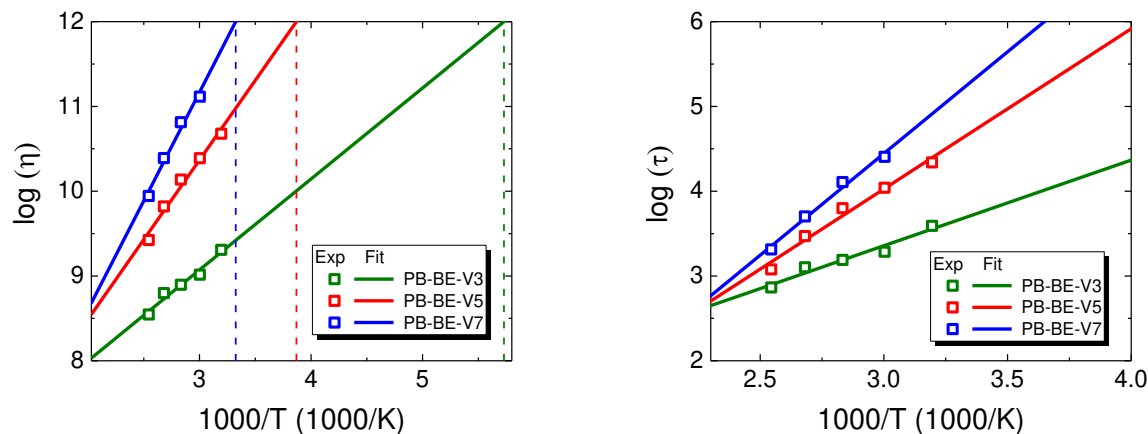

Figure 2.15. Plots of log(η) (left) and log (τ) (right) versus 1000/T for **PB-BE-V3** (green), **PB-BE-V5** (red) and **PB-BE-V7** (blue) experimental points (squares) and linear fits (solid lines) to extract the activation energy from the slope and T_v from the abscissa at which log(η) = 12 (dashed lines). Viscosities were extracted from stress step-stress creep data with **Equation 2.1**. Relaxation times were extracted from step-stress creep data with **Equation 2.2.**

  These results not only illustrate that the dynamics of exchange at a given temperature depend on the cross-linking density, but more importantly, they demonstrate that the extent to which vitrimer flow properties respond to a change of temperature can be manipulated and adjusted by playing on the cross-linking density. Hypothetical T_v values were calculated by extrapolation of creep experiments, and found to be −98, −14 and 28 °C for **PB-BE-V3**, **PB-BE-V5** and **PB-BE-V7**, respectively (**Figure 2.15, Table 2.5**). Therefore, for a given exchange reaction and polymer matrix (chemical nature and M_n of the polymer precursor), the T_v and the viscous flow activation energy of vitrimers can be controlled and adjusted by adding a catalyst of the exchange reaction to the system[5,31] or by manipulating the crosslinking density, the topology and the functionality of the vitrimer network.

Table 2.4. Viscosities of vitrimers calculated from the fifth cycle of consecutive step stress creep-recovery experiments.

	PB-BE-V3	**PB-BE-V5**	**PB-BE-V7**
T (°C)	η (Pa.s)	η (Pa.s)	η (Pa.s)
40	2.0×10^9	4.8×10^{10}	-
60	1.0×10^9	2.4×10^{10}	1.3×10^{11}
80	7.9×10^8	1.4×10^{10}	6.5×10^{10}
100	6.3×10^8	6.6×10^9	2.5×10^{10}
120	3.5×10^8	2.7×10^9	8.8×10^9

Table 2.5. Summary of activation energy and T_v of vitrimers extracted from step stress creep-recovery experiments.

	PB-BE-V3	**PB-BE-V5**	**PB-BE-V7**
E_a (kJ/mol) from η	19.4	36.2	45.9
E_a (kJ/mol) from τ	20.5	36.0	49.3
T_v (°C)	-98	-14	28
T_g (°C)	-12	1	15

2.5 Dual Networks

As just demonstrated, the creep resistance of PB vitrimers can be adjusted by playing on the concentration of dioxaborolane cross-links. However, numerous properties depend on the cross-linking density. Therefore, we were interested to find alternative ways to improve the creep resistance without changing the cross-linking density nor losing the ability of vitrimers to be recycled. To do so, PB networks incorporating both dynamic dioxaborolane cross-links (**Bis-BE-SH**) and static cross-links, 1,6-hexanedithiol (HDT), were prepared (**Figure 2.1**).

2.5.1 Synthesis and solvent resistance

The combination of dynamic and static cross-links into a single network has been recently exemplified by Sumerlin et al.[46] as well as Torkelson et al.[47] Sumerlin et al. prepared networks incorporating boronic ester cross-links, static cross-links, and eventually free diols, to design self-healing materials with structural integrity. Torkelson et al. conducted a theoretical and experimental study on vitrimers containing various fractions of static and dynamic cross-links. They predicted and verified experimentally that vitrimers can be reprocessed with full recovery of cross-link density as long as the fraction of permanent non-dynamic cross-links is insufficient to form a percolated static network. Both studies were performed on networks prepared by a step growth process. Thus, these networks were made of polymers with exchangeable groups in their main chain. In the present study, the networks will not present exchangeable groups in the main chain of the polymers, and the use of a thermoplastic precursor to generate the networks will also induce significantly different gelation profiles.

Two dual networks containing 6 cross-linkers per PB chain in average, but with different ratios of static to dynamic cross-links were prepared and compared to networks containing solely static (**PB-HDT-5**) or dynamic (**PB-BE-V5**) cross-links. The first dual network (**DN-HDT-3-BE-3**) contained 50% of static cross-links and 50% of dynamic dioxaborolane cross-links, while the second dual network (**DN-HDT-4-BE-2**) contained 66% of static cross-links and 33% of dynamic cross-links. The four networks presented high and comparable insoluble fractions, between 85% and 95%, after immersion for 24 h in THF at room temperature (**Figure 2.16**). When similar experiments were conducted in the presence of 1,2-propanediol, the insoluble fraction of the static network remained the same, 94%, whereas the vitrimer

network entirely dissolved, as expected. The dual networks displayed an intermediate behaviour, with decreasing insoluble fractions with increasing content of dioxaborolane cross-links. **DN-HDT-3-BE-3** and **DN-HDT-4-BE-2** presented insoluble fraction of 61% and 75% in the presence of diols, respectively, clearly indicating that the proportion of static cross-links alone was sufficient to be above the gel point for both dual networks.
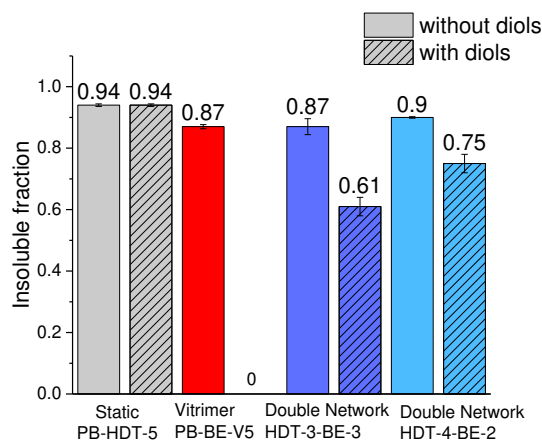

Figure 2.16. Insoluble fraction after 24h in THF at room temperature in the absence (left) and in the presence (right, striped) of free diols: static network **PB-HDT-5** (gray), vitrimer **PB-BE-V5** (red), dual networks **DN-HDT-3-BE-3** (blue) and **DN-HDT-4-BE-2** (cyan).

2.5.2 Creep resistance

The effect of the static cross-links onto the creep resistance was assessed by performing creep-recovery experiments. The networks were subjected to an elongational stress of 0.1 MPa for 100 min at 30 °C, and the residual stress was measured after 30 min of recovery at 30 °C (**Figures 2.17**).
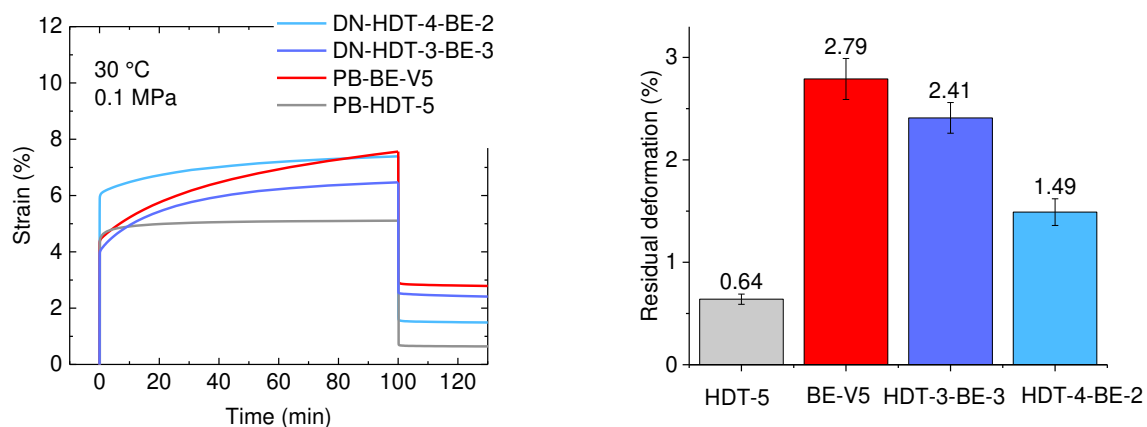
Figure 2.17. Creep resistance at 30 °C of static network **PB-HDT-5** (gray), vitrimer **PB-BE-V5** (red), dual networks **DN-HDT-3-BE-3** (blue) and **DN-HDT-4-BE-2** (cyan) after 100 min under a stress of 0.1 MPa and 30 min of recovery (no stress).

As expected, the creep resistance of the networks increased with the amount of static cross-linker. The residual deformation of the vitrimer was the highest, 2.79%, whereas the static network displayed a residual deformation of 0.64%. The residual deformation of the dual networks DN-**HDT-3-BE-3** and **DN-HDT-4-BE-2** lied in-between, with 2.41% and 1.49%, respectively. Hence the creep resistance of the dual network **DN-HDT-4-BE-2** was 1.9 higher than that of the vitrimer.

2.5.3 Recyclability

The ability of the dual networks to be recycled was also assessed. Stress-relaxation experiments indicated that the dual network **DN-HDT-3-BE-3** can relax more than 70% of the initial stress at 120 °C thanks to its dynamic dioxaborolane cross-links, even though the fraction of static cross-links (HDT) is sufficient to form a percolated permanent network, as evidenced by solubility tests in the presence of free 1,2-diols (**Figure 2.16**). The recyclability of the dual networks was evaluated by performing consecutive cycles of reprocessing and mechanical testing (**Figures 2.18 and 2.19**). Although, the Young's moduli of the four networks are comparable, the stress and elongation at break are clearly affected by the content of dynamic cross-links. As the content of dioxaborolane cross-links is increased, the elongation at break and the stress at break both increase. These results tend to indicate that the dioxaborolane cross-links are dynamic under the conditions of the tensile tests, *e.g.* at room temperature with a crosshead speed of 10 mm/min. Interestingly, the mechanical properties of the dual network **DN-HDT-3-BE-3** were unmodified after 3 recycling cycles, the Young's

modulus, stress and elongation at break after 3 cycles being 5.6% higher, 2.6% higher and 3.3% lower, respectively (**Figures 2.18 and 2.19**).
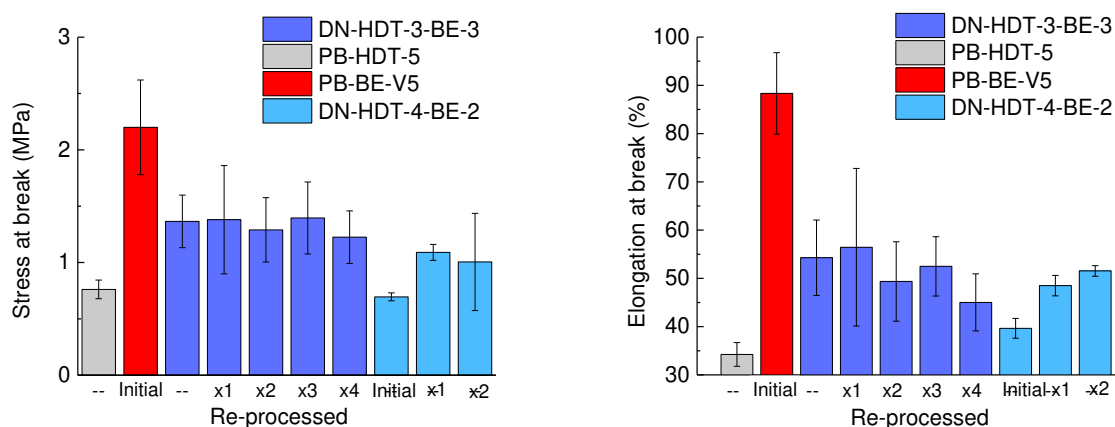

Figure 2.18. Stress (left) and elongation (right) at break at 25 °C of static network PB-HDT-5 (gray), vitrimer **PB-BE-V5** (red), and dual networks **DN-HDT-3-BE-3** (blue) and **DN-HDT-4-BE-2** (cyan).

Furthermore, DMA of the initial and reprocessed dual network showed that the T_g of the network as well as the storage modulus below and above the T_g were unmodified by the consecutive cycles of processing and mechanical testing (**Figure 2.19**). On the other hand, the mechanical properties of the dual network **DN-HDT-4-BE-2** were affected by recycling: the Young's modulus, stress and elongation at break all increased with recycling cycles (**Figures 2.18 and 2.19**). It should also be mentioned that the dual network **DN-HDT-4-BE-2** was difficult to reprocess by compression moulding. The material was prone to wrinkle and smooth surfaces were difficult to obtain.
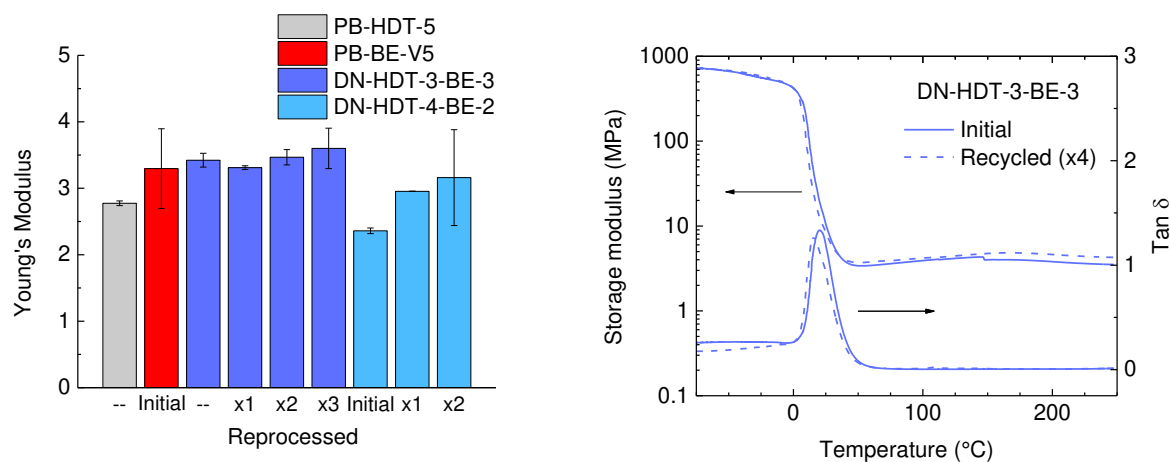

Figure 2.19. Left side: Young's modulus (bottom) at 25 °C of **PB-HDT-5** (gray) static network, **PB-BE-V5** (red) vitrimer, **DN-HDT-3-BE-3** (blue) and **DN-HDT-4-BE-2** (cyan) dual networks. Right side: Storage modulus and tan delta of **DN-HDT-3-BE-3** dual network before and after recycling.

116

2.5.4 Adhesion of Dual Networks

The possibility to create a strong adhesion between permanently cross-linked networks and cross-linked composites is an important feature of vitrimers.[6,7,48] Therefore, we were interested to test the possibility to generate a strong adhesion between dual networks, thanks to the formation of covalent bonds at the interface through dioxaborolane metathesis (**Figure 2.20**). To this aim, lap-shear experiments were conducted. Double networks were molded under press at 150 °C for 10 min into a rectangular shape and allowed to cool down to room temperature. The samples still in their molds were subsequently overlapped with a length of 15 mm and pressed at 150 °C for 2 min. Lap joints were left to slowly cool down to room temperature, de-molded and submitted to lap-shear tests. For both **DN-HDT-3-BE-3** and **DN-HDT-4-BE-2** dual networks, the adhesion was so strong even after 2 min at 150 °C that the fracture systematically occurred in bulk. Yet, the elongation and the force at rupture were consistently higher for the dual network containing more dioxaborolane cross-links (**Figure 2.20**). These results, consistent with the mechanical characterization performed (**Figures 2.14** and **2.19**) and the higher content of exchangeable cross-links in **DN-HDT-3-BE-3**, indicates that dual networks containing high fraction of static cross-links can also lead to strong interfacial adhesion, thanks to dioxaborolane metathesis between dynamic cross-links.
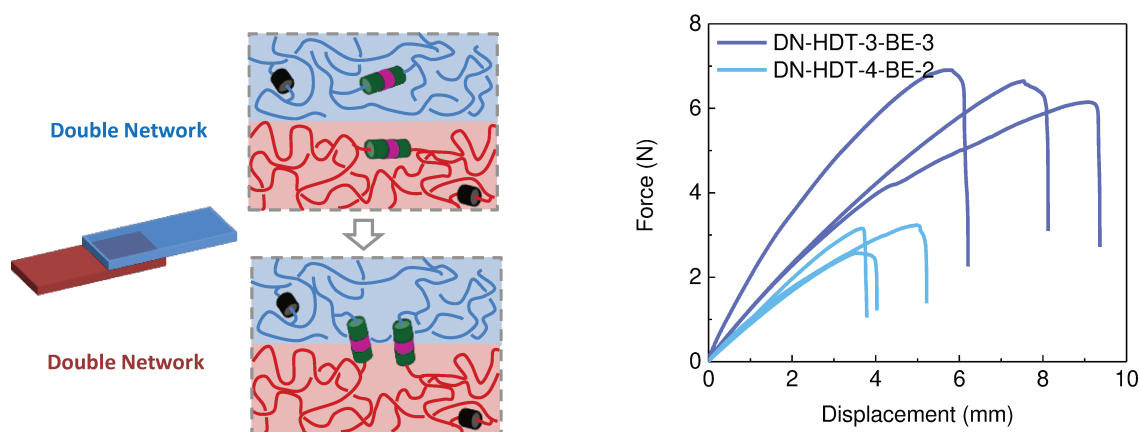

Figure 2.20. Adhesion test between dual networks: schematic representation of the exchange reaction at the interface and photographs of the double joints before, during and after the lap-shear test.

2.6 Conclusion

Vitrimers have been prepared from a commercial polybutadiene oligomer by radical grafting of a bis-thiol dioxaborolane. Network formation occurred without chain scission of the PB chains or formation of detectable permanent static cross-links via radical recombination. The cross-linking density and the properties of the vitrimers could be easily tuned by adjusting the content of dioxaborolane cross-linkers, even though the introduction of rigid phenyl-dioxaborolane pendant groups and cross-links significantly increases the T_g of the polymer matrix. Vitrimer networks with high insoluble fractions in THF and toluene were obtained. However, because of the low molar mass of the PB precursor, the limited number of cross-links per chain, and the dynamics of diaxaborolane cross-links under the conditions of the solubility tests, vitrimers dissolved after prolonged immersion time in THF. These results indicate that solubility tests are not always an appropriate way to assess the cross-linking density of vitrimers, if the tests are performed when cross-links are dynamic. Theoretical and experimental model studies should be conducted to quantify the extent and kinetics of dissolution of vitrimers as a function of the molecular structure of the network, life-time of the dynamic links, and solvent fraction and quality.

All the prepared vitrimers could entirely relax stress and their viscosities at a given temperature could be modulated by as much as two orders of magnitude by varying the cross-linking density by a factor of 2.3 only. More importantly, we showed that the viscous flow activation energy of vitrimers can be controlled by the molecular structure of the network. As a result, starting from the same PB oligomer and using the same dioaxoborolane cross-linker, vitrimers with hypothetical T_v varying by more than 120 °C were obtained. This result illustrates the complex dependance of vitrimer flow properties on the dynamics of exchange of the cross-links as well as on the mobility and accessibility of the exchangeable bonds. These parameters can be adjusted by manipulating the cross-linking density, the topology, and the functionality of the vitrimer network. This finding indicates that it is possible to optimize simultaneously creep resistance at room temperature and processability at high temperature. In an attempt to optimize creep resistance for a given given crossliniking density, and while preserving reprocessability, dual networks containing static and dynamic cross-links were prepared. We showed that in the case of dual networks prepared from thermoplastic oligomers, it is possible to maintain an excellent recyclability and to improve at the same time creep resistance by introducing static cross-links in proportion sufficient to form a percolated

network. Furthermore, it was demonstrated that such dual networks present the ability to create a strong adhesion between permanently cross-linked materials, just like vitrimers.

4.7 References

(1) Denissen, W.; M. Winne, J.; Prez, F. E. D. Vitrimers: Permanent Organic Networks with Glass-like Fluidity. *Chem. Sci.* **2016**, *7* (1), 30–38. https://doi.org/10.1039/C5SC02223A.

(2) Scott, T. F.; Schneider, A. D.; Cook, W. D.; Bowman, C. N. Photoinduced Plasticity in Cross-Linked Polymers. *Science* **2005**, *308* (5728), 1615–1617. https://doi.org/10.1126/science.1110505.

(3) Nicolaÿ, R.; Kamada, J.; Van Wassen, A.; Matyjaszewski, K. Responsive Gels Based on a Dynamic Covalent Trithiocarbonate Cross-Linker. *Macromolecules* **2010**, *43* (9), 4355–4361. https://doi.org/10.1021/ma100378r.

(4) Montarnal, D.; Capelot, M.; Tournilhac, F.; Leibler, L. Silica-Like Malleable Materials from Permanent Organic Networks. *Science* **2011**, *334* (6058), 965–968. https://doi.org/10.1126/science.1212648.

(5) Capelot, M.; Unterlass, M. M.; Tournilhac, F.; Leibler, L. Catalytic Control of the Vitrimer Glass Transition. *ACS Macro Lett.* **2012**, *1* (7), 789–792. https://doi.org/10.1021/mz300239f.

(6) Capelot, M.; Montarnal, D.; Tournilhac, F.; Leibler, L. Metal-Catalyzed Transesterification for Healing and Assembling of Thermosets. *J. Am. Chem. Soc.* **2012**, *134* (18), 7664–7667. https://doi.org/10.1021/ja302894k.

(7) Röttger, M.; Domenech, T.; Weegen, R. van der; Breuillac, A.; Nicolaÿ, R.; Leibler, L. High-Performance Vitrimers from Commodity Thermoplastics through Dioxaborolane Metathesis. *Science* **2017**, *356* (6333), 62–65. https://doi.org/10.1126/science.aah5281.

(8) Altuna, F. I.; Hoppe, C. E.; Williams, R. J. J. Shape Memory Epoxy Vitrimers Based on DGEBA Crosslinked with Dicarboxylic Acids and Their Blends with Citric Acid. *RSC Adv.* **2016**, *6* (91), 88647–88655. https://doi.org/10.1039/C6RA18010H.

(9) Pei, Z.; Yang, Y.; Chen, Q.; Terentjev, E. M.; Wei, Y.; Ji, Y. Mouldable Liquid-Crystalline Elastomer Actuators with Exchangeable Covalent Bonds. *Nat. Mater.* **2014**, *13* (1), 36–41. https://doi.org/10.1038/nmat3812.

(10) Zhang, Z. P.; Rong, M. Z.; Zhang, M. Q. Polymer Engineering Based on Reversible Covalent Chemistry: A Promising Innovative Pathway towards New Materials and New Functionalities. *Prog. Polym. Sci.* **2018**, *80*, 39–93. https://doi.org/10.1016/j.progpolymsci.2018.03.002.

(11) Brutman, J. P.; Delgado, P. A.; Hillmyer, M. A. Polylactide Vitrimers. *ACS Macro Lett.* **2014**, *3* (7), 607–610. https://doi.org/10.1021/mz500269w.

(12) Denissen, W.; Rivero, G.; Nicolaÿ, R.; Leibler, L.; Winne, J. M.; Du Prez, F. E. Vinylogous Urethane Vitrimers. *Adv. Funct. Mater.* **2015**, *25* (16), 2451–2457. https://doi.org/10.1002/adfm.201404553.

(13) Obadia, M. M.; Mudraboyina, B. P.; Serghei, A.; Montarnal, D.; Drockenmuller, E. Reprocessing and Recycling of Highly Cross-Linked Ion-Conducting Networks through Transalkylation Exchanges of C–N Bonds. *J. Am. Chem. Soc.* **2015**, *137* (18), 6078–6083. https://doi.org/10.1021/jacs.5b02653.

(14) Fortman, D. J.; Brutman, J. P.; Cramer, C. J.; Hillmyer, M. A.; Dichtel, W. R. Mechanically Activated, Catalyst-Free Polyhydroxyurethane Vitrimers. *J. Am. Chem. Soc.* **2015**, *137* (44), 14019–14022. https://doi.org/10.1021/jacs.5b08084.

(15) Snyder, R. L.; Fortman, D. J.; De Hoe, G. X.; Hillmyer, M. A.; Dichtel, W. R. Reprocessable Acid-Degradable Polycarbonate Vitrimers. *Macromolecules* **2018**, *51* (2), 389–397. https://doi.org/10.1021/acs.macromol.7b02299.

(16) Hendriks, B.; Waelkens, J.; Winne, J. M.; Du Prez, F. E. Poly(Thioether) Vitrimers via Transalkylation of Trialkylsulfonium Salts. *ACS Macro Lett.* **2017**, *6* (9), 930–934. https://doi.org/10.1021/acsmacrolett.7b00494.

(17) Dhers, S.; Vantomme, G.; Avérous, L. A Fully Bio-Based Polyimine Vitrimer Derived from Fructose. *Green Chem.* **2019**, *21* (7), 1596–1601. https://doi.org/10.1039/C9GC00540D.

(18) Ishibashi, J. S. A.; Kalow, J. A. Vitrimeric Silicone Elastomers Enabled by Dynamic Meldrum's Acid-Derived Cross-Links. *ACS Macro Lett.* **2018**, *7* (4), 482–486. https://doi.org/10.1021/acsmacrolett.8b00166.

(19) Stukenbroeker, T.; Wang, W.; Winne, J. M.; Prez, F. E. D.; Nicolaÿ, R.; Leibler, L. Polydimethylsiloxane Quenchable Vitrimers. *Polym. Chem.* **2017**, *8* (43), 6590–6593. https://doi.org/10.1039/C7PY01488K.

(20) Nishimura, Y.; Chung, J.; Muradyan, H.; Guan, Z. Silyl Ether as a Robust and Thermally Stable Dynamic Covalent Motif for Malleable Polymer Design. *J. Am. Chem. Soc.* **2017**, *139* (42), 14881–14884. https://doi.org/10.1021/jacs.7b08826.

(21) Lessard, J. J.; Garcia, L. F.; Easterling, C. P.; Sims, M. B.; Bentz, K. C.; Arencibia, S.; Savin, D. A.; Sumerlin, B. S. Catalyst-Free Vitrimers from Vinyl Polymers. *Macromolecules* **2019**, *52* (5), 2105–2111. https://doi.org/10.1021/acs.macromol.8b02477.

(22) Ricarte, R. G.; Tournilhac, F.; Leibler, L. Phase Separation and Self-Assembly in Vitrimers: Hierarchical Morphology of Molten and Semicrystalline Polyethylene/Dioxaborolane Maleimide Systems. *Macromolecules* **2019**, *52* (2), 432–443. https://doi.org/10.1021/acs.macromol.8b02144.

(23) Caffy, F.; Nicolaÿ, R. Transformation of Polyethylene into a Vitrimer by Nitroxide Radical Coupling of a Bis-Dioxaborolane. *Polym. Chem.* **2019**, *10* (23), 3107–3115. https://doi.org/10.1039/C9PY00253G.

(24) Lu, Y.-X.; Tournilhac, F.; Leibler, L.; Guan, Z. Making Insoluble Polymer Networks Malleable via Olefin Metathesis. *J. Am. Chem. Soc.* **2012**, *134* (20), 8424–8427. https://doi.org/10.1021/ja303356z.

(25) Imbernon, L.; Norvez, S. From Landfilling to Vitrimer Chemistry in Rubber Life Cycle. *Eur. Polym. J.* **2016**, *82*, 347–376. https://doi.org/10.1016/j.eurpolymj.2016.03.016.

(26) Imbernon, L.; Oikonomou, E. K.; Norvez, S.; Leibler, L. Chemically Crosslinked yet Reprocessable Epoxidized Natural Rubber via Thermo-Activated Disulfide Rearrangements. *Polym. Chem.* **2015**, *6* (23), 4271–4278. https://doi.org/10.1039/C5PY00459D.

(27) Cromwell, O. R.; Chung, J.; Guan, Z. Malleable and Self-Healing Covalent Polymer Networks through Tunable Dynamic Boronic Ester Bonds. *J. Am. Chem. Soc.* **2015**, *137* (20), 6492–6495. https://doi.org/10.1021/jacs.5b03551.

(28) Chen, Y.; Tang, Z.; Zhang, X.; Liu, Y.; Wu, S.; Guo, B. Covalently Cross-Linked Elastomers with Self-Healing and Malleable Abilities Enabled by Boronic Ester Bonds. *ACS Appl. Mater. Interfaces* **2018**, *10* (28), 24224–24231. https://doi.org/10.1021/acsami.8b09863.

(29) Chen, Y.; Tang, Z.; Liu, Y.; Wu, S.; Guo, B. Mechanically Robust, Self-Healable, and Reprocessable Elastomers Enabled by Dynamic Dual Cross-Links. *Macromolecules* **2019**, *52* (10), 3805–3812. https://doi.org/10.1021/acs.macromol.9b00419.

(30) Cao, L.; Fan, J.; Huang, J.; Chen, Y. A Robust and Stretchable Cross-Linked Rubber Network with Recyclable and Self-Healable Capabilities Based on Dynamic Covalent Bonds. *J. Mater. Chem. A* **2019**, *7* (9), 4922–4933. https://doi.org/10.1039/C8TA11587G.

(31) Denissen, W.; Droesbeke, M.; Nicolaÿ, R.; Leibler, L.; Winne, J. M.; Prez, F. E. D. Chemical Control of the Viscoelastic Properties of Vinylogous Urethane Vitrimers. *Nat. Commun.* **2017**, *8*, 14857. https://doi.org/10.1038/ncomms14857.

(32) Guerre, M.; Taplan, C.; Nicolaÿ, R.; Winne, J. M.; Du Prez, F. E. Fluorinated Vitrimer Elastomers with a Dual Temperature Response. *J. Am. Chem. Soc.* **2018**, *140* (41), 13272–13284. https://doi.org/10.1021/jacs.8b07094.

(33) Obadia, M. M.; Jourdain, A.; Cassagnau, P.; Montarnal, D.; Drockenmuller, E. Tuning the Viscosity Profile of Ionic Vitrimers Incorporating 1,2,3-Triazolium Cross-Links. *Adv. Funct. Mater.* 27 (45), 1703258. https://doi.org/10.1002/adfm.201703258.

(34) *Boronic Acids: Preparation and Applications in Organic Synthesis and Medicine*; Hall, D. G., Ed.; Wiley-VCH Verlag GmbH & Co. KGaA: Weinheim, FRG, 2005. https://doi.org/10.1002/3527606548.

(35) Martin, R.; Buchwald, S. L. Palladium-Catalyzed Suzuki−Miyaura Cross-Coupling Reactions Employing Dialkylbiaryl Phosphine Ligands. *Acc. Chem. Res.* **2008**, *41* (11), 1461–1473. https://doi.org/10.1021/ar800036s.

(36) Mó, O.; Yáñez, M.; Eckert-Maksić, M.; Maksić, Z. B.; Alkorta, I.; Elguero, J. Periodic Trends in Bond Dissociation Energies. A Theoretical Study. *J. Phys. Chem. A* **2005**, *109* (19), 4359–4365. https://doi.org/10.1021/jp050857o.

(37) Campa, J. G. de L.; Pham, Q.-T. Polybutadiènes Hydroxytéléchéliques, 5. Addition Des Thiols Sur Les Double Liaisons Des Polybutadiènes Hydroxytéléchéliques Radicalaire et Anionique. Etude Des Mécanismes d'addition Par 1H et 13C NMR. *Makromol. Chem.* **1981**, *182* (5), 1415–1428. https://doi.org/10.1002/macp.1981.021820514.

(38) Justynska, J.; Hordyjewicz, Z.; Schlaad, H. Toward a Toolbox of Functional Block Copolymers via Free-Radical Addition of Mercaptans. *Polymer* **2005**, *46* (26), 12057–12064. https://doi.org/10.1016/j.polymer.2005.10.104.

(39) David, R. L. A.; Kornfield, J. A. Facile, Efficient Routes to Diverse Protected Thiols and to Their Deprotection and Addition to Create Functional Polymers by Thiol−Ene Coupling. *Macromolecules* **2008**, *41* (4), 1151–1161. https://doi.org/10.1021/ma0718393.

(40) Sun, H.; Kabb, C. P.; Sims, M. B.; Sumerlin, B. S. Architecture-Transformable Polymers: Reshaping the Future of Stimuli-Responsive Polymers. *Prog. Polym. Sci.* **2019**, *89*, 61–75. https://doi.org/10.1016/j.progpolymsci.2018.09.006.

(41) Bandzierz, K.; Reuvekamp, L.; Dryzek, J.; Dierkes, W.; Blume, A.; Bielinski, D. Influence of Network Structure on Glass Transition Temperature of Elastomers. *Materials* **2016**, *9* (7). https://doi.org/10.3390/ma9070607.

(42) James, H. M.; Guth, E. Theory of the Elastic Properties of Rubber. *J. Chem. Phys.* **1943**, *11* (10), 455–481. https://doi.org/10.1063/1.1723785.

(43) Deam R. T; Edwards Samuel Frederick. The Theory of Rubber Elasticity. *Philos. Trans. R. Soc. Lond. Ser. Math. Phys. Sci.* **1976**, *280* (1296), 317–353. https://doi.org/10.1098/rsta.1976.0001.

(44) Katz, D.; Tobolsky, A. V. Rubber Elasticity in a Highly Crosslinked Epoxy System. *Polymer* **1963**, *4*, 417–421. https://doi.org/10.1016/0032-3861(63)90053-3.

(45) Katz, D.; Tobolsky, A. V. Rubber Elasticity in Highly Crosslinked Polyethyl Acrylate. *J. Polym. Sci. A* **1964**, *2* (4), 1595–1605. https://doi.org/10.1002/pol.1964.100020406.

(46) Cash, J. J.; Kubo, T.; Dobbins, D. J.; Sumerlin, B. S. Maximizing the Symbiosis of Static and Dynamic Bonds in Self-Healing Boronic Ester Networks. *Polym. Chem.* **2018**, *9* (15), 2011–2020. https://doi.org/10.1039/C8PY00123E.

(47) Li, L.; Chen, X.; Jin, K.; Torkelson, J. M. Vitrimers Designed Both To Strongly Suppress Creep and To Recover Original Cross-Link Density after Reprocessing: Quantitative Theory and Experiments. *Macromolecules* **2018**. https://doi.org/10.1021/acs.macromol.8b00922.

(48) Chabert, E.; Vial, J.; Cauchois, J.-P.; Mihaluta, M.; Tournilhac, F. Multiple Welding of Long Fiber Epoxy Vitrimer Composites. *Soft Matter* **2016**, *12* (21), 4838–4845. https://doi.org/10.1039/C6SM00257A.

Chapter 3

Model Study of Exchange Reactions of Dioxaborolanes and Dioxaborinanes

Table of Contents

Chapter 3 – Model Study of Exchange Reactions of Dioxaborolanes and Dioxaborinanes

3.1 Introduction

Small molecules that contain boronic acid moieties have been widely used in various applications.[1–10] In organic chemistry, they are utilised as protecting groups, in carbon-carbon coupling reactions, such as Suzuki-Miyaura, Chan-Lam and Liebeskind-Srogl reactions, but also in conjugate addition, oxidation, homologation, C-H coupling reaction and molecular self-assembly.[11–23] Thanks to their low toxicity and biofunctionality, macromolecules containing boronic acids and boronic acid derivatives are used in medicine, as boron neutron capture therapy agents, enzymatic inhibitors in anticancer drugs, or as chemical sensors of biomolecules like glucose, fructose or other polysaccharides.[24–35] Moreover, they have found others applications, such as injectable hydrogels,[36] dynamic covalent networks,[37,38] separation,[39] surface post-functionalization,[40] nanomaterials, intelligent molecular systems,[41] cages, cell captures,[42] controlled drug delivery[43,44] and others.[45] Their extraordinary broad utility is a consequence of their dynamic behaviour, which is related to the dynamic covalent bonding between diols and boronic acids.

The first synthesis of a boronic acid was reported by Frankland in 1860.[46] Triethyl borate was treated with diethylzinc to obtain a highly air–sensitive triethylborane, which provided ethylboronic acid through its oxidation in ambient air. Indeed, one of the three carbon linked to the boron atom of the trialkylborane is first hydrolysed to get a borinic acid, *i.e.* a boron specie with only one hydroxyl group (**Scheme 3.1**). More stable than its borane counterpart, but still reactive, the ethyl borinic acid can be further hydrolysed to yield ethyl boronic acid, and even boric acid, where all alkyls groups have been replaced by hydroxyls (**Scheme 3.1**). The latest product is the most stable of all considered compounds. But nowadays, the most common way to produce boronic acid is the reaction of organolithium or organomagensium reagents with trialkyl borates, followed by successive hydrolysis.[47,48]
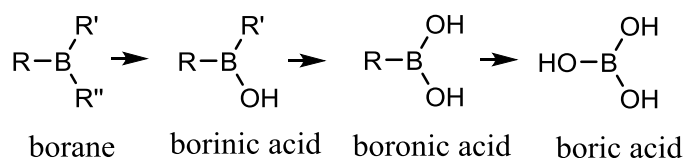
Scheme 3.1. General scheme of the synthetic route of boronic acid.

In the neutral form, the boron atom of boronic acid is sp^2-hybridized with six valence electrons and one vacant p orbital orthogonal to the three substituents, which are oriented in a trigonal planar configuration with an O-B-O angle of 120°. As a consequence of its electron-deficiency and moderate electronegativity, boron possesses a weak Lewis acidic character and can form complex with Lewis bases, thereby changing from sp^2 to sp^3 hybridisation state and adopting a tetrahedral configuration with bond angle of 109.5°. Under basic conditions in water, the boron atom reacts with hydroxyl-ions to form a hydroxyboronate anion. Depending on the pH and pKa of the boronic acid, an equilibrium is reached between these two species; the boronate anion and its neutral counterpart. The pKa of boronic acids is defined as the pH-value at which half of the boron is present as sp^2 boronic acid and half as sp^3 hydroxyboronate anion. The pKa is strongly correlated to the substitution pattern of boronic acids. The presence of electron-withdrawing substituents on the aryl groups of the boronic acid favours the formation and stabilisation of the corresponding boronate anion, decreasing its pKa, while electron-donating groups increase the pKa.[49–53] Additionally, bulky substituents close to boron hamper the formation of the tetrahedral boronate ion due to steric hindrance and thus increase the pKa value.[54] Therefore, pKa values of the aryl boronic acids are higher than the alkyl ones. Due to all these different effects, the pKa range varies from 10.4 to 4.0 for 3-pyridylboronic acid that mainly exists as a zwitterion in water. If Lewis acidity plays an important role in the reactivity of boronic acid, Brønsted acidity is much more unusual and is observed only when the formation of a tetrahedral boronate is highly unfavourable (**Scheme 3.2**).[55] In this case, the conjugate base is formed through proton transfer instead of coordinating with the hydroxide ion.
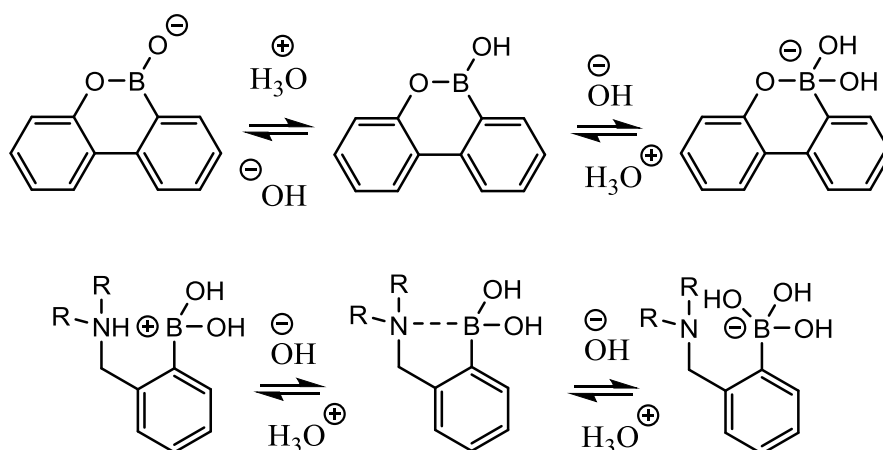
Scheme 3.2. Ionization equilibrium for a six-membered ring boronic acid (top) and for a 2-aminomethyl-phenylboronic acid derivative.

B-O bonds are shorter than B-C bonds, 1.37 and 1.57 Å, respectively. This translates into a higher bond dissociation energy of the B-O bond, *ca.* 630 kJ/mol, as compared to the B-C bond, *ca.* 430 kJ/mol.[56] As a consequence, B-C oxidation is thermodynamically favoured, but the oxidative cleavage of this bond with oxygen or water is very slow, so many common boronic acids are kinetically stable. This is true for arylboronic species, which are stable in water over a wide range of pH, but not so for alkylboronic acids, which are prone to atmospheric oxidation when left under ambient air, yielding an alcohol and boric acid.
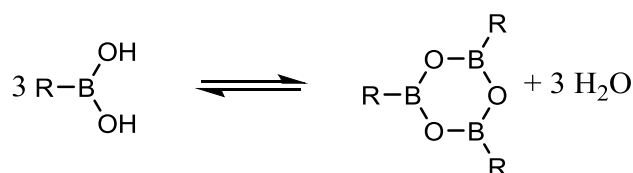
Scheme 3.3. Equilibrium between a boronic acid and boroxine, a trimeric cyclic boronic anhydride.

If boronic acids are stable compounds towards atmospheric oxidation, they can form cyclotrimeric anhydride species through the condensation of boronic acids, named boroxine. (**Scheme 3.3**).[57] Boroxines often coexist in solution and in solid state with their boronic acid counterparts. A ^{1}H- NMR study of different phenyl boronic acids showed that the reaction was reversible at room temperature in $CDCl_3$ but with equilibrium constants rather small.[58] Steric hindrance and electron-withdrawing groups were found to play a key role in this constant, decreasing the stability of the boroxines. The planar boroxine ring is isoelectronic to benzene and possess a partial aromatic character. Boroxines can interact with bases, just like their boronic acid analogues, involving only one boron atom of the B_3O_3 ring. Indeed, the coordination with another equivalent of base is strongly disfavoured due to steric strain. The

eight-membered cyclotetrameric boronic anhydride also exists but presents significantly more ring strain than its six-membered counterpart, and is thus more prone to hydrolysis.[59] The reactivity of cyclic boronic anhydrides with water makes them interesting for imparting recyclability and self-healing properties to polymer networks.[60–64]

$$R-B\begin{smallmatrix}OH\\OH\end{smallmatrix} + 2\,H_2O \quad\underset{}{\overset{K_a}{\rightleftharpoons}}\quad R-B^{\ominus}\begin{smallmatrix}OH\\OH\\OH\end{smallmatrix} + H_3O^{\oplus}$$

$$K_E \quad\quad\quad\quad\quad K_E'$$

$$R-B\begin{smallmatrix}O\\O\end{smallmatrix} + 2\,H_2O \quad\underset{}{\overset{K_a'}{\rightleftharpoons}}\quad R\blacktriangleright B^{\ominus}\begin{smallmatrix}HO\;O\\O\end{smallmatrix} + H_3O^{\oplus}$$

$$+\,2\,H_2O \quad\quad\quad\quad\quad +\,2\,H_2O$$
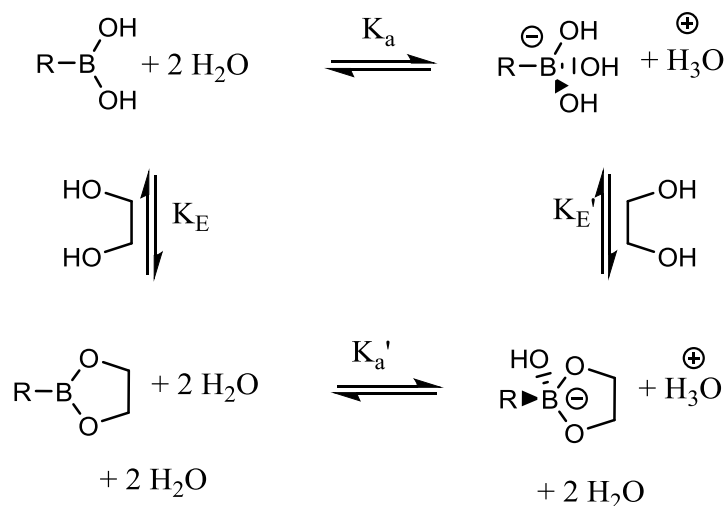
Scheme 3.4. Reaction landscape of boronic ester formation. Both neutral and anionic forms of boronic acid exist in thermodynamic equilibrium with cis-diols in aqueous solution, forming boronic and boronate esters via condensation reactions. K_E and K_E' are the equilibrium reaction constants for the pathways between the trigonal neutral and the tetrahedral anionic forms, respectively. Ka and Ka' are the ionization constants of the boronic acid and boronic ester, respectively. (Adapted from reference [45])

Boronic acids can also react with diols yielding boronic esters and water (**Scheme 3.4**). This equilibrium between boronic acids, diols, water and boronic esters was studied firstly in details by Loran and Edwards in 1959, looking at the dissociation equilibrium constant K_{eq}.[65] But the study considered only tetrahedral boronate anions to react with diols, while neutral form can also form boronic esters. Lots of studies about the complex boronic acid-diol equilibrium in aqueous media have been conducted since.[58,66–69] It was shown that boronic ester formation is favoured at high pH and that free boronic acids have lower Lewis acidity than their ester counterparts.[45] Intramolecular and intermolecular complexation, like in Wulff-type boronic acids, with internal coordination between the nitrogen or carbonyl lone pair and boron's vacant orbital, can change the pKa and the stability of boronic esters.[70–73] Consequently, diethanolamine boronic esters are formed in high yields, without water trapping agents as they crystallise out of solution. Furthermore, the choice of the diol is the key factor that will affect the most K_{eq}.[73] For instance, as compared to ethylene glycol, the formation of the ester is 10 times more favoured with glycerol, 1000 times with mannitol and 10 000 times with catechol.[65] The boronic ester formation is driven by removing water during

the reaction, thanks to Dean-Stark apparatus, or with the addition of dehydrating agents such as magnesium sulphate or molecular sieves. Under these conditions, boronic esters can be obtained in very good to quantitative yields.

Boronic esters can give back the boronic acids and diols when exposed to water. For acyclic boronic esters or unhindered cyclic ones, as those obtained with ethylene or propylene glycol (**Scheme 3.5**, compounds **1** and **2**, respectively), hydrolysis is very fast and can occur with contact to atmospheric moisture only.[74,75] Catechol based boronic esters (**Scheme 3.5**, compound **3**) are also sensitive to hydrolysis. However, hydrolysis can be slowed down and significantly decreased with hindered cyclic esters, such as pinacol, pinanediol and Hoffmann's camphor-derived diols (**Scheme 3.5, compounds 4, 5 and 6**).[76–82] In fact, these bulky boronic esters are quite complicated to convert into their starting boronic acids, as a further proof of their excellent stability. As forehead mentioned, diethanolamine and other *N*-substituted derivatives based boronic esters are even more resistant to hydrolysis due to the intramolecular dative N-B bond.[83,84] Stereochemistry may also play an important role on the thermodynamic stability of boronic esters. For instance, boronic esters made from trans-1,2-cyclohexanediol are less robust to hydrolysis than their cis counterpart due to the unfavourable orientation of the hydroxyl groups.[85]
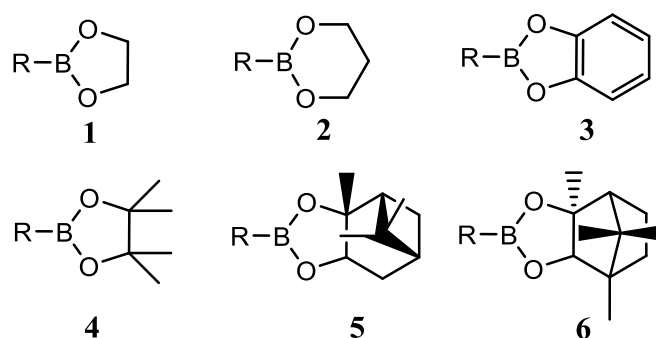
Scheme 3.5. Some common boronic esters.

Moreover, five membered boronic esters, knowns as dioxaborolanes, are more prone to hydrolysis than six membered boronic esters, called dioxaborinanes.[86] Indeed, the 1,3-diols form more stable boronic esters than their 1,2 counterparts, due to the absence of ring strain in dioxaborinanes. The complexation of 5-membered boronic esters induces a release of angle strain; O-B-O and B-O-C bond angles changing from 120° to 109°, when going from a planar configuration of the sp^2 boron atom to a tetrahedral configuration of the sp^3 boron atom.
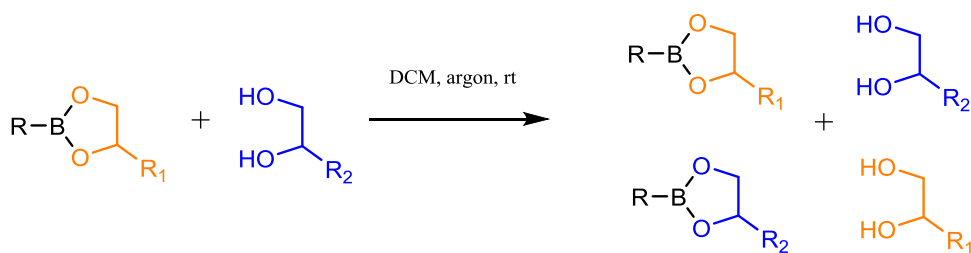
Scheme 3.6. Transesterification between a dioxaborolane and 1,2-diol.

Boronic esters can also react with free diols through transesterification to yield a mixture of different boronic esters and diols. The stoichiometric balance between the different boronic esters, once the thermodynamic equilibrium is reached, reflects their respective stability (**Scheme 3.6**). The rate of the transesterification depends on the nature of the boronic ester and diol. Transesterification is typically faster with dioxaborolanes containing unhindered aliphatic diols and/or which carry electron-withdrawing substituents. More hindered boronic esters obtained from pinacol or pinanediol do not undergo transesterification, or extremely slowly.[87,88] Diethanolamine containing dioxaborolanes are too stable to be reactive towards these species. Due to their increased stability, dioxaborinanes reacts slower than their 1,2-diols analogues.
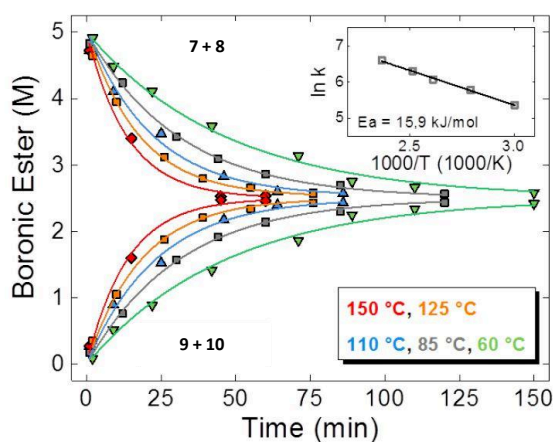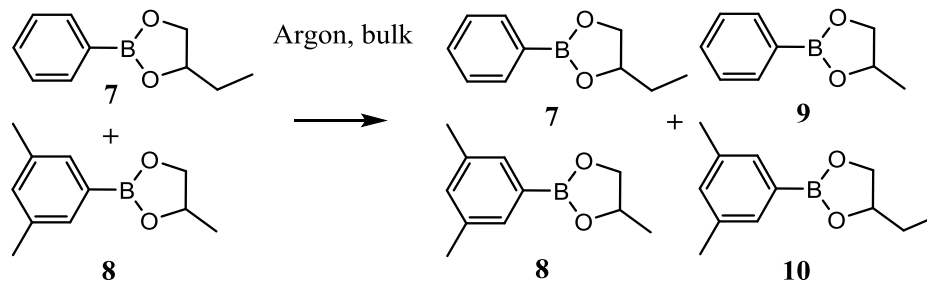

Figure 3.1. Kinetic data of the metathesis of dioxaborolanes 7 and 8 in bulk under argon protective atmosphere (adapted from reference [89]).

130

Nicolaÿ, Leibler and coworkers reported a new dynamic covalent reaction involving boronic esters: a metathesis reaction between dioxaborolanes (**Figure 3.1**).[89] A direct exchange occurred without any detectable traces of free diol, water or boronic acid. When two different dioxaborolanes were mixed in THF at 20 °C under protective atmosphere, no exchange was observed even after 200 minutes, while at 60 °C in bulk, the metathesis products were detected and the reaction reached equilibrium after 160 minutes. As the kinetic of exchange was followed from 60 °C to 180 °C and fitted with a second order model assuming a single metathesis rate, the activation energy was determined from the Arrhenius law to be 15.9 kJ/mol. Compared to other covalent exchange reactions, *e.g.* transesterification (88 kJ/mol) or vinylogous urethanes transamination (59 kJ/mol), the energy is quite low, meaning the temperature has a lower influence on the kinetics of the reaction.

Interestingly, boronic esters are very stable compounds even at high temperatures and thus are not prone to side reactions. Direct metathesis between boronic esters offers the possibility to implant a highly dynamic covalent chemistry without using diols. Indeed, diols are highly polar compounds so they can induce phase separation when they are incorporated into apolar polymeric matrices. Moreover, diols are much more sensitive to oxidation than boronic esters, and as good nucleophiles they can also react with many functional groups leading to the formation of a static covalent crosslinks.

As presented in chapter 2, the direct reaction between dioxaborolanes led to inherent creep for the considered elastomers, even at ambient temperature. To overcome this problem, while keeping the excellent chemical and oxidative stability of boronic esters, a kinetic study of the possible exchange reaction between dioxaborinanes was conducted and will be presented in this chapter. First, the association and dissociation equilibrium constants of dioxaborinanes were calculated and compared to those of dioxaborolanes. Transesterification exchange kinetics between dioxaborinanes and 1,2 or 1,3-diols are also presented. Then, the direct exchange between two highly pure dioxaborinanes under protective atmosphere was studied in details in solution and then in bulk.

3.2 General experimental methods

Chemicals, solvents and gases: Boronic acids, diols and other chemicals were purchased from Sigma Aldrich, Alfa Aesar, TCI, Acros and Fischer. Solvents and deuterated solvents were stored under inert atmosphere over fresh and dried molecular sieves 3Å. The respective ratio of molecular sieves to solvent (% mass/volume) and the minimum time to achieve dryness for each solvent were taken from literature.[90] The diols used as reactants were dried over $MgSO_4$ and filtered. After concentration under reduced pressure at elevated temperature to remove any traces of water, they were stored under inert atmosphere. Argon in highest available purity (alphagaz 2, <0.5 ppm H_2O) was purchased from Air Liquide.

Glassware: Glassware was oven-dried and purged with nitrogen or argon while heating with a heat gun before addition of the chemicals.

NMR analyses: ^{1}H-NMR and ^{13}C-HNMR analyses were conducted on a Bruker Ultra Shield machine at 400 MHz and 100 MHz, respectively. NMR tubes were oven dried. If not stated otherwise, samples of 10 mg in 500 μL of deuterated solvent were analysed and the obtained data were internally referred to the standard shift of the respective deuterated solvent.

GC analysis: GC analysis was conducted on a Shimadzu gas chromatograph GC-2014 equipped with a Zebron-5HT "inferno" column and helium as carrier gas. Injection was done manually by injecting 1 μL sample volumes using a 10 μL syringe from Hamilton (gastight 1701). Before running analysis, the entire set-up was pre-heated to 350 °C and kept at constant carrier gas flow of 5 mL/min and split ratio of 2.0 for at least 30 minutes. The GC method (T_{inj}, T_{col}, T_{det}, gas flow, split ratio) was chosen according to the nature of the studied molecules and the respective exchange reaction. The column was reconstituted regularly by heating to 350 °C.

3.3 Synthesis, purification, storage and characterisation of boronic esters

3.3.1 Synthesis, purification and storage of boronic esters

The most straightforward route to synthesise boronic esters is the condensation of a diol with a boronic acid in the presence of a water trapping agent (**Schemes 3.7** and **3.8**). Two different strategies were used. Decent purity was achieved for boronic esters used for external calibration and experiments under air thanks to the strategy 2, while highly pure compounds used for experiments under inert atmosphere were prepared via strategy 1.
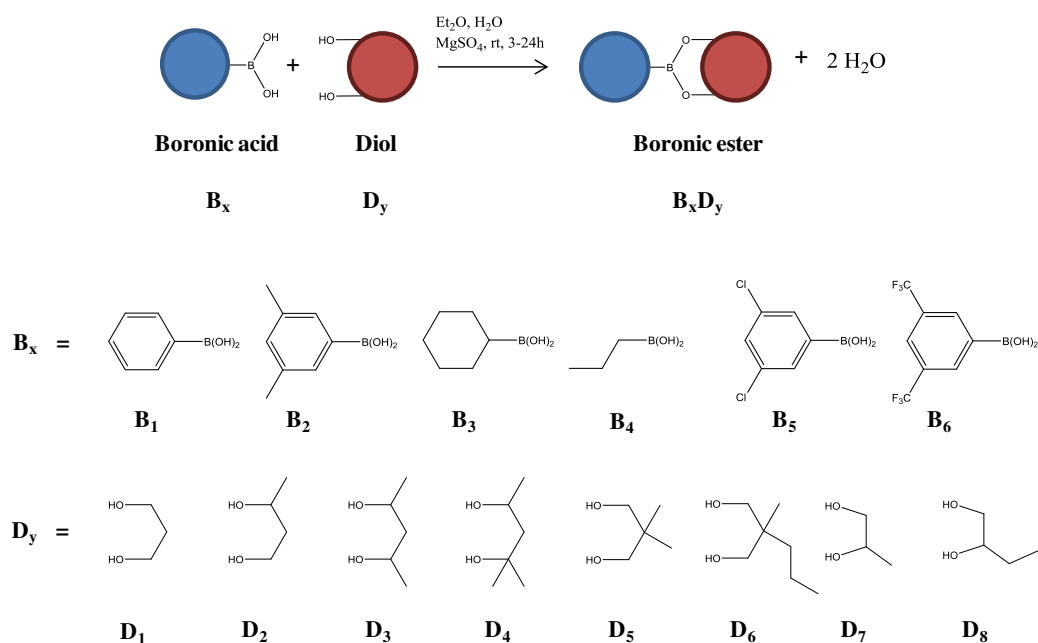
Scheme 3.7. Boronic ester formation (top). Various boronic acids (middle) and diols (bottom) were used to prepare model compounds.

Strategy 1: **B_1D_1** and **B_2D_2**

The diol (1.0 eq), the boronic acid (1.05 eq) and 0.1 vol% of water were mixed in Et$_2$O (2 mL/1 mmol boronic acid) at room temperature and stirred until complete dissolution of all compounds. MgSO$_4$ (3.0 eq) was added stepwise and the mixture was stirred at room temperature for 5-24 hours. The suspension was filtered and concentrated under reduced pressure. The resulting oil was distilled at 90 °C (**B_1D_1**) or 140 °C (**B_2D_2**) under high vacuum to yield the target compounds in very high purity as a colourless oil (**B_1D_1**) or a white solid

(B₂D₂) (70-85%). The purified boronic esters were transferred directly to dried and purged Schlenk flasks and kept under inert atmosphere (argon).

Strategy 2: **B₁D₂, B₁D₃, B₁D₄, B₁D₅, B₁D₆, B₁D₇, B₁D₈, B₂D₁, B₂D₇, B₃D₂, B₄D₂, B₅D₂, B₆D₂**

The diol (1.0 eq), the boronic acid (1.05 eq) and 0.1 vol% of water were mixed in Et₂O or THF (2 mL/1 mmol boronic acid) at room temperature and stirred until complete dissolution of all compounds. MgSO₄ (3.0 eq) was added stepwise and the mixture was stirred at room temperature for 5-24 hours. The suspension was filtered and concentrated under reduced pressure to yield the target compounds as colourless oils or white solids (60-82%). The boronic esters were transferred directly to small septum closed vials and kept under inert atmosphere (argon).
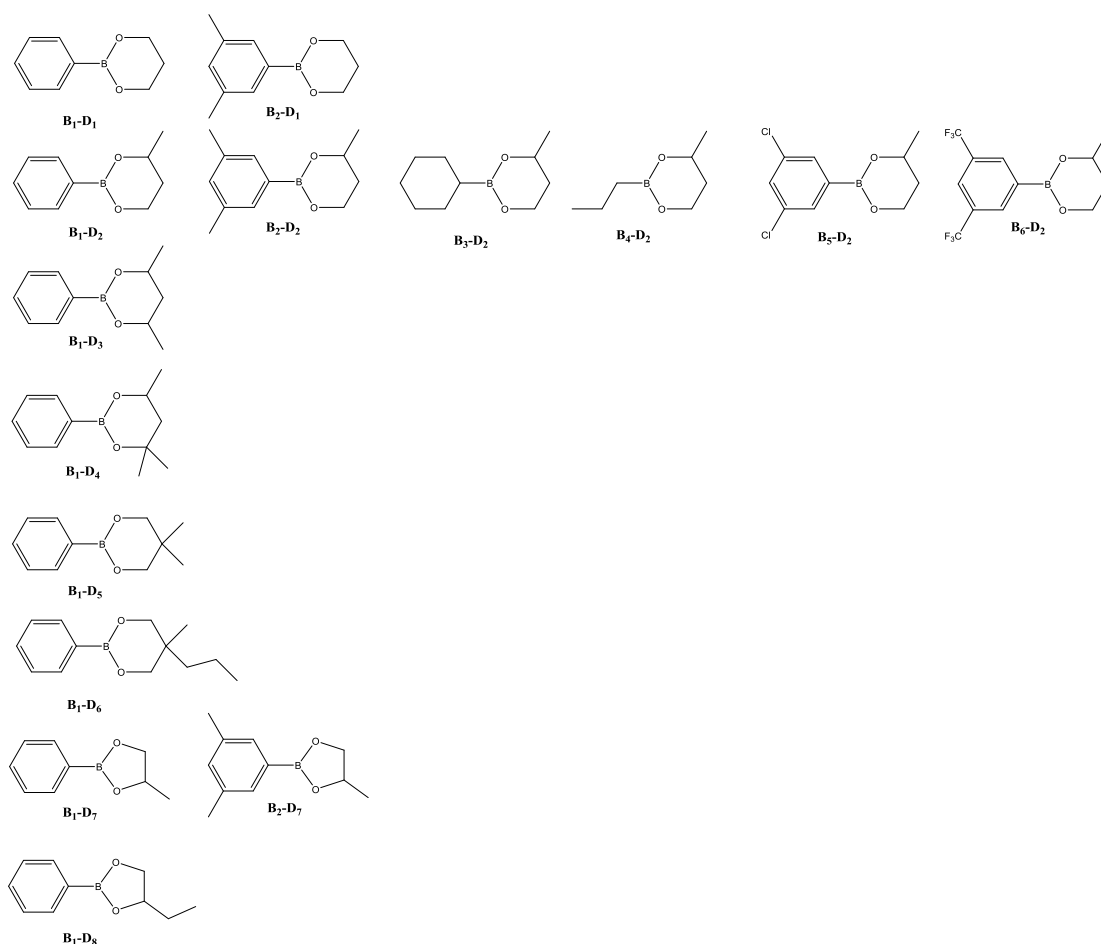
Scheme 3.8. Boronic esters synthesised and studied in model experiments, organized according to the boronic acid part (column) and the diol part (row).

3.3.2 Detection limit of 1,3-propanediol and 1,3-butanediol in ^{1}H-NMR spectroscopy

To determine the purity of boronic esters generated via strategy 1, the detection limit for free diols in ^{1}H-NMR analysis was estimated by deliberately decreasing the concentration of 1,3-propanediol (D_1) and 1,3-butanediol (D_2) in $CDCl_3$ (**Table 3.1**). Stock solutions of D_1 and D_2 at a concentration of 25.5 mM were generated and further diluted with the deuterated solvent. Styrene was added as internal standard (at a concentration of 25.0 mM) to the deuterated chloroform before it was dried with molecular sieves and the stock solutions were prepared.
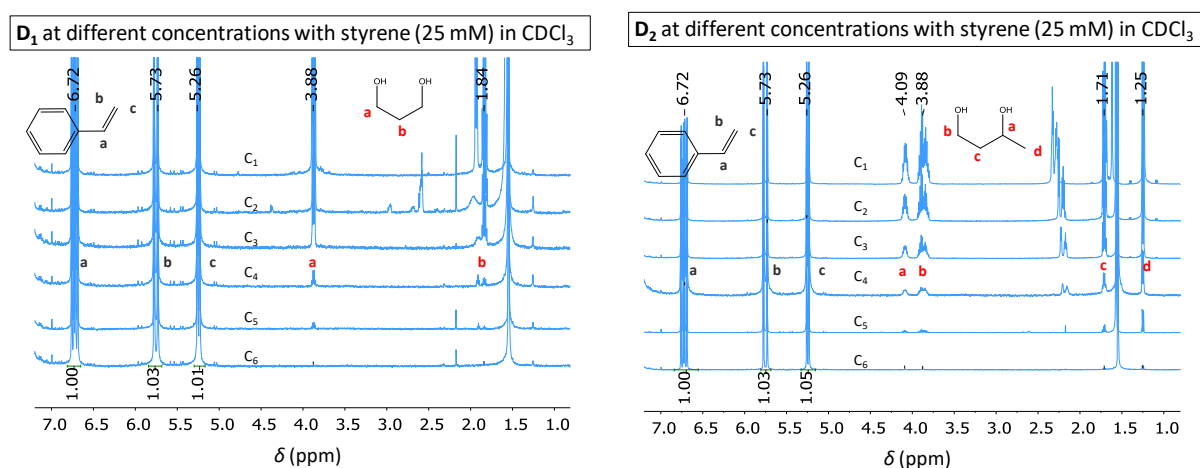

Figure 3.2. Determination of the detection limit of 1,3-propanediol (D_1, left) and 1,3-butanediol (D_2, right) in ^{1}H-NMR with a constant concentration of styrene as internal standard.
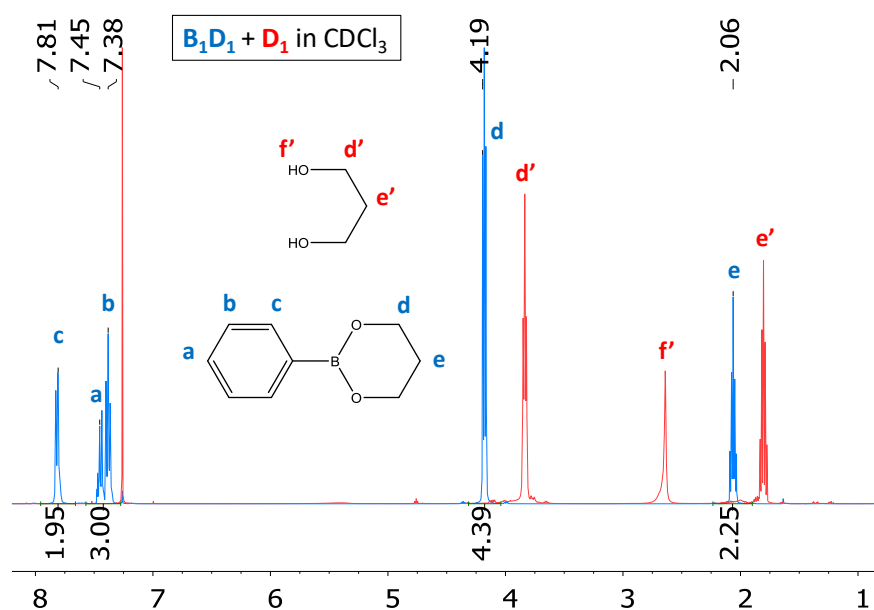

**Figure 3.3.** ^{1}H-NMR analysis in $CDCl_3$ of B_1D_1 (1 M) overlapped with free D_1.
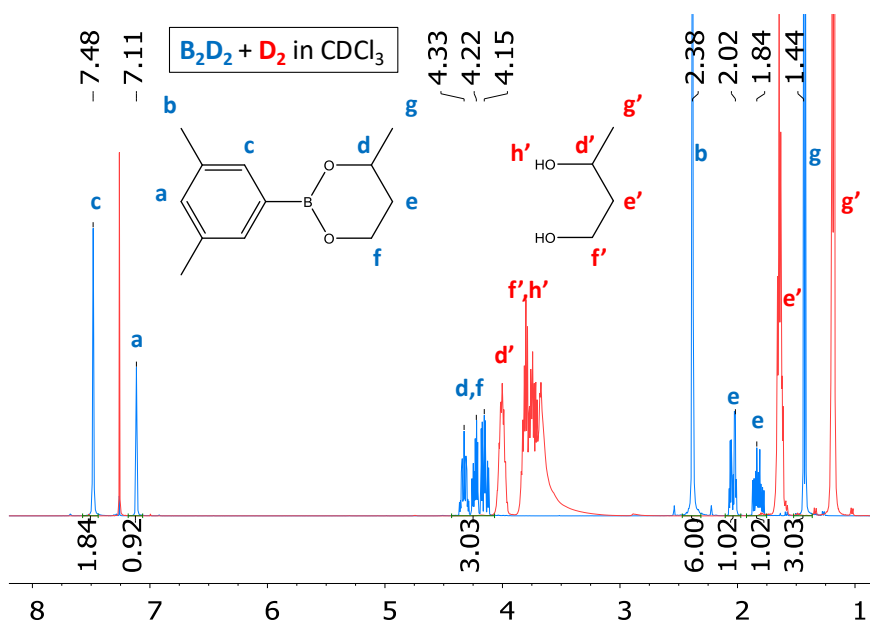
Figure 3.4. ^{1}H-NMR analysis in CDCl$_3$of **B$_2$D$_2$** (1 M,) overlapped with free **D$_2$**.

In total twelve solutions were analysed. In the ^{1}H-NMR spectrum of the 5.10^{-4} mol/L solution, **D$_1$** and **D$_2$** can still be detected and the integration values of the different signals match rather well. At a concentration of 1.10^{-4} mol/L, the signals of **D$_1$** cannot be detected anymore and only the CH$_3$-signal of **D$_2$** at 1.25 ppm is still detectable at this concentration (**Figure 3.2**).

Assuming a detection limit of 5.10^{-4} mol/L, the maximum free diol content in the synthesised boronic esters, **B$_1$D$_1$** and **B$_2$D$_2$,** was estimated by analysing highly concentrated boronic ester solutions in 1H-NMR spectroscopy (**Figures 3.3 and 3.4**).

Table 3.1. Determination of the detection limit of 1,3-propanediol (**D$_1$,** top) and 1,3-butanediol (**D$_2$,** bottom) in ^{1}H-NMR spectroscopy: Concentration and integration values of **D$_1$** and **D$_2$** in CDCl$_3$.

#	C	Chemical shift (ppm) and integration					
	D$_1$ (M)	Styrene			**D$_1$**		
		6,72 (1H)	5,73 (1H)	5,26 (1H)	3,88 (4H)	1,82 (2H)	-
C1	2,50E-02	1	1,06	1,07	1,19	0,61	-
C2	1,00E-02	1	1,03	1,02	0,4	0,28	-
C3	5,00E-03	1	1,06	1,03	0,18	0,12	-
C4	1,00E-03	1	1,05	1,06	0,102	0,044	-
C5	5,00E-04	1	1,13	1,1	0,03	nd*	-
C6	1,00E-04	1	1,12	1,07	nd*	nd*	-

#	C	Chemical shift (ppm) and integration					
	D$_2$ (M)	Styrene			D$_2$		
		6,72 (1H)	5,73 (1H)	5,26 (1H)	4,1 (1H)	1,7 (1H)	1,25 (3H)
C1	2,50E-02	1	1,01	0,99	1,16	2,4	3,61
C2	1,00E-02	1	1,02	1,02	0,44	0,92	1,51
C3	5,00E-03	1	1,02	0,99	0,2	0,5	0,69
C4	1,00E-03	1	0,99	0,98	0,03	0,15	0,12
C5	5,00E-04	1	1,08	1,08	0,02	0,06	0,09
C6	1,00E-04	1	1,02	1,06	nd*	nd*	0,03

*nd = not detectable

The diol signals of **D$_1$** and **D$_2$** are undetectable in the ^{1}H-NMR spectra of **B$_1$D$_1$** and **B$_2$D$_2$,** respectively. The maximum diol content in the boronic esters can be calculated using the above estimated detection limit and the following relation:

$$[diol]_{max} = \frac{[diol]_{max}}{[diol]_{max} + [boronic\ ester]}$$

$$[diol]_{max} = \frac{5.10^{-4} \text{mol/L}}{5.10^{-4} \text{mol/L} + 1.000\ \text{mol/L}}$$

**Equation 3.1.** $\qquad\qquad [diol]_{max} = 0.05\ \text{mol\%}$

Thus, the boronic esters **B$_1$D$_1$** and **B$_2$D$_2$** prepared via strategy 1 possess a minimum purity of 99.95 mol% with respect to their corresponding diols.

Similarly, in the ^{1}H-NMR spectra of the boronic esters synthesised via strategy 2 no free diol signals were detected. The maximum free diol content was calculated via the same procedure as mentioned above. Among all the studied diols, **D$_5$** and **D$_6$** possess the highest detection limit respectively with 0.35% and 0.27%. The boronic esters synthesised via strategy 2 possess thus a minimum purity of 99.65 mol% with respect to their corresponding diols.

3.4 Association and dissociation equilibrium constants of boronic esters

3.4.1 Determination of the association equilibrium constant from diol and boronic acid

In order to assess the equilibrium composition of boronic acids, diols and boronic esters in the absence of a water trapping agent, the association constant (K_{ass}) was determined.
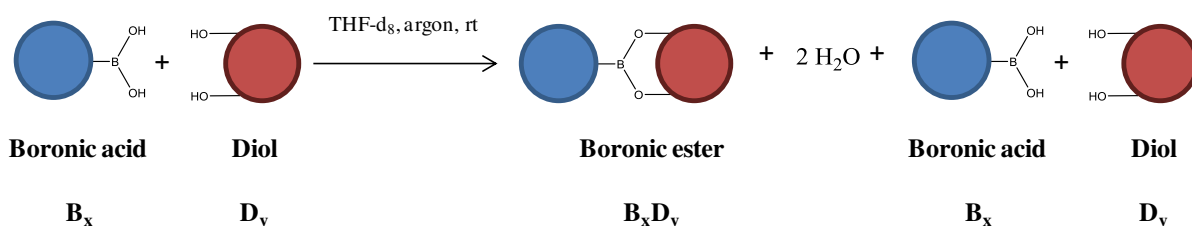
Scheme 3.8. Formation of boronic esters B_xD_y in THF-d_8.

Phenylboronic acid (B_1) was dissolved in dried THF-d_8 at room temperature and mixed with an equimolar amount of a solution of diol in dried THF-d_8 at the same concentration (0.2 mol.L^{-1}) (**Scheme 3.8**). After mixing 20 hours, the solution was analysed by ^{1}H-NMR spectroscopy using an oven dried NMR tube purged with argon to prevent the presence of water. Characteristic isolated signals of boronic esters and diols were used. For instance, the signal at 1.32 ppm (-CH$_3$) of the boronic ester B_1D_2 was compared to the corresponding peak from the diol at 1.09 ppm (**Figure 3.5**), while for B_1D_1 the peak at 2.06 ppm (-CH$_2$) was studied. The total concentration of boronic esters and diols should be equal to the initial concentration of diols (prior to mixing), that is to say 0.1 mol.L^{-1}. The exact concentration of water, boronic esters, boronic acids and diols could be calculated. Consequently, the association equilibrium constant was determined assuming negligible amount of boroxines in the starting boronic acid and using the following equation:

Equation 3.2.
$$K_{ass} = \frac{[B_xD_y]*[H_2O]^2}{[B_x]*[D_y]}$$

The value appeared to be very different between dioxaborolanes and dioxaborinanes (**Table 3.2**). For the former, the constant was calculated to be 20 M (B_1D_7) and 26 M (B_1D_8), while the latter had association constants four to twelve times higher (**Table 3.2**). Chemically different dioxaborinanes were tested to study the effect of the substitution pattern on the association constant. For a fixed boronic acid, phenyl boronic acid (B_1), different diols, D_y, were added to form the corresponding boronic esters. As a general trend, the more the diol is

substituted the higher is the association constant. For instance, the boronic ester **B₁D₄**, with 3 methyl groups on the diol, possess an association constant of 312 M, while **B₁D₁**, with the unsubstitued 1,3-propanediol **D₁**, has an association constant of 139 M. Interestingly, the position of the methyl groups has an influence on the overall stability of dioxaborinanes. **B₁D₅**, with two methyl groups born by the carbon which is not attached to oxygen atoms, has an association constant estimated to be 303 M, while **B₁D₃** with same number of methyl groups but closer to C-O bond had a lower constant at 92 M. Then the diol was fixed, 1,3-butanediol, **D₂**, and the boronic acid, **Bₓ**, was varied. The equilibrium composition is also strongly related to the structure of the boronic acid. For instance, halogen-substituted, **B₂D₅**, and trifluoromethyl-substituted dioxaborinanes, **B₂D₆**, have an association constant estimated to be 830 and 499 M, respectively, while the association constant of the 3,5-dimetyl-susbtituted boronic ester **B₂D₂** was found to be 108 M.

The ratio boronic ester/water (1/2 according to ^{1}H-NMR) was consistent with the equation of the reaction, for which two molecules of water are released for every molecule of boronic ester formed. The observed boronic ester/water ratio indicates that no (or very limited) quantities of boroxine was formed under these conditions. However, the concentration of water may be imprecise because of its labile protons that can exchange with those of diols.

These experiments indicate that simple mixing of diols and boronic acids, without removing the resulting water, produces dioxaborolanes and dioxaborinanes in high yields. The association equilibrium constant is ten times higher for the dioxaborinanes than for the dioxaborolanes.
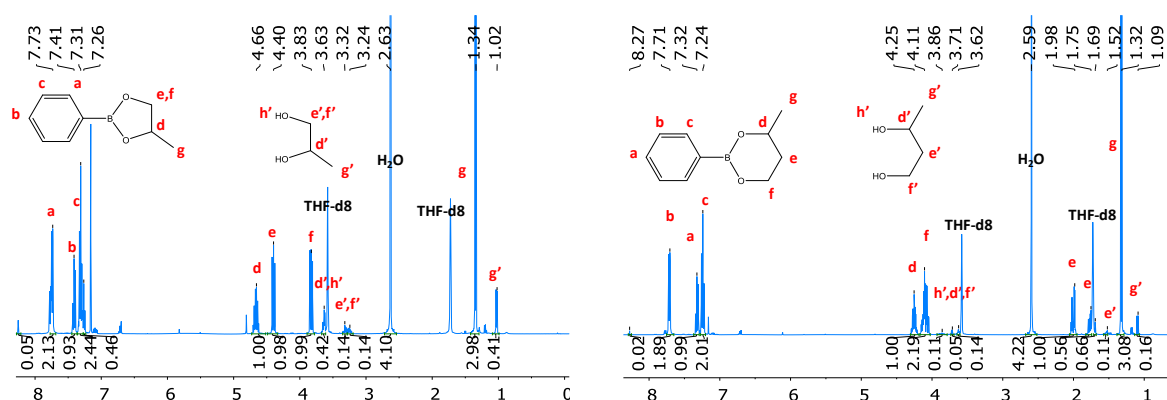

**Figure 3.5.** ^{1}H-NMR of the formation of boronic esters **B₁D₇,** and **B₁D₂**, after 18h at room temperature.

Table 3.2. Determination of the association equilibrium constant K_{ass} via ^{1}H-NMR.

B_xD_y	$[B_xD_y+Dy]$	$[B_xD_y]/[Dy]$	$[B_xD_y]$	$[H_2O]$	$[B_x]$	$[D_y]$	K_{ass}
-	(M)	-	(M)	(M)	(M)	(M)	(M)
	theoritic	Measured	Calculated	Calculated	Calculated	Calculated	Calculated
B_1D_1	0,1	18,2	9,5E-02	2,0E-01	5,2E-03	5,2E-03	139
B_1D_2	0,09	19,3	8,6E-02	1,8E-01	4,4E-03	4,4E-03	141
B_1D_3	0,10	15,3	9,4E-02	1,9E-01	6,1E-03	6,1E-03	92
B_1D_4	0,10	26,5	9,6E-02	2,1E-01	3,6E-03	3,6E-03	312
B_1D_5	0,10	26,1	9,6E-02	2,1E-01	3,7E-03	3,7E-03	303
B_1D_7	0,10	7,3	8,8E-02	1,8E-01	1,2E-02	1,2E-02	20
B_1D_8	0,10	7,9	8,9E-02	1,9E-01	1,1E-02	1,1E-02	26
B_2D_2	0,10	15,8	9,4E-02	2,0E-01	6,0E-03	6,0E-03	108
B_3D_2	0,10	21,4	9,6E-02	2,1E-01	4,5E-03	4,5E-03	203
B_4D_2	0,10	29,7	9,7E-02	2,1E-01	3,3E-03	3,3E-03	394
B_5D_2	0,10	42,9	9,8E-02	2,1E-01	2,3E-03	2,3E-03	830
B_6D_2	0,10	33,3	9,7E-02	2,1E-01	2,9E-03	2,9E-03	499

3.4.2 Determination of the dissociation equilibrium constant through hydrolysis

As discussed above, boronic esters are formed by the reversible condensation of a free diol with a boronic acid with the release of two equivalents of water. Consequently, the presence of water can lead to the hydrolysis of pure boronic esters. Hydrolysis depends on many parameters such as the solvent, temperature, pH, etc... In order to investigate the stability of boronic esters in the presence of water, hydrolysis experiments were conducted on **B_1D_7**, **B_1D_1** and **B_1D_4** in THF-d_8. To determine the amount of hydrolysed boronic esters, precise quantities of water were added to THF-d_8 stock solutions containing a known concentration of boronic esters (**Scheme 3.9**). After 48 hours, when the equilibrium is reached, the samples were handed to ^{1}H-NMR spectroscopy. All the tubes were oven-dried, and solutions were

prepared and kept under argon. The dissociation equilibrium constant was studied in detail at room temperature through four different ratios of **B₁D₇**/H₂O, **B₁D₁**/H₂O and **B₁D₄**/H₂O (**Table 3.3**). Stabilities of dioxaborolanes and dioxaborinanes were compared.
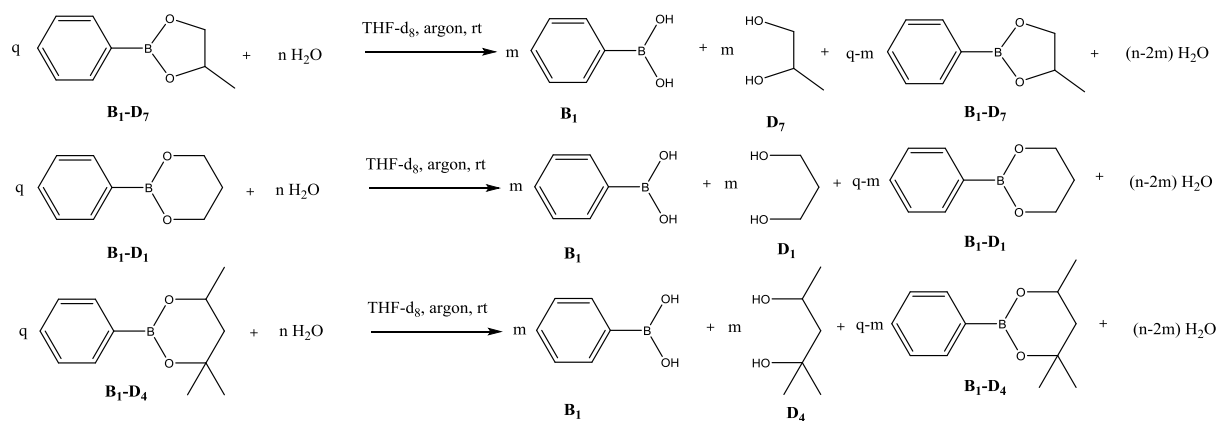
Scheme 3.9. Hydrolysis of boronic esters **B₁D₇**, **B₁D₁** and **B₁D₄** in THF-d₈.

Table 3.3. Reactants quantities used to investigate the hydrolysis of boronic esters **B₁D₇**, **B₁D₁** and **B₁D₄**.

C#	*ratio*	**Reactant**	*m*	*M*	*n*	*V*	*C*
	H₂O/BₓDᵧ		(mg)	(g/mol)	(mmol)	(µL)	(M)
		B₁D₇	12,3	161,99	0,08	600	0,13
C1	20		27,3		1,52	27	2,53
C2	10	H₂O	13,7	18	0,76	14	1,27
C3	5		6,8		0,38	7	0,63
C4	1		1,4		0,08	1	0,13
		B₁D₁	12,3	161,99	0,08	600	0,13
C1	20		27,3		1,52	27	2,53
C2	10	H₂O	13,7	18	0,76	14	1,27
C3	5		6,8		0,38	7	0,63
		B₁D₄	12,3	204,07	0,06	600	0,10
C1	20		21,7		1,21	22	2,53
C2	10	H₂O	10,8	18	0,60	11	1,27
C3	5		5,4		0,30	5	0,63

Boronic esters can be sensitive to hydrolysis and their water stability depends on their substitution pattern. The dissociation constants of the boronic esters were calculated via the following equation:

Equation 3.3.

$$K_{diss} = \frac{[B_x]*[D_y]}{[B_xD_y]*[H_2O]^2}$$

Two methods were used to determine the concentration of water. The first one (method 1) relies on the integration of the signal of water whose protons can exchange with the deuterated THF, which may lead to an incorrect assessment of the water content. In contrast, the second method (method 2) calculates the water concentration according to the following equation:

Equation 3.4.
$$[H_2O]_t = [H_2O]_0 - 2 \times [D_y]_t$$

Method 2 is based on the theoretical initial water concentration minus two times the quantity of generated diols. Tuning the ratio of $H_2O/\mathbf{B_1D_7}$ leads to modify the equilibrium composition between boronic esters, free diols and boronic acids. According to method 1, the dissociation constant was estimated to be $K_{diss} = 1.5 \times 10^{-1}$ M^{-1} for $\mathbf{B_1D_7}$ (**Table 3.4**). This value corresponds to $K_{ass} = 7$ M, which is of the same order of magnitude with the measured 20 M. Method 2 gave lower values for K_{diss} *ca.* 2.6×10^{-2} M^{-1}. In contrast with dioxaborolanes, the two methods gave similar results for the 6-membered boronic esters. Dissociation constants of dioxaborinanes were calculated to be one or two orders of magnitude lower than those of dioxaborolanes, with K_{diss} of 7.6×10^{-3} M^{-1} and 1.4×10^{-3} M^{-1} for $\mathbf{B_1D_1}$ and $\mathbf{B_1D_4}$, respectively, (**Figure 3.6**). $\mathbf{B_1D_4}$, which has three methyl groups bore by the diol part, has a dissociation constant which is five times lower than the same boronic ester without methyl group, *i.e.* $\mathbf{B_1D_1}$. The presence of these side groups might decrease the hydrolysis through steric hindrance. The association constant of $\mathbf{B_1D_1}$ calculated from $1/K_{diss} = 131$ M is consistent with the value of 139 M as mentioned above, while for $\mathbf{B_1D_4}$, $1/K_{diss} = 741$ M is twice higher than the value determined by initially mixing the diol and the boronic acid. The presence of boroxines and/or imprecise determination of concentration of water might be responsible for this discrepancy when estimating K_{ass} and K_{diss}.

Table 3.4. Determination of the dissociation equilibrium constant K_{diss} via ^{1}H-NMR spectroscopy.

B_xD_y	C#	[B_xD_y+Dy] (M)	[B_xD_y]/[Dy] -	[B_xD_y] (M)	[H_2O] (M)	[B_x] (M)	[D_y] (M)	K_{diss} (M^{-1})	K_{ass} (M)	[H_2O] (M)	K_{diss} (M^{-1})	K_{ass} (M)
-	-	Theoritical	Measured	Measured	Measured	Estimated	Measured	Method 1		Estimated	Method 2	
B_1D_7	C1	0,10	0,7	4,1E-02	8,4E-01	5,9E-02	5,9E-02	1,2E-01	8	2,4E+00	1,4E-02	69
	C2	0,10	1,2	5,5E-02	5,2E-01	4,5E-02	4,5E-02	1,4E-01	7	1,2E+00	2,7E-02	37
	C3	0,10	2,8	7,4E-02	2,5E-01	2,6E-02	2,6E-02	1,6E-01	6	5,8E-01	2,9E-02	35
	C4	0,10	14,3	9,3E-02	5,1E-02	6,5E-03	6,5E-03	1,7E-01	6	1,2E-01	3,4E-02	30
B_1D_1	C1	0,10	1,4	5,8E-02	2,2E+00	4,2E-02	4,2E-02	6,2E-03	162	2,4E+00	5,0E-03	202
	C2	0,10	3,1	7,6E-02	1,0E+00	2,4E-02	2,4E-02	7,2E-03	140	1,2E+00	5,2E-03	193
	C3	0,10	5,7	8,5E-02	5,3E-01	1,5E-02	1,5E-02	9,5E-03	105	6,0E-01	7,3E-03	137
B_1D_4	C1	0,10	7,2	8,8E-02	1,6E+00	1,2E-02	1,2E-02	6,9E-04	1450	2,5E+00	2,7E-04	3707
	C2	0,10	10,8	9,2E-02	7,8E-01	8,4E-03	8,4E-03	1,3E-03	790	1,3E+00	5,0E-04	2017
	C3	0,10	18,3	9,5E-02	3,7E-01	5,2E-03	5,2E-03	2,1E-03	477	6,2E-01	7,4E-04	1351

143
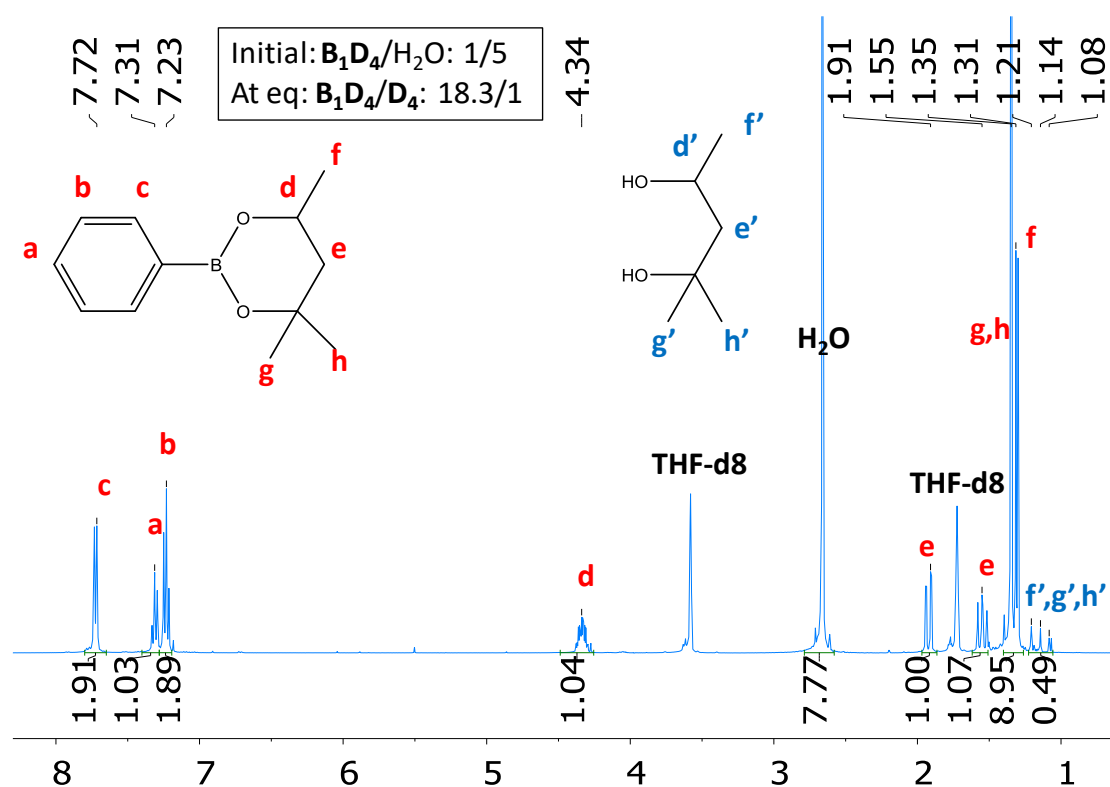
Figure 3.6. ^{1}H-NMR in THF-d$_8$ of **B$_1$D$_4$** and **D$_4$** after hydrolysis reaction with an initial ratio **B$_1$D$_4$/H$_2$O**: 1/5.

In this section, the association and dissociation equilibrium constants of boronic esters, K_{ass} and K_{diss}, were estimated. Phenyl boronic acid (**B$_1$**) was mixed, in dry THF-d$_8$ and under protective atmosphere, with equimolar amounts of various diols. The thermodynamic association constants were calculated to be 20 M and 26 M for **B$_1$D$_7$** and **B$_1$D$_8$**, respectively, while the thermodynamic association constant ranges between 92 and 312 M for dioxaborinanes. Even in the absence of water trapping agent, the proportion of generated boronic esters is higher than the amount of corresponding diols or boronic acids, 8 times for dioxaborolanes and from 15 to 42 times for dioxaborinanes. It was shown that the more the boronic esters are sterically hindered the higher is their water stability. The dissociation equilibrium constants, K_{diss}, of three different pure boronic esters were estimated under the same conditions and matched well with the above association equilibrium constants as K_{ass} = $1/K_{diss}$. The constants range varies from 0.15 M^{-1} for dioxaborolane **B$_1$D$_7$** and 7.6×10^{-3} M^{-1} to 1.4×10^{-3} M^{-1} for dioxaborinanes **B$_1$D$_1$** and **B$_1$D$_4$**, respectively. The higher stability against hydrolysis of diaxoborinanes as compared to dioxaborolanes reflects the absence of ring strain in the 6-membered ring boronic esters unlike the 5-membered ring species. To investigate the rate of different exchanges that can occur between boronic esters with and without diols in organic solvent and in bulk, the following experiments were conducted.

3.5 Exchange reactions under air

The studies of exchange reactions taking place in mixtures of dioxaborolanes or dioxaborinanes are presented in the following sections. Experiments were performed under different conditions. In this subchapter, the influence of water and atmospheric moisture on boronic esters exchange is investigated to see if pure boronic esters can exchange in these conditions. Kinetic experiments were followed under air via GC analysis.

3.5.1 GC methods: internal and external calibrations and usual procedure

Kinetic studies of the possible exchange reaction between boronic esters were followed by gas chromatography (GC). To calculate the exact molar quantity of the different boronic esters involved in the reactions from GC raw data, internal and external calibrations methods were used.

External calibrations curves were obtained for each boronic ester. Each compound was analysed at four different concentrations at a constant sample volume of 1 μL and specific response factors were generated for every boronic ester. When no internal calibration was used, then only the percentage of each boronic ester could be calculated.

For internal calibration, an internal standard (IS) was added and the boronic esters signals were referred to this standards signal. The standard was chosen according to its column compatibility, retention time, temperature stability, polarity and its inert character towards boronic esters. Dodecane or tetradecane were used as internal standards. They were dried and stored over molecular sieves at least four days under argon atmosphere before use.
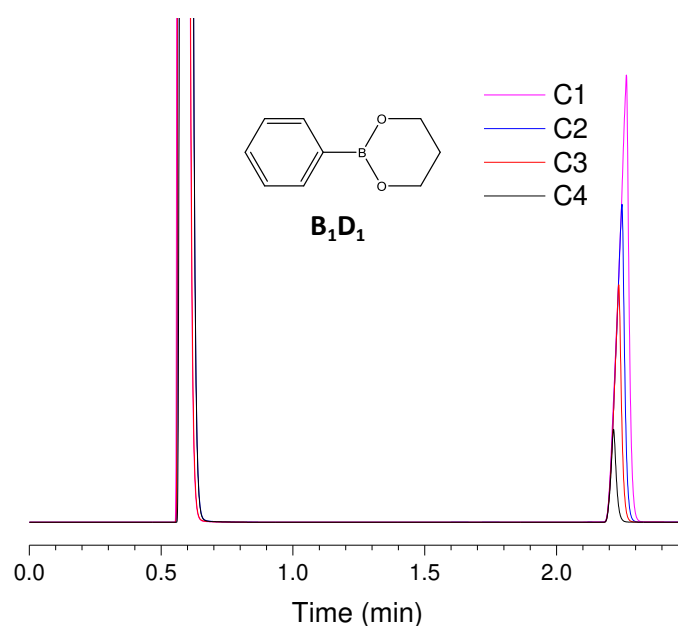
Figure 3.7. Example of the GC raw data used for the external calibration curve of boronic ester **B₁D₁**.

All calibration curves were generated as follow. Stock solutions of each boronic ester and inert standard were prepared by adding 0.1 mmol of the corresponding molecule to 1 mL of the respective solvent. 100, 50, and 10 μL of these stock solutions were subsequently diluted with the anhydrous solvent to reach the targeted concentrations, between 140 mM and 9 mM, and characterised by GC using an injection volume of 1 μL (**Figure 3.7**). Concentrations were corrected for diol or boronic acid impurities, as quantified by prior ¹H-NMR analysis. The slope of the linear fit of the four resulting points was used as external calibration reference to obtain the concentration – area dependence for each molecule as depicted in **Figure 3.8**.
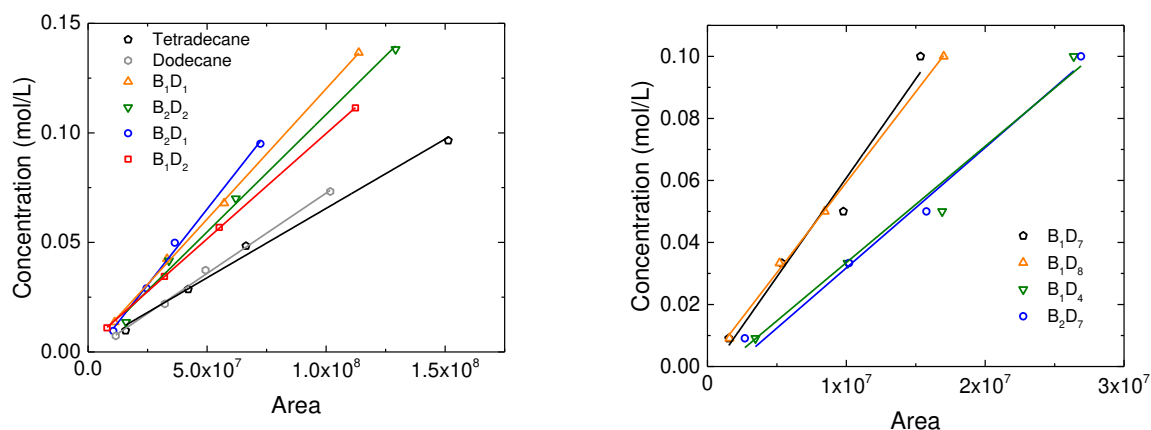
Figure 3.8. External calibration curves of the boronic esters used for model exchange reactions.

GC analysis was conducted on a Shimadzu gas chromatograph GC-2014 equipped with a Waxplus column, a flame ionization detector and helium as carrier gas. Injection was done manually by injecting 1 µL sample volumes using a 10 µL syringe from Hamilton. Before running analysis, the entire set-up was pre-heated at 350 °C and kept at constant carrier gas flow of 5 mL/min and split ratio of 2.0 for at least 20 min.

GC methods were adapted to the nature of the studied boronic esters, meaning polarity and molar mass, and the speed of the exchange reaction. The methods varied in detection/injection temperature, starting temperature of the column and the temperature program. The carrier gas flow was adjusted when necessary. These parameters were chosen as a compromise between short retention time, to maximise the number of measures in a given time, and good separation between the products, to improve the precision and reproducibility of the results. **Table 3.5** depicts the totality of used GC methods.

Table 3.5. Gas chromatography methods used for kinetic studies of boronic ester exchanges.

$T_{inj/det}$	T_{col}	Column flow	Split ratio	Temperature program
(°C)		(mL)	-	Hold time (min) / ramp (°C/min) / aimed temperature (°C)
Reactions with only dioxaborolanes				
300	100	3.0	2.0	0/30/200
Reactions with dioxaborolanes and dioxaborinanes				
300	100	5.0	2.0	0.5/30/250
Reactions involving only dioxaborinanes				
270	100	8.5	10	0.5/8/119 - 1/4/124 - 1/4/135

3.5.2 Study of the exchange reaction between two dioxaborinanes under air

The direct reaction between two dioxaborinanes was investigated in the presence of atmospheric moisture (**Figure 3.9**). To this aim, the following series of experiments were

performed. Stock solutions with a concentration of 0.1 M of **B₁D₁** and 0.1 M of **B₂D₂** were generated under argon in toluene and a stoichiometric amount of **B₂D₂** (2 mL) was added to **B₁D₁** (2mL) under ambient atmosphere at the considered temperature.
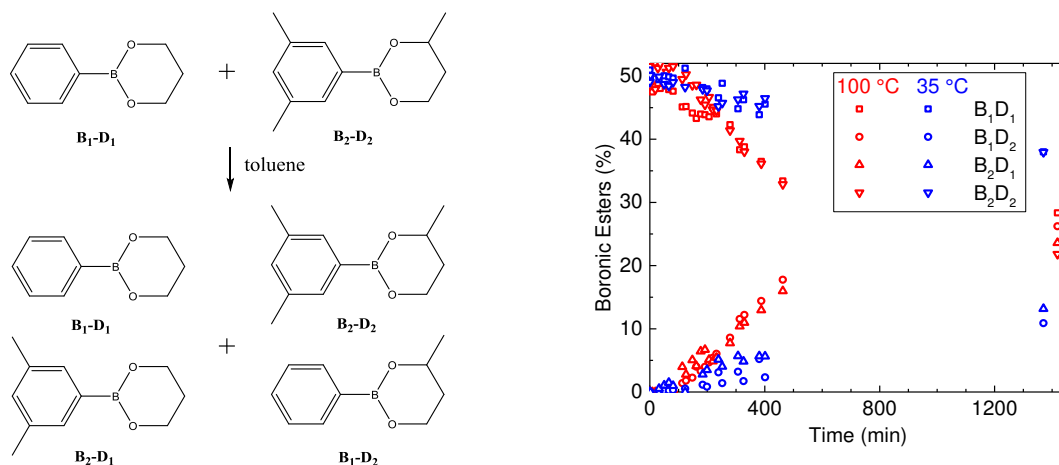

Figure 9. Exchange between **B₁D₁** and **B₂D₂** under air in toluene at 100 °C (red) and 35 °C (blue).

The reaction at 35 °C presented an induction period of 180 min, where no reaction occurred (**Figure 3.9**). After 100 min, the reaction began to proceed slowly with an equilibrium time superior to 1400 min at 35 °C. Increasing the temperature to 100 °C decreased the induction period to 100 min and the equilibrium state was reached after more than 500 min.

3.5.3 Study of exchange reaction between a dioxaborinane and a dioxaborolane under air
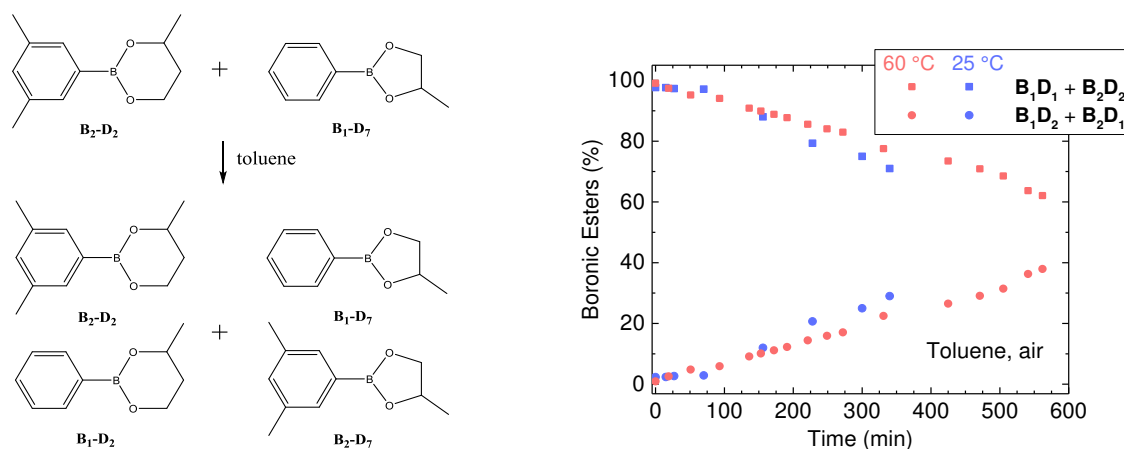
Figure 3.**10.** Exchange between dioxaborolane B_1D_7 and dioxaborinane B_2D_2 under air in toluene at 60 °C (red) and 25 °C (blue).

The influence of the structure of boronic ester was studied under similar conditions, *i.e.* in solution under ambient atmosphere (**Figure 3.10**). The exchange between dioxaborinane B_2D_2 and dioxaborolane B_1D_7 is faster than between two dioxaborinanes made solely from 1,3-aliphatic diols. This observation reflects the higher reactivity, thus lower stability, of the 5-membered boronic ester rings because of ring strain. The kinetics data reveal that at 60 °C the dioxaborinane B_2D_2 does not react before 60 min, while the dioxaborolane concentration of B_1D_7 started to decrease as from 20 min. This can be explained by the higher water stability of dioxaborinanes. Interestingly, cooling down the system to 25 °C did not result in a decreased equilibrium time, which indicates a low activation energy of the exchange reaction through hydrolysis and transesterification.

149

3.6 Exchange reactions under protective atmosphere

The transesterification of dioxaborinanes was studied with different diols in solution. Finally, the exchange reaction between highly pure boronic esters was studied in concentrated solutions and in bulk. Key parameters of the direct exchange, such as the rate constant k and the activation energy, E_a, of the reaction, were estimated. Out of stoichiometry experiments were conducted to determine the global order of the reaction.

3.6.1 Transesterification reactions

3.6.1.1 Transesterification of dioxaborolanes with 1,2-butanediol

To better understand the role of diols in solution of boronic esters, a series of experiments was performed under argon atmosphere. Under these conditions, the presence of water can be neglected and the effect of diols can be isolated from hydrolysis.

To study the kinetic of the direct transesterification reaction of a boronic ester with an aliphatic diol, the following experiments were conducted. Stock solutions with a concentration of 0.1 M of B_1D_7 and 0.1 M of dried D_8 were generated and a stoichiometric amount of D_8 (2 mL) was added to B_1D_7 (2mL) in DCM under argon atmosphere at 20 °C.
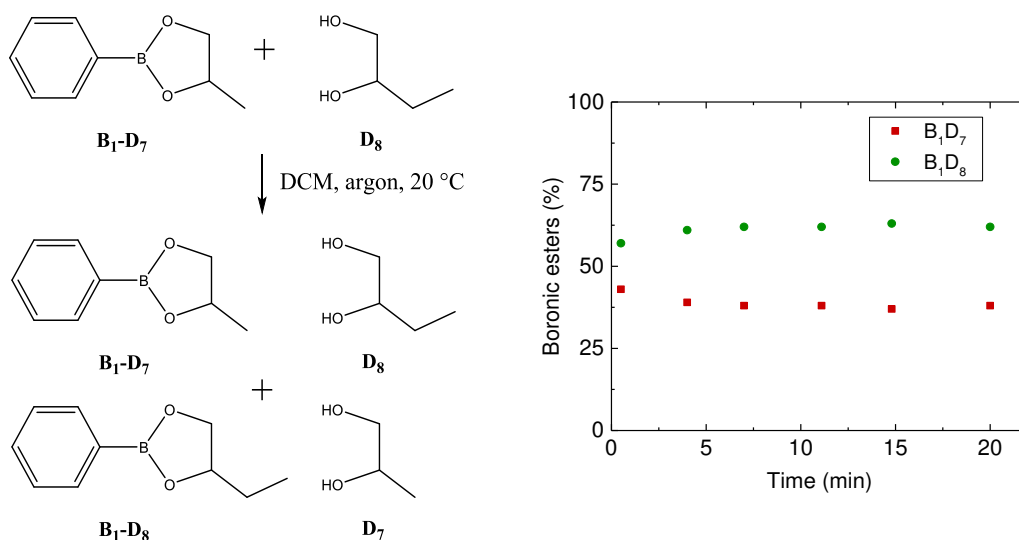

Figure 3.11. Transesterification of dioxaborolane B_1D_7 with a monosubstituted 1,2-aliphatic diol, D_8, in DCM at 20 °C.

Only boronic esters B_1D_7 and B_1D_8 could be detected via GC analysis because of the very short retention time of the free diols, no matter the parameters used in GC. **Figure 3.11** shows

the consumption of B_1D_7 and the generation of B_1D_8. The reaction is extremely fast, reaching its equilibrium within less than five minutes. The dioxaborolane products are not present in stoichiometric proportions, 62 mol% for B_1D_8 and 38 mol% for B_1D_7. This non stoichiometric distribution reveals that boronic ester B_1D_8 is more stable than B_1D_7 in DCM at room temperature.

3.6.1.2 Transesterification of dioxaborinanes with 1,3-butanediol

To compare the behaviour of dioxaborinanes and dioxaborolanes toward transesterification, a similar reaction was studied involving 6-membered ring boronic esters and a 1,3-aliphatic diol. Stock solutions with a concentration of 0.1 M of B_1D_1 and 0.1 M of died D_2 were generated, and various amounts of D_2 (in 2 mL) were added to B_1D_1 (2mL) in DCM under argon atmosphere at 20 °C.
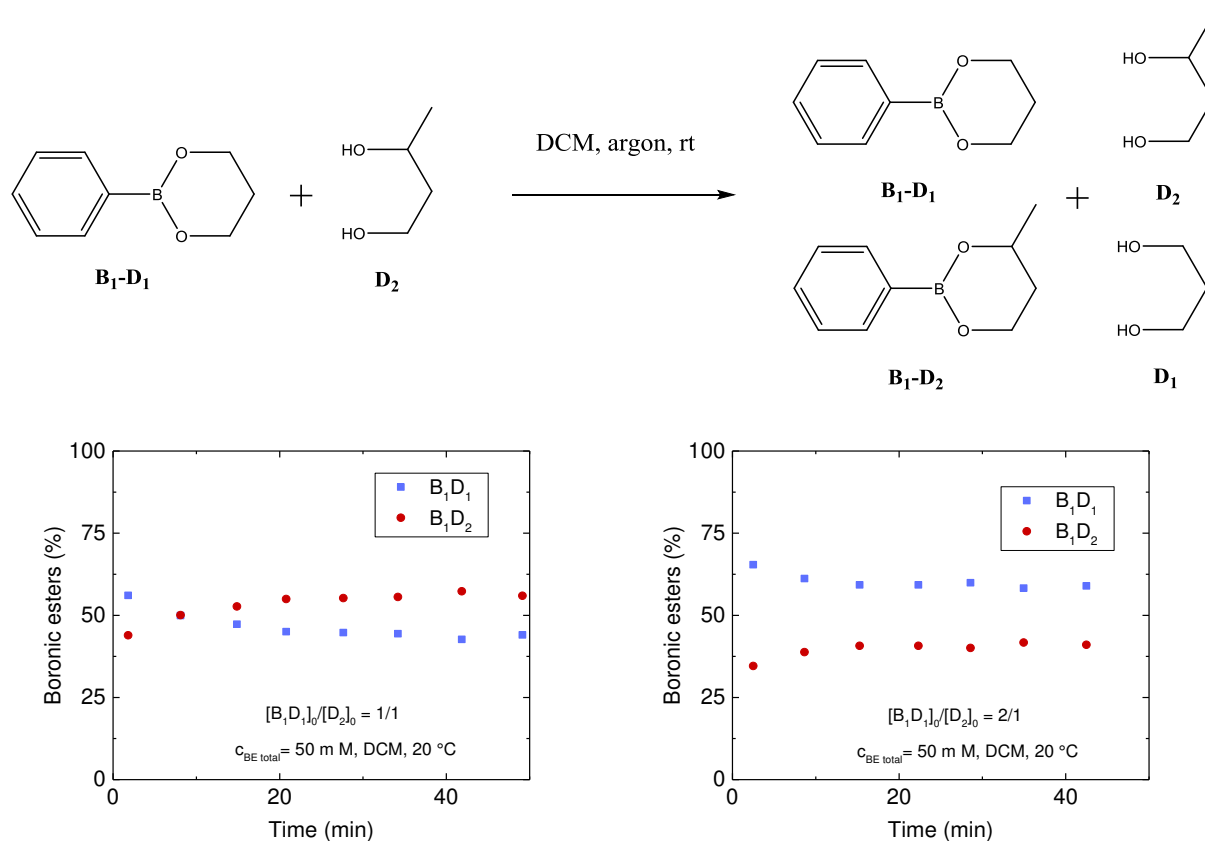
Figure 3.12. Transesterification of dioxaborinane B_1D_1 with a 1,3-aliphatic diol, D_2, in DCM at 20 °C, with different boronic ester/diol ratios.

The transesterification of dioxaborinanes was more than twice slower than the similar reaction with dioxaborolanes (**Figure 3.12**). This may be explained by the higher stability of the 6-

151

membered boronic esters. The equilibrium was reached after 20 minutes. As should be expected, the equilibrium composition was different depending on the initial ratio of B_1D_1 and D_2. For instance, with an equimolar initial ratio of B_1D_1 and D_2, the transesterification led to a product distribution of 43% for B_1D_1 and 57 % for B_1D_2. B_1D_2 is slightly more stable than B_1D_1 thanks to the extra methyl group of D_2. With a lower ratio D_2/B_1D_1 equilibrium was displaced to a higher B_1D_1 concentration also within 20 minutes.

To investigate the influence of the substitution pattern of the boronic ester, a different dioxaborinane, B_1D_4, made from phenylboronic acid and a bulky diol with three methyl groups, the 2,4-dimethylpentanediol, was used to study transesterification. Stock solutions with a concentration of 0.1 M of B_1D_4 and 0.1 M of dried D_2 were generated, and an equimolar amount of D_2 (2 mL) was added to B_1D_4 (2mL) in DCM under argon atmosphere at 20 °C.
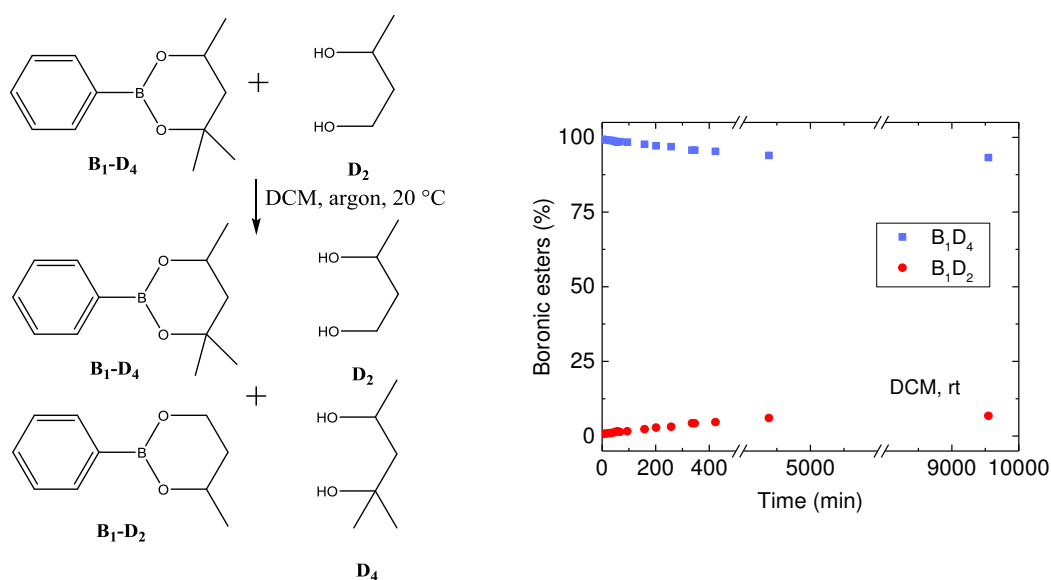

Figure 3.13. Transesterification of dioxaborinane B_1D_4 with a 1,3-aliphatic diol D_2 in DCM at 20 °C.

The exchange was extremely slow as compared to the transesterification between B_1D_1 and D_2. Indeed, the reaction needed more than 4300 minutes to reach the equilibrium (**Figure 3.13**). The steric hindrance of B_1D_4 only due to the diol part likely explains the slow rate of transesterification. Indeed, it was reported that pinacol (four methyl groups) based dioxaborolanes do not undergo transesterification.[82,87,88] The ratio B_1D_4 / B_1D_2, which is measured to be 13.7 is consistent with the higher stability of B_1D_4.

3.6.1.3 Transesterification of dioxaborolanes with 1,3-butanediol

One last transesterification was studied to confirm that the rate of transesterification mostly depends on the structure of the boronic ester rather than on the nature of the diol involved, 1,2 or 1,3-diol. The exchange between dioxaborolane B_1D_7 and 1,3-butanediol D_2 was conducted. The two compounds were mixed in equimolar amounts in DCM under argon atmosphere at 20 °C.
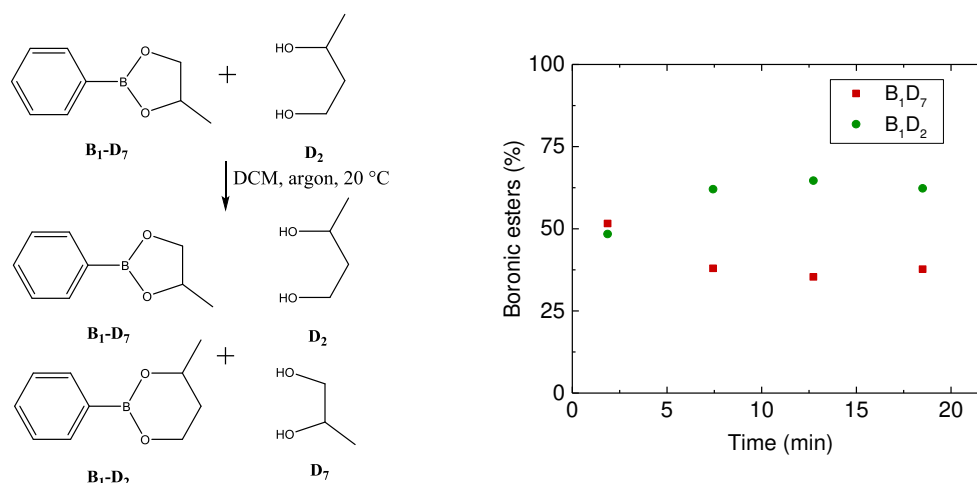

Figure 3.14. Transesterification of dioxaborolane B_1D_7 with a 1,3-aliphatic diol D_2 in DCM at 20 °C.

The kinetic was similar to those of B_1D_7 with the 1,2-butanediol D_8, with equilibrium reached within 7 minutes, and a product distribution in favour of the dioxaborinane; 65% of the dioxaborolane was converted into the most stable 6-membered boronic ester (**Figure 3.14**). Interestingly, this composition is not very different from the one observed with 1,2-butanediol, but 1,3-pentanediol should be used instead of 1,3-butanediol for a rigorous comparison, *i.e.* with a similar ethyl group as substituent on the diol part.

All the reactions of transesterification were slower for 6-membered boronic esters than for 5-membered boronic esters, but the exchange was always faster than between two boronic esters as observed in the previous section.

3.6.2 Exchange of dioxaborinanes in solution at room temperature

The two highly pure boronic esters B_1D_1 and B_2D_2 were mixed in an equimolar ratio under protective atmosphere in THF at an overall boronic ester concentration of 0.1 mM, and the evolution of the reaction was followed by GC.
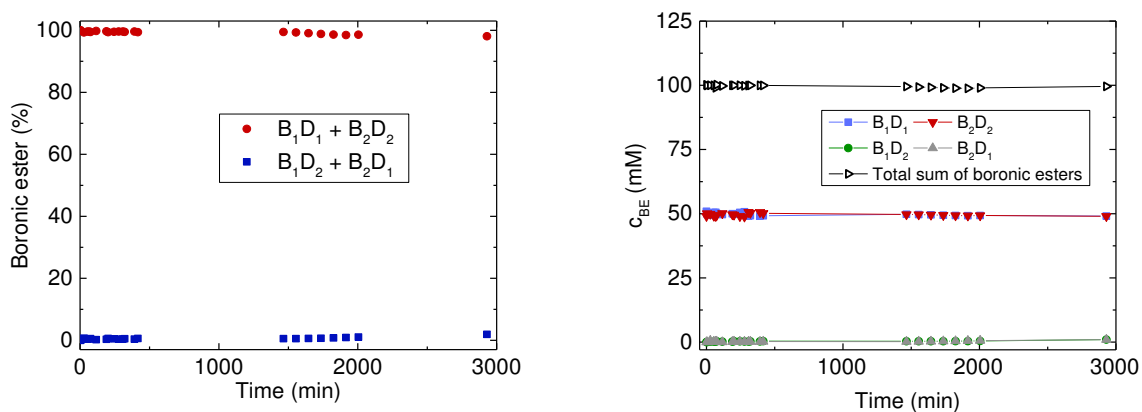

Figure 3.15. Reaction between B_1D_1 and B_2D_2 under argon protective atmosphere in THF at 20 °C. Signals are referred to the internal standard tetradecane and are given in mol% (left, plotted are the sums of reactants and products) and in concentration (right, individual curves for each species).

Almost no exchange reaction was detected under these conditions. After 2900 min, the generated B_1D_2 and B_2D_1 were still inferior to 0.5 mol% (**Figure 3.15**). As the presence of diols would lead to fast transesterification reaction, we can conclude to the absence of diols and water in this case. This experiment is a further evidence of the very high purity of the two compounds B_1D_1 and B_2D_2. It also validates this experimental set-up to perform exchange reactions in the absence of moisture.

3.6.3 Exchange of dioxaborinanes in highly concentrated medium and in bulk

When working in anhydrous conditions and under inert atmosphere, no exchange was observed between dioxaborinanes B_1D_1 and B_2D_2 in THF at an overall concentration of boronic esters of 100 mM. However, in a similar case as for dioxaborolanes, without detectable traces of water and diols, the reaction could occur in bulk through a direct exchange between boronic esters, or through transesterification due to the presence of undetectable traces of diols or water. The exchange reaction between dioxaborinanes B_1D_1 and B_2D_2 was studied at different temperatures in highly concentrated solution and in bulk

under protective atmosphere. Importantly, no traces of free diol could be detected by ^{1}H-NMR at the beginning and the end of all the conducted reactions.

3.6.3.1 Exchange between dioxaborinanes in highly concentrated medium

Here is presented the study of the exchange between the highly pure dioxaborinanes $\mathbf{B_1D_1}$ and $\mathbf{B_2D_2}$. The exchange was conducted in a highly concentrated dodecane solution (this section) and in bulk (next section). In both cases, the reaction was conducted under argon protective atmosphere at different temperatures, without the addition of diol.
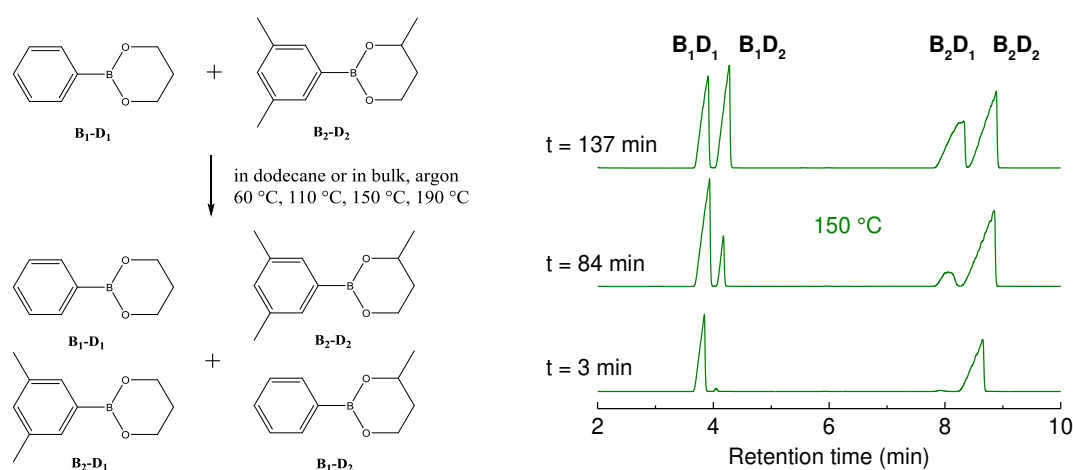
Figure 3.16. Left side: Metathesis of highly pure dioxaborinanes $\mathbf{B_1D_1}$ and $\mathbf{B_2D_2}$ at different temperatures under argon protective atmosphere. Right side: Gas chromatography traces of the reaction medium after 3min (bottom), 84 min (middle) and 137 min (top) during the exchange at 150 °C.

The dioxaborinane $\mathbf{B_1D_1}$ (2.7 mmol) was mixed with dodecane (2.4 mL) then an equimolar amount of dioxaborinane $\mathbf{B_2D_2}$ (2.7 mmol) was added under argon at different temperatures. The densities of the boronic esters were measured and the concentration of all boronic esters was calculated to be 1.6 mol.L^{-1}. At 190 °C, the equilibrium was reached after 45 min, whereas at 150 °C it needed more than 2 hours of reaction, and at 60 °C the system was still out of equilibrium after 24 hours (**Figures 3.16 and 3.17**).
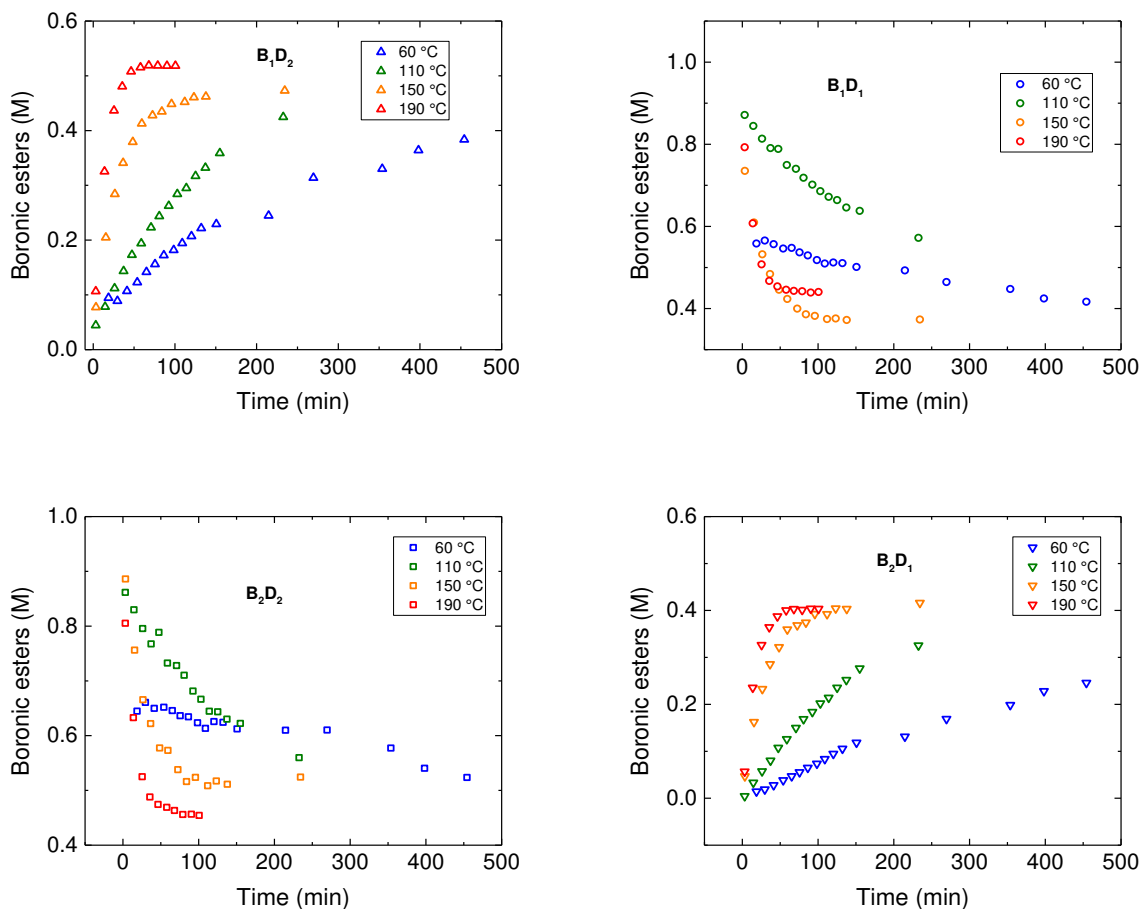
Figure 3.17. Kinetic plots of the exchange reaction between boronic esters **B₁D₁** and **B₂D₂ B₂D₂** in dodecane at different temperatures and under argon protective atmosphere.

The kinetic data of the exchange reaction are fitted with a second order model and assuming a single metathesis rate *k*. Consequently, the rate constant of dioxaborinanes metathesis can be estimated using the following expression (see appendix for details, 3.8.2.2) with *a*, the initial concentration of **B₁D₁**:

Equation 3.5.
$$ln\left(\frac{a}{a-2x}\right) = 2a\ kt$$

Equation 3.6.
$$k = Ae^{-\frac{E_a}{RT}}$$

According to **equation 3.6**, the activation energy determined via the logarithmic plot of the rate constant versus the inverse temperature was estimated to be 39.1± 0.4 kJ/mol (**Figure 3.18**). The pre-exponential factor *A* was assumed to be temperature independent and determined from the intercept of the linear fit of Arrhenius law to be 1.5 ± 0.1 L.mol⁻¹s⁻¹. This factor represents the frequency of collision between reactant molecules. It includes steric effects of the boronic esters, indeed the molecules have to collide to give the corresponding

156

products but also to be in the correct orientation. Dioxaborinanes are 6-membered cyclic species that possess different cycle conformations, with six classical forms.[91] They are switching from a conformation to another all the time, changing the orientation of the O-B-O plan and thus making the co-planar overlap of two dioxaborinanes highly difficult. Samples of the reaction medium were analysed by ^{1}H-NMR spectroscopy just after mixing at t = 4 min and at the equilibrium. The amount of free diols was below the diol detection limit in both cases.
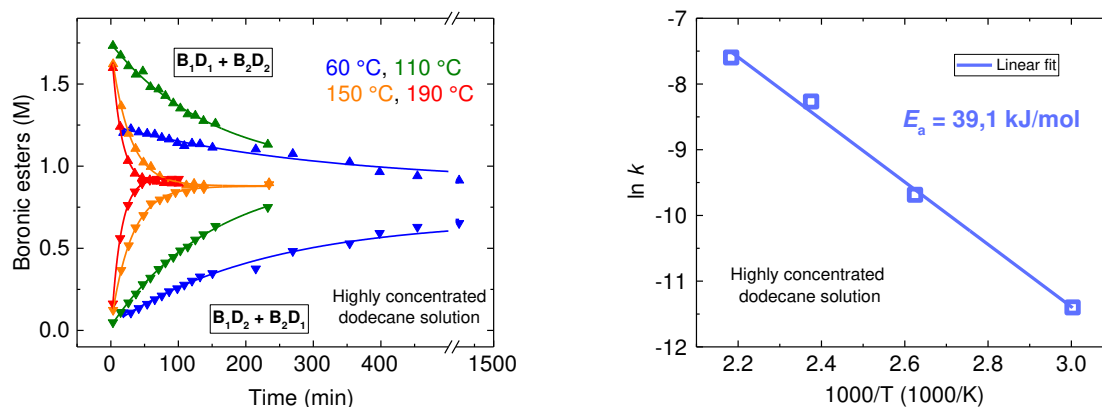
Figure 3.18. Left: Exchange of highly pure boronic esters in dodecane at different temperatures and under argon protective atmosphere. Right: Activation energy of the reaction.

The presence of dodecane had two potential benefits; on one hand it was useful for calculating the exact concentration of boronic esters, and on the other hand, dodecane can mimic in some ways the elastomer or olefin matrix, as a molecule made only from carbon and hydrogen. However, in order to confirm these promising results, and to obtain the characteristic parameters such as the rate constant of the metathesis reaction and the activation energy of the exchange reaction in a different chemical environment, the exchange reaction was also performed in bulk.

## 3.6.3.2 Exchange between dioxaborinanes in bulk
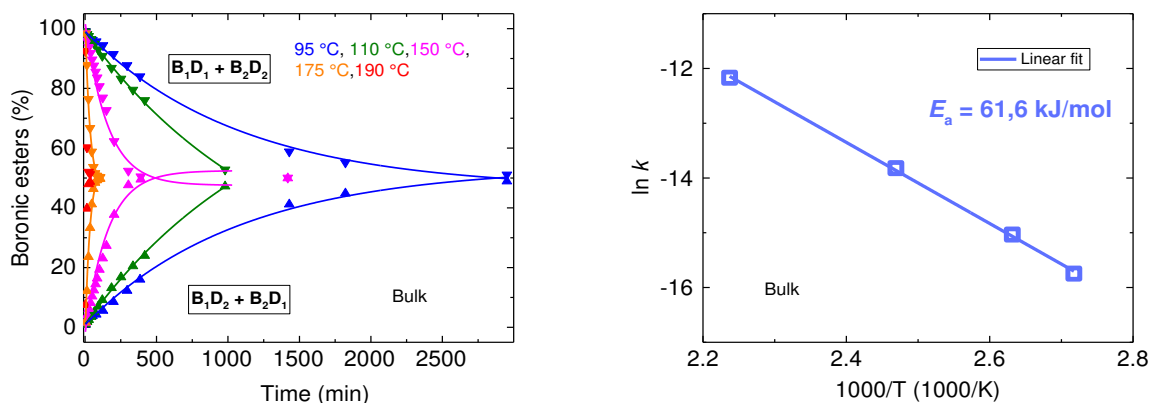
Figure 3.19. Left: Exchange of highly pure boronic esters in bulk at different temperature and under argon protective atmosphere. Right: Activation energy of the reaction.

The dioxaborinanes **B₁D₁** and **B₂D₂** (2.7 mmol) were mixed in equimolar amounts under argon at different temperatures. The overall concentration of boronic esters was estimated to be 5.7 mol.L^{-1}. At 190 °C, the condensation of the lightest dioxaborinane **B₁D₁** was observed on the walls of the Schlenk flask. Thus, in order to homogenise the reaction medium, the walls were rinsed four times with the reaction mixture before sampling at this temperature.

It was observed that the reaction was faster in bulk at 190 °C than in dodecane (**Figure 3.19**). At this temperature, the equilibrium was reached after only 36 min, while with the internal standard it required 45 min. However, at 150 °C the equilibrium was reached after 390 min of reaction in bulk, while it only required 137 min in dodecane. This suggests a higher activation energy of the metathesis reaction in bulk. The plot of ln k versus 1000/T gave an activation energy, E_a, of 61.6 ± 1.4 kJ/mol and a pre-factor, A, of 83 ± 2.3 L.mol^{-1}s^{-1}. The pre-factor is really low as compared to the pre-factor calculated from the metathesis of dioxaborolanes in bulk, for which A was found to be 6600 L.mol^{-1}s^{-1}.[92] This means that dioxaborinanes requires 80 times more collisions before to react than dioxaborolanes. Dioxaborolanes, as 5-memebered cyclic compounds, have less difficulty than dioxaborinanes to overlap between each other, because all the atoms of the dioxaborolane cycle are in the same plan. Compared to the experiment with dodecane, the order of magnitude of the pre-factor is two times higher, and the activation energy is 1.5 times higher. Changing the conditions, *i.e.* from solution to bulk, resulted in modification of activation energy and frequency factor in the same direction. Such behaviour might suggest that the variation of the nature of the solvent alters the degree of solvation of the transition state and/or of the reactants. Most importantly, both in bulk (5.4

158

mol.L^{-1}) or at high concentration (1.6 mol.L^{-1}), the exchange between two highly pure dioxaborinanes was observed, while in solution in THF the exchange reaction did not occur at room temperature. The concentration might play an important role on the kinetic, as well as the complexation of the boron atom by the lone pair of the oxygen of THF, which decreases the Lewis character of dioxaborinanes. The role of undetectable traces of free diols and boronic acids cannot be excluded during the exchange of highly pure dioxaborinanes, through a catalytic process of transesterification with dioxaborinanes.

3.6.4 Determination of the reaction order of dioxaborinane metathesis in solution

In an attempt to verify the assumptions made to fit the kinetic data, the global order of the reaction between two highly pure dioxaborinanes **B$_1$D$_1$** and **B$_2$D$_2$** was determined.

Stock solutions in xylene with a concentration of 0.8 M of **B$_2$D$_2$** and different concentrations of **B$_1$D$_1$** were generated and various amounts of **B$_1$D$_1$** (in 2 mL) were added to **B$_2$D$_2$** (2mL) in xylene under argon atmosphere at 110 °C (**Scheme 3.10**).

Assuming that only metathesis, *i.e.* one elementary step, occurred during the exchange reaction between boronic esters with [A] = [**B$_1$D$_1$**], [B] = [**B$_2$D$_2$**], [C] = [**B$_1$D$_2$**], [D] = [**B$_2$D$_1$**], the reaction can be described as follow:

$$[A] + [B] \quad \underset{k_2}{\overset{k_1}{\rightleftharpoons}} \quad [C] + [D]$$
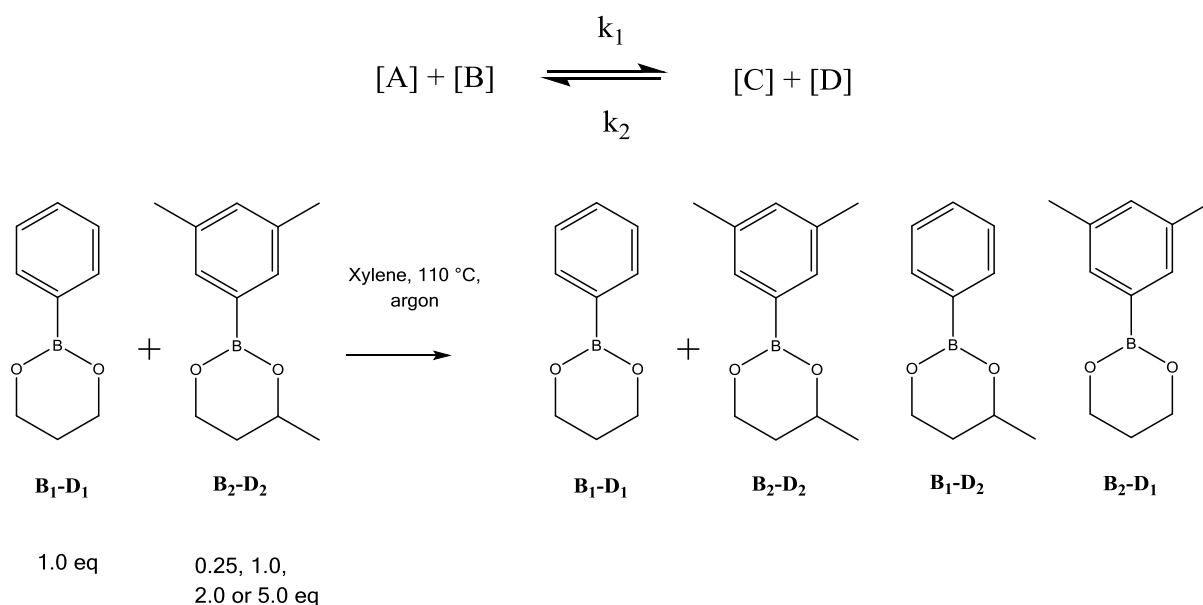
Scheme 3.10. Exchange reaction of **B$_1$D$_1$** with **B$_2$D$_2$** in xylene under argon at 110 °C, with different initial boronic ester ratios.

159
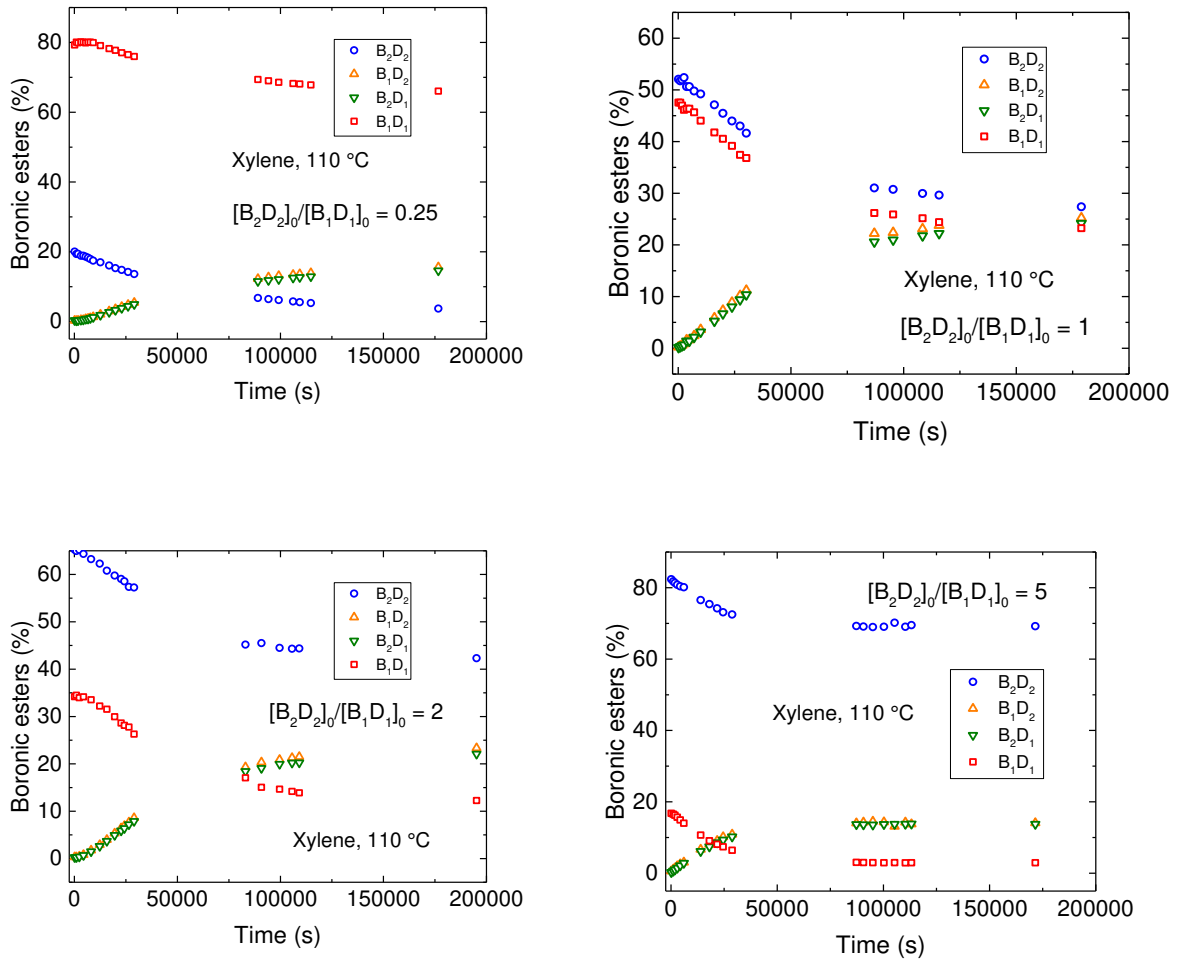
Figure 3.20. Exchange of boronic esters in xylene at 110 °C under argon with different initial boronic ester ratios.

Let us assume that initially $[\mathbf{B_1D_1}]_0 = a$, $[\mathbf{B_2D_2}]_0 = b$ while $[\mathbf{B_1D_2}]_0$ and $[\mathbf{B_2D_1}]_0$ are zero, we obtain the following equation (see appendix for details, 3.8.2.1):

Equation 3.7.
$$ln\left(\frac{x_e}{x_e-x}\right) = k(a+b)a^{p-1}b^{q-1}t$$

$ln(x_e\text{-}x)$ is plotted against t to yield the slope k', which may be equalled to:

$$k' = k(a+b)a^{p-1}b^{q-1}$$

Rearranging **equation 7**, we obtain:

Equation 3.8.
$$ln\left(\frac{k'}{a+b}\right) = ln(k) + (p-1)ln(a) + (q-1)ln(b)$$

The overall reaction order is determined by:

Equation 3.9. $$n = p + q$$

To determine the order p of the reaction with respect to $[A]_0 = a = [B_1D_1]_0$, 4 different experiments were performed at 110 °C in which the initial concentration of [A] was varied, while $[B]_0 = b = [B_2D_2]_0$ was kept constant (**Figure 3.20**). The different ratio a / b were 0.25, 1, 2 and 5 for an initial concentration of $[B]_0 = b = 0.8$ mol.L^{-1}. As *ln b* is a constant, *ln {k'/(a+b)}* is plotted against *ln a* to determine the slope, which is equalled to *p - 1*. According to **equation 3.8** and **Figure 3.21**, the reaction order with respect to B_1D_1, was calculated to be 1.15 ± 0.08. As B_1D_1 and B_2D_2 possess similar structures their partial order of reaction should be equal. Thus the overall reaction order is calculated to be 2.3 ± 0.16 (**Equation 3.9**). This value seems to confirm the above assumption of a second order model for the boronic ester exchange.
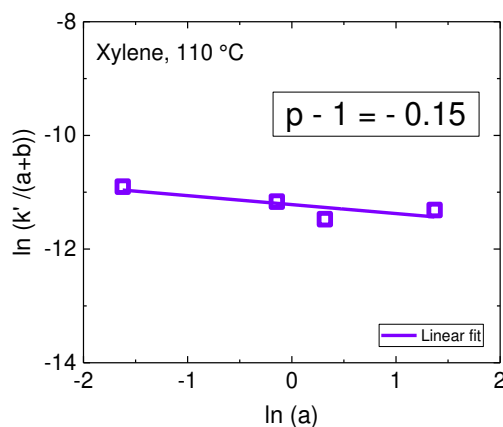

Figure 3.21. The logarithmic plot of the rate constant *k'* versus *ln a* to determine the order of the exchange reaction between two dioxaborinanes.

3.7 Conclusion

In this chapter a method was presented to analyse the dynamic covalent exchange reactions between two boronic esters, and between boronic esters and diols. Compounds were synthesised in high to very high purities (diol below the detection limit of NMR, content below 0.05 mol%). The association and dissociation constants of dioxaborolanes and dioxaborinanes were studied in the presence of water under argon via ^{1}H-NMR spectroscopy. Dioxaborinanes possess a water stability, or resistance to hydrolysis, 10 to 100 times higher than the corresponding dioxaborolanes.

The transesterification was studied and was proven to be faster for dioxaborolanes (equilibrium time, t_{eq}, < 5 min) than for dioxaborinanes (t_{eq} *ca.* 20 min). The substitution pattern might strongly affect the speed of reaction as demonstrated for **B$_1$D$_4$** (t_{eq} > 4300 min).

While in a dry THF solution of two highly pure dioxaborinanes no exchange could be observed at room temperature under protective atmosphere, the exchange reaction was observed at high concentration and in bulk. An activation energy of E_a = 39.1 kJ/mol was calculated in dodecane at high concentration, while the E_a was estimated to be 61.6 kJ/mol in bulk, with a frequency factor 55 times higher as compared to dodecane solution. Diols influence the speed of exchange. Although neither free diols (nor boronic acids) could be detected via ^{1}H- NMR, the presence of traces of diols, acting as a catalyst, cannot be excluded in bulk under the tested conditions. The overall reaction order was studied and estimated to be 2.3 and thus, close to the second order assumed to fit the kinetic data.

Compared to dioxaborolane metathesis, dioxaborinane metathesis has an activation energy 3 times higher and a frequency factor 100 times lower. These two combined characteristics are highly interesting. For instance, at 60 °C, the rate constant of dioxaborolanes exchange was estimated to be k = 10 L.mol^{-1}s^{-1} versus k = 1.10^{-9} L.mol^{-1}s^{-1} for dioxaborinanes. Consequently the exchange is drastically slowed down at room temperature for 6-membered cyclic boronic esters as compared to their 5-membered counterparts, likely because of the ring strain present in the 5-membered boronic esters and absent in the 6-membered species. Introducing dioxaborinane groups into elastomeric matrices could be extremely interesting: not only for their high stability and compatibility with a wide range of polymer backbones, but because the exchange reaction is quenched at room temperature, freezing the topology of the network thus

preventing it to creep while at higher temperatures (150-190 °C) the reaction is 1000 times faster allowing rapid rearrangement of the network and thus processability. Consequently, we aimed to incorporate dioxaborinanes into polybutadiene to generate reprocessable elastomers with higher creep resistance.

3.8 Appendix

3.8.1 Characterisation of boronic esters
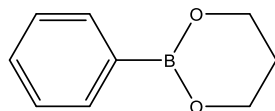
B$_1$-D$_1$

^{1}H-NMR (CDCl$_3$, 400 MHz): δ (ppm) 7.78 (d, J = 8.0 Hz, 2H), 7.43 (m, 1H), 7.36 (m, 2H), 4.18 (t, J = 5.5 Hz, 4H), 2.06 (qt, J = 5.5 Hz, 2H).

^{13}C-NMR (CDCl$_3$, 100 MHz): δ (ppm) 133.4, 130.4, 127.5, 61.8, 61.5, 27.8, 21.2. Carbon adjacent to boron not detected. Purity: no impurities detected via GC and ^{1}H-NMR.
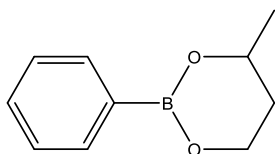

B$_1$-D$_2$

^{1}H-NMR (CDCl$_3$, 400 MHz): δ (ppm) 7.86 (d, J = 8.0 Hz, 2H), 7.47 (m, 1H), 7.41 (m, 2H), 4.33 (m, 1H), 4.23 (m, 1H), 4.15 (m, 1H), 2.03 (m, 1H), 1.82 (m, 1H), 1.42 (d, J = 6.3 Hz, 3H).

^{13}C-NMR (CDCl$_3$, 100 MHz): δ (ppm) 133.4, 130.4, 127.7, 67.9, 61.5, 33.9, 22.82. Carbon adjacent to boron not detected. Purity: no impurities detected via GC and ^{1}H-NMR.
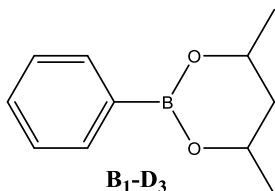

B$_1$-D$_3$

^{1}H-NMR (THF-d$_8$, 400 MHz): δ (ppm) 7.71 (d, J = 8.0 Hz, 2H), 7.30 (m, 1H), 7.22 (m, 2H), 4.38 (m, 1H), 4.23 (m, 1H), 2.03 (m, 1H), 1.83 (t, J = 5.3 Hz, 1H), 1.32 (m, 6H).

B₁-D₄
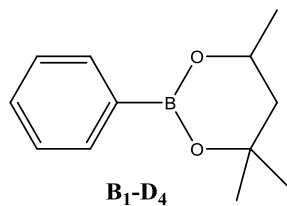
^{1}H-NMR (THF-d$_8$, 400 MHz): δ (ppm) 7.71 (d, J = 6.6 Hz, 2H), 7.31 (m, 1H), 7.23 (m, 2H), 4.34 (m, 1H), 1.92 (m, 1H), 1.55 (m, 1H), 1.35 (m, 6H), 1.31 (d, J = 6.2 Hz, 3H).

B₁-D₅
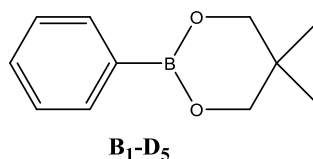
^{1}H-NMR (THF-d$_8$, 400 MHz): δ (ppm) 7.75 (d, J = 6.4 Hz, 2H), 7.34 (m, 1H), 7.26 (m, 2H), 3.75 (s, 4H), 0.99 (s, 6H).


B₁-D₆
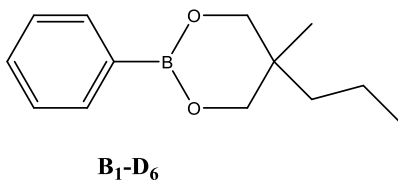
^{1}H-NMR (THF-d$_8$, 400 MHz): δ (ppm) 7.3 (d, J = 6.6 Hz, 2H), 7.32 (m, 1H), 7.25 (m, 2H), 3.81 (d, J = 5.4 Hz, 2H), 3.75 (d, J = 5.4 Hz, 2H), 1.33 (m, 4H), 0.95 (s, 3H), 0.91 (t, J = 6.3 Hz, 3H).

B₁-D₇
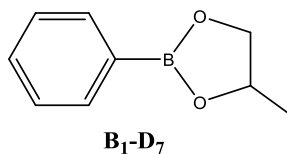
^{1}H-NMR (CDCl$_3$, 400 MHz): δ (ppm) 7.73 (d, J = 6.7 Hz, 2H), 7.41 (m, 1H), 7.31 (m, 2H), 4.66 (m, 1H), 4.40 (dd, J = 1.1 Hz, J = 8.3 Hz), 3.83 (dd, J = 1.1 Hz, J = 8.3 Hz), 1.34 (d, J = 6.2 Hz, 3H).

^{13}C-NMR (CDCl$_3$, 100 MHz): δ (ppm) 134.4, 131.6, 127.9, 73.7, 72.5, 21.9. Carbon adjacent to boron not detected. Purity: no impurities detected via GC and ^{1}H-NMR.

165
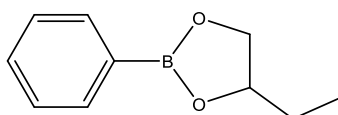
B₁-D₈

¹H-NMR (CDCl₃, 400 MHz): δ (ppm) 7.84 (d, J = 6.4. Hz, 2H), 7.41 (m, 1H), 7.31 (m, 2H), 4.56 (m, 1H), 4.43 (dd, J = 1.2 Hz, J = 8.3 Hz), 3.88 (dd, J = 1.2 Hz, J = 8.3 Hz), 1.72 (m, 2H), 1.06 (t, J = 7.8 Hz, 3H).

¹³C-NMR (CDCl₃, 100 MHz): δ (ppm) 134.7, 131.5, 127.7, 78.7, 70.8, 21.9, 20.5. Carbon adjacent to boron not detected. Purity: no impurities detected via GC and ¹H-NMR.
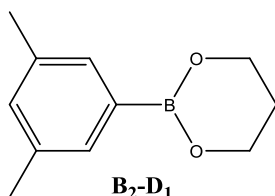
B₂-D₁

¹H-NMR (CDCl₃, 400 MHz): δ (ppm) 7.46 (s, 2H), 7.11 (s, 1H), 4.19 (t, J = 5.5 Hz, 4H) , 2.37 (s, 6H), 2.07 (qt, J = 5.5 Hz, 2H).

¹³C-NMR (CDCl₃, 100 MHz): δ (ppm) 136.7, 132.2, 131.3, 61.9, 27.1, 21.2. Carbon adjacent to boron not detected. Purity: no impurities detected via GC and ¹H-NMR
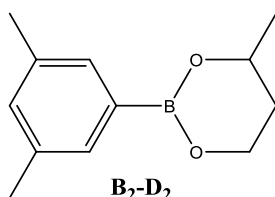
B₂-D₂

¹H-NMR (CDCl₃, 400 MHz): δ (ppm) 7.48 (s, 2H), 7.12 (s, 1H), 4.33 (m, 1H), 4.23 (m, 1H), 4.15 (m, 1H), 2.38 (s, 6H), 2.04 (m, 1H), 1.82 (m, 1H), 1.43 (d, J = 6.3 Hz, 3H).

¹³C-NMR (CDCl₃, 100 MHz): δ (ppm) 136.7, 132.2, 131.3, 67.9, 61.0, 34.2, 22.9, 21.2. Carbon adjacent to boron not detected. Purity: no impurities detected via GC and ¹H-NMR.

B₂-D₇
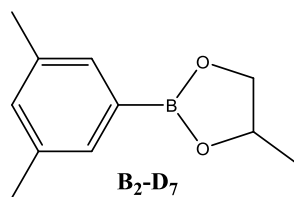
¹H-NMR (CDCl₃, 400 MHz): δ (ppm) 7.44 (s, 1H), 7.11 (s, 1H), 4.46 (m, 1H), 4.40 (dd, J = 1.1 Hz, J = 8.8 Hz), 3.83 (dd, J = 1.1 Hz, J = 8.8 Hz), 2.34 (s, 6H), 1.43 (d, J = 6.2 Hz, 3H).

¹³C-NMR (CDCl₃, 100 MHz): δ (ppm) 1347.4, 133.6, 132.9, 73.7, 72.5, 21.9, 21.2. Carbon adjacent to boron not detected. Purity: no impurities detected via GC and ¹H-NMR.

B₃-D₂
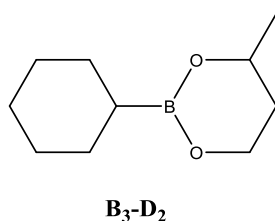
¹H-NMR (THF-d₈, 400 MHz): δ (ppm) 4.03 (m, 1H), 3.89 (m, 2H), 1.85 (m, 1H), 1.58 (m, 7H), 1.23 (m, 5H), 1.17 (d, J = 6.3 Hz, 3H), 0.74 (m, 1H).

¹³C-NMR (THF-d₈, 100 MHz): δ (ppm) 61.34, 35.1, 29.3, 28.9, 28.1, 27.8, 23.1. Carbon adjacent to boron not detected.

B₄-D₂
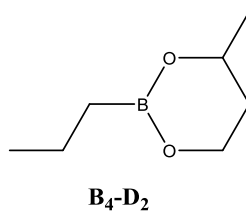
¹H-NMR (THF-d₈, 400 MHz): δ (ppm) 4.03 (m, 1H), 3.88 (m, 2H), 1.88 (m, 1H), 1.56 (m, 1H), 1.34 (m, 2H), 1.17 (d, J = 6.3 Hz, 3H), 0.86 (m, 3H), 0.58 (t, J = 7.6 Hz, 2H).

¹³C-NMR (THF-d₈, 100 MHz): δ (ppm) 67.0, 61.3, 35.1, 23.1, 17.4, 17.1. Carbon adjacent to boron not detected.

B₅-D₂
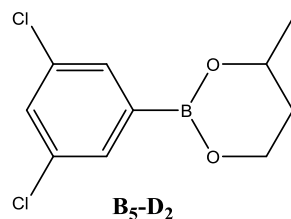
¹H-NMR (THF-d₈, 400 MHz): δ (ppm) 7.58 (s, 2H), 7.45 (s, 1H), 4.28 (m, 1H), 4.12 (m, 2H), 2.03 (m, 1H), 1.77 (m, 1H), 1.34 (d, $J = 6.3$ Hz, 3H).

¹³C-NMR (THF-d₈, 100 MHz): δ (ppm) 135.0, 132.4, 130.7, 68.9, 62.2, 34.5, 22.3. Carbon adjacent to boron not detected.

B₆-D₂
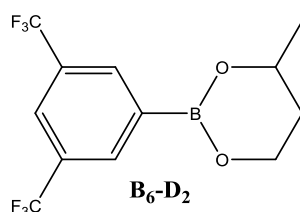
¹H-NMR (THF-d₈, 400 MHz): δ (ppm) 8.21 (s, 2H), 8.01 (s, 1H), 4.34 (m, 1H), 4.18 (m, 2H), 2.09 (m, 1H), 1.82 (m, 1H), 1.37 (d, $J = 6.3$ Hz, 3H).

¹³C-NMR (THF-d₈, 100 MHz): δ (ppm) 134.1, 126.0, 123.3, 69.1, 62.3, 34.8, 22.8. Carbon adjacent to boron not detected.

3.8.2 Equations for the exchange reactions

3.8.2.1 Equations for the estimation of the reaction order

If only metathesis occurs between boronic esters with [A] = [**B₁D₁**], [B] = [**B₂D₂**], [C] = [**B₁D₂**], [D] = [**B₂D₁**]:

$$[A] + [B] \underset{k_2}{\overset{k_1}{\rightleftharpoons}} [C] + [D]$$
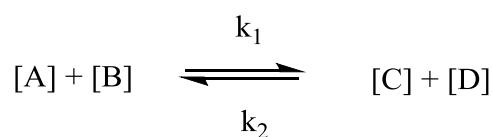
Exchange reaction may be expressed as following: [93]

168

Equation 3.10.
$$\frac{dx}{dt} = a^p b^q \left(k_1 \frac{(a-x)(b-x)}{ab} - k_2 \frac{x^2}{ab} \right)$$

We suppose that the equilibrium constant equals 1 thanks to the thermodynamic stability of all the reactants and products, as a consequence $k_1 = k_2 = k$.

Equation 3.11.
$$\frac{dx}{dt} = k \, a^p b^q \left\{ \frac{(a-x)(b-x)}{ab} - \frac{x^2}{ab} \right\}$$

With the equilibrium constant: $K = \frac{(a-x_e)(b-x_e)}{x_e^2}$

$$x_e = \frac{ab}{a+b}$$

Rearranging **equation 3.11**:

$$\frac{dx}{dt} = k \, a^{p-1} b^{q-1} (a+b)(x_e - x)$$

Integrating and using the fact that x = 0 when t = 0, we have:

$$ln\left(\frac{x_e}{x_e - x} \right) = k(a+b)a^{p-1}b^{q-1}t$$

3.8.2.2 Equations for the assessment of the rate constants

Restarting from **equation 3.11** and assuming that the observed exchange follows second order reaction kinetics, *i.e.* p = 1 and q = 1, the rate constant of the reaction can be determined using the following relations:

$$\frac{dx}{dt} = k \left\{ (a-x)(b-x) - x^2 \right\}$$

After the integration between t = 0 and t:

$$ln\left(\frac{ab}{ab - (a+b)x} \right) = (a+b) \, kt$$

When the two reactants are mixed in stoichiometric proportions, thus $a = b$, the above equation becomes:

$$ln\left(\frac{a}{a - 2x} \right) = 2a \, kt$$

169

3.9 References

(1) Hall, D. G. Boronic Acid Catalysis. *Chem. Soc. Rev.* **2019**. https://doi.org/10.1039/C9CS00191C.

(2) Xu, S.; Che, S.; Ma, P.; Zhang, F.; Xu, L.; Liu, X.; Wang, X.; Song, D.; Sun, Y. One-Step Fabrication of Boronic-Acid-Functionalized Carbon Dots for the Detection of Sialic Acid. *Talanta* **2019**, *197*, 548–552. https://doi.org/10.1016/j.talanta.2019.01.074.

(3) Zhao, H.; Peng, K.; Lv, F.; Liu, L.; Wang, S. Boronic Acid-Functionalized Conjugated Polymer for Controllable Cell Membrane Imaging. *ACS Appl. Bio Mater.* **2019**. https://doi.org/10.1021/acsabm.9b00212.

(4) Chen, X.; Zhang, H.; Ci, C.; Sun, W.; Wang, Y. Few-Layered Boronic Ester Based Covalent Organic Frameworks/Carbon Nanotube Composites for High-Performance K-Organic Batteries. *ACS Nano* **2019**. https://doi.org/10.1021/acsnano.9b00165.

(5) Zhang, X.; Chai, L.; Nie, S.; Lv, C.; Wang, Q.; Li, Z. Facile Synthesis of Boronic Acid-Decorated Carbon Nanodots as Optical Nanoprobes for Glycoprotein Sensing. *Analyst* **2019**. https://doi.org/10.1039/C8AN02192A.

(6) Smithmyer, M. E.; Deng, C. C.; Cassel, S. E.; LeValley, P. J.; Sumerlin, B. S.; Kloxin, A. M. Self-Healing Boronic Acid-Based Hydrogels for 3D Co-Cultures. *ACS Macro Lett.* **2018**, *7* (9), 1105–1110. https://doi.org/10.1021/acsmacrolett.8b00462.

(7) Wang, S.; Xing, X.; Zhang, X.; Wang, X.; Jing, X. Room-Temperature Fully Recyclable Carbon Fibre Reinforced Phenolic Composites through Dynamic Covalent Boronic Ester Bonds. *J. Mater. Chem. A* **2018**, *6* (23), 10868–10878. https://doi.org/10.1039/C8TA01801D.

(8) Salonen, L. M.; Medina, D. D.; Carbó-Argibay, E.; Goesten, M. G.; Mafra, L.; Guldris, N.; Rotter, J. M.; Stroppa, D. G.; Rodríguez-Abreu, C. A Supramolecular Strategy Based on Molecular Dipole Moments for High-Quality Covalent Organic Frameworks. *Chem. Commun.* **2016**, *52* (51), 7986–7989. https://doi.org/10.1039/C6CC02170K.

(9) Liu, C.; Yu, Y.; Zhang, W.; Zeng, Q.; Lei, S. Room-Temperature Synthesis of Covalent Organic Frameworks with a Boronic Ester Linkage at the Liquid/Solid Interface. *Chem. – Eur. J.* **2016**, *22* (51), 18412–18418. https://doi.org/10.1002/chem.201603547.

(10) Baldock, C.; Deene, Y. D.; Doran, S.; Ibbott, G.; Jirasek, A.; Lepage, M.; McAuley, K. B.; Oldham, M.; Schreiner, L. J. Polymer Gel Dosimetry. *Phys. Med. Biol.* **2010**, *55* (5), R1–R63. https://doi.org/10.1088/0031-9155/55/5/R01.

(11) Petasis, N. A.; Zavialov, I. A. A New and Practical Synthesis of α-Amino Acids from Alkenyl Boronic Acids. *J. Am. Chem. Soc.* **1997**, *119* (2), 445–446. https://doi.org/10.1021/ja963178n.

(12) de la Herrán, G.; Segura, A.; Csákÿ, A. G. Benzylic Substitution of Gramines with Boronic Acids and Rhodium or Iridium Catalysts†. *Org. Lett.* **2007**, *9* (6), 961–964. https://doi.org/10.1021/ol063042m.

(13) Sieber, J. D.; Liu, S.; Morken, J. P. Catalytic Conjugate Addition of Allyl Groups to Styryl-Activated Enones. *J. Am. Chem. Soc.* **2007**, *129* (8), 2214–2215. https://doi.org/10.1021/ja067878w.

(14) Chan, D. M. T.; Monaco, K. L.; Li, R.; Bonne, D.; Clark, C. G.; Lam, P. Y. S. Copper Promoted C-N and C-O Bond Cross-Coupling with Phenyl and Pyridylboronates. *Tetrahedron Lett.* **2003**, *44* (19), 3863–3865. https://doi.org/10.1016/S0040-4039(03)00739-1.

(15) Lam, P. Y. S.; Vincent, G.; Bonne, D.; Clark, C. G. Copper-Promoted/Catalyzed C-N and C-O Bond Cross-Coupling with Vinylboronic Acid and Its Utilities. *Tetrahedron Lett.* **2003**, *44* (26), 4927–4931. https://doi.org/10.1016/S0040-4039(03)01037-2.

(16) Ley, S. V.; Thomas, A. W. Modern Synthetic Methods for Copper-Mediated C(Aryl)-O, C(Aryl)-N, and C(Aryl)-S Bond Formation. *Angew. Chem. Int. Ed.* **2003**, *42* (44), 5400–5449. https://doi.org/10.1002/anie.200300594.

(17) Miyaura, Norio.; Suzuki, Akira. Palladium-Catalyzed Cross-Coupling Reactions of Organoboron Compounds. *Chem. Rev.* **1995**, *95* (7), 2457–2483. https://doi.org/10.1021/cr00039a007.

(18) Ishiyama, T.; Murata, M.; Miyaura, N. Palladium(0)-Catalyzed Cross-Coupling Reaction of Alkoxydiboron with Haloarenes: A Direct Procedure for Arylboronic Esters. *J. Org. Chem.* **1995**, *60* (23), 7508–7510. https://doi.org/10.1021/jo00128a024.

(19) Roush, W. R.; Adam, M. A.; Walts, A. E.; Harris, D. J. Stereochemistry of the Reactions of Substituted Allylboronates with Chiral Aldehydes. Factors Influencing Aldehyde Diastereofacial Selectivity. *J. Am. Chem. Soc.* **1986**, *108* (12), 3422–3434. https://doi.org/10.1021/ja00272a043.

(20) Liebeskind, L. S.; Srogl, J. Thiol Ester−Boronic Acid Coupling. A Mechanistically Unprecedented and General Ketone Synthesis. *J. Am. Chem. Soc.* **2000**, *122* (45), 11260–11261. https://doi.org/10.1021/ja005613q.

(21) Hyland, S. N.; Meck, E. A.; Tortosa, M.; Clark, T. B. α-Amidoboronate Esters by Amide-Directed Alkane CH Borylation. *Tetrahedron Lett.* **2019**, *60* (16), 1096–1098. https://doi.org/10.1016/j.tetlet.2019.03.020.

(22) Keerthi Krishnan, K.; Saranya, S.; Rohit, K. R.; Anilkumar, G. A Novel Zinc-Catalyzed Suzuki-Type Cross-Coupling Reaction of Aryl Boronic Acids with Alkynyl Bromides. *J. Catal.* **2019**, *372*, 266–271. https://doi.org/10.1016/j.jcat.2019.03.005.

(23) Thomas, A. A.; Zahrt, A. F.; Delaney, C. P.; Denmark, S. E. Elucidating the Role of the Boronic Esters in the Suzuki–Miyaura Reaction: Structural, Kinetic, and Computational Investigations. *J. Am. Chem. Soc.* **2018**, *140* (12), 4401–4416. https://doi.org/10.1021/jacs.8b00400.

(24) Trippier, P. C.; McGuigan, C. Boronic Acids in Medicinal Chemistry: Anticancer, Antibacterial and Antiviral Applications. *MedChemComm* **2010**, *1* (3), 183–198. https://doi.org/10.1039/C0MD00119H.

(25) Cambre, J. N.; Sumerlin, B. S. Biomedical Applications of Boronic Acid Polymers. *Polymer* **2011**, *52* (21), 4631–4643. https://doi.org/10.1016/j.polymer.2011.07.057.

(26) Edwards, N. Y.; Sager, T. W.; McDevitt, J. T.; Anslyn, E. V. Boronic Acid Based Peptidic Receptors for Pattern-Based Saccharide Sensing in Neutral Aqueous Media, an Application in Real-Life Samples. *J. Am. Chem. Soc.* **2007**, *129* (44), 13575–13583. https://doi.org/10.1021/ja073939u.

(27) Tarus, D.; Hachet, E.; Messager, L.; Catargi, B.; Ravaine, V.; Auzély-Velty, R. Readily Prepared Dynamic Hydrogels by Combining Phenyl Boronic Acid- and Maltose-Modified Anionic Polysaccharides at Neutral PH. *Macromol. Rapid Commun.* **2014**, *35* (24), 2089–2095. https://doi.org/10.1002/marc.201400477.

(28) Bruen, D.; Campos, P. P.; Ferreira, M.; Diamond, D.; Delaney, C.; Florea, L. Boronic Acid Homopolymers as Effective Polycations for Sugar-Responsive Layer-by-Layer Assemblies. *ACS Appl. Polym. Mater.* **2019**, *1* (5), 990–996. https://doi.org/10.1021/acsapm.9b00017.

(29) Daum, S.; Toms, J.; Reshetnikov, V.; Özkan, H. G.; Hampel, F.; Maschauer, S.; Hakimioun, A.; Beierlein, F.; Sellner, L.; Schmitt, M.; et al. Identification of Boronic Acid Derivatives as an Active Form of N-Alkylaminoferrocene-Based Anticancer Prodrugs and Their Radiolabeling with 18F. *Bioconjug. Chem.* **2019**, *30* (4), 1077–1086. https://doi.org/10.1021/acs.bioconjchem.9b00019.

(30) Lee, J.; Park, J. M.; Jang, W.-D. Fructose-Sensitive Thermal Transition Behaviour of Boronic Ester-Bearing Telechelic Poly(2-Isopropyl-2-Oxazoline). *Chem. Commun.* **2019**, *55* (23), 3343–3346. https://doi.org/10.1039/C8CC09835B.

(31) Gaballa, H.; Theato, P. Glucose-Responsive Polymeric Micelles via Boronic Acid–Diol Complexation for Insulin Delivery at Neutral PH. *Biomacromolecules* **2019**, *20* (2), 871–881. https://doi.org/10.1021/acs.biomac.8b01508.

(32) Müller, J.; Kirschner, R. A.; Geyer, A.; Klebe, G. Conceptional Design of Self-Assembling Bisubstrate-like Inhibitors of Protein Kinase A Resulting in a Boronic Acid Glutamate Linkage. *ACS Omega* **2019**, *4* (1), 775–784. https://doi.org/10.1021/acsomega.8b02364.

(33) Zhang, Y.-H.; Zhang, Y.-M.; Yu, J.; Wang, J.; Liu, Y. Boronate-Crosslinked Polysaccharide Conjugates for PH-Responsive and Targeted Drug Delivery. *Chem. Commun.* **2019**. https://doi.org/10.1039/C8CC09956A.

(34) Guy, C. S.; Gibson, M. I.; Fullam, E. Targeting Extracellular Glycans: Tuning Multimeric Boronic Acids for Pathogen-Selective Killing of Mycobacterium Tuberculosis: Supplementary Information. **2019**. https://doi.org/10.1101/529743.

(35) Cai, B.; Luo, Y.; Guo, Q.; Zhang, X.; Wu, Z. A Glucose-Sensitive Block Glycopolymer Hydrogel Based on Dynamic Boronic Ester Bonds for Insulin Delivery. *Carbohydr. Res.* **2017**, *445*, 32–39. https://doi.org/10.1016/j.carres.2017.04.006.

(36) Huang, Z.; Delparastan, P.; Burch, P.; Cheng, J.; Cao, Y.; B. Messersmith, P. Injectable Dynamic Covalent Hydrogels of Boronic Acid Polymers Cross-Linked by Bioactive Plant-Derived Polyphenols. *Biomater. Sci.* **2018**, *6* (9), 2487–2495. https://doi.org/10.1039/C8BM00453F.

(37) Tang, J.; Yang, J.; Yang, H.; Miao, R.; Wen, R.; Liu, K.; Peng, J.; Fang, Y. Boronic Ester-Based Dynamic Covalent Ionic Liquid Gels for Self-Healable, Recyclable and Malleable Optical Devices. *J. Mater. Chem. C* **2018**, *6* (46), 12493–12497. https://doi.org/10.1039/C8TC03639J.

(38) Chen, Y.; Tang, Z.; Zhang, X.; Liu, Y.; Wu, S.; Guo, B. Covalently Cross-Linked Elastomers with Self-Healing and Malleable Abilities Enabled by Boronic Ester Bonds. *ACS Appl. Mater. Interfaces* **2018**, *10* (28), 24224–24231. https://doi.org/10.1021/acsami.8b09863.

(39) Liu, C.; Gong, H.; Liu, W.; Lu, B.; Ye, L. Separation and Recycling of Functional Nanoparticles Using Reversible Boronate Ester and Boroxine Bonds. *Ind. Eng. Chem. Res.* **2019**. https://doi.org/10.1021/acs.iecr.9b00253.

(40) Taleb, S.; Noyer, E.; Godeau, G.; Darmanin, T.; Guittard, F. Switchable Surface Wettability by Using Boronic Ester Chemistry. *ChemPhysChem* **2016**, *17* (2), 305–309. https://doi.org/10.1002/cphc.201500873.

(41) Hebel, M.; Riegger, A.; Zegota, M. M.; Kizilsavas, G.; Gačanin, J.; Pieszka, M.; Lückerath, T.; Coelho, J. A. S.; Wagner, M.; Gois, P. M. P.; et al. Sequence Programming with Dynamic Boronic Acid/Catechol Binary Codes. *J. Am. Chem. Soc.* **2019**. https://doi.org/10.1021/jacs.9b03107.

(42) Karimi, F.; Collins, J.; Heath, D. E.; Connal, L. A. Dynamic Covalent Hydrogels for Triggered Cell Capture and Release. *Bioconjug. Chem.* **2017**, *28* (9), 2235–2240. https://doi.org/10.1021/acs.bioconjchem.7b00360.

(43) Sun, W.; Jiang, H.; Wu, X.; Xu, Z.; Yao, C.; Wang, J.; Qin, M.; Jiang, Q.; Wang, W.; Shi, D.; et al. Strong Dual-Crosslinked Hydrogels for Ultrasound-Triggered Drug Delivery. *Nano Res.* **2019**, *12* (1), 115–119. https://doi.org/10.1007/s12274-018-2188-4.

(44) Chen, Y.; Diaz-Dussan, D.; Wu, D.; Wang, W.; Peng, Y.-Y.; Asha, A. B.; Hall, D. G.; Ishihara, K.; Narain, R. Bioinspired Self-Healing Hydrogel Based on Benzoxaborole-Catechol Dynamic Covalent Chemistry for 3D Cell Encapsulation. *ACS Macro Lett.* **2018**, *7* (8), 904–908. https://doi.org/10.1021/acsmacrolett.8b00434.

(45) Dufort, B. M.; Tibbitt, M. W. Design of Moldable Hydrogels for Biomedical Applications Using Dynamic Covalent Boronic Esters. *Mater. Today Chem.* **2019**, *12*, 16–33. https://doi.org/10.1016/j.mtchem.2018.12.001.

(46) Frankland, E.; Duppa, B. Vorläufige Notiz Über Boräthyl. *Justus Liebigs Ann. Chem.* **1860**, *115* (3), 319–322.

(47) Michaelis, A.; Becker, P. Ueber Monophenylborchlorid Und Die Valenz Des Bors. *Berichte Dtsch. Chem. Ges.* **1880**, *13* (1), 58–61. https://doi.org/10.1002/cber.18800130118.

(48) Michaelis, A.; Becker, P. Ueber Monophenylborchlorid Und Einige Derivate Desselben. *Berichte Dtsch. Chem. Ges.* **1882**, *15* (1), 180–185. https://doi.org/10.1002/cber.18820150143.

(49) Branch, G. E. K.; Yabroff, D. L.; Bettman, B. The Dissociation Constants of the Chlorophenyl and Phenetyl Boric Acids1. *J. Am. Chem. Soc.* **1934**, *56* (4), 937–941. https://doi.org/10.1021/ja01319a053.

(50) Bettman, B.; Branch, G. E. K.; Yabroff, D. L. Dissociation Constants of Organic Boric Acids. *J. Am. Chem. Soc.* **1934**, *56* (9), 1865–1870. https://doi.org/10.1021/ja01324a012.

(51) Yabroff, D. L.; Branch, G. E. K.; Bettman, B. The Relative Strengths of Some Hydrocarbon Derivatives of Boric Acid. *J. Am. Chem. Soc.* **1934**, *56* (9), 1850–1857. https://doi.org/10.1021/ja01324a009.

(52) Torssell, K.; McCLENDON, J. H.; Somers, G. Chemistry of Arylboric Acids VIII. The Relationship between Physico-Chemical Properties and Activity in Plants. *Acta Chem Scand* **1958**, *12* (7), 1373.

(53) Singhal, R. p.; Ramamurhy, B.; Govindraj, N.; Sarwar, Y. New Ligands for Boronte Affinity Chromatography: Synthesis and Propertiesa. *J. Chromatogr. A* **1991**, *543*, 17–38. https://doi.org/10.1016/S0021-9673(01)95752-8.

(54) Torssell, K. The Chemistry of Boronic and Borinic Acids. *Progr Boron Chem* **1964**, *1*, 369–415.

(55) Dewar, M. J.; Jones, R. New Heteroaromatic Compounds. XXV. Studies of Salt Formation in Boron Oxyacids by Boron-11 Nuclear Magnetic Resonance. *J. Am. Chem. Soc.* **1967**, *89* (10), 2408–2410.

(56) Mó, O.; Yáñez, M.; Eckert-Maksić, M.; Maksić, Z. B.; Alkorta, I.; Elguero, J. Periodic Trends in Bond Dissociation Energies. A Theoretical Study. *J. Phys. Chem. A* **2005**, *109* (19), 4359–4365. https://doi.org/10.1021/jp050857o.

(57) L. Korich, A.; M. Iovine, P. Boroxine Chemistry and Applications: A Perspective. *Dalton Trans.* **2010**, *39* (6), 1423–1431. https://doi.org/10.1039/B917043J.

(58) Tokunaga, Y.; Ueno, H.; Shimomura, Y. Formation of Boroxine: Its Stability and Thermodynamic Parameters in Solution. *Heterocycles* **2002**, *57* (5), 787–790.

(59) Beckmann, J.; Dakternieks, D.; Duthie, A.; Lim, A. E. K.; Tiekink, E. R. T. Ring Strain in Boroxine Rings: Computational and Experimental Considerations. *J. Organomet. Chem.* **2001**, *633* (1), 149–156. https://doi.org/10.1016/S0022-328X(01)01060-9.

(60) Bao, C.; Jiang, Y.-J.; Zhang, H.; Lu, X.; Sun, J. Room-Temperature Self-Healing and Recyclable Tough Polymer Composites Using Nitrogen-Coordinated Boroxines. *Adv. Funct. Mater.* **2018**, *28* (23), 1800560. https://doi.org/10.1002/adfm.201800560.

(61) Ogden, W. A.; Guan, Z. Recyclable, Strong, and Highly Malleable Thermosets Based on Boroxine Networks. *J. Am. Chem. Soc.* **2018**, *140* (20), 6217–6220. https://doi.org/10.1021/jacs.8b03257.

(62) Bao, C.; Guo, Z.; Sun, H.; Sun, J. Nitrogen-Coordinated Boroxines Enable the Fabrication of Mechanically Robust Supramolecular Thermosets Capable of Healing and Recycling under Mild Conditions. *ACS Appl. Mater. Interfaces* **2019**. https://doi.org/10.1021/acsami.9b00006.

(63) Delpierre, S.; Willocq, B.; Manini, G.; Lemaur, V.; Goole, J.; Gerbaux, P.; Cornil, J.; Dubois, P.; Raquez, J.-M. Simple Approach for a Self-Healable and Stiff Polymer Network from Iminoboronate-Based Boroxine Chemistry. *Chem. Mater.* **2019**. https://doi.org/10.1021/acs.chemmater.9b00750.

(64) Yuan, D.; Delpierre, S.; Ke, K.; Raquez, J.-M.; Dubois, P.; Manas-Zloczower, I. Biomimetic Water-Responsive Self-Healing Epoxy with Tunable Properties. *ACS Appl. Mater. Interfaces* **2019**, *11* (19), 17853–17862. https://doi.org/10.1021/acsami.9b04249.

(65) LORAND, J. P.; EDWARDS, J. O. Polyol Complexes and Structure of the Benzeneboronate Ion. *J. Org. Chem.* **1959**, *24* (6), 769–774. https://doi.org/10.1021/jo01088a011.

(66) Springsteen, G.; Wang, B. A Detailed Examination of Boronic Acid–Diol Complexation. *Tetrahedron* **2002**, *58* (26), 5291–5300. https://doi.org/10.1016/S0040-4020(02)00489-1.

(67) Fujita, N.; Shinkai, S.; James, T. D. Boronic Acids in Molecular Self-Assembly. *Chem. – Asian J.* **2008**, *3* (7), 1076–1091. https://doi.org/10.1002/asia.200800069.

(68) Arzt, M.; Seidler, C.; Ng, D. Y.; Weil, T. Reversible Click Reactions with Boronic Acids to Build Supramolecular Architectures in Water. *Chem. Asian J.* **2014**, *9* (8), 1994–2003.

(69) Marinaro, W. A.; Prankerd, R.; Kinnari, K.; Stella, V. J. Interaction of Model Aryl- and Alkyl-Boronic Acids and 1,2-Diols in Aqueous Solution. *J. Pharm. Sci.* **2015**, *104* (4), 1399–1408. https://doi.org/10.1002/jps.24346.

(70) Wulff, G.; Lauer, M.; Böhnke, H. Rapid Proton Transfer as Cause of an Unusually Large Neighboring Group Effect. *Angew. Chem. Int. Ed. Engl.* **1984**, *23* (9), 741–742.

(71) Hughes, M. P.; Smith, B. D. Enhanced Carboxylate Binding Using Urea and Amide-Based Receptors with Internal Lewis Acid Coordination: A Cooperative Polarization Effect. *J. Org. Chem.* **1997**, *62* (13), 4492–4499. https://doi.org/10.1021/jo9702249.

(72) Yang, X.; Lee, M.; Sartain, F.; Pan, X.; Lowe, C. R. Designed Boronate Ligands for Glucose-selective Holographic Sensors. *Chem. Eur. J.* **2006**, *12* (33), 8491–8497.

(73) Goldberg, A. R.; Northrop, B. H. Spectroscopic and Computational Investigations of The Thermodynamics of Boronate Ester and Diazaborole Self-Assembly. *J. Org. Chem.* **2016**, *81* (3), 969–980. https://doi.org/10.1021/acs.joc.5b02548.

(74) Haruta, R.; Ishiguro, M.; Ikeda, N.; Yamamoto, H. Chiral Allenylboronic Esters: A Practical Reagent for Enantioselective Carbon-Carbon Bond Formation. *J. Am. Chem. Soc.* **1982**, *104* (26), 7667–7669. https://doi.org/10.1021/ja00390a052.

(75) Roush, W. R.; Walts, A. E.; Hoong, L. K. Diastereo- and Enantioselective Aldehyde Addition Reactions of 2-Allyl-1,3,2-Dioxaborolane-4,5-Dicarboxylic Esters, a Useful Class of Tartrate

Ester Modified Allylboronates. *J. Am. Chem. Soc.* **1985**, *107* (26), 8186–8190. https://doi.org/10.1021/ja00312a062.

(76) Ray, R.; Matteson, D. S. Osmium Tetroxide Catalyzed Hydroxylation of Hindered Olefins. *Tetrahedron Lett.* **1980**, *21* (5), 449–450. https://doi.org/10.1016/S0040-4039(00)71429-8.

(77) Matteson, D. S.; Kandil, A. A. (S, S)-Diisopropylethanediol ("DIPED"): A New Chiral Director for the α-Chloro Boronic Ester Synthesis. *Tetrahedron Lett.* **1986**, *27* (33), 3831–3834. https://doi.org/10.1016/S0040-4039(00)83891-5.

(78) Luithle, J. E. A.; Pietruszka, J. (2R,3R)-1,4-Dimethoxy-1,1,4,4-Tetraphenyl-2,3-Butanediol: Chiral Auxiliary and Efficient Protecting Group for Boronic Acids. *J. Org. Chem.* **2000**, *65* (26), 9194–9200. https://doi.org/10.1021/jo0056601.

(79) Herold, T.; Schrott, U.; Hoffmann, R. W.; Schnelle, G.; Ladner, W.; Steinbach, K. Stereoselektive Synthese von Alkoholen, VI1) Asymmetrische Synthesen von 4-Penten-2-ol Über Allylboronsäureester Chiraler Glycole. *Chem. Ber.* **1981**, *114* (1), 359–374.

(80) Luithle, J. E. A.; Pietruszka, J. Synthesis of Enantiomerically Pure Cyclopropanes from Cyclopropylboronic Acids. *J. Org. Chem.* **1999**, *64* (22), 8287–8297. https://doi.org/10.1021/jo9910278.

(81) Ditrich, K.; Bube, T.; Stürmer, R.; Hoffmann, R. W. Total Synthesis of Mycinolide V, the Aglycone of a Macrolide Antibiotic of the Mycinamycin Series. *Angew. Chem. Int. Ed. Engl.* **1986**, *25* (11), 1028–1030.

(82) Bernardini, R.; Oliva, A.; Paganelli, A.; Menta, E.; Grugni, M.; Munari, S. D.; Goldoni, L. Stability of Boronic Esters to Hydrolysis: A Comparative Study. *Chem. Lett.* **2009**, *38* (7), 750–751. https://doi.org/10.1246/cl.2009.750.

(83) Letsinger, R. L.; Skoog, I. Organoboron Compounds. IV. 1 Aminoethyl Diarylborinates. *J. Am. Chem. Soc.* **1955**, *77* (9), 2491–2494.

(84) Demianenko, E.; Rayevsky, A.; Soriano-Ursúa, M. A.; Trujillo-Ferrara, J. G. Theoretical Coupling and Stability of Boronic Acid Adducts with Catecholamines. *Lett. Drug Des. Discov.* **2019**, *16* (4), 467–475. https://doi.org/10.2174/1570180815666180710101604.

(85) Sugihara, J. M.; Bowman, C. M. Cyclic Benzeneboronate Esters. *J. Am. Chem. Soc.* **1958**, *80* (10), 2443–2446. https://doi.org/10.1021/ja01543a024.

(86) Bowie, R. A.; Musgrave, O. C. 749. Organoboron Compounds. Part V. The Hydrolysis of Cyclic Phenylboronates. *J. Chem. Soc. Resumed* **1963**, No. 0, 3945–3949. https://doi.org/10.1039/JR9630003945.

(87) Roy, C. D.; Brown, H. C. A Comparative Study of the Relative Stability of Representative Chiral and Achiral Boronic Esters Employing Transesterification. *Monatshefte Für Chem. - Chem. Mon.* **2007**, *138* (9), 879–887. https://doi.org/10.1007/s00706-007-0699-x.

(88) Roy, C. D.; Brown, H. C. Stability of Boronic Esters – Structural Effects on the Relative Rates of Transesterification of 2-(Phenyl)-1,3,2-Dioxaborolane. *J. Organomet. Chem.* **2007**, *692* (4), 784–790. https://doi.org/10.1016/j.jorganchem.2006.10.013.

(89) Röttger, M.; Domenech, T.; Weegen, R. van der; Breuillac, A.; Nicolaÿ, R.; Leibler, L. High-Performance Vitrimers from Commodity Thermoplastics through Dioxaborolane Metathesis. *Science* **2017**, *356* (6333), 62–65. https://doi.org/10.1126/science.aah5281.

(90) Williams, D. B. G.; Lawton, M. Drying of Organic Solvents: Quantitative Evaluation of the Efficiency of Several Desiccants. *J. Org. Chem.* **2010**, *75* (24), 8351–8354. https://doi.org/10.1021/jo101589h.

(91) Boeyens, J. C. A. The Conformation of Six-Membered Rings. *J. Cryst. Mol. Struct.* **1978**, *8* (6), 317–320. https://doi.org/10.1007/BF01200485.

(92) Roettger, M. Associative Exchange Reactions of Boron or Nitrogen Containing Bonds and Design of Vitrimers, Université Pierre et Marie Curie, 2016.

(93) Logan, S. The Kinetics of Isotopic Exchange Reactions. *J. Chem. Educ.* **1990**, *67* (5), 371.

Chapter 4

Polybutadiene Vitrimers based on Dioxaborinane Chemistry

Table of Contents

Chapter 4 - Polybutadiene Vitrimers based on Dioxaborinane Chemistry

4.1 Introduction

The following chapter describes the synthesis of a divalent and a trivalent molecule containing a 6-membered boronic ester and a thiol function, respectively two thiol functions, in order to generate polybutadiene vitrimers based on the dioxaborinane exchange reaction. To conduct a relevant comparative study between dioxaborolane and dioxaborinane vitrimers, the same low molar mass unentangled polybutadiene (PB) was chosen as a vitrimer precursor. The crosslinking was achieved in solution and the resulting network was processed by compression moulding. The thermoplastic properties of these materials, *i.e.* ability to flow and to be recycled, were analysed, as wells as their thermosetting properties. Important features such as the insoluble fraction, the swelling ratio, the storage moduli, the elongation at break and the creep resistance were compared to the corresponding dioxaborolane vitrimer.
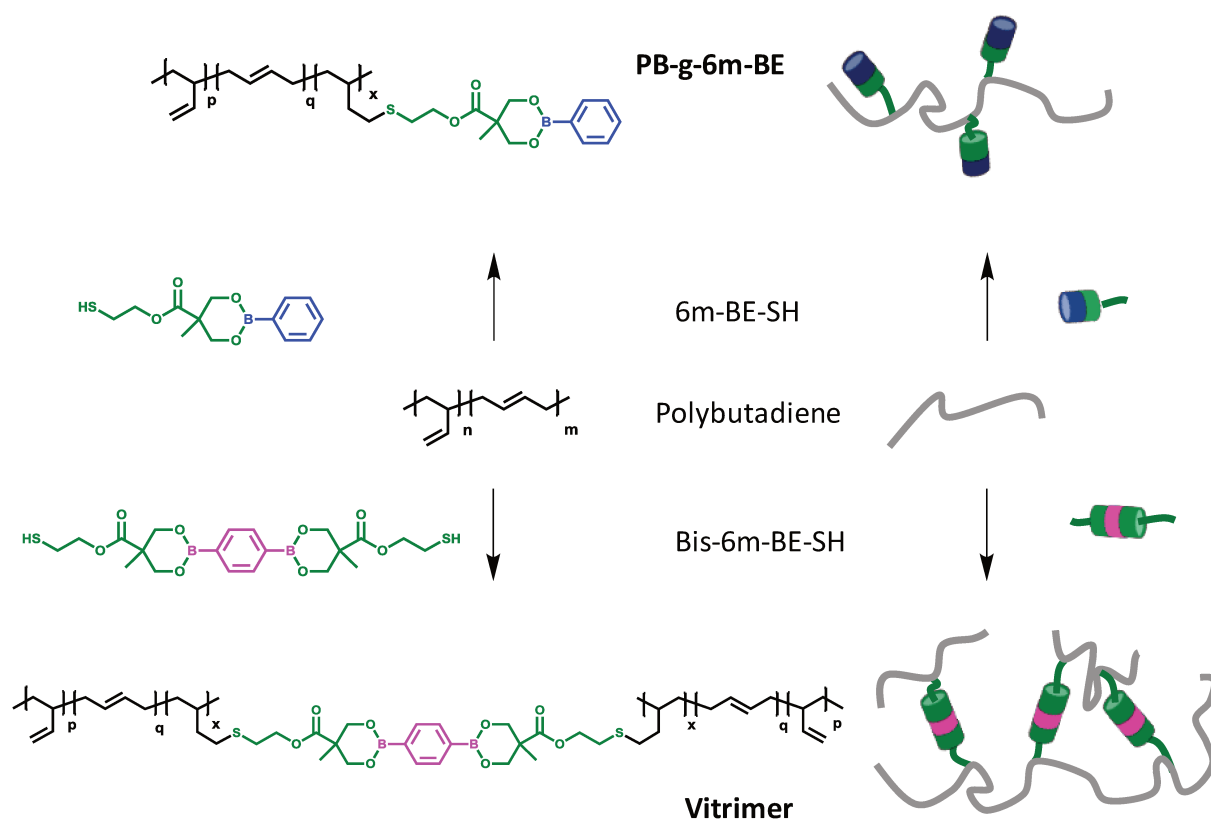

Figure 4.1. Synthesis of: polybutadiene grafted with dioxaborinanes (top) and polybutadiene vitrimers (bottom).

177

4.2 Experimental section

4.2.1 Materials

Polybutadiene (PB) (vinyl content = 84 mol%, M_n = 3.9 kDa, $Đ$ = 1.48), high molecular weight polybutadiene (HW PB) (vinyl content = 9 mol%, M_n = 84 kDa, $Đ$ = 1.99), and all other chemical compounds were purchased from Sigma-Aldrich. Acetone, toluene, anisole, tetrahydrofuran (THF) and methanol were obtained from Carlos Erba and deuterated solvents from Eurisotop. Unless otherwise noted, reagents were used without further purification. Solvents (including deuterated solvents) were dried over activated 3Å molecular sieves under an inert atmosphere for at least 72 hours prior to use. Glassware used for dioxaborinane and vitrimer syntheses was oven-dried and then heated with a heat gun while being purged with dry argon (< 0.5 ppm H_2O).

4.2.2 Characterisation

Size exclusion chromatography (SEC). SEC was performed on a Viscotek GPCmax/VE2001 connected to a triple detection array (TDA 305) from Malvern. Molecular weights were determined using a conventional calibration based on monodisperse polystyrene (PS) standards.

Fourier-transform infrared (FT-IR) spectroscopy. FT-IR spectroscopy was conducted on a Tensor 37 spectrometer from Bruker in solid state and recorded in attenuated total reflectance (ATR) mode and converted to absorbance spectra.

Nuclear magnetic resonance (NMR) spectroscopy. ^{1}H and ^{13}C NMR spectra were recorded at 297 K on a Bruker AVANCE 400 spectrometer at 400 MHz and 100 MHz, respectively, and referenced to the residual solvent peaks (^{1}H, δ 7.26 for $CDCl_3$; ^{13}C, δ 77.16 for $CDCl_3$).

Rheological characterizations. Viscoelastic properties of polybutadiene samples were determined using a TA Instruments ARES G2 rotational rheometer equipped with parallel plate geometry (25 mm in diameter) in a convection oven under air.

178

Step stress-creep recovery experiments. Creep-recovery tests were carried out at 28 °C by imposing a constant stress over time (creep) and releasing it for a certain period of time (recovery) while measuring the strain.

Differential scanning calorimetry (DSC). Glass transitions of materials were determined by DSC. Sequences of temperature ramps (heating, cooling, heating) in the −50 °C to 60 °C range were performed at 10 °C/min using a TA Instruments Q1000 equipped with a liquid nitrogen cooling accessory and calibrated using sapphire and high purity indium metal. All samples were prepared in hermetically sealed pans (5−10 mg/sample) and were referenced to an empty pan. The reported T_g values are from the second heating cycle.

Thermogravimetric analysis (TGA). TGA analyses were conducted on a TG 209 F1 Libra from Netzsch under nitrogen flow. The samples were heated at a constant rate of 10 °C/min from 25 to 500 °C.

Dynamic mechanical analysis (DMA). DMA were conducted on a TA Instruments Q800 in tension mode. Heating ramps were performed from -75 °C to 120, 150 or 250 °C at a constant rate of 3 °C/min with a maximum strain amplitude of 1% at a fixed frequency of 1 Hz.

Tensile tests and recycling. Uniaxial tensile tests were performed on dumbell-shaped specimens (gauge length 10 mm) using an Instron 5564 tensile machine mounted with a 100 N cell. Specimens were tested in quintuplicates at a fixed crosshead speed of 10 mm/min. Testing was carried out at room temperature for all materials. Engineering stress-strain curves were obtained through measurements of the tensile force F and crosshead displacement Δl by defining the engineering stress as $\sigma = F/S_0$ and the strain as $\gamma = \Delta l/l_0$, where S_0 and l_0 are the initial cross-section and gauge length of the specimens, respectively. The Young's modulus was determined as the initial slope of the engineering stress-strain curves. Following tensile testing, the vitrimer specimens were cut down to small fragments and reshaped via compression moulding for 10 min at 150 °C under a load of 3 tons in order to test their recyclability over several reprocessing cycles. Tensile tests were repeated at room temperature for each generation.

4.2.3 Syntheses
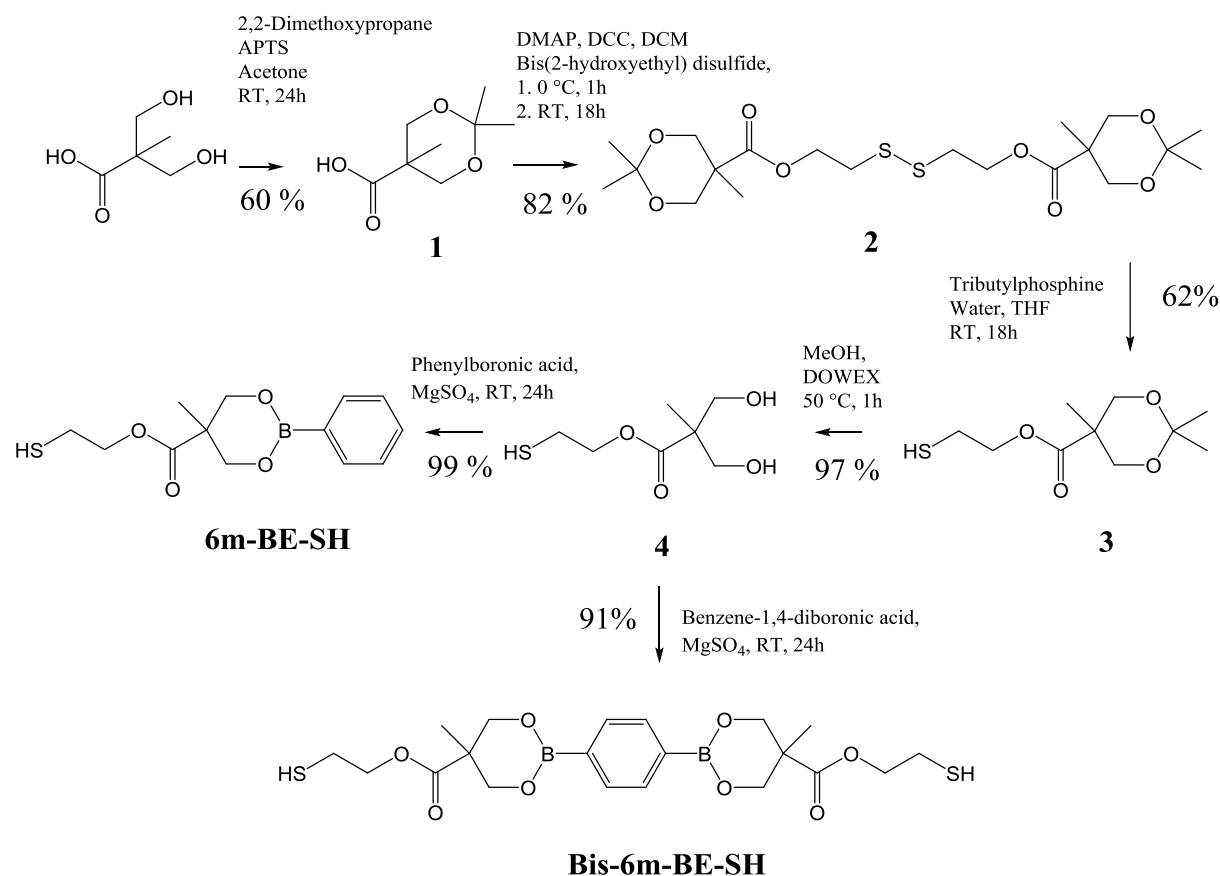
Scheme 4.1. Syntheses of a dioxaborinane carrying one thiol function, **6m-BE-SH,** and a bis-dioxaborinane bearing two thiol groups, **Bis-6m-BE-SH**.

Synthesis of compound **1**: 2,2-bis(hydroxymethyl)propionoic acid (10.00 g, 74.6 mmol), 2,2-dimethoxypropane (14 mL, 112 mmol) and toluenesulfonic acid monohydrate (0.71 g, 3.7 mmol) were added to acetone (50 mL). After reacting for 2 hours, a NH₃/EtOH mixture (1 mL, 50 : 50) was added to the solution to neutralize the catalyst. Afterwards, the solution was evaporated to remove all the solvent and a white solid was obtained. The solid was dissolved in CH₂Cl₂ (250 mL) and washed twice with water (30 mL). Finally, the solution was dried over MgSO₄, filtered and the CH₂Cl₂ evaporated to obtain the product **2** (7.75 g, 60%).

^{1}H NMR (CDCl₃, 400 MHz): δ (ppm), 1.21 (s, 3H), 1.42 (s, 3H), 1.45 (s, 3H), 3.67 (d, J = 12 Hz, 2H), 4.18 (d, J = 12 Hz, 2H).

Synthesis of compound **2**: Compound **1** (4.00 g, 23.0 mmol, 2.4 equiv) was dissolved in 50 mL of CH₂Cl₂ with bis(2-hydroxyethyl) disulfide (1.48 g, 9.6 mmol, 1 equiv) and DMAP (4-dimethylaminopyridine) (0.47 g, 3.8 mmol, 0.4 equiv). The solution was kept at 0 °C upon

addition of dicyclohexylcarbodiimide (DCC) (4.74 g, 23.0 mmol, 2.4 equiv). The reaction was left overnight to reach room temperature. The slurry was filtered and the crude solution was concentrated and purified by flash chromatography (SiO_2) eluting the product in 20:80 EtOAc : hexanes. The product was recovered as a colourless viscous oil (3.68 g, 82%).

^{1}H NMR ($CDCl_3$, 400 MHz,): δ (ppm) 1.19 (s, 6H), 1.38 (s, 6H), 1.42 (s, 6H), 2.94 (t, J = 6.5 Hz, 4H), 3.63 (d, J = 11.9 Hz, 4H), 4.18 (d, J = 11.9 Hz, 4H), 4.40 (t, J = 6.5 Hz, 4H). ^{13}C NMR ($CDCl_3$, 100 MHz): δ (ppm), 18.8, 22.7, 24.9, 37.2, 42.1, 62.6, 66.1, 98.2, 174.2

Synthesis of compound **3**: A stirred solution of compound **2** (4.00 g, 8.6 mmol, 1 equiv) in THF-H_2O mixture (THF-H_2O, 10 : 1) was flushed thoroughly with N_2, then tributylphosphine (2.60 g, 12.9 mmol, 1.5 equiv) was added at room temperature. After having 18 h of stirring at room temperature, the reaction mixture was concentrated in vacuum, the residue re-dissolved in EtOAc and washed with HCl (1M) followed by saturated aqueous NaCl. The combined organic phases were dried over $MgSO_4$, and the solvent was removed in vacuum. Purification by flash column chromatography (Et_2O : pentane 80:20 → 50:50) yielded the product as a colourless oil (2.48 g, 62%).

^{1}H NMR ($CDCl_3$, 400 MHz,): δ (ppm) 1.17 (s, 3H), 1.38 (s, 3H), 1.42 (s, 3H), 1.59 (t, J = 8.5 Hz, 1H), 2.77 (m, 2H), 3.64 (d, J = 11.9 Hz, 2H), 4.19 (d, J = 11.9 Hz, 2H), 4.27 (t, J = 6.5 Hz, 2H). ^{13}C NMR ($CDCl_3$, 100 MHz): δ (ppm) 18.7, 22.2, 23.5, 25.5, 42.1, 66.1, 66.2, 98.3, 174.1. ν = 2561 cm^{-1}

Synthesis of compound **4**: Compound **3** (2.88 g, 12.3 mmol) was dissolved in 50 mL of MeOH at room temperature. An acidic catalyst resin, DOWEX® 50W-X2, was added. When the full conversion of the acetonide to hydroxyl groups was achieved, the acidic resin was filtered off and the filtrate was concentrated by evaporation of the solvent. The product was collected as a colourless viscous oil (2.32 g, 97%).

^{1}H NMR ($CDCl_3$, 400 MHz,): δ (ppm) 1.07 (s, 3H), 1.58 (t, J = 8.5 Hz, 1H), 2.77 (m, 2H), 3.68 (d, J = 11.2 Hz, 2H), 3.85 (d, J = 11.2 Hz, 2H), 4.25 (t, J = 6.5 Hz, 2H). ^{13}C NMR ($CDCl_3$, 100 MHz): δ (ppm) 17.3, 23.4, 49.5, 66.0, 66.2, 67.4, 175.6

Synthesis of **6m-BE-SH**: Compound **4** (1.16 g, 6.0 mmol, 1.0 eq) and phenylboronic acid (0.73 g, 6.0 mmol, 1.0 eq) were mixed in tetrahydrofuran (THF) (2 mL/1 mmol boronic acid) at room temperature and stirred until complete dissolution of all compounds. MgSO$_4$ (2.16 g, 17.9 mmol, 3.0 eq) was added stepwise and the mixture was stirred at room temperature for 5 hours, filtered and concentrated under reduced pressure to obtain **6m-BE-SH** as a white powder. The purified boronic esters were transferred directly to dried and purged Schlenk flasks and kept under protective atmosphere (1.67 g, 99%).

^{1}H-NMR (400 MHz, CDCl3): δ (ppm) 7.78 (d, J = 6.6 Hz, 2H), 7.43 (m, 1H), 7.34 (m, 2H), 4.46 (d, J = 11.0 Hz, 2H), 4.25 (t, J = 6.5 Hz, 2H), 3.93 (d, J = 11.0 Hz, 2H), 2.71 (m, 2H), 1.48 (t, J = 8.6 HZ, 1H), 1.27 (s, 3H). ^{13}C-NMR (100 MHz, CDCl3): δ (ppm) 18.4, 23.4, 44.4, 66.4, 68.0, 127.7, 131.1, 134.0, 173.2 Carbon adjacent to boron not detected.

Synthesis of **Bis-6m-BE-SH**: Compound **4** (1.16 g, 6.0 mmol, 1.0 eq), phenyl 1,4 diboronic acid (0.50 g, 3.0 mmol, 0.5 eq) were mixed in tetrahydrofuran (THF) (2 mL/1 mmol boronic acid) at room temperature and stirred until complete dissolution of all compounds. MgSO$_4$ (2.16 g, 17.9 mmol, 3.0 eq) was added stepwise and the mixture was stirred at room temperature for 5 hours, filtered and concentrated under reduced pressure to obtain **Bis-6m-BE-SH** as a white powder. The purified boronic ester was transferred directly to dried and purged Schlenk flasks and kept under protective atmosphere (1.32 g, 91%).

^{1}H-NMR (400 MHz, CDCl3): δ (ppm) 7.74 (s, 4H), 4.45 (d, J = 11.0 Hz, 4H), 4.25 (t, J = 6.5 Hz, 4H), 3.92 (d, J = 11.0 Hz, 4H), 2.69 (m, 4H), 1.46 (t, J = 8.6 HZ, 2H), 1.26 (s, 6H). ^{13}C-NMR (100 MHz, CDCl3): δ (ppm) 18.4, 23.3, 44.3, 66.4, 68.0, 131.1, 173.2 Carbon adjacent to boron not detected.

Grafting procedure of BE-SH onto polybutadiene: In a typical experiment, polybutadiene (PB) (1.00 g, 15.5 mmol of vinyl groups) was dissolved in anhydrous anisole (20 wt%), followed by **6m-BE-SH** (0.41 g, 1.5 mmol). Then, AIBN (1.2 mg, 0.008 mmol) was dissolved in anisole (0.5 mL) in another vial and added to the solution of polybutadiene and **BE-SH**. The mixture was bubbled with argon for 30 min. Then, the argon flow was stopped and the mixture was heated at 100°C for 60 min (9 × τ$_{1/2}$). Finally, the polymer was

precipitated into 20 mL of anhydrous methanol. The isolated residue was dried under high vacuum overnight at 100 °C.

Vitrimers synthesis: In a typical experiment, PB (1.00 g, 15.5 mmol of vinyl groups) was dissolved in anhydrous anisole (20 wt%), followed by **Bis-6m-BE-SH** (0.36 g, 0. mmol). Then, AIBN (0.73 mg, 0.004 mmol) was dissolved in anisole (0.5 mL) in another vial and added to the solution of polybutadiene and **Bis-6m-BE-SH**. The mixture was bubbled with argon for 30 min. Then, the argon flow was stopped and the mixture was heated at 100°C for 60 min ($9 \times \tau_{1/2}$). The obtained gel was dried under high vacuum overnight at 100 °C.

4.3 Grafting of dioxaborinanes

With the aim to quantify the grafting efficiency as a function of the targeted functionalisation degree, PB was first modified with **6m-BE-SH** (**Figure 4.1**). The grafting of PB was conducted in anisole, keeping a constant ratio [**6m-BE-SH**]/[AIBN] of 100, and varying the [**BE-SH**]/[C=C] ratio to tune the functionalization degree.

4.3.1 ^{1}H-NMR analysis

The efficiency of **6m-BE-SH** grafting onto PB was quantified by conducting ^{1}H NMR spectroscopy of grafted PBs before and after purification by precipitation into anhydrous methanol. **Figure 4.2** shows a typical spectrum of an isolated **6m-BE-SH**-grafted PB after purification by precipitation into anhydrous methanol.
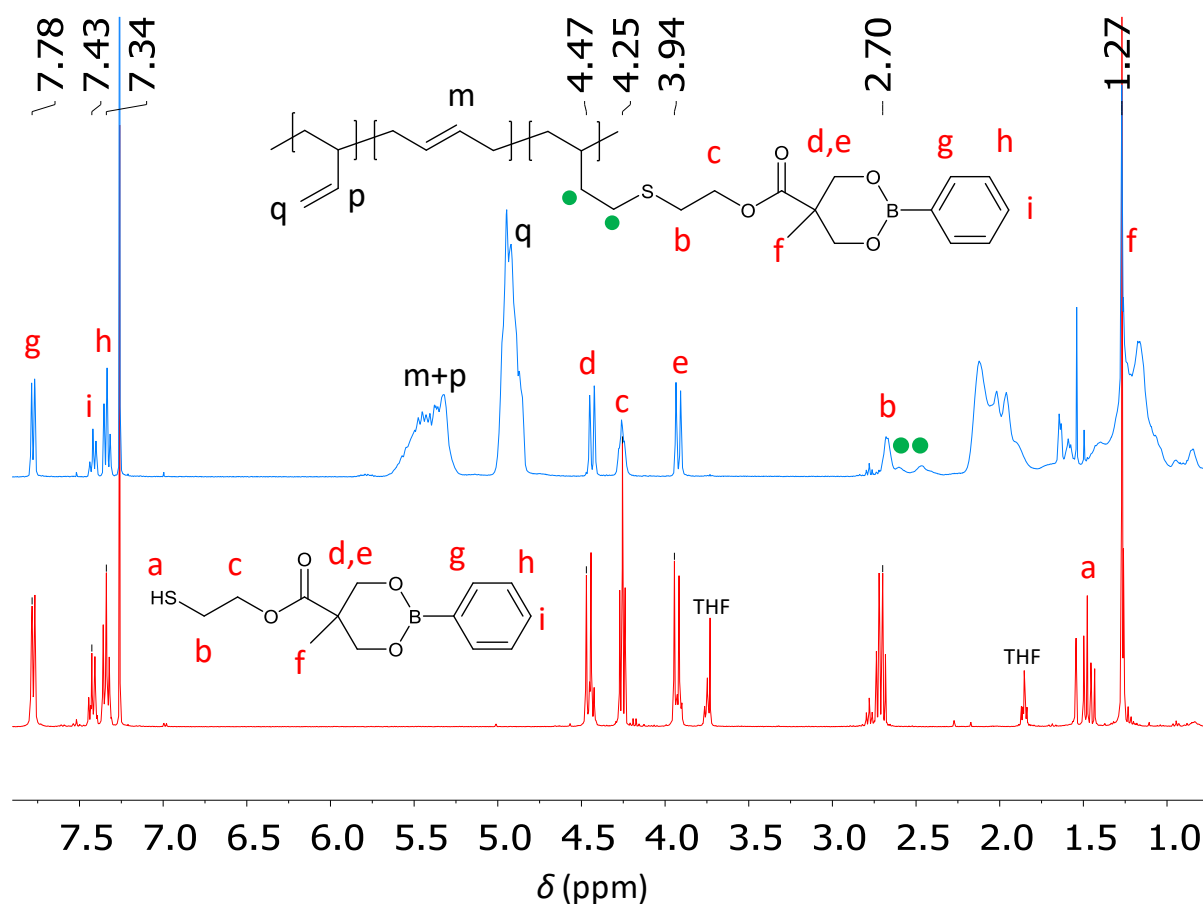

Figure 4.2. ^{1}H-NMR spectra in CDCl$_3$ of **PB-6m-BE-6** after purification by precipitation into anhydrous methanol (grafting yield = 65%, f = 6%) (top, blue) and **6m-BE-SH** (bottom, red).

Peaks at 7.78, 7.43 and 7.34 ppm, characteristic of the phenyl group of the phenylboronic ester, as well as peaks corresponding to the proton of the dioxaborinane ring (-OCH2- and –CH-C), *e.g.* 4.47 and 3.94 ppm, confirmed the grafting of **6m-BE-SH** onto PB. The functionalization degree, which corresponds to the number of repeating unit carrying a pendant dioxaborolane, and the grafting yields are reported in **Table 4.1**. They were calculated according to the following equations:

Equation 4.1.
$$f(\%) = \frac{Integration\ proton\ d}{(Integration\ all\ protons - 11\ x\ Integration\ proton\ d\ )/6}$$

Equations 4.2.
$$Grafting\ yield\ (\%) = \frac{Integration\ proton\ d\ after\ precipitation}{Integration\ proton\ d\ before\ precipitation}$$

Grafting yields were moderate regardless of the targeted functionalization degree. Yet, they slightly increased with the molar ratio [**6m-BE-SH**]/[C=C], going from 66% to 77% with functionalization degrees increasing from 3 to 9%, which is consistent with results reported in the literature for the grafting of cysteine onto PB.[1] However, these yields are inferior to those determined for the dioxaborolane **BE-SH**, with values between 81% and 92% (*cf.* Chapter 2). Such significant differences may be explained by the lower solubility of **6m-BE-SH** in anisole, as compared to **BE-SH**.

Table 4.1. Characterization of polybutadiene grafted with **6m-BE-SH**.

Sample	6m-BE-SH per chain	Grafting yield (%)	f(%) measured	Vinyl (%)[a]	Vinylene (%)[b]	f measured + vinyl + vinylene (%)	$M_{n,exp}$ (g/mol)	Đ
PB	-	-	-	85	15	100	3900	1.47
PB-6m-BE-3	3	66 ± 13	3 ±0.6	76	15	94 ± 4	4230	1.62
PB-6m-BE-5	6	65 ± 9	6 ± 0.8	71	14	91 ± 2	4460	1.59
PB-6m-BE-9	9	77 ± 4	9 ± 0.5	57	13	79 ± 5	5020	1.68

[a] From equation 4.3; [b] From equation 4.4.

Interestingly, the sum (measured functionalization degree + vinyl + vinylene) was studied as a function of the functionalization degree (**Table 4.1**). Indeed, in the absence of side reactions

consuming carbon-carbon double bonds, this sum should not change irrespective of the functionalization degree. The greater the difference, the more side reactions are taking place. Going from a functionalization degree of 3 to 9%, the percentage of vinyl bonds decreased from 85 to 57%, while the percent of vinylene bonds only decreased from 15 to 13%. These values were calculated based on the following equations:

Equation 4.3. $\quad Vinyl\ (\%) = \dfrac{(Integration\ proton\ q)/2}{(Integration\ all\ protons-\ 11\ x\ Integration\ proton\ d\ )/6}$

Equation 4.4. $\quad Vinylene\ (\%) = \dfrac{((Integration\ proton\ m+p)-\frac{Integration\ proton\ q}{2})/2}{(Integration\ all\ protons-\ 11\ x\ Integration\ proton\ d\ )/6}$

Consequently, vinyl groups are more reactive towards thiyl radicals and thereby, are more prone to intramolecular cyclizations and than their vinylene counterparts as known in literature.[2,3] The exact same trend was observed during the grafting of dioxaborolane **BE-SH** (*cf.* Chapter 2).

4.3.2 SEC measurements

As expected, the number average molar mass, M_n, of the grafted PBs increased with the grafting functionality (**Table 4.1**). The low dispersities of the various grafted PB samples show the absence of undesirable reactions under the tested conditions, as for instance, radical cross-linking and chain scission.

4.4 Vitrimer formation and characterisation

As for the dioxaborolane PB vitrimers, the dynamic network was synthesised using the same procedure as for PB grafting, simply replacing **6m-BE-SH** with **Bis-6m-BE-SH** (**Figure 4.1**). Only one cross-linking density was tested, that is to say 6 **Bis-6m-BE-SH** cross-linker per chain. The obtained material was hazy, neither clear nor transparent like the dioxaborolane PB vitrimers. This could be due to a macrophase separation in the final material. Furthermore, no gel was observed during the cross-linking, only an increase of the viscosity. However, once dried, the resulting material behaved like a solid. The grafting of **Bis-6m-BE-SH** onto PB was confirmed by FT-IR after reaction, with the complete disappearance of the S-H stretching vibration band around 2560 cm^{-1}.

4.4.1 Analysis after diolysis

4.4.1.1 Grafting yield

In order to quantify the grafting of the cross-linker, **Bis-6m-BE-SH**, an excess of 1,3-propanediol was added to the network immersed in THF. Within less than one hour, the material was completely dissolved proving that the network is formed thanks to dynamic dioxaborinane bonds and that radical coupling reactions are limited. The reaction medium was then precipitated into methanol to isolate the functionalised PB thermoplastic from the bis-dioxaborinane, compound **5** and 1,2-propanediol as shown in **Scheme 4.2**.
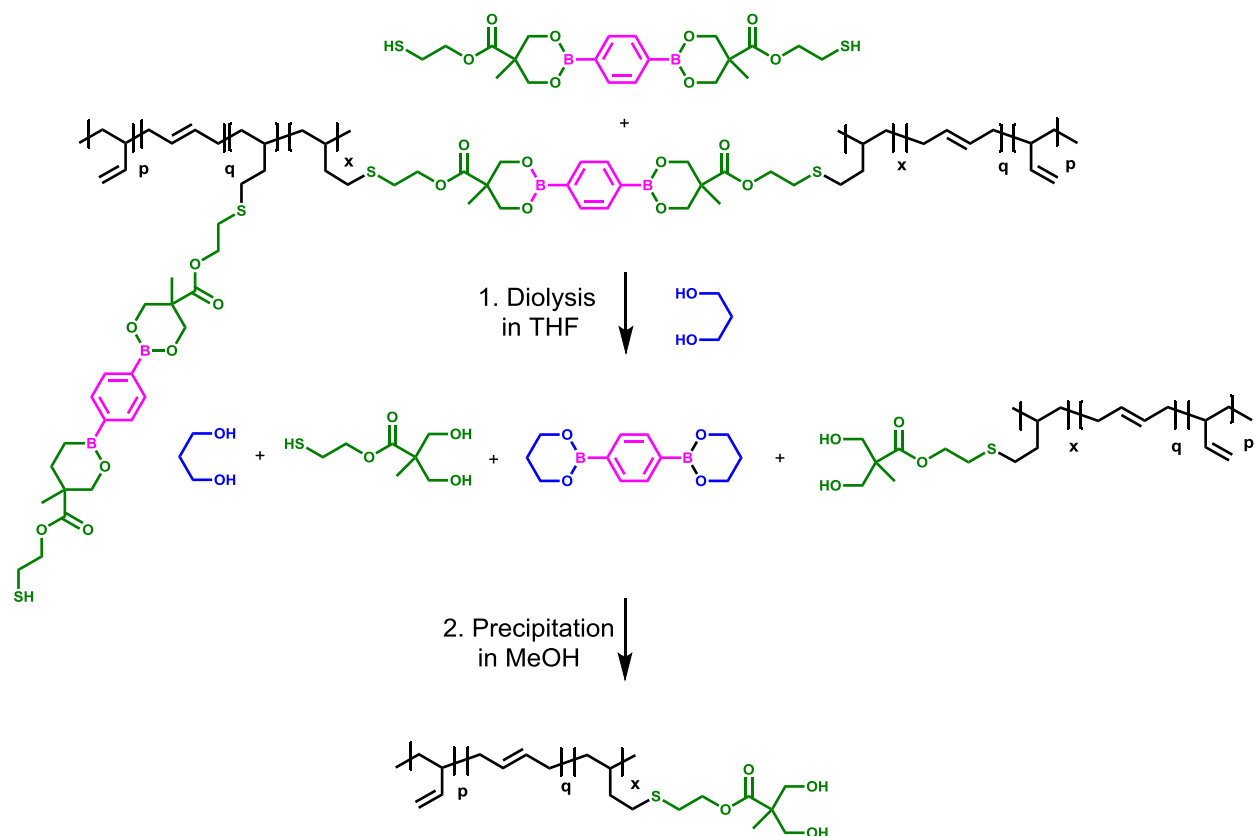
Scheme 4.2. Diolysis of the vitrimer followed by the precipitation into methanol, to isolate the functionalised PB thermoplastic.

The precipitated polymer was dried and analysed by ^{1}H-NMR. The theoretical functionalisation degree was taken as reference. The grafting yield was calculated as the ratio between the measured and the theoretical functionalisation degree and was estimated to be 56%, which was a bit lower than the yield of **PB-6m-BE-6** (65 ± 9) but in the same range. This decrease may be explained by the rise of viscosity that occurs during the crosslinking reaction, impeding the crosslinker **Bis-6m-BE-SH** to react with the polybutadiene backbone.

4.4.1.2 SEC analysis

The polymer isolated after precipitation was further analysed by SEC. The results are displayed in **Figure 4.3.** The diolysed polymer had an M_n of around 4510 Da, while the number average molar mass of **PB-6m-BE-6**, the linear grafted polybutadiene, was estimated to be 4460 Da. Dispersities were also similar. Consequently, the dynamic crosslinking based on **Bis-6m-BE-SH** did not lead to main chain scission, branching or static irreversible cross-linking.
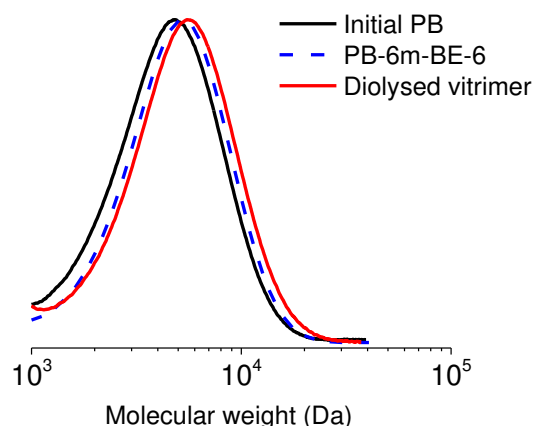
Figure 4.3. Overlap of SEC chromatograms of the initial PB (solid line, black), **PB-6m-BE-6** (dashed line, blue) and diolysed vitrimer (solid line, red).

4.4.2 Solubility

Swelling experiments were also conducted. Samples were immersed in dried THF at room temperature and weighed after 24 h and 144 h. The results are summarised in **Table 4.2**. The network was insoluble under these conditions, with insoluble fractions of 68% after 24 h. Nevertheless, the insoluble fraction of the corresponding dioxaborolane vitrimer **PB-BE-V6** reached 90%. This difference could be due to less effective grafting of the dioxaborinane as mentioned in the above subchapter. Interestingly, the 6 membered boronic ester based network exhibited still an insoluble fraction of 14% after 144 hours of immersion, while the 5 membered counterpart was totally dissolved after only 72 hours. This improvement of the solvent resistance shows that the former network rearranged slower than the latter one, due to slower dioxaborinane exchange reaction as compared to dioxaborolanes.

With the aim to investigate the dissolution mechanism, furthers experiments were performed. Molecular sieves were introduced in the vial and the whole set-up was purged with argon in order to prevent the atmospheric moisture to hydrolyse some of the boronic ester bonds. The soluble fraction decreased from 32% to 22% after 24 hours and from 86% to 40% after 144 hours highlighting the decisive role of water in the dissolution of these vitrimers. As should be expected, swelling ratios decreased, by a factor 2, as the insoluble fractions increased.

Table 4.2. Insoluble fractions and swelling ratios of the vitrimer in THF at room temperature under different conditions

	Insoluble fraction		Swelling ratio
Molecular sieves	24 h	144 h	24 h
without	68%	14%	12
with	78%	60%	6

To check if the dissolution follows a hydrolytic process and/or an exchange between dioxaborinanes, the following experiment was conducted. The vitrimer was immersed 24 hours or 6 days THF without adding molecular sieves. The soluble fraction was isolated, dried, re-dissolved in CDCl₃ and analysed by ¹H-NMR spectroscopy.
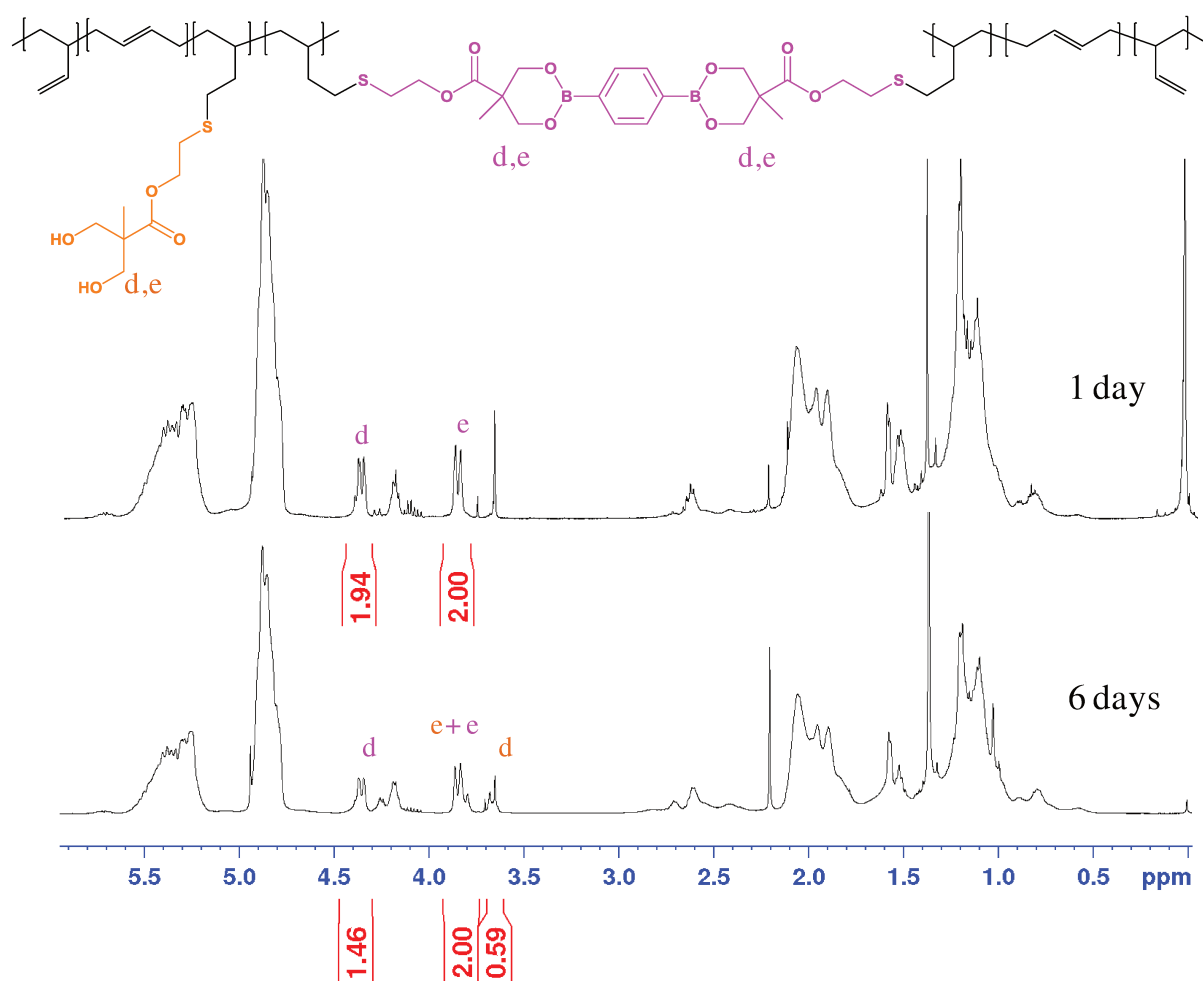

Figure 4.4. ¹H-NMR spectra in CDCl₃ of soluble fractions, after 24 hours (top) and 6 days (144 hours ; bottom) in THF, dried and re-dissolved in CDCl₃.

The ^{1}H-NMR spectra are shown in **Figure 4.4**. After 24 hours, no diol could be detected, consequently no or amount of diols below the NMR detection limit were generated. After 144 hours, the results were different; the integrations of protons attached to the boronic esters did not match between each others. Indeed, the integration of the peak at 4.44 ppm (proton d) decreased from 1.94 to 1.46 while for the peak at 3.92 ppm (proton e) it did not change and matched with the aromatic peaks of the boronic ester. Furthermore, new peaks at 3.64 ppm corresponding to the diol part, appeared. The diol proportion was estimated to be 29% of the total amount of crosslinker.

Nonetheless, the drying of the soluble fractions affects the dynamic of the system because the connectivity and the conformation of the soluble macromolecules depend on their concentration in the solution and on the nature of the solvent. When the solution part was extracted and concentrated, an elastic network was formed but could be dissolved in CDCl$_3$. In order to obtain a meaningful and rigorous study, the experimental conditions were changed.

To overcome this problem, the swelling test was conducted in deuterated THF. The soluble fractions were directly analysed without being dried and without changing the solvent for the NMR analysis. After 7 days, diols peaks were detected while after 1 day they were below the NMR detection limit (**Figure 4.5**). Atmospheric moisture leads to the partial hydrolysis of the crosslinks. With this experimental set-up, which better mimic the solubility tests, only 15% of the bis boronic esters were hydrolysed after 168 hours, which is not sufficient to cleave all the cross-links and to dissolve the vitrimer. The appearance of diols significantly accelerates the dioxaborinane exchange reaction by transesterification, resulting in faster topological rearrangement of the network and eventually leading to its total dissolution.
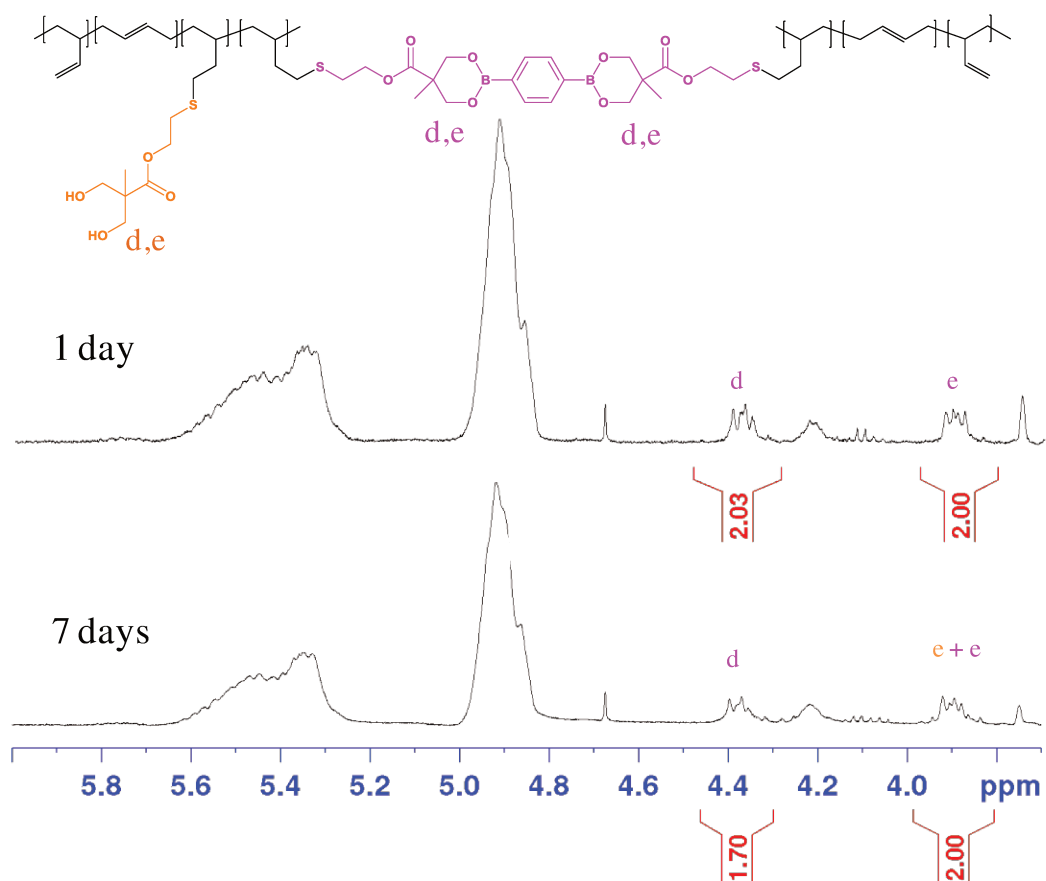
Figure 4.5. ^{1}H-NMR spectra in THF-d_8 of soluble fractions, after 24 hours and 7 days (168 hours) in THF-d_8.

To investigate the water resistance of the crosslinker, **Bis-6m-BE-SH** was dissolved in THF-d_8 and 1 equivalent of water was added, the evolution of its water stability was then monitored by ^{1}H-NMR spectroscopy. A control experiment was also conducted without purposely adding water.

The results are displayed in **Figure 4.6**. To quantify the hydrolysis, the peak at 1.23 ppm corresponding to the methyl group of the boronic ester (**Figure 4.6**, pink, labelled c) was followed and compared to the methyl group of the diol equivalent which is shifted to 1.07 ppm (**Figure 4.6**, orange, labelled c). One can observe that 2h30 after the introduction of water the dioxaborinane was hydrolysed to a small extent, with 3 mol% of generated diols, while no diol was detected without adding water. Although the tubes were sealed with parafilm, water appeared after 6 days (even when no water was intentionally added at the beginning of the experiment) and 5 mol% of the boronic esters were converted into their diol counterpart. The value reached 7% when 1 equivalent of water was incorporated at the beginning of the experiment. Considering that the soluble fractions are composed of chains crosslinked with 3 to 5 crosslinkers in average, the hydrolysis of 15 mol% of dioxaborinanes

is too low to lead to the full dissolution of the vitrimers. Diols, generated by hydrolysis, accelerate the exchange reaction between the crosslinks resulting in a quicker rearrangement of the system which can start to dissolve.
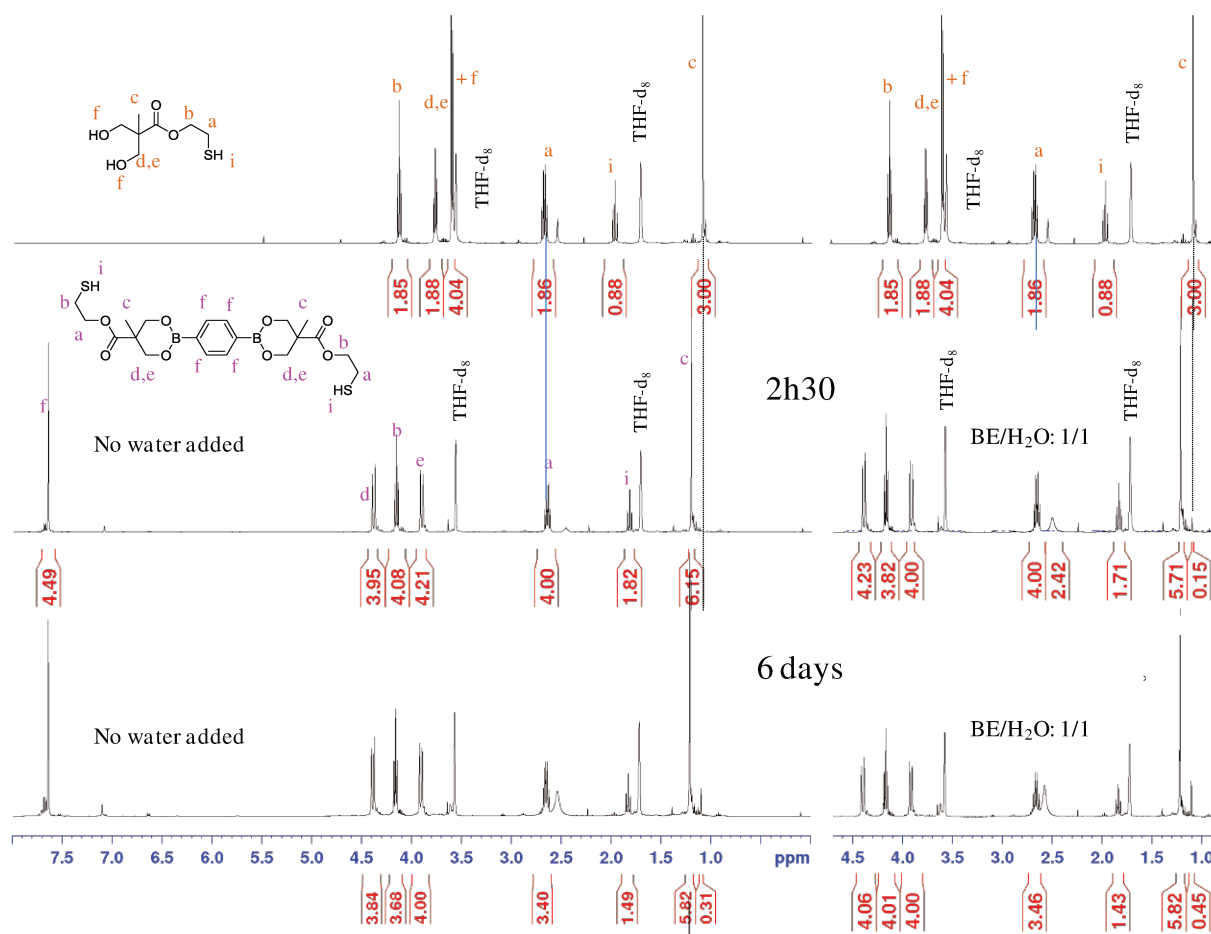

Figure 4.6. ^{1}H-NMR spectra of the kinetic study of Bis-6m-BE-SH hydrolysis in THF-d$_8$ (c = 0.1 mol.L^{-1}) at room temperature, in the presence (right) or in the absence (left) of 1 equivalent of water.

4.4.3 Ageing of the vitrimers

4.4.3.1 DMA

The ageing of vitrimers was studied because the properties of the material were changing over time. This unexpected behaviour was investigated according to the following procedure. After its synthesis, the vitrimer was stored in a dark place at room temperature for twenty days. The network was then analysed by DMA, with an elongational creep-recovery test followed by a temperature ramp at 1 Hz from -80 to 200 °C. The material was recovered and reprocessed 10 minutes at 150 °C under 3 tons by compression moulding and analysed again. Finally, 8 days after these two steps, the vitrimer was analysed one last time. The results are displayed in **Figure 4.7**.

193

The creep tests gave very different results depending on the ageing of the vitrimer. After 20 days and 8 days the material deformed of 3.5 % after 100 min under 0.1 MPa, while the reprocessed material crept of about 20%, the rearrangement was drastically accelerated. The DMA results show the presence of a pseudo plateau between 25 °C and 75 °C after the glass transition, this regime is followed by a second plateau, the expected rubbery state with a storage modulus of 1 MPa. The former plateau around 10 MPa is well pronounced after the ageing but not just after the reprocessing at 150 °C. Interestingly, when the vitrimer is cooled down after the heating ramp, the first plateau is not observed anymore as depicted in **Figure 4.8**. This result confirmed that heating to 200 °C led to a change in the morphology of the vitrimer with a structuration of the material.
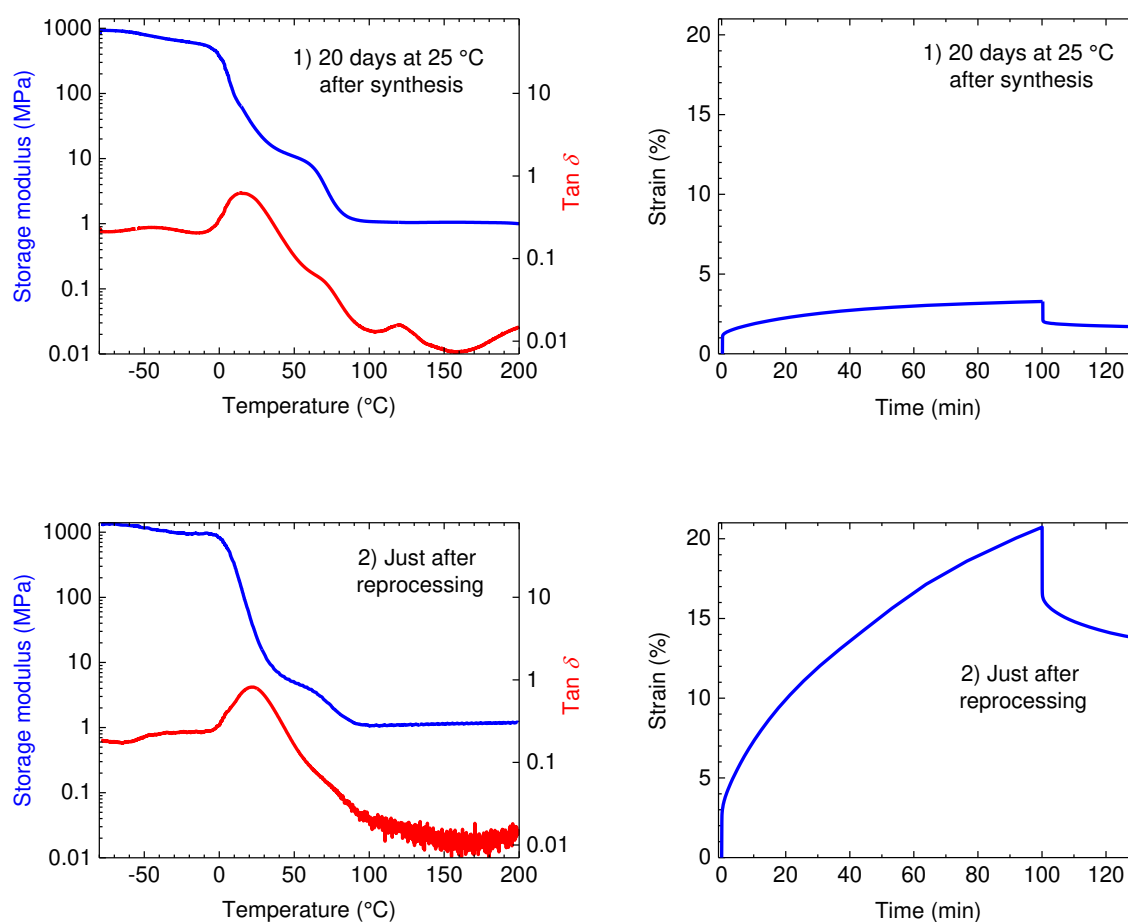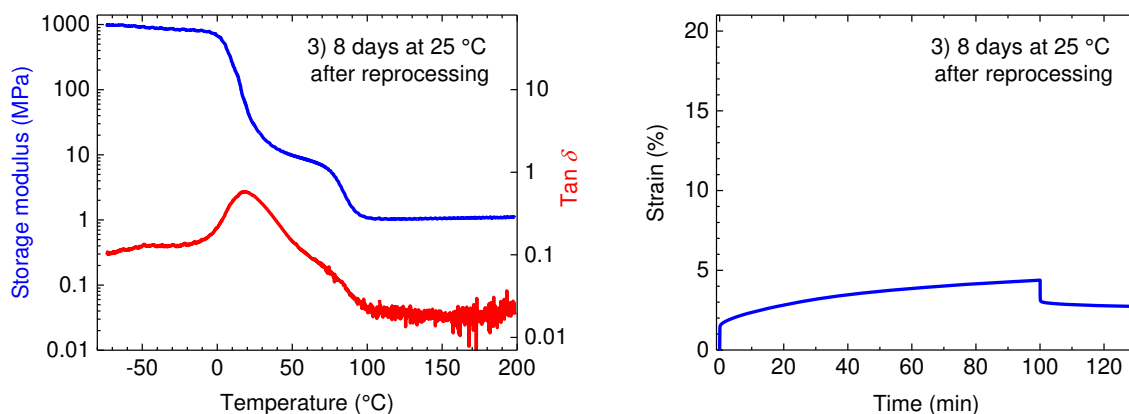
Figure 4.7. Thermo-mechanical analysis of vitrimer aged 20 days (top), reprocessed (middle) and after 8 days of ageing (bottom). Left side: DMA from -80 to 200 °C. Right side: creep (0.1 MPa for 100 min) recovery (0 MPa for 30 min) experiment at 28 °C.
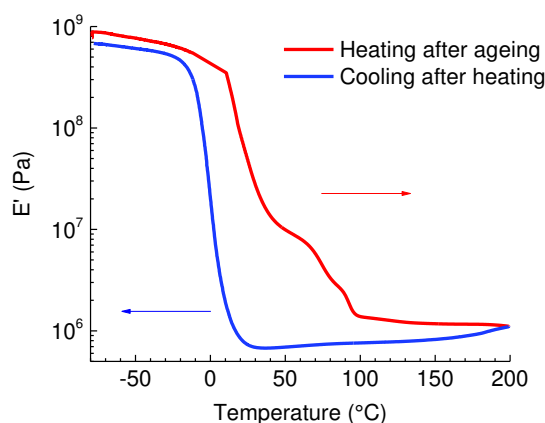

Figure 4.8. DMA of the vitrimer after 8 days of ageing during the heating (1st part, red) followed by the cooling (2nd part, blue) ramp.

4.4.3.2 Calorimetry

The different materials, as synthesised and after ageing, were analysed by DSC. **Figure 4.9** displays the results. Right after the synthesis, a T_g of -2 °C is observed, while after 20 days, the glass transition shifted to -5 °C on the first heating ramp and an enthalpic peak corresponding to a melting peak appeared at 68 °C. During the 2nd heating ramp of the aged material, the T_g reached -2 °C again, whereas the melting peak disappeared. The crosslinker, **Bis-6m-BE-SH**, is a solid at ambient temperature. Its melting temperature was calculated to be 157 °C, which is considerably higher that peak observed for the aged material. The vitrimer reorganises its structure over time at room temperature, which leads to a macrophase separation between the crosslinker and the polybutadiene matrix. This phase separation disappeared by the annealing, but slowly occurs again.

195
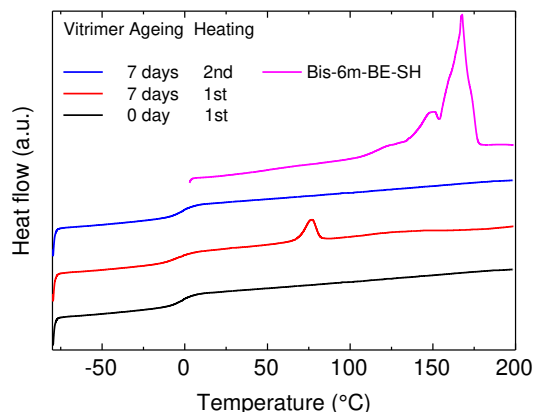
Figure 4.9. DSC curves of vitrimer as synthesised (black), after 20 days of ageing during the 1st heating (red), 2nd heating (blue) and crosslinker **Bis-6m-BE-SH** (pink).

4.4.4 Tensile tests and recycling

The recyclability of the vitrimer (**6 m BE**) as synthesised, *i.e.* without ageing, was evaluated by tensile tests, which were followed by reprocessing by compression moulding for 10 min at 150 °C and tensile testing again up. This procedure was repeated over 3 cycles. The results were compared to dioxaborolane PB vitrimer (**5 m BE**) and are displayed in **Figure 4.10**. The elongation at break did not change when switching from dioxaborolane to dioxaborinane networks, while the stress at break and the Young's modulus were divided by a factor 4. The less efficient grafting led to less crosslinked network for the 6 membered boronic esters based network. Consequently, the mechanical properties were inferior as shown also in DMA analysis. Interestingly, the keys properties of the dioxaborinane vitrimer tended to increase over the recycling cycles. The elongation at break increased by 13% between the initial test and the 3rd recycling, the stress at break raised by 29%, to reach 0.72 MPa, and the Young's modulus gained 36% to reach 1.2 MPa.
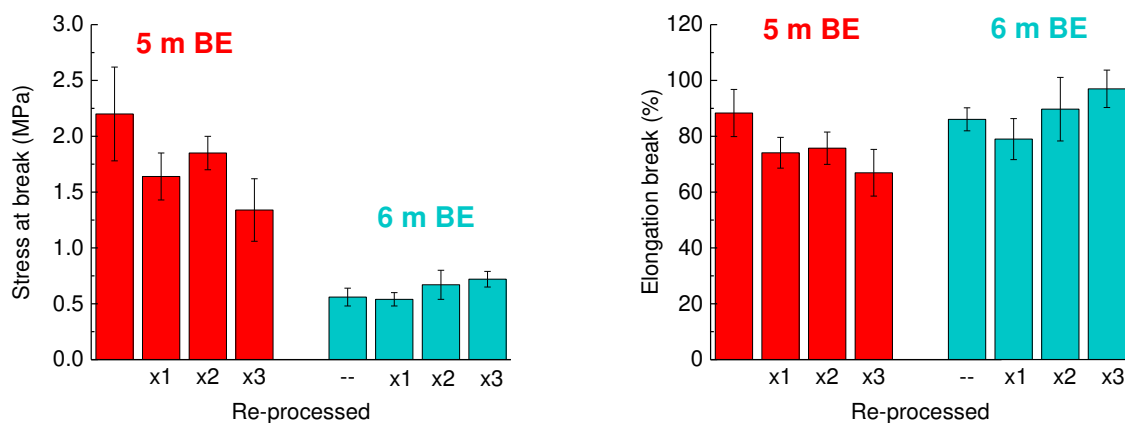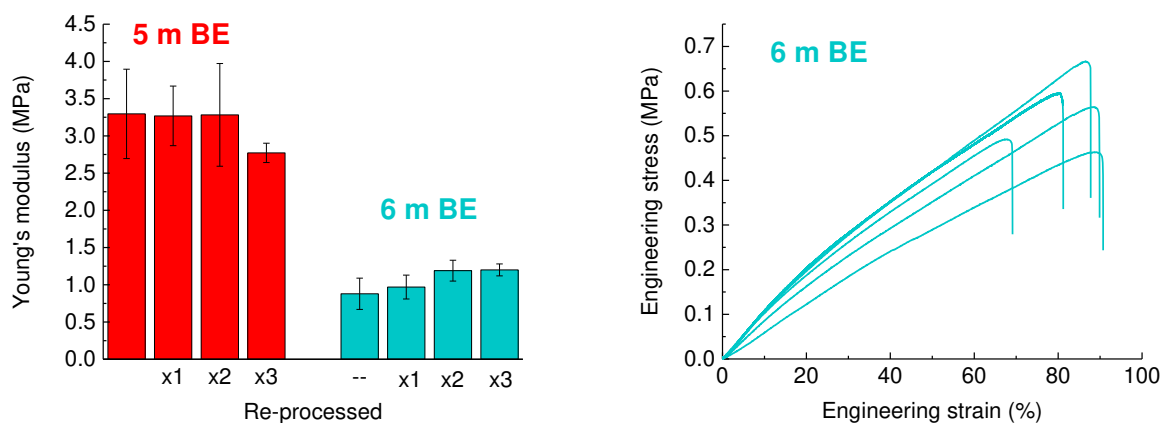
Figure 4.10. Stress at break (top, left), elongation at break (top, right) and Young's modulus (bottom, left) of the dioxaborolane based vitrimer **5 m BE** (red) and the dioxaborinane based vitrimer **6 m BE** (cyan). Tensile stress-strain curves at 25 °C for the initial **6 m BE**. Results on multiple specimens are shown for reproducibility (bottom, right).

4.5 High molar mass polybutadiene

In order to decrease the concentration of boronic esters required to obtain a 3D-network, and potentially avoid phase separation, a higher molecular weight polybutadiene (HW PB) (M_n = 84 000 g/mol, Đ = 1.99) with a vinyl content of 9 mol% was used.
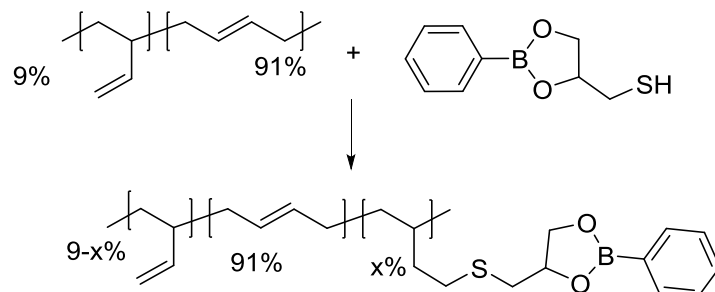
Scheme 4.3. Grafting of dioxaborolane **BE-SH** onto a high molecular weight, low vinyl content polybutadiene.

The dioxaborolane **BE-SH** was chosen as model molecule before switching to the dioxaborinane **6m-BE-SH**, because it was easier to synthesise in large quantity (**Scheme 4.3).**

The polymer contains 140 vinyl groups per chain with a polymerization degree (DP_n) of 1550. The targeted functionalisation degree was set to 6%, which corresponds to a ratio [**BE-SH**]/[vinyl] = 97/140, *i.e.* 69%. In a first attempt to functionalise HW PB, the polymer was dissolved in anisole, at a concentration of 5 wt%. The reaction medium was then highly viscous; the grafting yield was really low, *i.e.* inferior to 2%. Only 2 pendant boronic esters were grafted onto HW PB. The nitrogen bubbling was perhaps not efficient or reactive species could not easily diffuse into the mixture. The polymer concentration was then decreased to 1.5 wt%, thus the solution was far less viscous. The grafting was improved to 6%.

In order to get rid of the effect of possible inhibitors, the amount of added AIBN was increased from [**BE-SH**]/[AIBN] = 70/1 to 7/1. It resulted in a similar grafting yield, *ca.* 7%.

Changing the solvent from anisole to toluene did not change the overall yield at 5%, still inferior to 10%.

Table 4.3. Grafting conditions of BE-SH onto HW PB

Sample	Solvent	Concentration (wt%)	[BE-SH]/ [PB]	[BE-SH] / [AIBN]	Conditions	Grafting yield (%)
HW-PB-BE-1	anisole	5	6%	70	100°C, 1h	< 2
HW-PB-BE-2	anisole	1,5	6%	70	100°C, 1h	6
HW-PB-BE-3	anisole	1,5	6%	7	100°C, 1h	7
HW-PB-BE-4	toluene	1,5	6%	70	80°C, 4h	5

As summarised in **Table 4.3**, the grafting onto HW PB did not exceed 7%, which corresponds to 7 pendant **BE-SH** per chain. This is far less than the grafting yields obtained for polybutadiene with high vinyl content, for which grafting yields were ranging from 60 to 90%. Nonetheless these results are consistent with literature data. [4,5]

198

4.6 Conclusion

This chapter describes the synthesis of a divalent and a trivalent molecule containing a 6-membered boronic ester and a thiol function, respectively two thiol functions. These compounds were synthesised in 5 steps with an overall yield of 29% and 27%, respectively, which corresponds to an average yield per step of 78% and 77%, respectively. The mono thio-functionalised dioxaborinane **6m-BE-SH** was successfully grafted onto polybutadiene. A dynamic covalent network was then formed via the grafting of the bis-thiol dioxaborinane, **Bis-6m-BE-SH**. The resulting vitrimer exhibited an increased solvent resistance as compared to its dioxaborolane counterpart, even if a significant part of the networks (up to 86%) could be dissolved under specific conditions. It was shown that the hydrolysis is not the major process involved in the dissolution of the vitrimer under the conditions tested. Indeed, minor traces of diols and water were detected by ^{1}H-NMR spectroscopy. However, these molecules lead to the acceleration of the exchange reaction between dioxaborinanes through transesterification. As a result, the network could rearrange faster its topology than without diols, to eventually be partially dissolved through loop formation and partial hydrolysis. Further investigations should be conducted to determine the precise rearrangement of the macromolecules in the solvent, and quantify the significance of hydrolysis and network rearrangement. The material was prone to creep at room temperature. The lower grafting efficiency could be one the reasons of this unexpected result. Moreover, the systems led to macrophase separation. In order to prevent such phenomenon, a less polar dioxaborinane than **Bis-6m-BE-SH** should be used. However, the tensile tests reveal that the vitrimer possess a good recyclability even if its mechanical properties were inferior to those of the dioxaborolane vitrimer.

Eventually, grafting onto a high molar mass polybutadiene with a low vinyl content was attempted but all grafting yields were inferior to 8%, regardless of the tested conditions. Consequently, the thiol-ene chemistry in solution is not suitable for such polymers. Therefore, other grafting conditions, such as reactive extrusion, or chemistries have to be found and developed in order to transform efficiently commercially available linear polydienes into vitrimers.

4.7 References

(1) Lotti, L.; Coiai, S.; Ciardelli, F.; Galimberti, M.; Passaglia, E. Thiol-Ene Radical Addition of L-Cysteine Derivatives to Low Molecular Weight Polybutadiene. *Macromol. Chem. Phys.* **2009**, *210* (18), 1471–1483. https://doi.org/10.1002/macp.200900164.

(2) Campa, J. G. de L.; Pham, Q.-T. Polybutadiènes Hydroxytéléchéliques, 5. Addition Des Thiols Sur Les Double Liaisons Des Polybutadiènes Hydroxytéléchéliques Radicalaire et Anionique. Etude Des Mécanismes d'addition Par 1H et 13C NMR. *Makromol. Chem.* **1981**, *182* (5), 1415–1428. https://doi.org/10.1002/macp.1981.021820514.

(3) Justynska, J.; Hordyjewicz, Z.; Schlaad, H. Toward a Toolbox of Functional Block Copolymers via Free-Radical Addition of Mercaptans. *Polymer* **2005**, *46* (26), 12057–12064. https://doi.org/10.1016/j.polymer.2005.10.104.

(4) Trovatti, E.; Lacerda, T. M.; Carvalho, A. J. F.; Gandini, A. Recycling Tires? Reversible Crosslinking of Poly(Butadiene). *Adv. Mater.* **2015**, *27* (13), 2242–2245. https://doi.org/10.1002/adma.201405801.

(5) David, R. L. A.; Kornfield, J. A. Facile, Efficient Routes to Diverse Protected Thiols and to Their Deprotection and Addition to Create Functional Polymers by Thiol−Ene Coupling. *Macromolecules* **2008**, *41* (4), 1151–1161. https://doi.org/10.1021/ma0718393.

Chapter 5

Transformation of Polyisoprene into Vitrimers using Azide Chemistry

Table of Contents

Chapter 5 - Modification of Polyisoprene into Vitrimers using Azide Chemistry

5.1 Introduction

5.1.1 Azides

Azide compounds are nitrogenous chemicals carrying a N_3 group. They are involved in a number of reactions, such as Staudinger reaction, Schmidt reaction and Curtius rearrangement. One of the major uses of azides is the Huisgen cycloaddition. This is a [2+4] cycloaddition involving 5 atoms between a dipolarophile, as alkenes and alkynes, and an azide or another 1,3-dipolar compound. It can operate at elevated temperature without a catalyst or at room temperature when catalysed by copper.[1] This reaction is highly selective and easy to conduct under biological conditions.[2] Moreover, under specific conditions, azides can lead to the formation of nitrenes, which are very reactive compounds. As a consequence, organic azides are used in a wide range of applications, such as photochemical cross-linking of polymers, including rubber, couplings agents, modification of polymer surfaces, dyes, blowing agents, propellants, biological compounds and polymerization initiators.[3–8]

5.1.2 Definition of nitrenes

Nitrenes are derivatives of electroneutral nitrogen, R-N, having only six valence electrons at the nitrogen. Two electronic configurations of low energies are involved in the chemical reactions of nitrenes: singlet and triplet states, as depicted in **Scheme 5.1**. Nitrenes are the nitrogen analogous of carbenes.[9]

Singlet nitrenes have two non-bonding lone pairs of electrons and one empty orbital and needs an electron pair to have fully occupied orbitals. Consequently, they are strong electrophilic species, especially when the R substituent is electron withdrawing. Triplet nitrenes have two unpaired electrons. They are less electrophilic than their singlet counterpart.
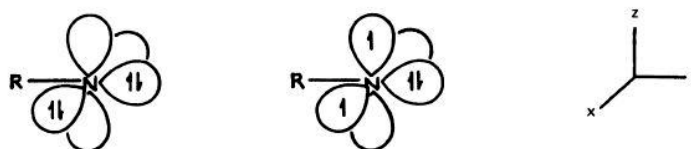
Scheme 5.1. Nitrenes singlet (left) and triplet (right) states.

Under suitable triggers, organic azides can form nitrenes through N_2 loss. Nitrenes are very reactive species whose selectivity depends on their chemical structure. A wide diversity of azides exists; among them, alkyl, vinyl, allyl, aryl, acyl, alkoxycarbonyl, also named azidoformates ($RO-CO-N_3$), sulfonyl and phosphoryl azides possess different behaviours towards dienes and others chemical functionalities. In infrared spectroscopy, the N_3 group exhibits a strong asymmetric stretching vibration around 2100 cm^{-1} and a medium symmetric stretching vibration around 1260 cm^{-1}. Azides show an UV absorption around 285 nm, enabling energy transfer and nitrogen loss. Therefore, UV light is a way to generate nitrenes, called photolysis.

5.1.3 The formation of nitrenes

Nitrenes can be formed through different pathways as shown in **Table 5.1**. Thermolysis and photolysis are the two main possibilities to generate nitrenes. Thermolysis usually yields singlet nitrenes. Azidoformates or alkoxycarbonyl nitrenes, $RO-CO-N_3$, vinyl azides and other similar compounds, possess a decomposition temperature between 60 and 120 °C, which makes them suitable to react in the melt with polymers whose T_m or T_g are below this range, and thus elastomers. However, other azides can yield nitrenes but they require higher temperatures. For example, sulfonyl and alkyl azides typically decompose at 120 and 175 °C, respectively. Under these conditions, the products and the rubber may be unstable.

Table 5.1. Practical pathways to nitrenes.

Nitrenes		Photolysis	α Elimination	Thermolysis	
Alkyl	R-N	+	-	+	175 °C
Vinyl	C=C-N	+	-	+	100 °C
Acyl	R-CO-N	+	-	-	-
Azidoformate	RO-CO-N	+	+	+	60-100 °C
Sulfonyl	R-SO$_2$-N	(+)	-	+	> 120 °C

+, commonly used; (+), occasionally used; -, unsuccessful, others reactions predominate.

Photolysis of azides yields predominantly singlet nitrenes, but triplet states can also be generated by using triplet sensitizers such as carbonyl compounds. With long life times, these nitrenes are good nitrogen abstractors to yield amides.

Another possibility to form alkoxycarbonylnitrenes is the α-elimination of arenesulfonate ion from alkyl *N*-(arenesulfonyloxy)urethanes using triethylamine as a base. For instance, carbethoxynitrene (EtOOCN) can be generated by α-elimination from the anion of *N*-p-nitrobenzenesulfonoxyurethan.[10] Thus, this method does not require to use azides.

5.1.4 Reactions involving nitrenes: C-H insertion and C=C addition

Nitrenes are involved in different reactions, regardless of the singlet or triplet state: addition to a carbon-carbon double bond, insertion into a C-H bond, and interaction with a non-bonding lone pair of electrons of a heteroatom. Depending on the electronic state, nitrene reactions follow different mechanisms. Singlet nitrenes react commonly in a single step to fill their electron deficiency, leading to stereospecific insertion or addition. On contrary to singlet nitrenes, triplet nitrenes react in two steps through radical reactions, which are non-stereospecific. As a consequence, the analysis of the products may be used to determine the nature of nitrene electronic states involved in the reaction, or their respective importance. If most of the reactions of acylnitrenes are reactions with singlet nitrenes, both singlet and triplet nitrenes are strong electrophilic species. However, due to their inherent high reactivity, nitrenes may suffer from rearrangements or fragmentations, thereby decreasing the overall yield of the targeted reaction.

5.1.4.1 C-H insertion

Nitrenes can insert into C-H bonds making new C-N and N-H bonds, while breaking at the same time the C-H bond (**Scheme 5.2**). C-H insertion into a classical C-H bond requires highly energetic and electrophilic species, such as nitrenes. The reaction is easier if the bond dissociation energy is lower, increasing the rate of insertion. Therefore, the order of reactivity for C-H bonds is as following: tertiary > secondary > primary.[11] The reactivity of secondary derivatives is ten times higher than that of primary C-H bonds, and 3 times higher for tertiary as compared to secondary. The C-H insertion leads to the full retention of configuration, whatever the stimulus used to produce nitrenes.

Triplet nitrenes seem to react with C-H bonds by abstraction-recombination, to yield apparent C-H insertion products (**Scheme 5.2**). For instance, hydrogen abstraction may be followed by a radical recombination. In this two-step process, the triplet insertion into C-H bonds proceeds with loss of configuration.
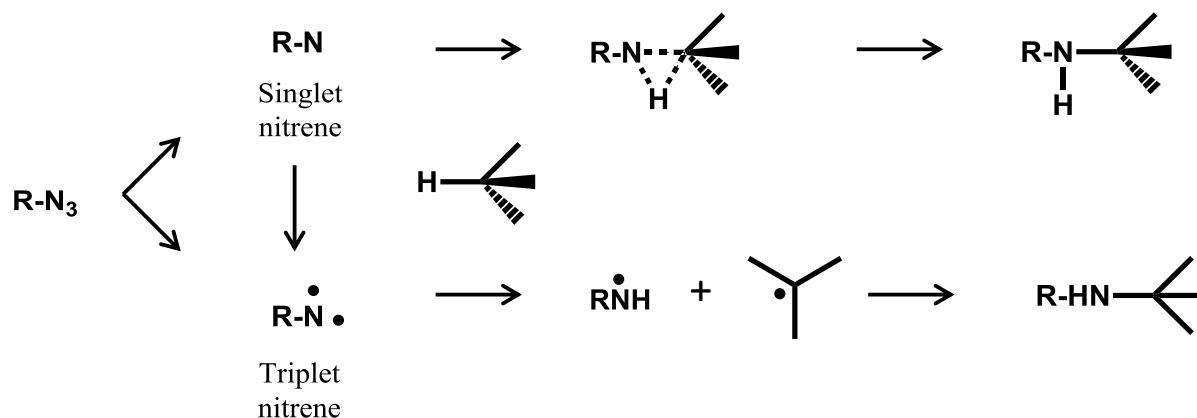
Scheme 5.2. Mechanism of C-H insertion of a nitrene.

5.1.4.2 Addition of acylnitrenes to olefins

Nitrenes add onto olefinic double bonds leading to the formation of aziridines. Aziridines can be generated with both triplet and singlet alkoxycarbonyl nitrenes, but following different mechanisms of addition onto C=C double bonds.

Singlet nitrenes addition is stereospecific, as for the C-H insertion, while triplet nitrenes add via a two-step mechanism leading to non-stereospecific addition (**Scheme 5.3**). The formation of a 1,3-diradical during the first step enables a free rotation about the C-C single bond. The ring closure occurs in the second step, to yield a cis-trans mixture of aziridines.
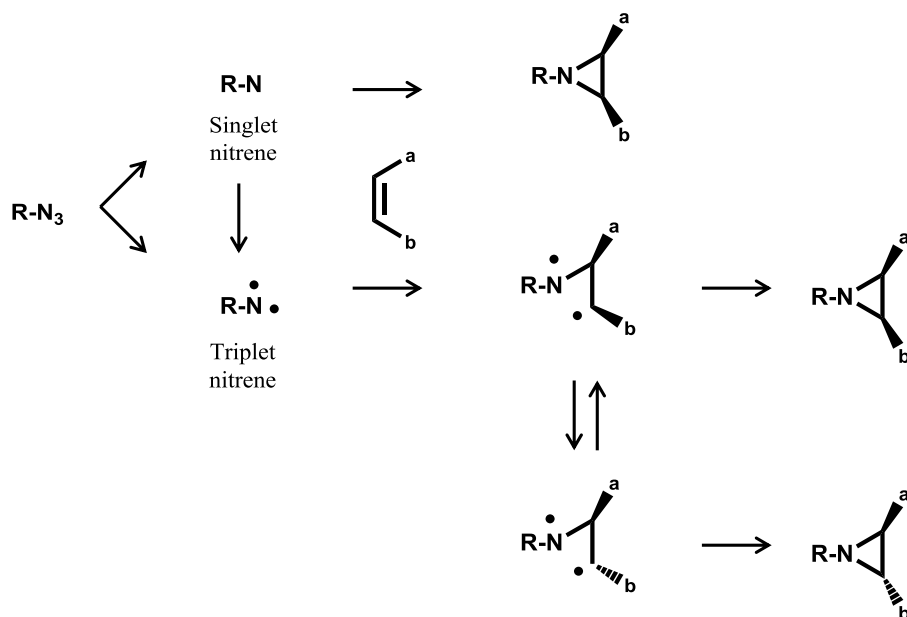
Scheme 5.3. Mechanism of nitrene addition onto C=C .

According to Lwowski and McConaghy, thermally generated nitrenes are in the singlet state, which can subsequently yield triplet nitrenes through intersystem crossing.[12] For instance, azidoformate nitrenes lead to stereospecific addition via C-H insertion, through their singlet state, but yield non stereospecific reactions via the triplet state formed by intersystem crossing. As a consequence, it was demonstrated that the higher the concentration of the olefin, the higher the stereospecificity, because singlet nitrenes have less time to cross to triplet state.[13] Consequently, it was extrapolated at infinite concentration of olefins, that additions were 100% stereospecific when alkoxycarbonyl nitrenes were generated by azide thermolysis. This indicates that in these conditions only singlet nitrenes are formed. In contrast, with photolysis, one third of nitrenes are directly generated in the triplet state, leading to non-stereospecific products. It was confirmed by electron paramagnetic resonance (EPR), which was employed to detect diphenylmethylene, a ground state triplet. Dilute solutions of the azides were irradiated with mercury arc at 77 °K, and the resonance absorptions were recorded. No resonance was observed for cyclohexyl azide, styryl azide, ethyl azidoformate and phenyl azidoformate, whereas EPR was detected with phenyl, p-toluenesulfonyl and benzenesulfonyl azides, and the signal were stable for at least eighteen hours, proving the existence of a ground state triplet.[14]

5.1.5 A wide range of azides

If a wide variety of species can be used as nitrene precursors. However many azides are prone to side reactions (**Scheme 5.4**), limiting the overall reaction yield and thus their interest for grafting onto polydienes.
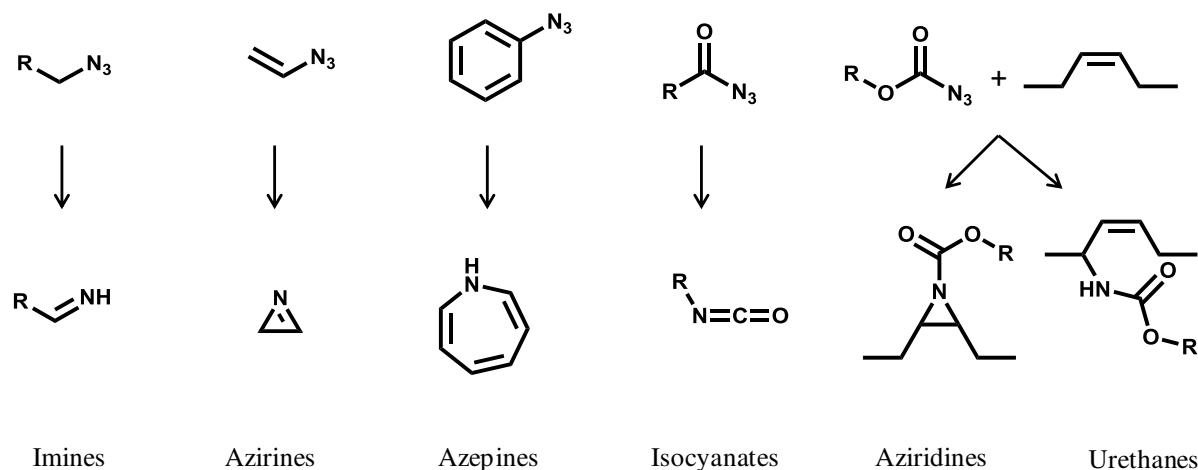
Scheme 5.4. Potential (side-)reactions of alkyl, vinyl, aryl, acyl, alkoxycarbonyl azides.

Alkyl azides are prone to undergo rearrangement into imines, HCN, NH_3, acetylene and methane. Pyrolysis of hydrogen azide gives both singlet and triplet nitrenes. The nitrene formation is the rate limiting step of the global reaction.[15] Temperatures superior to 175 °C are required to thermally decompose alkyl azides. Thermolysis of alkyl azides generates nitrenes through N_2 loss, which subsequently rearrange into imines (**Scheme 5.4**) or amines. For instance, thermolysis of methyl azide yields methylimine. During photolysis, the electronic transition yields a singlet excited azide, which losses nitrogen to give an imine directly without nitrene intermediate. Regardless of the trigger used, alkyl azides generate C-H insertion and aziridines products in minor quantities.[16]

Vinyl and allyl azides are prone to side reactions. For example, as nitrenes can insert into double bonds, intramolecular and intermolecular insertions onto themselves are observed for vinyl azides, which is leading to azirine products (**Scheme 5.4**) and ketenimines.[17] These side products have been observed during both the thermolysis and the photolysis of vinyl azides. For their part, allyl azides can spontaneously rearrange to form a mixture of isomers under a mechanism, which has been named the Winstein rearrangement.[18] As a consequence, using these kinds of azides for the grafting onto polydienes leads to low yields.

Aryl azides can lead to a wide variety of products due to their conversion into an amino group, azobenzene or derivatives of aniline, their insertion into a C-H bonds, their addition to double bonds and their ring expansion of a benzene into an azepine (**Scheme 5.4**). In the latter case, arylnitrene attacks the π system of the aromatic reactant yielding azepine, but can also further rearrange to give an C-H insertion product.

Acyl azides, R-CO-N$_3$ (R = alkyl or aryl), are sensitive to the Curtius rearrangement, during which they are converted into isocyanates (R-NCO) (**Scheme 5.4**) via both thermolysis and photolysis.[19] More precisely, photolysis gives two kinds of reactions. On one hand the photo Curtius rearrangement produces isocyanates, and on the other hand, singlet carbonyl nitrenes are also generated. In contract to photolysis, the thermal activation of acyl azides only generates isocyanates.[20–22]

Unlike the above mentioned azides, **azidoformates,** RO-CO-N$_3$, are less prone to side reactions. They decompose under the action of light[23] or heat,[24,25] into carbalkoxynitrenes (RO-CO-N), which mainly insert into C-H bond and add to double bonds of alkene, such as polydienes for example (**Scheme 5.4**). Under UV light exposure, a mixture of ethyl azidoformate and cyclohexene gave an aziridine product with a yield of more than 50%.[26] Carbon-carbon double bonds were no longer observable by IR spectroscopy, and no N-H band, from a hypothetical amide group, could be observed. The evolution of nitrogen was simultaneous to the azide disappearance, showing that no triazoline intermediate was formed during the reaction. It was confirmed that the main product of the reaction was the aziridine (50%), and the minor products were urethanes (12%) and coupling products of cyclohexene (5%).[27] The presence of oxygen or the variation of the reaction temperature did not change these results. When the azide was heated up to 88 °C, the aziridine compound was still predominant. However, after 118 hours of reaction the ratio cyclohexenylurethane versus aziridine was inverted. This slow rearrangement was not observed when a highly pure aziridine was refluxed over 114 hours. The same reaction, but under UV light and with cyclohexane instead of cyclohexene, led to the formation of a urethane as confirmed by IR and NMR. The reaction operates through C-H insertion and gives a yield superior to 50%.

Many studies have been conducted to determine the nature of the alkoxycarbonyl nitrene; singlet or triplet state. Hafner, Kaiser and Puttner have observed that the photolysis of methyl azidoformate in the presence of cis-butan-2-ene at 30 °C yielded an aziridine through a stereospecific process.[28] This result shows that the formation of singlet nitrenes is

210

predominant under these conditions. McConaghy and Lwowski reported that during the photolysis of ethyl azidoformate, one third of nitrene is generated in the triplet state, while two-thirds are produced in the singlet state. Under thermal activation, nitrene is assumed to be in the singlet state but intersystem crossing to triplet state can occur.[29] According to Wan *et al.*, phenyl azidoformate, $PhO-CO-N_3$, gives triplet ground state upon photolysis followed by Curtius rearrangement. In contrast, the thermal decomposition, which does not promote this reaction, yields intramolecular cyclization.[30] Li and co-workers presented the triplet multiplicity of methoxycarbonylnitrene by direct observation.[31]

5.1.6 Towards the functionalization of polydienes

Nitrene compounds are very reactive species that can graft onto polydienes through two main reactions: C-H insertion and C=C addition. As just presented, nitrenes possess two electronic configurations: the triplet and the singlet state. Both can generate insertion and addition products with polydienes, but through different mechanisms. However, many nitrenes are prone to undergo side-reactions, like intramolecular rearrangements. Rearrangement or fragmentation, for instance transferring the element of a nitrene to an acceptor molecule, would not produce the expected grafting product. When reacting with dienes, azidoformate nitrenes can give aziridines and urethanes without predominant rearrangement, and thereby, with decent yields. Furthermore, the temperature decomposition of such azides, between 60 °C and 100 °C, is well adapted to the modification of elastomers. Indeed, this range of temperature is high enough to enable a fine control of the reaction but also low enough to avoid thermal degradation of polydienes, especially polyisoprene, which are particularly temperature sensitive.

5.2 Hydroquinone-based azidoformate

5.2.1 Synthesis and characterisation of the hydroquinone-based azidoformate dioxaborolanes

5.2.1.1 Synthesis

As azidoformates are activated at temperatures around 100 °C, they have been used to cross-link elastomers through insertion into C-H bonds. They have been used as vulcanizing agents for a wide range of elastomer, such as cis-1,4-polybutadiene, styrene-butadiene copolymers, butyl rubber, EPDM and cis-1,4-polyisoprene.[3]

With the overall aim to incorporate dynamic covalent bonds in polydienic rubbers, in particular polyisoprene (PI) and polybutadiene (PB) with low vinyl contents (inferior to 1 mol%), a difunctional molecule was designed. It should carry two different functional groups; the boronic ester part to introduce dynamic covalent links, and the azide part to graft onto the rubbers. According to the above bibliography, the azide chosen for this functionalisation was an azidoformate (RO-CO-N$_3$), where R is an aryl. Hydroquinone was used as the starting compound because of its commercial availability, low price and the presence of a phenol group that enables the formation of the azidoformate. After a 4 step synthesis, as depicted in **Scheme 5.5,** the targeted azidoformate dioxaborolane, **BE-N$_3$-1**, was obtained with an overall yield of 3.9%, which corresponds to an average yield per step of 44.4%. The detailed synthesis of **BE-N$_3$-1** is presented in subsection 5.7.3.1.
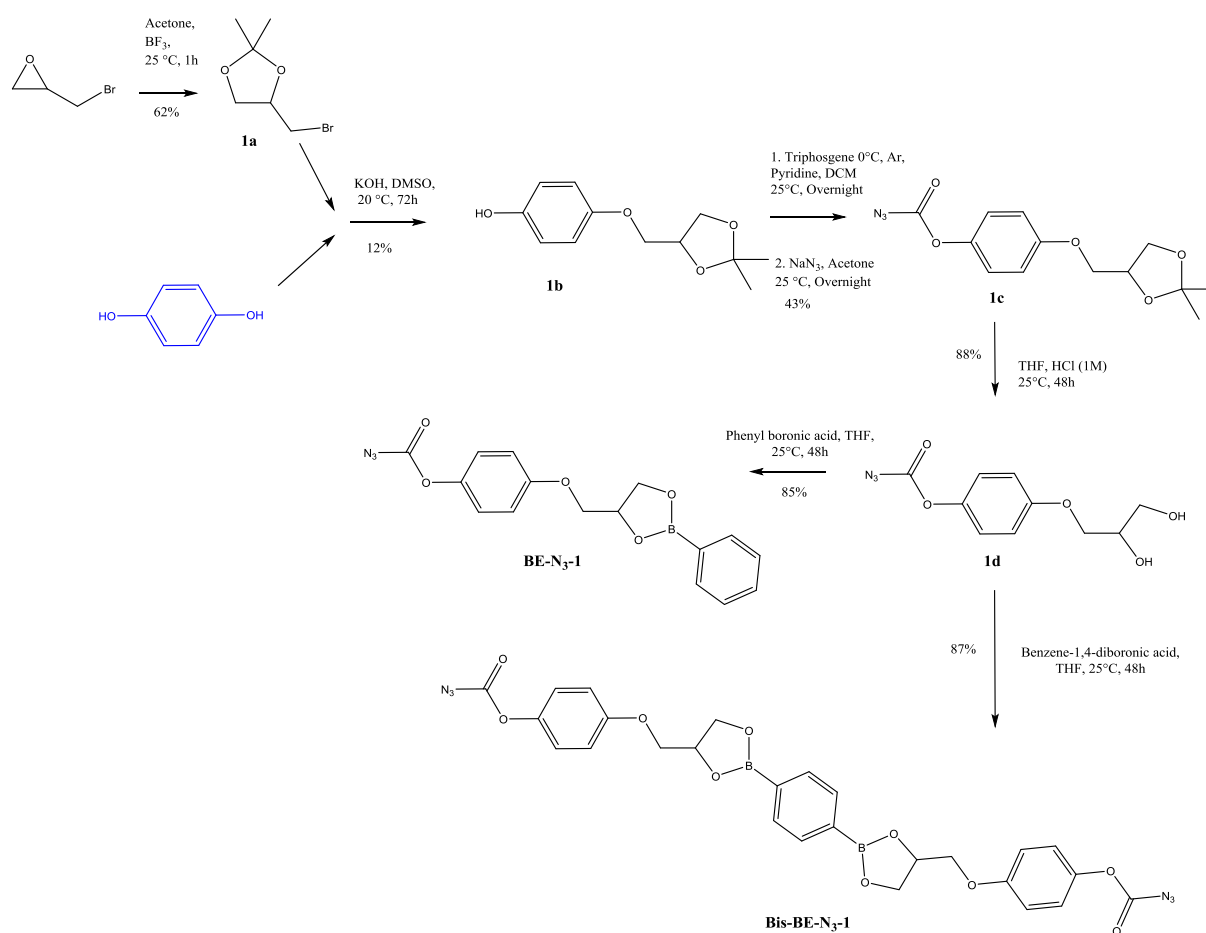
Scheme 5.5. Synthesis of **BE-N₃-1** and **Bis-BE-N₃-1** from hydroquinone, a mono azidoformate dioxaborolane and a bis-azidoformate dioxaborolane, respectively.

5.2.1.2 Thermogravimetric analysis (TGA)

BE-N₃-1 is expected to release a molecule of nitrogen under thermal excitation. The kinetic of the reaction was studied by TGA using a TG 209 F1 Libra from Netzsch. The temperature was either ramped at 20 °C/min or was hold in isothermal mode under nitrogen flow. The results are displayed in **Figure 5.1**.
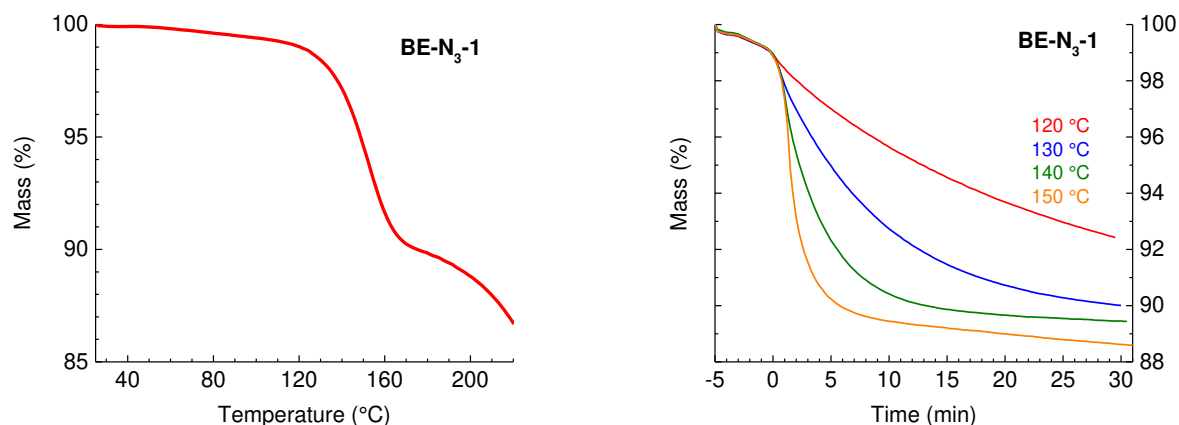
Figure 5.1. Thermogravimetric analysis of **BE-N$_3$-1**. Left side: Temperature ramp at 20 °C/min. Right side: Isothermal curves at 120 °C (red), 130 °C (blue), 140 °C (green) and 150 °C (orange).

During the heating ramp at 20 °C/min, the mass of the azide slowly decreases until 120 °C, above this temperature the loss accelerates until 160 °C, where a pseudo plateau is reached for a loss of around 9 wt% (**Figure 5.1**, left side). This drop is attributed to nitrogen emission which was calculated to be 8.3 wt% in theory. Above 190 °C, the molecule was not stable anymore, and further decomposition is observed.

In the case of the isotherms, the mass loss after 30 min depends on the temperature (**Figure 5.1**, right side). At 120 °C and 130 °C, the plateau is not reached within 30 min, while at 140 and 150 °C, the azide compound has lost 10.6 and 11.4 wt%, respectively. Traces of solvent and/or water could explain this difference between the mass loss observed experimentally and the theoretical one (*i.e.* 8.3 wt%). As expected, the decomposition rate is strongly related to the temperature. At 120 °C, all the nitrogen is not yet released after 30 min, whereas at 130 °C the decomposition is almost finished after 20 min and it required only 10 min at 140 °C and 5 min at 150 °C.

With the aim to further investigate the decomposition of the azidoformate **BE-N$_3$-1**, the following experiment was designed. TGA experiment coupled to infrared was performed on **BE-N$_3$-1** to examine the gaseous products released during the heating ramp at 20 °C/min from 25 to 500 °C. The gaseous products were analysed by FT-IR, while the azidoformate was weighted over time. No signal at all could be detected by FT-IR, confirming the hypothesis that the main product released during the heating of **BE-N$_3$-1** is nitrogen. No band around 2300 cm^{-1} was observed, showing that **BE-N$_3$-1** did not free carbon dioxide during its decomposition up to 200 °C.

5.2.1.3 Infrared analysis

Fourier-transform infrared (FT-IR) spectroscopy of **BE-N$_3$-1** was performed in the solid state using a Tensor 37 spectrometer from Bruker. Spectra were recorded in the attenuated total reflectance mode and converted to absorbance. **Figure 5.2** displays the FT-IR spectra of **BE-N$_3$-1** obtained at 25 °C and at 150 °C at various times between 0 and 20 min.
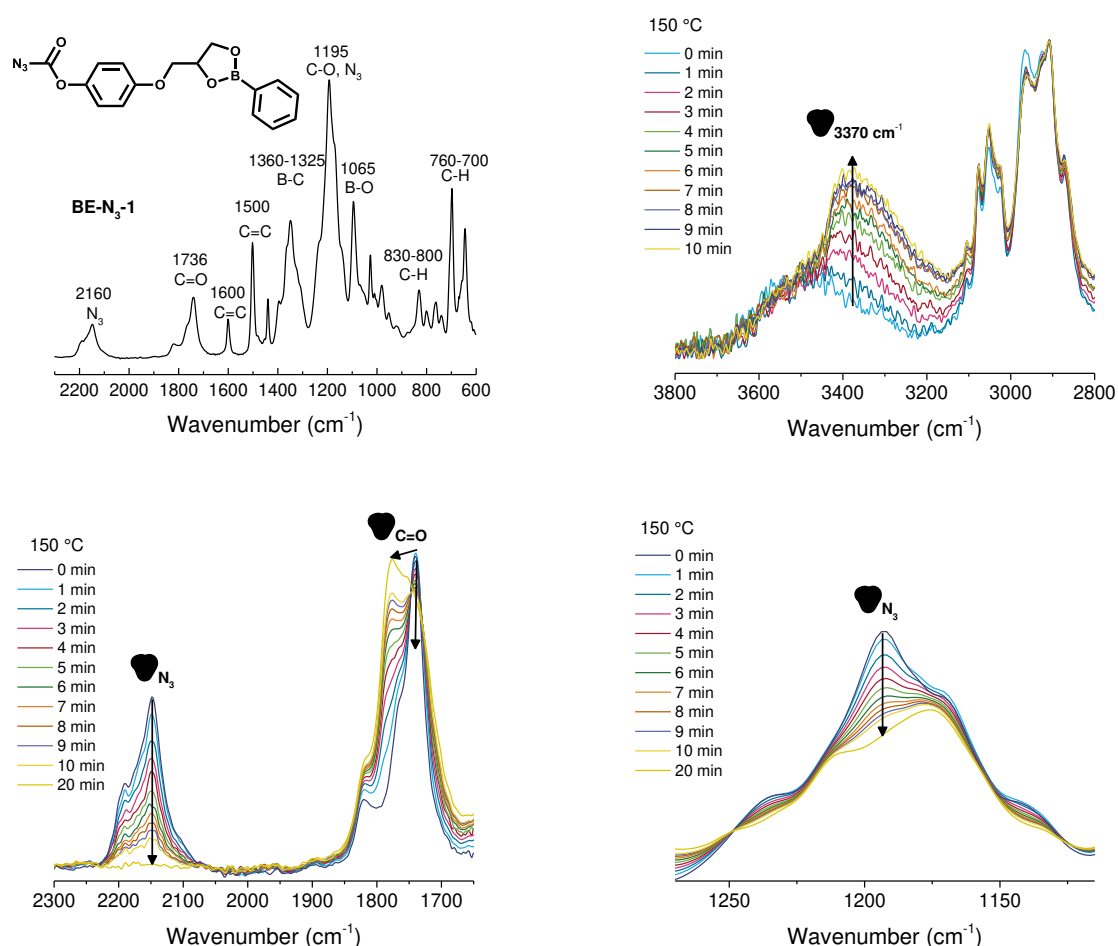
Figure 5.2. FT-IR spectra of **BE-N$_3$-1**. Top left: At 25 °C. Top right: Kinetic data of **BE-N$_3$-**1 at 150 °C in the C-H stretching region. Bottom left: N$_3$ vibration at 2160 cm^{-1} and carbonyl stretching vibration at 1736 cm^{-1} at 150 °C as a function of time. Bottom right: Kinetic data of the stretching vibration of N$_3$ at 1200 cm^{-1} at 150 °C.

At 25 °C, the asymmetric and symmetric stretching frequencies of the azido group are observed at 2160 and 1195 cm^{-1}, respectively.[32] Characteristic peaks reflecting the presence of the five membered boronic ester were also detected; the B-C stretching band at 1353 cm^{-1}, the symmetric stretching of C-O bonds around 1175 cm^{-1} and the symmetric stretching of B-O bonds at 1065 cm^{-1}.[33] Upon heating to 150 °C, both symmetric and asymmetric stretching vibrations of the N$_3$ group decreased with time, and totally disappeared after 20 min. The absence of a new peak around 2260 cm^{-1} proved that no isocyanate was formed during the

azide decomposition, which is consistent with literature data.[30] After 20 min at 150 °C, **BE-N₃-1** exhibits a new broad band at 3370 cm^{-1} corresponding to N-H vibration. This likely reflects the formation of an urethane group through an intramolecular cyclisation, or the intermolecular insertion of nitrenes into C-H bonds (**Scheme 5.6**).
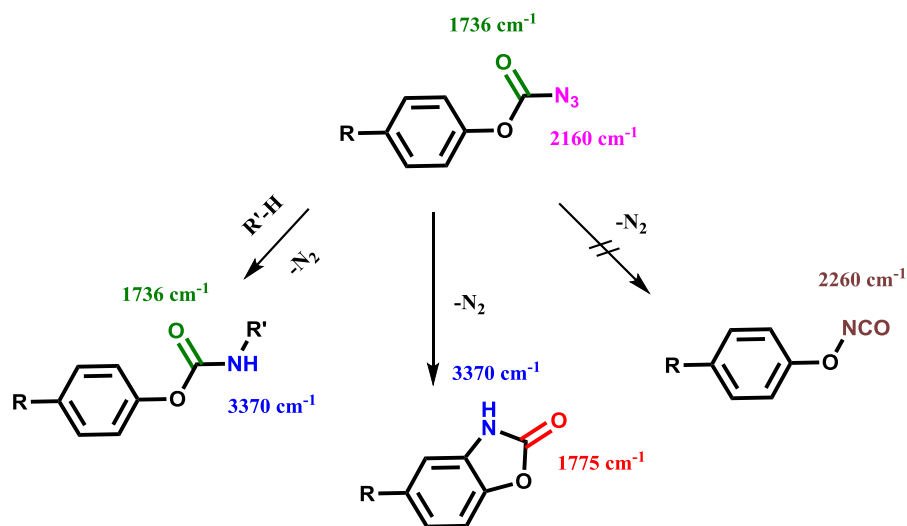
Scheme 5.6. Potential products of the decomposition of **BE-N₃-1**: acyclic urethane (left), 5-membered monocyclic urethane (middle) and isocyanate (right).

At the same time, the band at 1736 cm^{-1}, attributed to the carbonyl vibration, decreased and shifted to higher wavenumber which is consistent with the transformation of the azidoformate into a cyclic urethane (**Scheme 5.6**).[34] The infrared spectra were recorded over more than two hours at 150 °C without any detectable modification, proving that the products of the azide decomposition are stable under these conditions. The reaction was slower than measured by the TGA experiment during which the decomposition was complete within 5 min, while it required more than 10 min according to FT-IR. The inhomogeneous temperature of the FT-IR sample and diffusion effects might be the reason of this discrepancy between these two methods.

5.2.2 Grafting of hydroquinone-based azidoformate BE-N₃-1 onto PI by extrusion

5.2.2.1 Grafting in reactive extrusion

To obtain a vitrimer, moieties that are able to form dynamic cross-links must be introduced. Dynamic covalent bonds were incorporated into polyisoprene using azidoformate **BE-N₃-1**. The considered polyisoprene possesses an vinylene content estimated to be superior to 99%,

according to ^{1}H-NMR spectroscopy. While PI was soluble in THF, its molar mass could not be determined by SEC, as the polymer was of too high molar mass to pass through the 0.2 μm filter.

Reactive extrusion was chosen for the grafting process because of its environmentally friendly characteristics, industrial relevance, and mixing efficiency as compared to compression moulding (**Scheme 5.7**). Different conditions were tested to optimise the grafting.
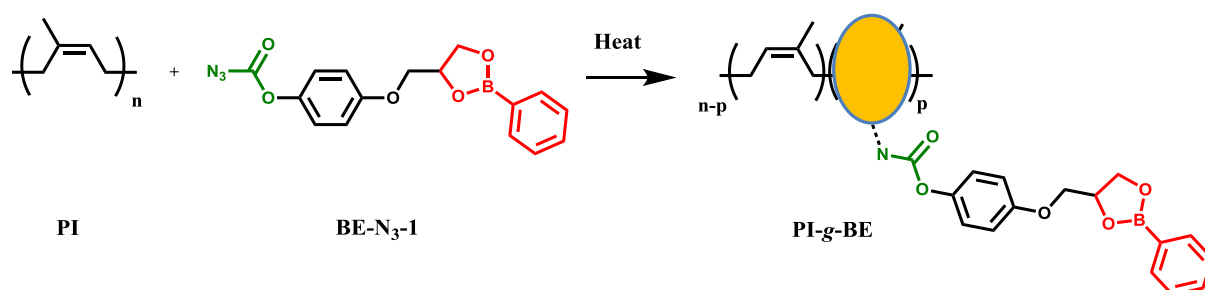
Scheme 5.7. Grafting of **BE-N$_3$-1** onto PI.

Azidoformate **BE-N$_3$-1** was grafted onto PI through reactive extrusion using a DSM Explore batch twin-screw extruder with a 5 cm^3 capacity, equipped with a conical screw profile and a recirculation channel to control the residence time. Mono azidoformate **BE-N$_3$-1** (0.360 g, 12 wt%, 2.7 mol%) was manually mixed with PI (2.60 g), previously cut into small pieces. The mixture was introduced into the barrel at a set temperature (120, 130 or 140 °C) and a screw speed of 100 rpm. Nitrogen flow was used to avoid thermal oxidation of PI. After 30 min at the considered temperature, the polymer was extruded by opening the valve. During the extrusion process, the axial force exerted on the screws by the blending process was recorded. This force depends on the temperature, the mixture composition and on the loading of the barrel. It is an indirect measure of the torque, and thus gives information about the viscosity: the higher the force, the higher the viscosity.

217
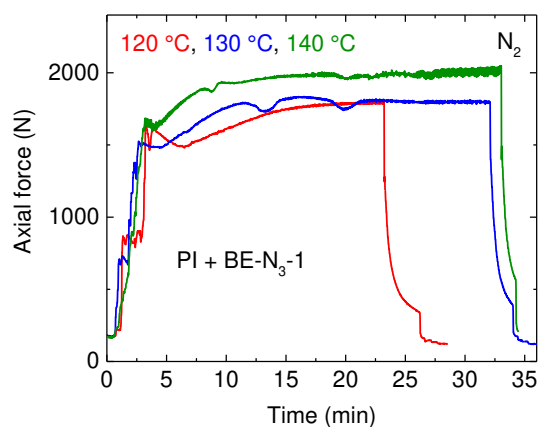
Figure 5.4. Reactive extrusion profiles of PI with 12 wt% (2.7 mol%) of **BE-N$_3$-1** at 120 °C (red), 130 °C (blue) and 140 °C (green) under nitrogen flow.

The **Figure 5.4** displays typical reactive extrusion profiles. In all cases, the measured force increased upon addition of the mixture of PI and **BE-N$_3$-1**. After complete addition, the force slightly decreased because the azidoformate **BE-N$_3$-1** was dispersed in the melt and might act as a plasticizer of the polymeric matrix. After one or two minutes, the axial force started to increase again. The azidoformate **BE-N$_3$-1** began to graft onto PI, modifying the linear polyisoprene into a functional polymer. A plateau regime was then reached, indicating the end of the grafting reaction. The constant regime appeared after 9 min of mixing at 140 °C, which is consistent with thermogravimetric analysis (10 min). However, for the grafting at 130 °C and 120 °C it required only 12 and 17 min, respectively, while the TGA experiments showed a longer decomposition time of 20 and more than 30 min, respectively. This difference may be explained by the high shear stress exercised in the cavity, which does not exist during the static measurement of TGA. Moreover, due to friction, the temperature of the melt may be slightly higher than the measured temperature, as the latter is determined by thermocouple sensors located in the barrel and thereby do not touch the melt. All the samples looked clear or a bit yellowish. As the initial polymer and all grafted PI could not be analysed by SEC measurements, due to their molar masses, solubility tests were performed instead. The samplings were immersed in THF overnight at room temperature and their solubility was then analysed by the naked eye. All these samples were soluble under these conditions.

In order to obtain a control sample, the following experiment was performed. Pure PI was extruded for 40 minutes at 140 °C under nitrogen flow and sampling was conducted (which corresponds to the abrupt drop of the axial force of the blue curve in **Figure 5.5**). The profile was slightly different than the one observed during the grafting of **BE-N$_3$-1**; after the initial increase, the force stabilised around 2400 N. The solubility tests revealed that the polymer became insoluble after 30 minutes of processing. Side reactions occurred in the extruder under these conditions and in proportions that were high enough to lead to a permanent chemical network.
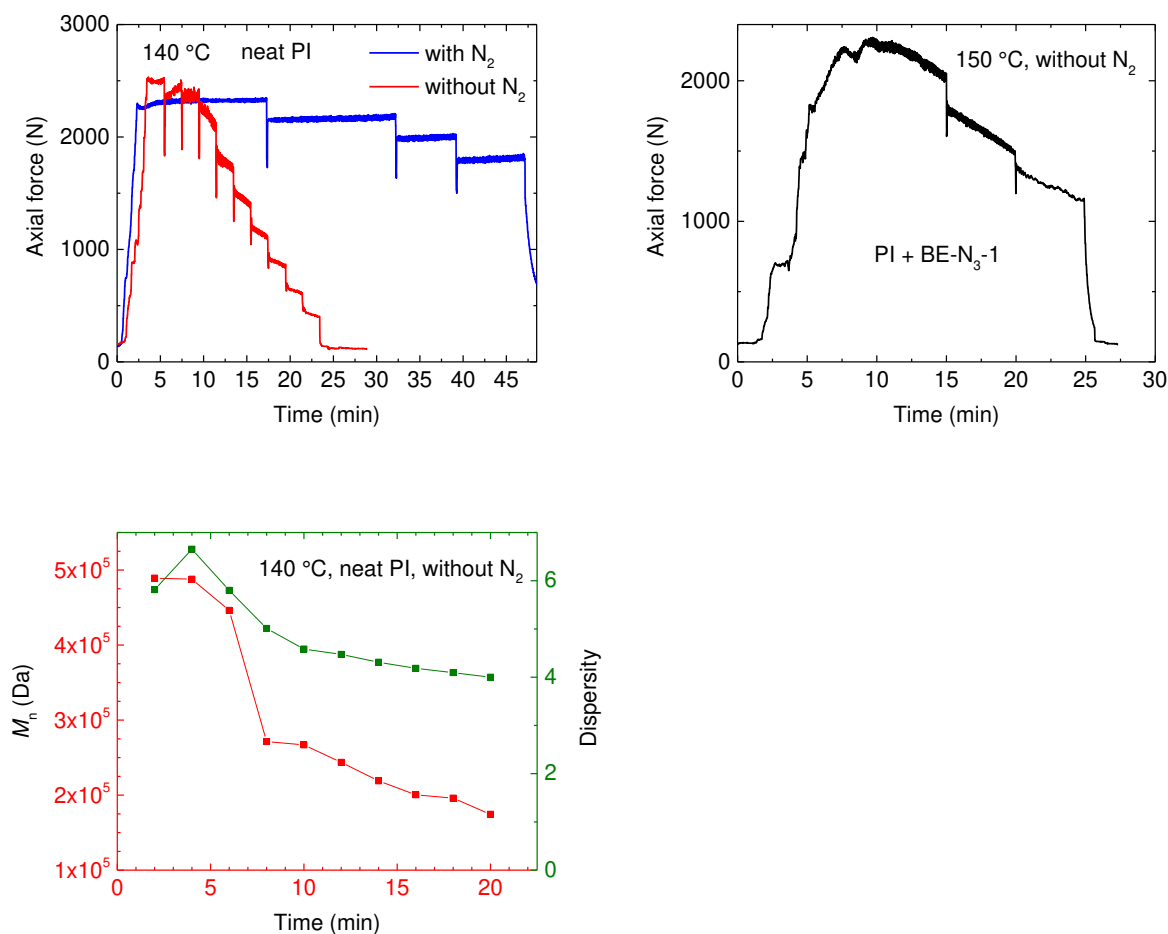
Figure 5.5. Top: Evolution of the force as function of time during extrusion of pure PI at 140 °C with and without N$_2$ flow (top, left) and during reactive extrusion of **BE-N$_3$-1** with PI at 150 °C without nitrogen flow (top, right). The steps observed for the axial force correspond to the samplings of the extruded material. Bottom: Evolution of number average molar mass and dispersity of pure PI extruded at 140 °C without N$_2$ flow.

The influence of the presence of oxygen was then investigated. When nitrogen flow was not used, the extrusion profile was completely different (**Figure 5.5**, red curve). A drastic drop of the force was observed after 10 min of extrusion. Interestingly, the polymer could be analysed by SEC from t = 2 min, which showed that the number average molar mass was following the same trend as the axial force. After a period of constant molar mass, it dropped to reach a pseudo-plateau regime at *ca.* M_n = 200 000 Da and Đ = 4.00. The presence of air combined with high shear strain led to the scission of the long chains into shorter ones, inducing a significant drop of viscosity. In summary, two opposite reactions occurred during the extrusion: static cross-linking and main chain scission. The absence of nitrogen had the same effect on the reactive extrusion with **BE-N$_3$-1** (**Figure 5.5**). Indeed, at 150 °C, the second increase of the force was not observed instead the force dropped drastically. The resulting

product after 20 min of extrusion had a number average molar mass and a dispersity of 202 000 Da and 3.88, respectively.

5.2.2.2 Characterisation of the grafting

The polymers extruded at 120, 130, 140 °C under nitrogen flow and at 150 °C under air, were collected to be analysed by FT-IR and ^{1}H-NMR spectroscopy before and after precipitation in acetone. The precipitation was necessary to remove the non-grafted boronic esters, in order to calculate the grafting efficiency, as well as to properly characterise the boronic ester grafted polyisoprene, **PI-*g*-BE**.

FT-IR analysis was performed to confirm the grafting. The FT-IR spectra of the non-purified blends after different grafting times are overlapped in **Figure 5.6** (top). The zoom around 2160 cm^{-1} shows that the peak of the azide completely disappeared after 13 min at 140 °C. No precipitation was performed before FT-IR analysis. Therefore, this result indicates that under these conditions all the azidoformate was decomposed after 13 min, as indicated by the extrusion profile shown in **Figure 5.4** (green line). This result is consistent with previous TGA experiments.
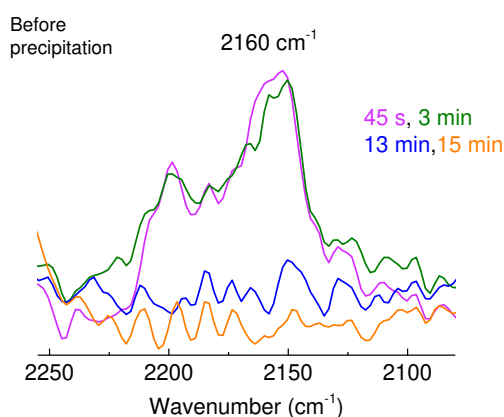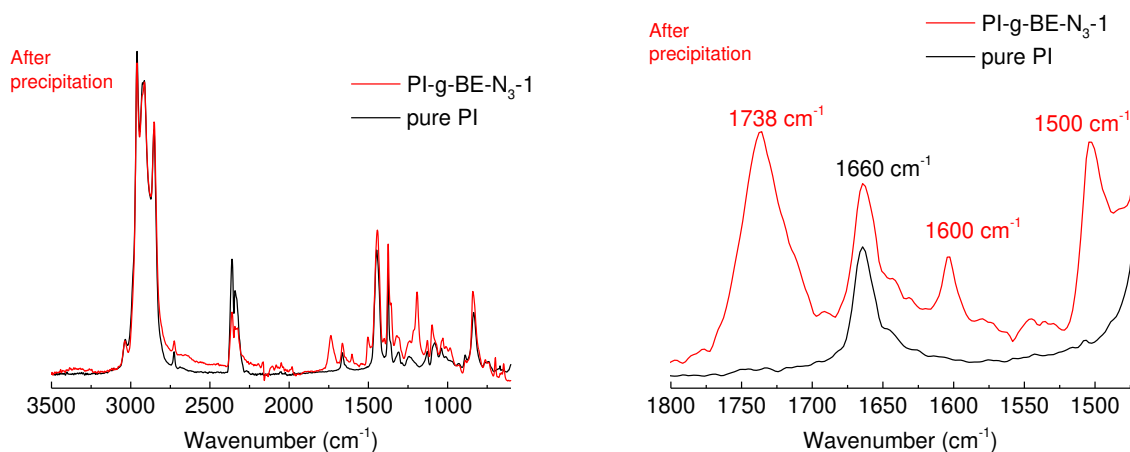
Figure 5.6. FT-IR spectra of the mixture PI + BE-N$_3$-1 after reactive extrusion. Top: At different extrusion times without precipitation prior to analysis; 45 s (pink), 3 min (green), 13 min (blue) and 15 min(orange). Bottom: Comparison of the starting PI (black) with the grafted polyisoprene, **PI-g-BE**, after precipitation (red). Left side: Full spectra. Right side: Zoom in the carbonyl group area.

After precipitation, the presence of a new band at 1738 cm^{-1}was observed on the extruded PI. This band corresponds to the stretching vibrations of the carbonyl moiety, thereby proving the grafting of the azidoformate **BE-N$_3$-1** onto PI (**Figure 5.6**, bottom). Interestingly, the shift of the wavenumber from 1738 to 1775 cm^{-1} was not observed here, unlike previous experiments conducted in the absence of PI. This can be interpreted as a proof of limited intramolecular reaction of the nitrene, due to the presence of polyisoprene and the lower concentration of **BE-N$_3$-1** (12 wt% versus 100 wt%). The urethane formation was confirmed by the presence of a large band at 3370 cm^{-1}, corresponding to the N-H stretching vibration. Two others new bands appeared, at 1600 and 1500 cm^{-1}, characteristic of the carbon-carbon double bonds of the aromatic ring of the dioxaborolane moiety, further confirming the grafting of **BE-N$_3$-1** onto PI. During the grafting, a new weak peak appeared at 1320 cm^{-1}, which might be due to the presence of substituted aziridine compounds.[35] In summary, the proposed reactions between PI and **BE-N$_3$-1** are the C-H insertion and the addition onto carbon-carbon double bonds to form urethane and aziridine moieties, as shown in **Scheme 5.8**.
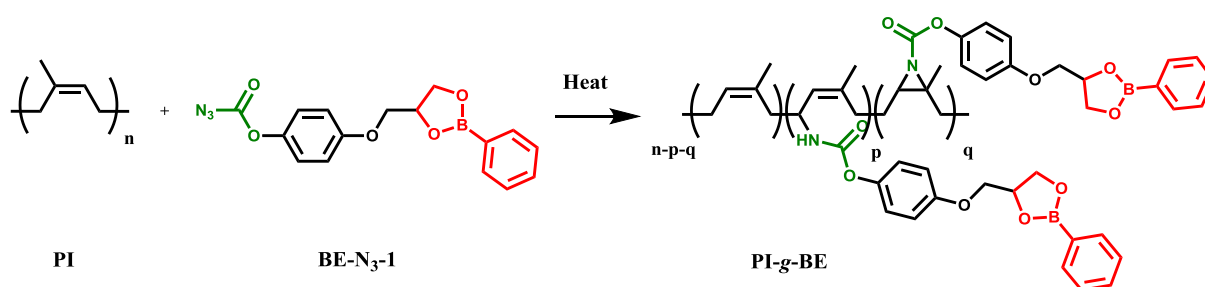
Scheme 5.8. Grafting of **BE-N$_3$-1** onto PI.

221

The functionalization of PI was also studied by ^{1}H-NMR spectroscopy to quantity the grafting efficiency as a function of temperature. To this aim, extruded samples were characterized by ^{1}H NMR before and after purification by precipitation into acetone. A typical spectrum of **BE-N$_3$-1** grafted PI, **PI-*g*-BE-3**, after precipitation is displayed in **Figure 5.7**. The peaks at 7.82, 7.48, 7.38 ppm, characteristic of the phenyl group of the phenylboronic ester, as well as peaks corresponding to the proton of the dioxaborolane ring, at 4.69, 4.52, 4.31 ppm, clearly confirmed the grafting of **BE-N$_3$-1** onto PI. The grafting yields were estimated by the average integration of these protons before and after precipitation. The signal at 5.12 ppm, corresponding to allylic proton of PI, was taken as reference because it should not change through the precipitation step.
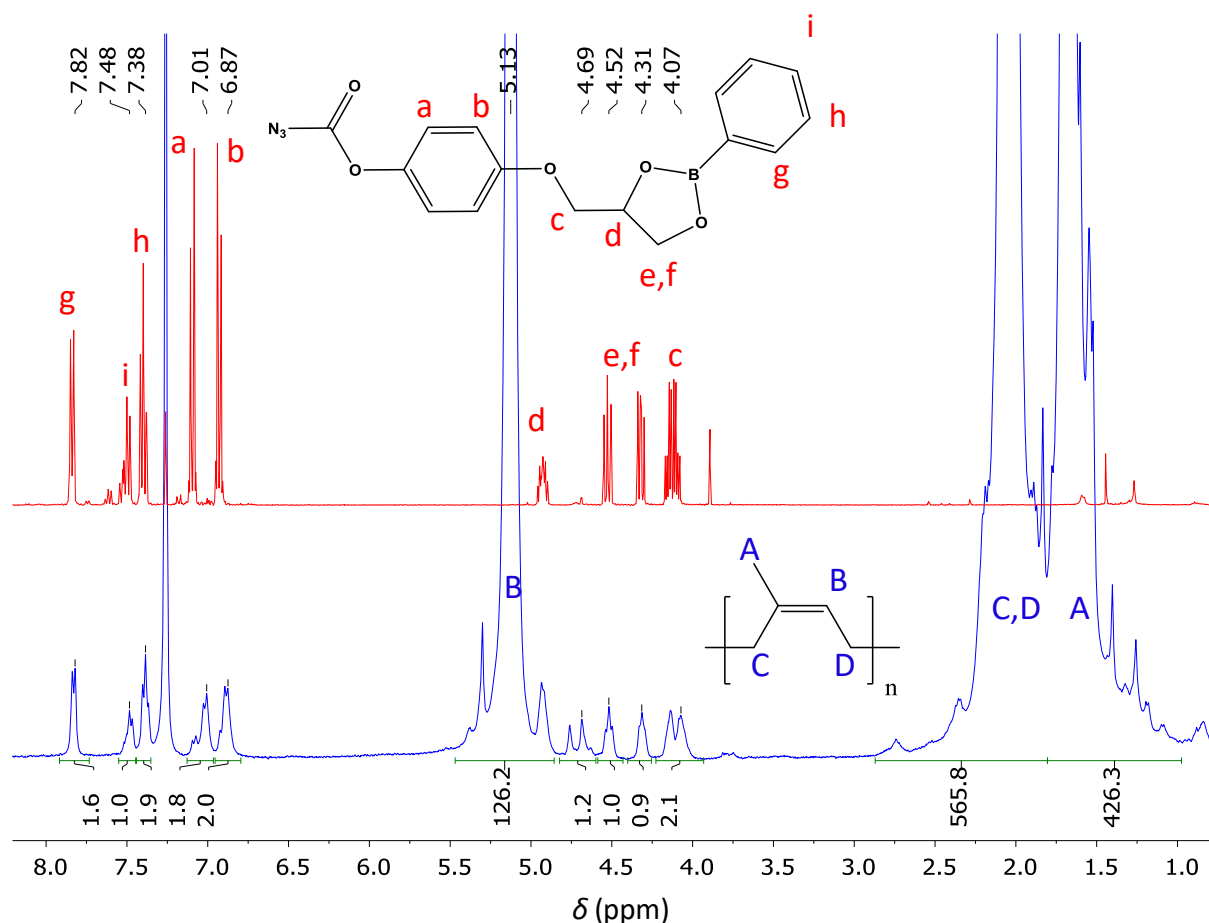

Figure 5.7. ^{1}H-NMR spectra in CDCl$_3$ of **BE-N$_3$-1** (top, red) and **PI-*g*-BE-3** after precipitation (grafting yield = 52%, $f = 0.7\%$) (bottom, blue).

The grafting yields and the functionalization degrees are reported in **Table 5.2**. They were calculated according to the following equations:

Equation 5.1. $f\ (\%) = \dfrac{Integration\ of\ proton\ e}{(Integration\ of\ all\ protons - 14 \times Integration\ of\ proton\ e\ )/8}$

Equations 5.2. $grafting\ yield\ (\%) = \dfrac{Integration\ of\ proton\ e\ after\ precipitation}{Integration\ of\ proton\ e\ before\ precipitation}$

Table 5.2. Characterisation of PI grafted with **BE-N$_3$-1**

Sample	T (°C)	Time (min)	N$_2$ flow	f (%)	Grafting yield (%)	C=C (%)	T_g (°C)	Solubility	M_n (kDa)	$Đ$
Initial PI	-	20	Yes	-	-	99 ± 0.7	-66	100%	-	-
PI-1	140	20	Yes	-	-	-	-65.5	100%	-	-
PI-2	140	30	Yes	-	-	-	-65.4	50%	-	-
PI-3	140	20	No	-	-	-	-	100%	174	4.00
PI-*g*-BE-1	120	20	Yes	0.4	31 ± 2.5	88 ± 0.5	-63.5	100%	-	-
PI-*g*-BE-2	130	30	Yes	0.7	48 ± 1.6	88 ± 0.8	-62.3	100%	-	-
PI-*g*-BE-3	140	30	Yes	0.7	52 ± 1.5	89 ± 0.2	-64.2	100%	-	-
PI-*g*-BE-4	150	20	No	0.6	50 ± 0.9	89 ± 1.2	-62.3	100%	202	3.88

Grafting yields were moderate. They slightly increased with temperature, going from 38 to 52% with temperature increasing from 120 to 140 °C, respectively. Interestingly, the sum of functionalization degree + the vinylene content gave some information about the modification of PI. The grafting can occur through two different mechanisms: C-H insertion or addition onto the carbon-carbon double bond. The former mechanism should not change the vinylene content, as the insertion takes place on the allylic carbon, while the latter mechanism should decrease the vinylene amount. The quantity of **BE-N$_3$-1** mixed with PI was too low to be solely responsible of the observed decrease of the vinylene content. Indeed, the percentage of vinylene bonds decreased from 99 to 88%, while the functionalization degree was not higher than 0.7 % for all the temperatures tested. Consequently, the majority of the vinylene bonds that disappeared during the grafting were not involved in the grafting reaction. They reacted with radical species generated during the extrusion that led to radical cross-linking and chain scission. These vinylene bonds were less affected by the quantity of azides incorporated than

by the temperature or the extrusion process. The targeted functionalization degree of 2.2 mol% was not achieved because of moderate yields of the grafting. Furthermore important loss of **BE-N₃-1** (*ca.* 40 wt%) were observed during the introduction of the mixture into the extruder because the azide is very viscous and glues to the walls of the hopper.

The absence of nitrogen flow at 150 °C did not affect the vinylene content (88%) nor the grafting efficiency (50%), but the sample looked dark brown for **PI-*g*-BE-4** or yellow for neat PI after extrusions, as well as softer and more viscous than the starting material in both cases. Therefore, chain scission was clearly significant under these conditions. The grafting method proposed here is an efficient and easy bulk process (*i.e.* solvent free), which allows transforming polymers during their (industrially relevant) processing.

The impact of the grafting yield on the T_g of the PI was investigated by DSC. The DSC curves of neat PI and modified **PI-*g*-BE-3** are displayed in **Figure 5.8**. The T_g did not increase significantly with the functionalisation degree, going from -65.4 °C for neat PI to -63.5 °C for $f = 0.7$ %. This low degree of functionalization did not alter the glass transition of the PI, which means that the elastomeric properties of the material are conserved during the chemical modification with the azidoformate **BE-N₃-1**.
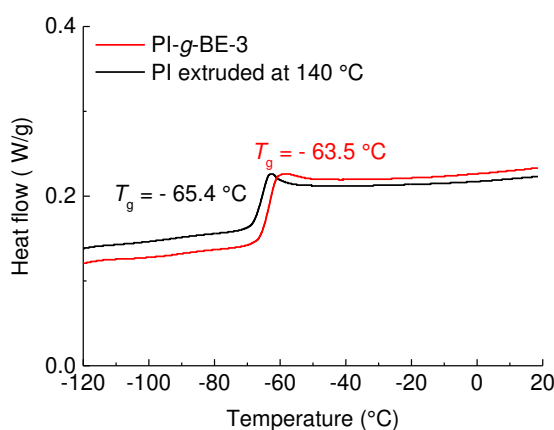
Figure 5.8. DSC curves of grafted **PI-*g*-BE-3** (red) and the polyisoprene precursor after extrusion 30 min at 140 °C under N₂ (black).

5.2.3 Grafting of azidoformate BE-N₃-1 onto polybutadiene

The functionalization of a commercial polybutadiene (PB-CB-24) (vinyl content inferior to 2 mol %, $M_n = 400$ kg/mol, $Đ = 1.78$) was also conducted with **BE-N₃-1**. All attempts resulted in materials cross-linked with non-dynamic bonds (**Scheme 5.9**).
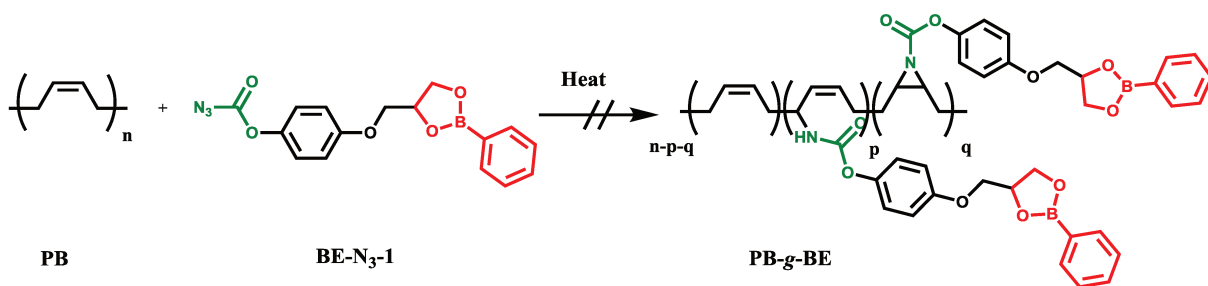
Scheme 5.9. Grafting of **BE-N$_3$-1** onto PB led to a permanently cross-linked network.

Reactive extrusions using the protocols described for PI were performed. Compounds ratios PI/**BE-N$_3$-1** of 100/2 and 100/1 were tested with sampling at fixed intervals. Other tests at lower temperatures (100 °C, 110 °C) were also attempted. All reactions led to cross-linked networks after 7 min of reaction or less. These materials did not dissolve after addition of THF but swelled. No further characterisation was conducted on these systems.

5.2.4 Cross-linking of PI in extrusion with the bis-azidoformate dioxaborolane Bis-BE-N$_3$-1

5.2.4.1 Reactive extrusion

As the mono azidoformate **BE-N$_3$-1** was successfully grafted onto PI, the vitrimer synthesis was considered, using a bis-azidoformate (**Scheme 5.10**). The cross-linking density was tuned by adjusting the amount of cross-linker incorporated.
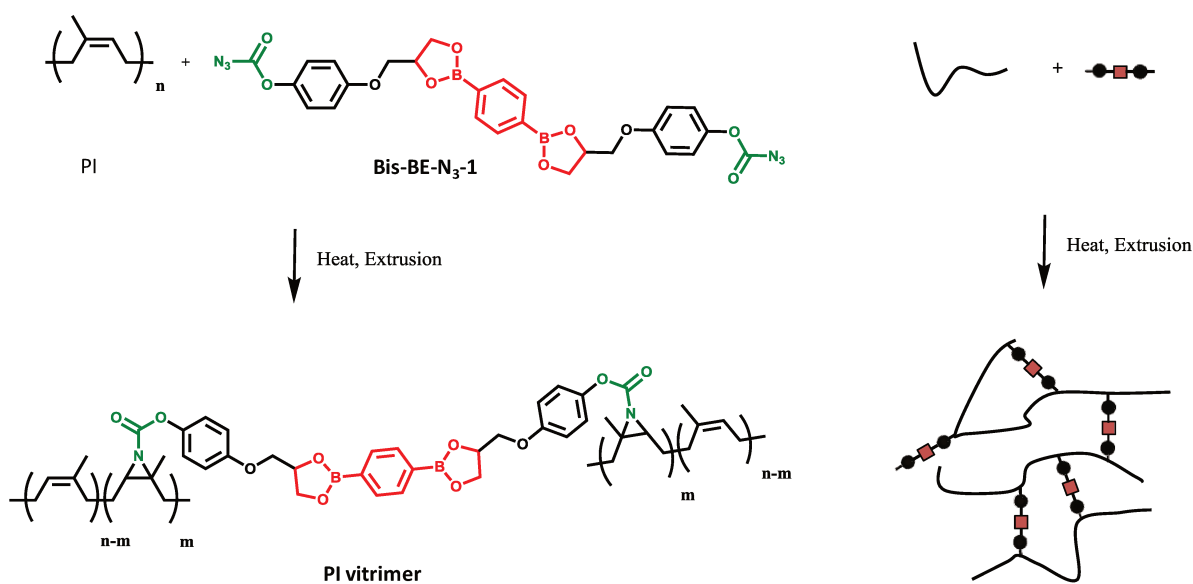
Scheme 5.10. Synthesis of PI vitrimer by reactive extrusion of PI with **Bis-BE-N$_3$-1**.

225

The cross-linking reaction was performed at 140 °C to synthesise vitrimer from **Bis-BE-N$_3$-1** following the same protocol as for the experiments with **BE-N$_3$-1**. The axial force exhibited a maximum within less than two minutes after complete addition of the mixture (**Figure 5.9**).
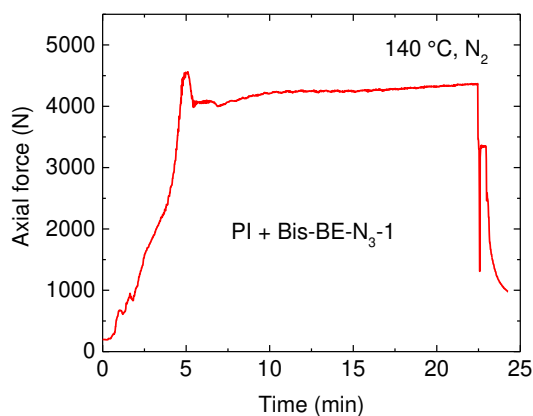
Figure 5.9. Extrusion profile of the cross-linking reaction of PI using **Bis-BE-N$_3$-1** at 140 °C under nitrogen flow.

The drop of the force was observed directly after the maximum was reached then the force showed a constant regime. This drop was interpreted as a wall slip due to the solid like behaviour of the new material. The system was so elastic that it could not really flow out of the extruder when the valve was opened. Moreover, the appearance of the network was not homogenous at all, revealing a macrophase separation of the cross-linker into the polymeric matrix.

5.2.4.2 Swelling tests

However, the materials were analysed to assess their cross-linked and dynamic behaviour. Usually, cured rubbers exhibit good solvent resistance and do not dissolve in good solvents of the constituting polymer chains, while the linear precursors normally dissolve in these solvents.

The samples (typically, with an initial mass of 200 mg) were immersed in dried THF (typically 15 mL) at room temperature and weighed after 24 h (mass of the swollen sample). Then, the samples were dried under vacuum at 120 °C until complete dryness and weighed again (mass of the dried sample). The insoluble fractions and the swelling ratios were calculated as follow:

Equation 5.3.
$$Insoluble\ fraction = \frac{Mass\ dried}{Initial\ Mass}$$

Equation 5.4.
$$Swelling\ ratio = \frac{Mass\ swollen - Mass\ dried}{Mass\ dried}$$

For vitrimers **PI-BE-V1, PI-BE-V2 and PI-BE-V3**, the insoluble fraction was rather high, 99, 94 and 87 wt% respectively, while the pure PI completely dissolves within 2 hours, showing the cross-linked nature of these systems (**Table 5.3**). Despite low soluble fractions, the swelling ratios were high, which is consistent with the low cross-linking of high molar mass polymer.

Table 5.3. Characterisation of the solvent resistance of vitrimers

Vitrimer	Temperature	Cross-linker (mol%)	Insolubility in THF (wt%)	Insolubility after diolysis (wt%)	Swelling ratio
PI-BE-V1	140 °C	1.1	99	0	7
PI-BE-V2	140 °C	0.56	94	0	11
PI-BE-V3	115, 140 °C	0.42	87	0	13
PI-BE-V4	140 °C	0.15	0	0	-

PI-BE-V4 with 0.15 mol% of bis-azidoformate did not reach the gel point, due to insufficient cross-link density. Assuming molecular weight around 400 000 g/mol and a grafting efficiency of 50%, this density should be around 1 per 1000 repetition units, which gives 7 cross-links per chain. This should be enough to create a percolated network with homogeneously distributed cross-links. However, as mentioned in the previous section, a phase separation occurred, which likely resulted in an inhomogeneous distribution of the cross-linker.

227

5.2.4.3 Selective de-cross-linking of the vitrimers by diolysis

In order to prove that the vitrimers were cross-linked by dynamic dioxaborolane bridges, the networks were swollen in THF and cleaved with an excess of 1,2-propanediol, as compared to **Bis-BE-N$_3$-1**.

The samples (initial mass: 100−250 mg polymer, n equiv. of dioxaborolane functions) were immersed in THF at room temperature and 1,2-propanediol (50−150 × n) was added. After 4 h of immersion at room temperature, all vitrimers completely dissolved (**Table 5.3**). The cleaved networks were then precipitated in acetone to recover the thermoplastic precursors. However, the diolysed vitrimers could not be analysed by SEC, as it was the case after the grafting of **BE-N$_3$-1** under nitrogen flow. Nevertheless, they were analysed by ^{1}H-NMR spectroscopy, as shown in **Figure 5.10** in the case of **PI-BE-V1**.
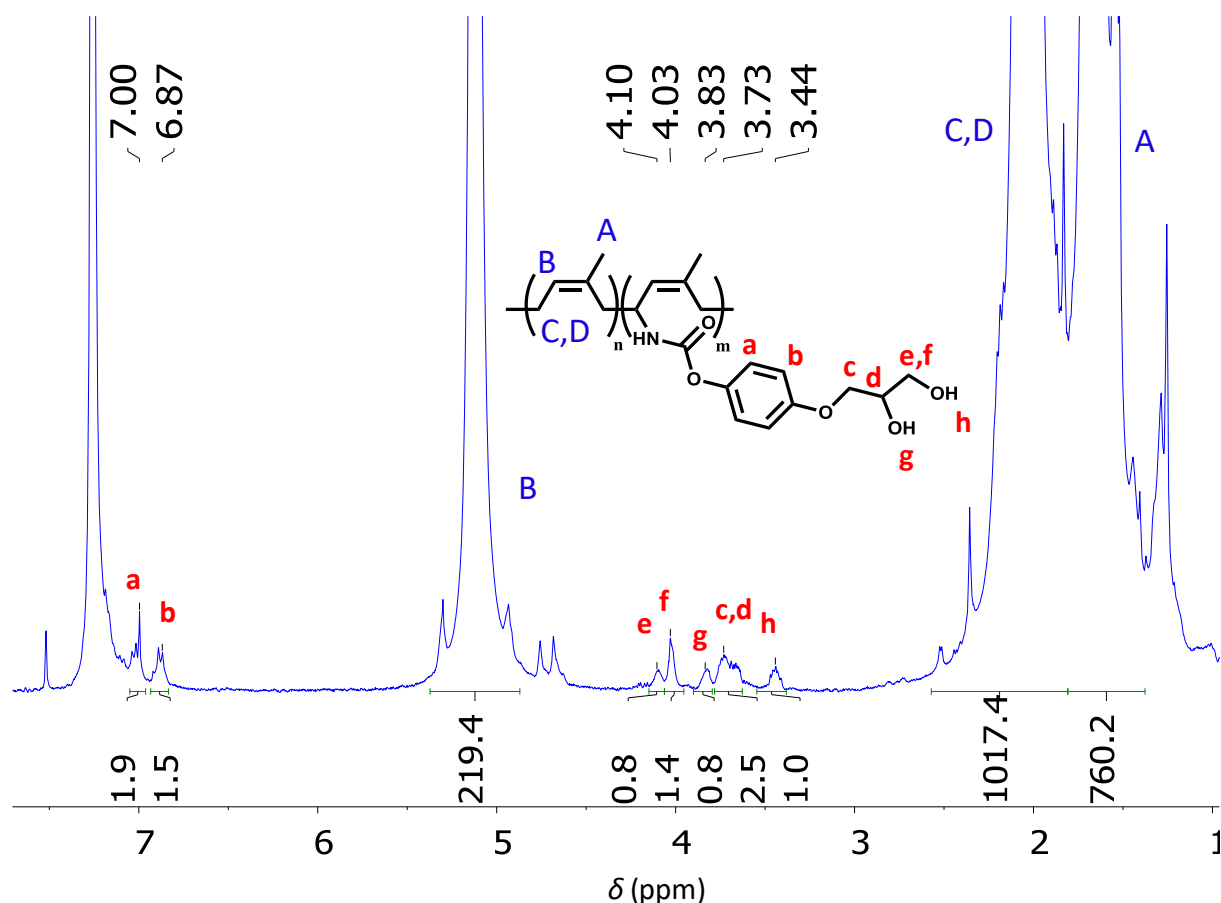

Figure 5.10. ^{1}H NMR spectrum in CDCl$_3$ of **PI-BE-V1** cleaved by diolysis and precipitated in acetone.

The integration of aliphatic protons from the attached diol allowed estimating the functionalisation degree and the grafting yield. They were calculated to be 0.46% and 54%,

228

respectively. The reference could not be taken by the value before diolysis/precipitation as it was still a network. Therefore, the reference was taken by the amount of cross-linker used for the reaction. As the cross-linker is a solid, very low losses were observed during the introduction of the mixture into the extruder. Interestingly, the grafting efficiency was similar to that of mono azide **BE-N$_3$-1**. Consequently, the macrophase separation observed in the final material did not seem to affect the grafting efficiency.

5.2.4.4 Stress relaxation

Conventionally cross-linked elastomers can neither flow nor relax stress, they have a solid-like behaviour regardless of the temperature. Unlike them, vitrimers can flow thanks to chemical exchange reactions taking place within the network. As a result, they can be processed and recycled while being permanently cross-linked. The dynamics of exchange within vitrimer networks depend on the rate constant of the chemical exchange reaction, as well as the concentration and the mobility of the chemical species involved in the exchange reaction. Therefore, for a given exchange reaction and a given thermoplastic precursor, rheological properties of vitrimers, such as viscosity, creep-recovery and relaxation times will depend on the cross-linking density, the concentration of pendant exchangeable groups (if present), and the temperature. In this section, vitrimer properties such as relaxation behaviour, viscosity and creep were measured. All the materials were analysed on an ARES G2 from TA Instruments in plate-plate geometry, using plates of 25 mm diameter in a convection oven. Samples were moulded into disc shapes at 150 °C for 30 minutes and placed in the preheated geometry under air. After 10 minutes of equilibration, the experiment was started.

Stress relaxation experiments were conducted by applying a constant shear strain of 1% and monitoring the stress applied by the rheometer to hold the sample at this strain. **Figure 5.11** shows that the two vitrimers tested, **PI-BE-V1** and **PI-BE-V2**, relax stresses but not completely, at least over the timescale of the experiment. The relaxation of pure PI is presented for comparison.
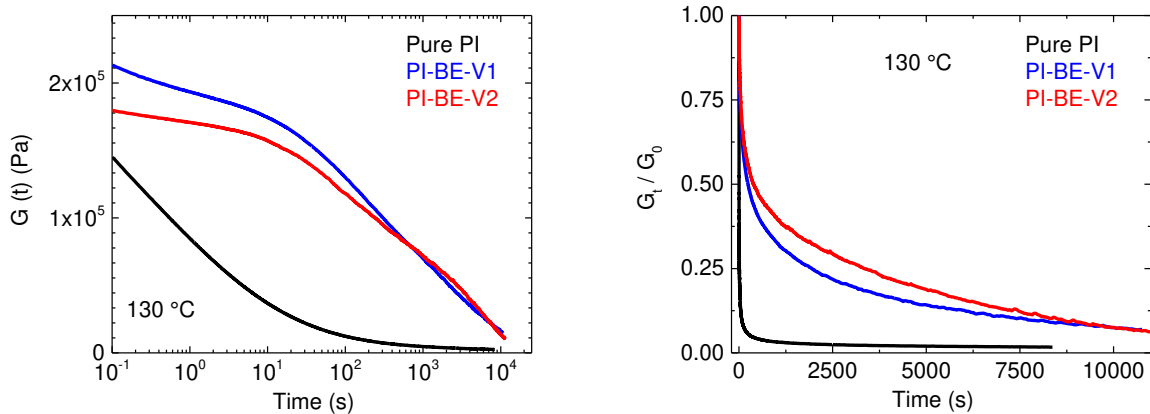
Figure 5.11. Left side: Stress relaxation curves of PI, **PI-BE-V1** and **PI-BE-V2** at 130 °C. Right side: Normalized relaxation curves of PI, **PI-BE-V1** and **PI-BE-V2** at 130 °C.

They have respectively still 6.9% and 5.7% of residual stresses after 10 700 s (2h58min) while the neat PI did not relax 1.6% for the same time. This result means that these systems require very long times to relax the stresses, in particular because of entanglements and the very low concentration of exchangeable cross-links. Thus, the full relaxation was not achieved during these experiments. Consequently, the previous equations used in chapter 3 and 5 to determine the characteristic relaxation times and zero shear viscosities are not valid in this case. This would lead to underestimate these key parameters. To give an estimation for these characteristic values, a mono exponential model was used with only one relaxation time τ which equals the relaxation of *ca.* 36.8% residual stress.

Equation 5.5.
$$G_{(t)} = G_{(0)} \, e^{-\frac{t}{\tau}}$$

Vitrimers exhibited at least two regimes of relaxation. The first regime corresponds to the relaxation of dangling chains and chain segments between cross-links. Then, the systems relax through covalent bond exchanges between the cross-links. The multi modal behaviour is marked by the relaxation of entanglement which slows down the overall relaxation process. The initial modulus is proportional to the cross-link density with 213 300 Pa for **PI-BE-V1** and 179 600 Pa for **PI-BE-V2**. The more cross-linked material relaxed faster than the less cross-linked system. Indeed, **PI-BE-V1** relaxed 63% of initial stress at 130 °C in 710 seconds, while it required 1350 seconds for **PI-BE-V2** to reach the same value. These results reflect the higher probability of exchange in the more cross-linked vitrimer, keeping in mind the very low cross-linking density of these vitrimers and the absence of pendant exchangeable groups.

From the characteristic relaxation times and the initial moduli, viscosities were calculated according to the following equation:

Equation 5.6.
$$\eta = G_{(0)} \times \tau$$

PI was found to have a viscosity $\eta = 5.8 \times 10^5$ Pa.s at 130 °C, which is close to literature values at low shear rates,[36] while **PI-BE-V1** and **PI-BE-V2** have viscosities as high as 1.5×10^8 Pa.s and 2.4×10^8 Pa.s at 130 °C.

5.2.4.5 Creep-recovery

Cross-linking should impart creep resistance to the elastomer as it gives dimensional stability. At the same time, this resistance highly depends on the rate of exchange of the dynamic cross-links in the vitrimer network. To check this behaviour step-stress elongational creep-recovery experiments were performed at 25 °C, 80 °C and 150 °C. A stress of 10 000 Pa was applied for 30 min then released for 20 min. The systems elongation was followed by using TA Instruments Q800. The results are display in **Figure 5.12**.
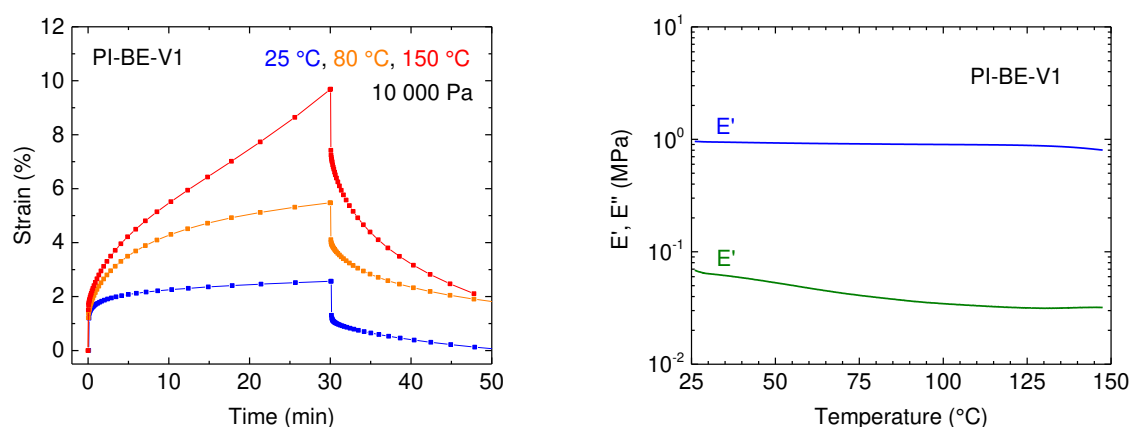
Figure 5.12. Left side: Creep-recovery experiments under a load of 10 000 Pa for 30 min followed by 20 min of recovery at different temperatures: 25 °C (blue), 80 °C (orange) and 150 °C (red) for **PI-BE-V1**. Right side: Dynamic mechanical analysis of **PI-BE-V1** between 25 and 150 °C.

Upon the application of an axial stress of 10 000 Pa, **PI-BE-V1** deformed of 1.2% at all the temperatures tested, which corresponds to an elastic modulus of 0.8 MPa and is consistent with the modulus measured by DMA. At 25 °C, the vitrimer exhibits a maximum deformation

of 2.6% and then shows a residual deformation as low as 0.03% but its behaviour at higher temperature is very different. At 80 °C, the vitrimer deforms much more and faster. This is due to the rearrangement of the network allowed by the exchange reaction between dynamic boronic ester cross-links, which is accelerated by the temperature. At 80 °C, the slope decreases with time to reach a steady state regime. At 150 °C, the slope increases with time because the applied stress is perhaps too important; the system might be outside of its linear regime. After 20 min of recovery, the strain is still decreasing, showing that the new equilibrium was not yet reached. In summary, it seems possible to activate the exchange reaction and thus the rearrangement of the network by heating, and freeze the topological reorganisation by cooling.

5.2.3.6 Tensile tests and recycling

Mechanical testing and recycling experiments were conducted to test the mechanical properties and re-processability of the vitrimers. Uniaxial tensile tests were performed on dumbbell-shaped specimens (gauge length 10 mm) using an Instron 5564 tensile machine mounted with a 100 N cell. The specimens were tested at a fixed cross-head speed of 10 mm/min. Testing was carried out at room temperature for all materials. Engineering stress−strain curves were obtained through measurements of the tensile force F and cross-head displacement Δl by defining the engineering stress as $\sigma = F/S_0$ and the strain as $\gamma = \Delta l/l_0$, where S_0 and l_0 are the initial cross section and gauge length of the specimens, respectively. The Young's modulus was determined according to the Mooney-Rivlin equation (see appendix for details). Following tensile testing, the vitrimer specimens were cut down to small fragments and reshaped via compression moulding for 30 min at 150 °C under a load of 3 tons in order to test their recyclability over several reprocessing cycles. Tensile tests were repeated at room temperature for each generation. The results are display in **Figure 5.13**.
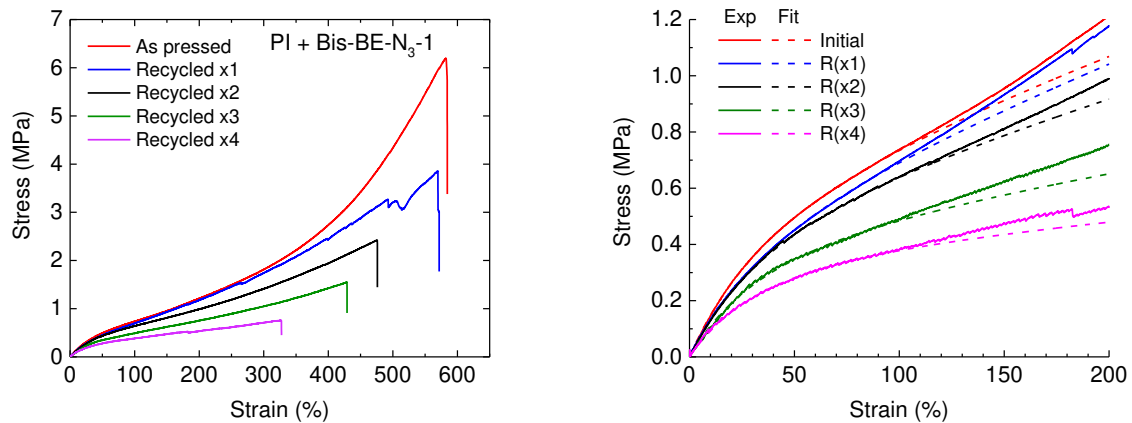
Figure 5.13. Left: Tensile stress-strain curves at 25 °C for initial and recycled (up to 4 times) **PI-BE-V1**. Right: Experimental data (solid lines) overlapped with Mooney-Rivlin fits (dashed lines).

All the characteristic mechanical properties decreased with reprocessing cycles: stress at break decreased from 6.2 to 0.8 MPa, and elongation at break from 584 to 327% after four recycling cycles. The decrease of the Young's modulus from 1.7 to 1.1 MPa shows that the cross-linking degree of the network falls. The systems cannot support such processing conditions. This drop of tensile properties reveals the poor recyclability of the considered systems by a thermo-mechanical process. Further experiments needs to be performed to verify the stability of the neat PI under these reprocessing conditions.

5.3 Allylphenol based azidoformate

5.3.1 Synthesis

As mentioned in the previous section, the polarity of the cross-linker **Bis-BE-N₃-1** was too high to be perfectly soluble and well dispersed into the apolar polyisoprene matrix. To overcome this phase separation issue, a new molecule, **BE-N₃-2**, was designed with three carbons added in comparison to **Bis-BE-N₃-1**. The low overall yield of the synthesis of **BE-N₃-1**, only 3.9 %, was due to the first step because of the symmetric nature of hydroquinone. Thus, mono and difunctional products were formed. Consequently, it was chosen to change the starting material to an asymmetric difunctional molecule. The commercially available allyphenol also is a good candidate. Although the new synthesis pathway required 5 steps, versus 4 steps for the previous cross-linker, the overall yield of the synthesis of **BE-N₃-2** reached 27 %, which corresponds to an average yield per step of 77% (**Scheme 5.11**).
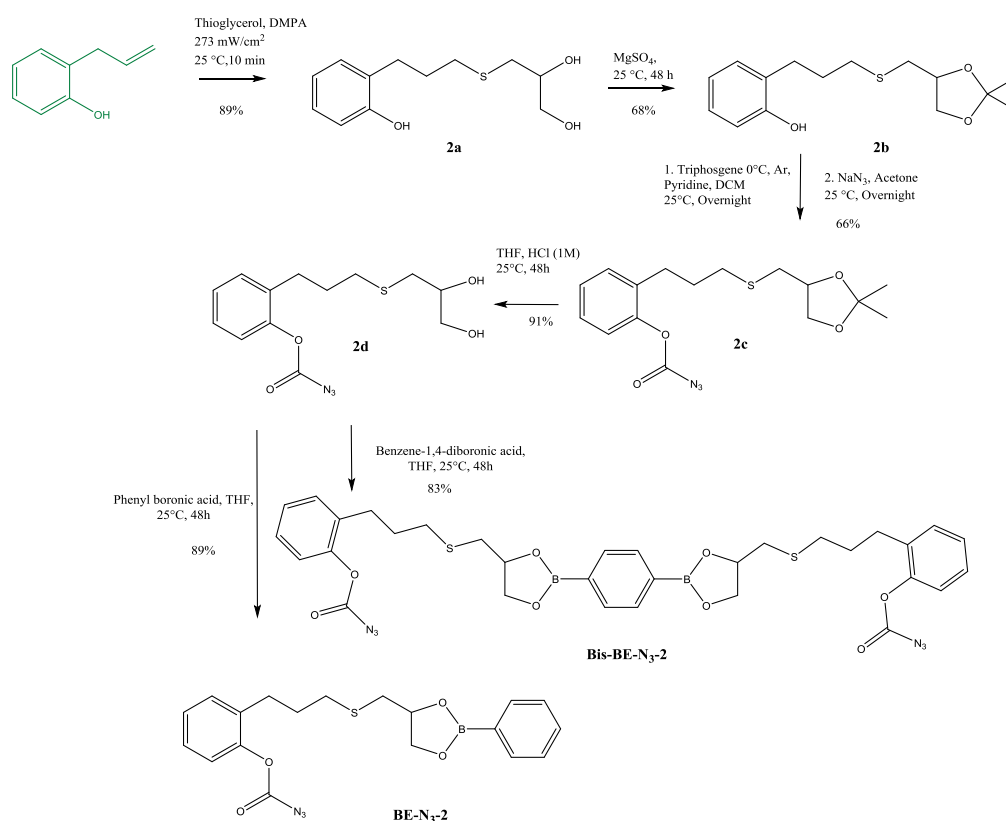
Scheme 5.11. Synthesis of **BE-N₃-2** and **Bis-BE-N₃-**2 from 2-allylphenol, a mono azidoformate dioxaborolane and a bis-azidoformate dioxaborolane, respectively.

As shown in **Figure 5.14**, **Bis-BE-N₃-1** starts to melt at 100 °C and ends at 130 °C while the azide decomposition begins at 120 °C. The cross-linker cannot diffuse totally into the polymer before it melts. As decomposition and melting proceed in the same range of temperature, **Bis-**

BE-N$_3$-1 melts and starts to react before being well mixed with PI, resulting in a macro phase separation visible with the naked eye. Unlike hydroquinone based cross-linker, **Bis-BE-N$_3$-2** did not exhibit any melting peak, which may improve its dispersion into PI. Its decomposition profile was shown to be similar to **Bis-BE-N$_3$-1** (Appendix, **Figure 5.21**).
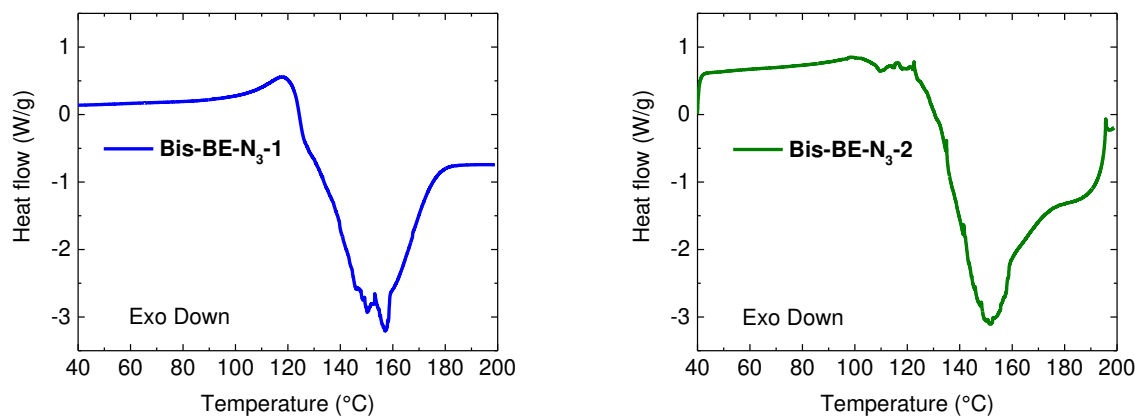
Figure 5.14. DSC curves of **Bis-BE-N$_3$-1** (left, blue) and **Bis-BE-N$_3$-2** (right, green).

5.3.2 Grafting of the allylphenol-based azidoformate dioxaborolanes onto PI by extrusion

Bis-BE-N$_3$-2 (1.1 mol%) cross-linked successfully PI by reactive extrusion at 140 °C for 20 minutes and no macrophase separation was visible. However, the obtained network could not be cleaved by the addition of an excess of 1,2-propanediol in THF, even with 150 equivalents of diols and stirring for 72 hours at room temperature. This is characteristic of conventional curing with static cross-links. The system cannot rearrange and behaves then like a classical chemically cross-linked rubber.

The grafting of the azidoformate dioxaborolane **BE-N$_3$-2** was also performed by reactive extrusion following the same procedure as for mono azide **BE-N$_3$-1**. **BE-N$_3$-2** (0.34 g, 2.2 mol%, 11.5 wt%,) was mixed with PI (2.70 g, 39 mmol), the mixture was extruded at 140 °C for 20 minutes under nitrogen flow. The resulting polymer could not be dissolved after one week in THF at 25 °C. The amount of **BE-N$_3$-2** was decreased to 1.1 and 0.5 mol%, but in all cases the reaction led to static cross-linked networks. Therefore, this molecule was not used anymore. The presence of sulphur atoms may be the reason of these side reactions; promoting intersystem crossing of the nitrene into its triplet state and thus stimulating radical coupling reactions.[37]

235

5.4 Eugenol-based azidoformate

5.4.1 Synthesis

New mono and bis-azidoformate dioxaborolane compounds that did not contain any sulphur atom, **BE-N$_3$-3** and **Bis-BE-N$_3$-3**, respectively, were synthesised starting from eugenol. The general route of synthesis contains 7 steps, thus 3 more than for **BE-N$_3$-1** Bis-BE-N$_3$-1, but the overall yield reached 14% and thus is 3.5 times higher than the ones of the hydroquinone based azidoformates (**Scheme 5.12**). The average yield per step of these syntheses is 75.5%.
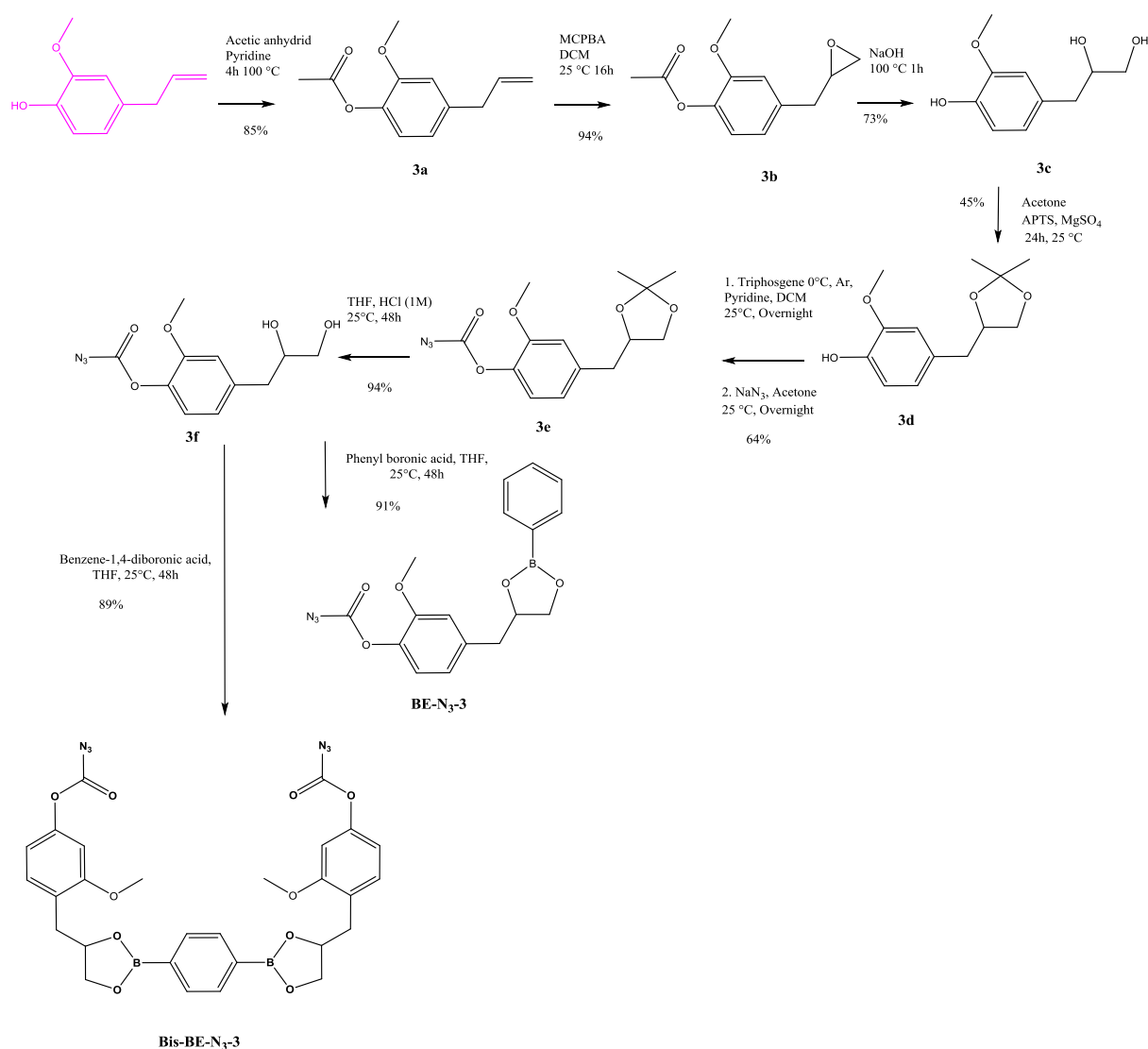
Scheme 5.12. Synthesis of **BE-N$_3$-3** and **Bis-BE-N$_3$-3** from eugenol, a mono azidoformate dioxaborolane and a bis-azidoformate dioxaborolane, respectively.

5.4.2 Grafting of the eugenol-based mono azidoformate dioxaborolane by extrusion and compression moulding

The kinetic of the grafting reaction of the mono azidoformate dioxaborolane **BE-N₃-3** on PI were followed. Two different processes were compared for the grafting reaction: extrusion and compression moulding.

With the aim to determine the effect of the grafting onto the molar mass distribution, PI was extruded 10 min at 140 °C in the presence of oxygen. The resulting material had a $M_n = 225$ kDa and a $Đ = 2.61$, as indicated by SEC analysis. It was then used instead of the initial PI.

In order to avoid significant losses on the extruder walls (due to the viscosity of the azide) and to obtain a homogenous grafting with the press, the mono azidoformate dioxaborolane **BE-N₃-3** (0.193 g, 0.5 mol%, 5.5 wt%) and pre-extruded PI (3.30 g, 50 mmol) were dissolved in dried THF. The two solutions were mixed before evaporating the solvent under reduced pressure. In extrusion, the procedure previously described for the grafting of **BE-N₃-1** was followed. Except that at fixed intervals, 0.100 g of the mixture was extruded by opening the valve letting the rest of the mixture still reacting until the reaction was stopped after 90 min. For the compression moulding, similar sampling was not possible, as it would require opening the press during the experiment and thus, drastic temperature variation would be unavoidable, potentially altering the grafting reaction. Therefore, the same batch was used for the kinetic study under press but they were as many experiments as the number of samplings.

After the reaction, all the samples were dissolved in THF and precipitated in dried acetone to remove the non-grafted boronic esters. The precipitated samples were subsequently dried under vacuum and analysed by ^{1}H-NMR spectroscopy and SEC analysis.

Regardless of the processing, extrusion or compression moulding, the characteristic peaks of **BE-N₃-3** were detected after purification of the polymer by precipitation (**Figure 5.15**). Aromatic peaks were observed on the precipitated polymer, at 7.79, 7,47, 7,37 ppm for the phenyl group of the phenylboronic ester and at 7.01, and 6.81 ppm for the benzene ring of the eugenol part. Aliphatic peaks from **BE-N₃-3** were also detected at 4.37, 4.06, 3.05 and 2.87 ppm, which reveals that the grafting was effective. All the integrations match pretty well proving that the integrity of **BE-N₃-3** was not altered during the grafting or the precipitation, in particular the boronic ester was not hydrolysed.

A new peak was detected at 2.74 ppm after the grafting. As all the protons of **BE-N₃-3** were already found, it might be attributed to allylic protons of the polymer backbone close to a heteroatom.
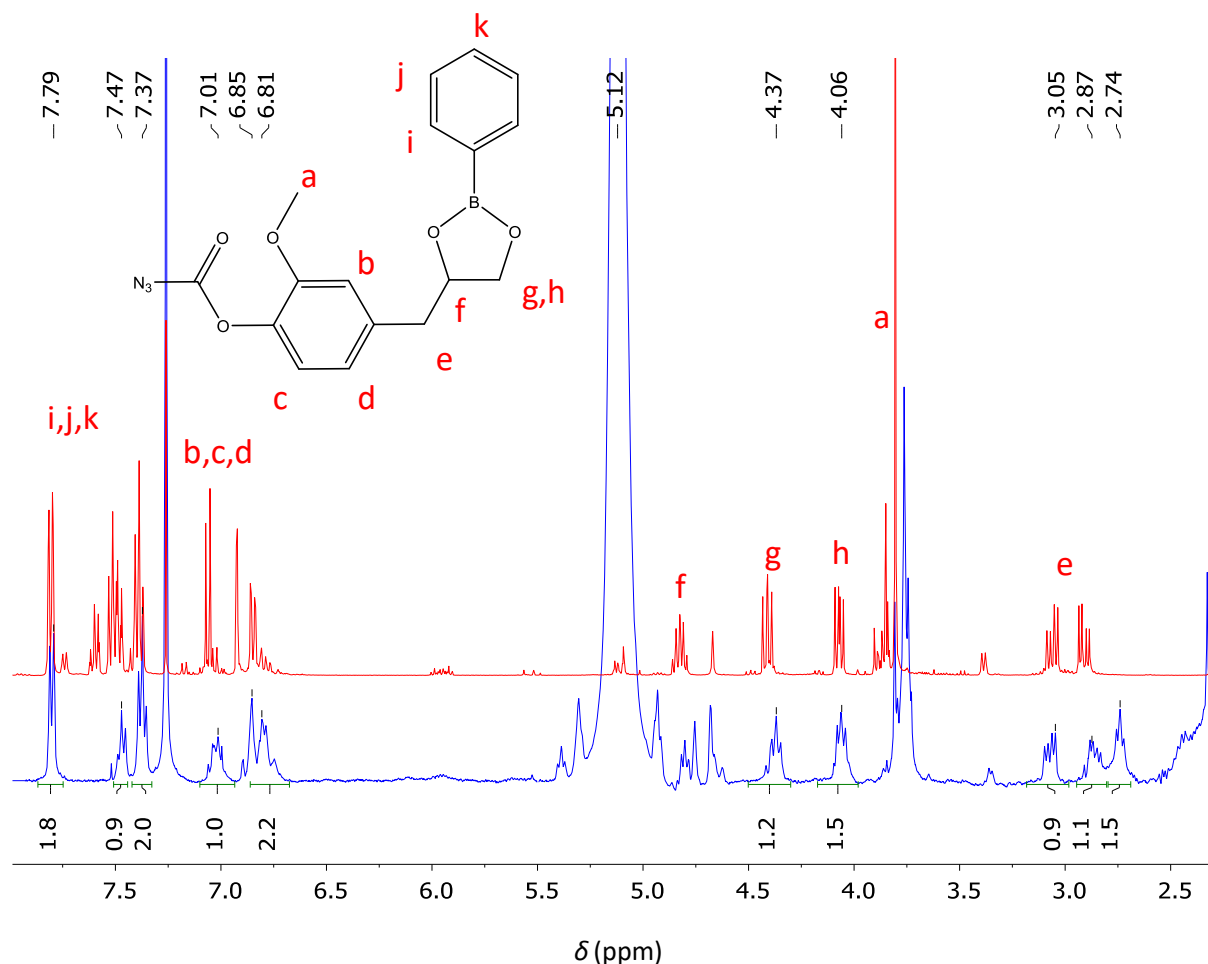
Figure 5.15. ¹H-NMR spectra in CDCl₃ of **BE-N₃-3** (top, red) and **PI grafted with BE-N₃-3** via extrusion after precipitation (bottom, blue).

Using the press, the reaction was over after 10 minutes at 140 °C with a grafting yield of 63% then started to decrease after 60 minutes (**Figure 5.16,** top left side). At 120 °C the grafting was slower as it required 60 min to reach the plateau value of 52%. These kinetic data were consistent with the results obtained by TGA. The molar masses were drastically affected by the reaction, with a constant increase of dispersity combined with a decrease from 250 000 Da at t = 0 min to 125 000 Da after 90 min at 120 °C. The same trend was observed for the two tested temperatures (**Figure 5.16**, middle left side).

To compare the processing conditions, the grafting was conducted by reactive extrusion but at only 120 °C under nitrogen flow. The results are displayed in **Figure 5.16** (top right side).

The speed of grafting was similar under these two conditions. However, the grafting was more efficient in extrusion with a yield around 70% while under press the yield stabilised around 50%. This could come from the better mixing in the extruder that may avoid or decrease intramolecular reactions. Opposite tendencies were observed for the evolution of molar masses (**Figure 5.16,** middle right side). The number average molar mass continuously decreased over time with the press while during the extrusion it increased for the first 30 minutes before reaching a plateau then it started to decrease after 80 minutes. This difference proves that the decomposition of the azide and its grafting onto pre-extruded PI tend to cross-link the chains potentially by radical coupling reactions, but in limited proportions. During the compression moulding, the presence of oxygen led to the thermodegradation of the pre-extruded PI, while the nitrogen flow used during the extrusion avoided such side reactions. But at long times in both cases, the polymer begins to degrade exhibiting its instability under these conditions.
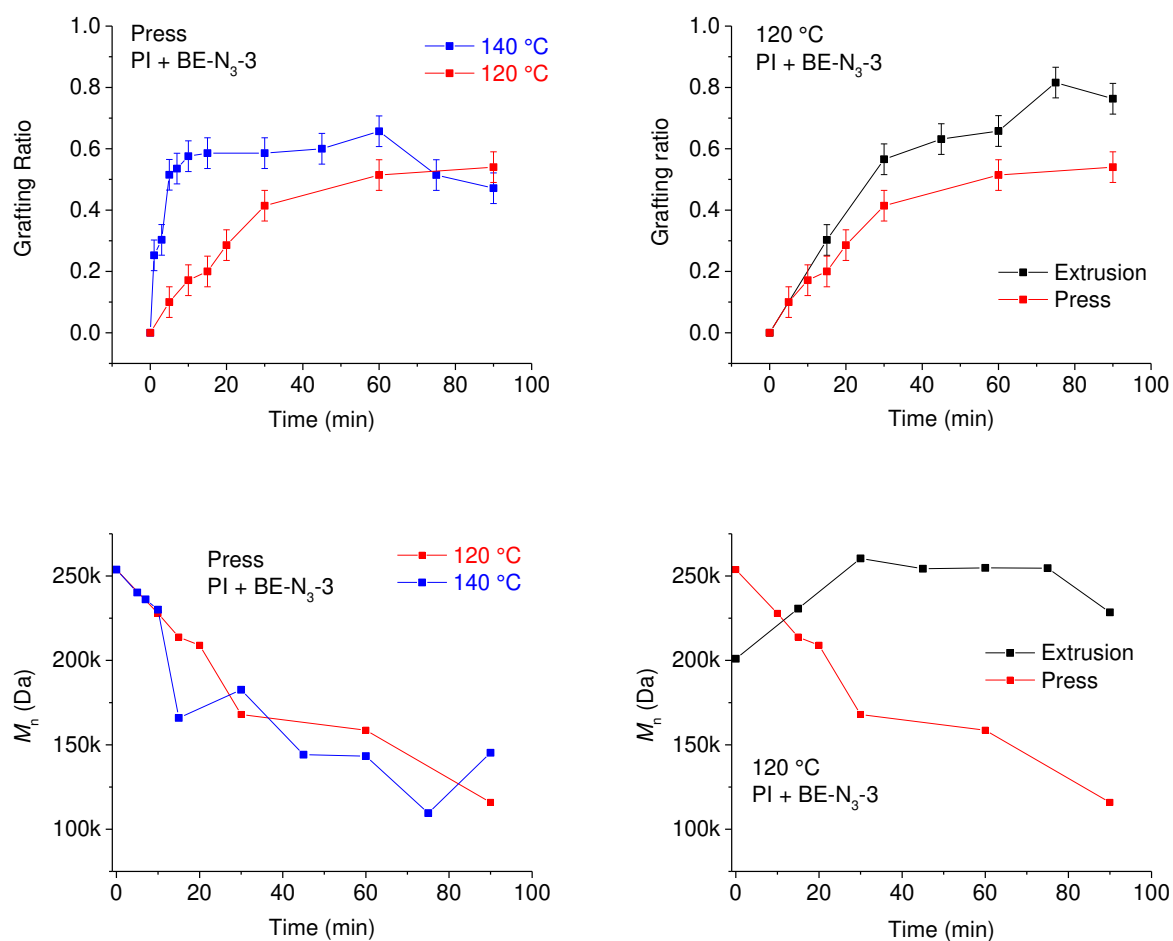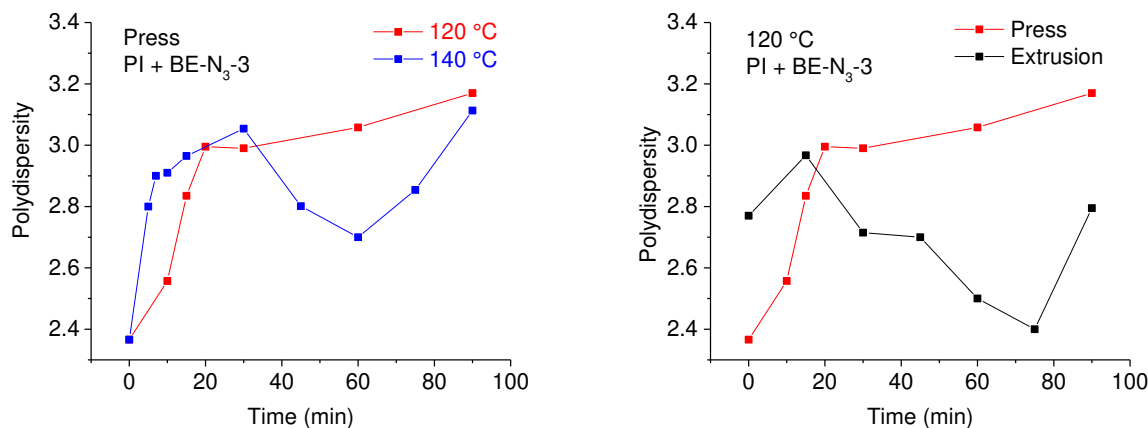
Figure 5.16. Kinetic data of the grafting reaction under different conditions: via compression moulding at 140 °C (blue), at 120 °C (red) and in reactive extrusion at 120 °C (black) under nitrogen atmosphere. Top: Grafting ratio determined by ^{1}H-NMR spectroscopy after purification by precipitation. Middle: Number average molar mass. Bottom: Dispersity.

5.4.3 Cross-linking of PI with the bis-azidoformate dioxaborolane Bis-BE-N₃-3

5.4.3.1 DSC analysis

As the grafting of **BE-N₃-3** was shown to be efficient, the bis-azidoformate dioxaborolane **Bis-BE-N₃** was analysed before being tested to cross-link pre-extruded PI. DSC analysis was performed in order to assess its melting temperature, as depicted in **Figure 5.17**. **Bis-BE-N₃-3** exhibited a melting temperature at 110 °C, thus the endothermic peak proceeded before the decomposition of the azide, which promotes a good dispersion of the cross-linker as it is melt before it reacts with PI, unlike **Bis-BE-N₃-1**.
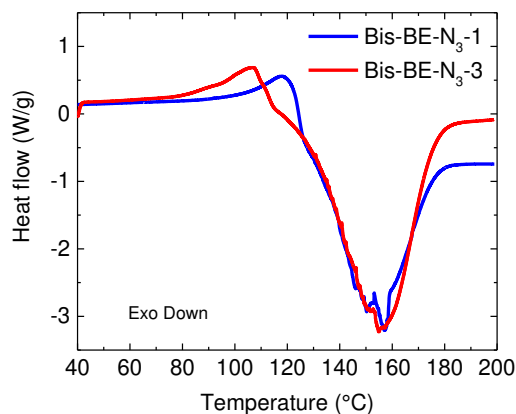
Figure 5.17. DSC curves of **Bis-BE-N₃-1** (blue) and **Bis-BE-N₃-3** (red).

5.4.3.2 Curing and stress relaxation experiments

The mixture pre-extruded PI / **Bis-BE-N$_3$-3** was prepared by dissolution in THF and evaporation with an azide content of 0.5 mol%. The cross-linking kinetics of the blends were monitored with an Anton Paar MCR 501 rheometer in plate-plate geometry. The evolution of the elastic shear modulus G' and the loss shear modulus G'' were recorded by oscillatory shear at 1% strain at 120 or 140 °C, with a heating rate of 1 °C.s^{-1} to bring the samples to the targeted temperature from 25 °C. This curing process was conducted under a nitrogen atmosphere to avoid oxidation.

First, thanks to the fast increase of temperature, G' begins to decrease as the rubber softens and the cross-linker melts acting as a plasticizer. Then, after 10 min, G' increases due to the cross-linking reaction (**Figure 5.18**). Then G' reaches a plateau after 20 min at 140 °C, while it required 60 to 80 minutes to reach the same plateau at 120 °C. These times are similar to the reaction times observed by ^{1}H-NMR spectroscopy during the grafting of the mono azidoformate dioxaborolane **BE-N$_3$-3**.
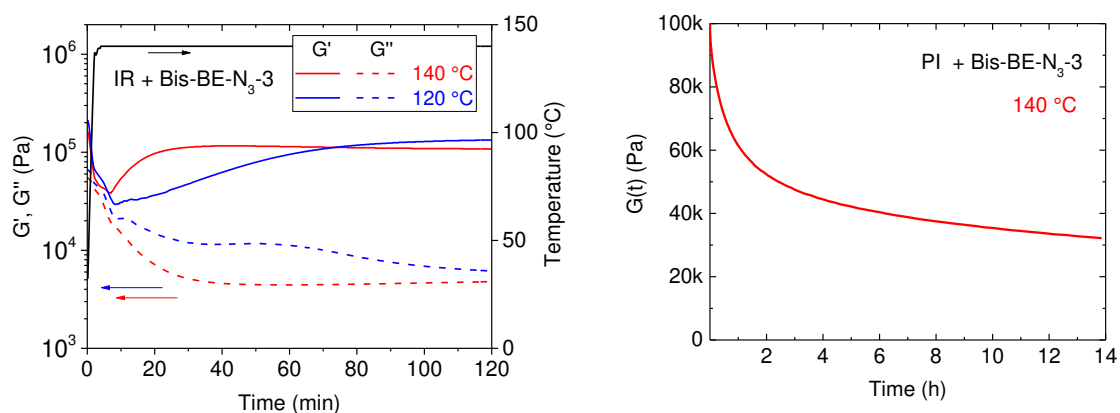
Figure 5.18. Left: The cross-linking kinetics of the PI / **Bis-BE-N$_3$-3** blend are monitored in the rheometer at 120 °C (blue) and 140 °C (red). Right: Stress relaxation experiment at 140 °C of the PI / **Bis-BE-N$_3$-3** blend right after the curing *in situ* at 140 °C.

The stress relaxation experiment was conducted after the *in situ* curing of the sample, **PI-BE-V5**, (cured 120 min at 140 °C) under nitrogen in the rheometer. 1 % strain was applied and the resulting stress was recorded over time. The material relaxes an important part of stresses, probably thanks to boronic ester exchanges, but did not fully relax even after 14 hours at 140 °C. A residual stress of 30% was observed. This is likely due to side reactions that generate static cross-links during the nitrene grafting. To verify the formation of a static network, diolysis was performed on the samples right after the curing following the method described

in subsection 5.2.4.3. Both networks did not dissolve after 48 hours in THF, thereby confirming the presence of parasite static cross-links which impede the topological rearrangement of the network through dynamic exchange reactions.

5.5 Another strategy to cross-link PI

5.5.1 Cross-linking in two steps

The higher are the temperatures, the more dynamic is the vitrimer and the easier it is for the network to rearrange its topology, thus to relax stress and be reprocessable. However too oxidative conditions should be avoided as it would alter the polymer backbone leading to irreversible degradation of the network and poor mechanical properties after thermo recycling. In order to obtain a recyclable network, a different method of cross-linking was used.
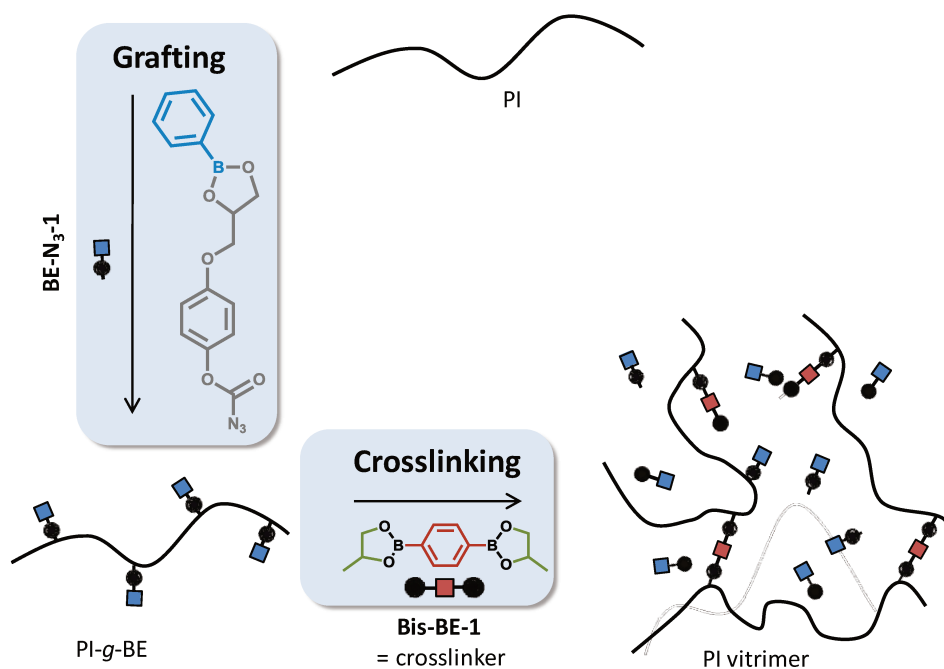
Scheme 5.13. Another strategy to cross-link PI. First PI was functionalised with pendant dioxaborolane units and then cross-linked by addition of a bis-dioxaborolane.

First, the mono azide **BE-N$_3$-1** was grafted onto the polyisoprene backbone then the non-functionalized cross-linker, **Bis-BE-1**, was incorporated in the precursor to obtain a dynamic network (**Scheme 5.13**). This new kind of cross-linker was synthesised through the condensation of benzene-1,4-diboronic acid and 1,2-propanediol. It is the complementary molecule of the pending boronic esters **BE-N$_3$-1** attached to the polymer backbone after grafting. The ratio of exchangeable pending groups / cross-linker can then be tuned to

promote the rearrangement of the network and thus decrease the viscosity of the vitrimer for a better reprocessability. Another advantage of this method is to avoid phase separation. Indeed, the functionalization of PI with mono azidoformate **BE-N$_3$-1** increases the polarity of the polymer backbone which promotes the miscibility of the cross-linker **Bis-BE-1** into the PI matrix. The melting of the latter cross-linker occurs at 95 °C and thus, 45 °C below than the processing temperatures.

5.5.2 Cross-linking in extrusion

PI was functionalised with 2.2 mol% of **BE-N$_3$-1** via reactive extrusion at 140 °C under nitrogen flow as reported in a previous subchapter. When the reaction of grafting was finished as proved by the plateau regime and ^{1}H-NMR analysis, the cross-linker **Bis-BE-1** was introduced into the barrel. The axial force increased for 15 minutes after the complete addition, before reaching a new plateau (**Figure 5.19**). This plateau regime corresponds to the equilibrium state of the exchange between the mono functional pendant groups and the cross-linkers. In other words, the cross-linking reaction ended when the force became constant again. The force increased from 2200 N after functionalisation to 3400 N after cross-linking, which is lower that the value obtained with the **Bis-BE-N$_3$-1** (4100 N). This lower viscosity is explained by a lower cross-linking degree and the presence of pendant groups and free molecule which promote the exchange reaction.
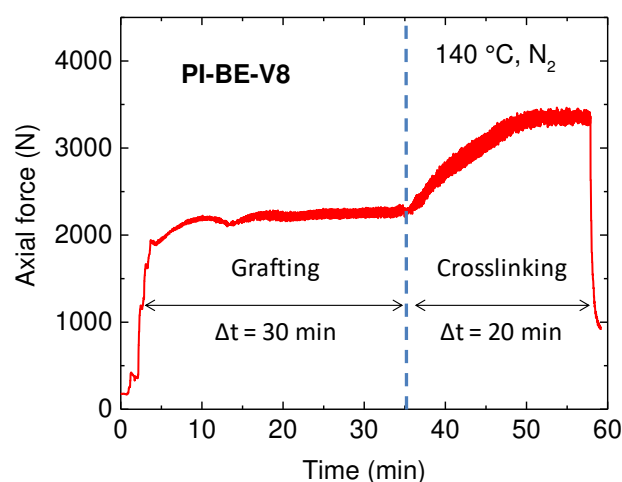
Figure 5.19. Extrusion profile of the grafting and cross-linking in two steps of **PI-BE-V8** at 140 °C.

Surprisingly, the time required to fully cross-link the functional PI was higher than the equilibrium time of the model reaction at 140 °C. This could be due to the slow diffusion of

the cross-linker into the polymeric matrix. As the functionalisation degree is pretty low around 1 mol%, the cross-linkers need a certain time to find an exchangeable partner for the cross-linking to occur.

5.5.3 Swelling tests and selective cleavage

To check the formation of a network, swelling tests were performed on the synthesised vitrimers. These tests were performed using the same procedure as described above in a previous subchapter. No sample dissolved during the test (**Table 5.4**).

Table 4. Characterisation of the solvent resistance of vitrimers obtained from the two step cross-linking.

Vitrimer	BE-N$_3$-1 (%mol)	Cross-linker (%mol)	Insolubility in THF (wt%)	Swelling ratio	Insolubility after diolysis (wt%)
PI-BE-V6	2.2	0.22	63	58	0
PI-BE-V7	2.2	0.56	64	47	0
PI-BE-V8	2.2	1.1	73	23	0

These results prove the insolubility of these vitrimers generated via a one-pot two step reactive processing from a commercial thermoplastic precursor. As should be expected, the insoluble fraction increased and the swelling ratio decreased with the amount of cross-linker The soluble fractions were lower than those measured with **PI-BE-V1**, **PI-BE-V2** and **PI-BE-V3** further confirming the lower cross-link density of these new vitrimers or their faster rearrangement

To verify the integrity of the dynamic boronic ester cross-links after processing 45 min at 140 °C, the network was selectively cleaved with an excess of 1,2-propanediol. After one night at room temperature all the vitrimers completely dissolved (**Table 5.4**). These results prove that the dynamic of the boronic ester bonds is kept even after the processing.

5.5.4 Mechanical properties
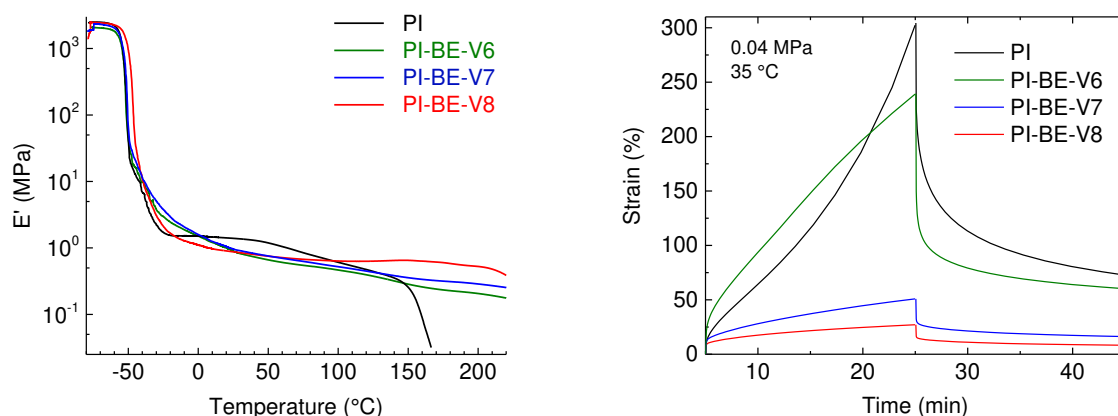
Figure 5.20. Left: Storage modulus of PI, **PI-BE-V6**, **PI-BE-V7** and **PI-BE-V8**, measured by DMA between -75 °C and 220 °C. Right: Creep experiment at 35 °C and 40 000 Pa for PI, **PI-BE-V6**, **PI-BE-V7** and **PI-BE-V8**.

To confirm the network formation, the thermo-mechanical properties of these vitrimers were tested. **Figure 5.20** displays the DMA curves for vitrimers **PI-BE-V6**, **PI-BE-V7** and **PI-BE-V8** with storage moduli in function of temperature. The T_g of the systems corresponds to the first decrease of E', which shows that the glass transition is not strongly affected by the cross-linking. The vitrimers exhibit a constant plateau regime above the glass transition up to 220 °C while for the linear precursor, E' reached a plateau thanks to entanglements followed by a drastic drop above 150 °C as the system is not cross-linked.

Step-stress recovery experiments were performed to check the creep resistance of the vitrimers. A stress of 40 000 Pa was applied to the samples at 35 °C for 25 min then released 20min. The initial elastic moduli were inversely proportional to the amount of cross-linker incorporated in PI (**Figure 5.20**). For all the samples tested, the vitrimers reached a linear deformation with the time unlike PI. However, the most cross-linked vitrimer **PI-BE-V6** possesses a residual deformation of 10 %. Consequently, even this network is too dynamic at service temperature leading to poor creep resistance. One of the reasons might be the presence of 50 mol% of non-grafted **BE-N₃-1** in the material before cross-linking. Consequently, the cross-linkers can react with the free non grafted mono boronic esters leading to a decrease of the cross-linking efficiency. Precipitation of the functional PI should be considered before achieving the dynamic cross-linking.

5.6 Conclusion

Various azidoformates dioxaborolanes were designed and synthesised in order to functionalize elastomer with a low vinyl content. The grafting was performed in bulk via two different processes, reactive extrusion and compression moulding. Moderate to good yields were achieved, between 50 and 82% regardless of the temperature used. The presence of oxygen did not alter the grafting but significantly decreased the molar masses of the polymer. Vitrimers were generated via two different strategies. The hydroquinone-based bis-azidoformate dioxaborolane **Bis-BE-N$_3$-1** was used as a cross-linker, resulting in a cross-linked material which was insoluble in a good solvent (THF) but could be dissolved by selective diolysis of the dynamic dioxaborolane cross-links. The system could relax the majority of stresses at elevated temperatures, but it could not recover its initial mechanical properties after reprocessing by compression moulding. The macrophase separation observed with **Bis-BE-N$_3$-1** led us to change the cross-linker with a new one having more atoms of carbon; an eugenol-based bis-azidoformate dioxaborolane **Bis-BE-N$_3$-3**. If the grafting of **BE-N$_3$-3** was improved, the system was no longer recyclable, as this bis-azidoformate dioxaborolane generates side reactions which produces static cross-links.

Therefore, another approach was considered. Polyisoprene was first functionalized with a mono azidoformate dioxaborolane, **BE-N$_3$-1,** and then cross-linked with a bis-dioxaborolane that did not carry any azido group. A cross-linked material was obtained with similar glass transition and enhanced three dimensional stability above T_g. The network was easily reprocessable but its mechanical properties were inferior to conventionally cured rubbers, especially the creep resistance at service temperature. The presence of ungrafted boronic ester may be one the reasons for this too fast rearrangement of the network at room temperature.

High molecular weight polyisoprene was functionalized with success using techniques which are common in the industry, such as reactive extrusion and compression moulding. However, the high reactivity of the nitrenes species combined with the low temperature resistance of the targeted polymer backbone led to the formation of static networks or too dynamic systems.

Process should be adjusted by adding an anti-oxidant and purifying the polymer after grafting the mono azidoformate **BE-N$_3$-1** in order to obtain a relevant recyclable elastomer. Moreover, the influence of carbon black on the properties of these vitrimers could be investigated.

5.7 Appendix

5.7.1 Materials

Commercially available polyisoprene, Nipol IR2200, was kindly provided by Zeon and polybutadiene, Buna CB24, by Arlanxeo. All other chemicals were purchased from Sigma-Aldrich, TCI Chemicals or Alfa Aesar. All hydrogenated solvents were obtained from Carlos Erba while deuterated solvents, *e.g.* THF-d$_8$, DMSO-d$_6$ and CDCl$_3$, were obtained from Eurisotop. Unless otherwise noted, reagents were used without further purification. Solvents (including deuterated solvents) were dried over activated 3 Å molecular sieves under an inert atmosphere for at least 72 h prior to use. The glassware used for dioxaborolanes' syntheses was oven-dried.

5.7.2 Characterisation

Differential Scanning Calorimetry

Glass transitions of the materials were determined by differential scanning calorimetry (DSC). For the elastomers, sequences of temperature ramps (heating, cooling, heating) in the −120 to 20 °C range were performed at 10 °C/min using a TA Instruments Q1000 equipped with a liquid nitrogen cooling accessory and calibrated using sapphire and high purity indium metal. For the elastomers, samples were prepared in hermetically sealed pans (5−10 mg/sample) and were referenced to an empty pan. The reported T_g values are from the second heating cycle. For the azides, sequences of temperature ramps (heating, cooling, heating) were performed in the 40 to 200 °C range and in opened pans.

Nuclear Magnetic Resonance Spectroscopy

^{1}H and ^{13}C-NMR spectra were recorded at 297 K on a Bruker AVANCE 400 spectrometer at 400 and 100 MHz, respectively, and referenced to the residual solvent peaks (^{1}H, δ 7.26 for CDCl$_3$; ^{13}C, δ 77.16 for CDCl$_3$).

Size Exclusion Chromatography

Size exclusion chromatography (SEC) was performed on a Viscotek GPCmax/VE2001 connected to a triple detection array (TDA 305) from Malvern. Molecular weights were determined based on conventional calibration obtained with monodisperse polystyrene standards.

Dynamic Mechanical Analysis

Dynamic mechanical analyses (DMAs) were conducted on a TA Instruments Q800 in tension mode. Heating ramps were performed from −75 to 220 °C at a constant rate of 3 °C/min, with a maximum strain amplitude of 1% at a fixed frequency of 1 Hz.

Determination of Young's Modulus

The classical theory of elasticity predicts that the engineering stress equals G (λ – 1/λ^2) with G the shear modulus.[38] However, in the first part of the mechanical curves, *ie.* before the up-turn, the experimental data cannot be fitted with this equation because of the slight difference observed for small deformations. To take into account this effect, the curves were fitted by the following equations proposed by Mooney and Rivlin:

Equation 5.7. $$\sigma = 2\left(C_1 + \frac{C_2}{\lambda}\right)\left(\lambda - \frac{1}{\lambda^2}\right)$$

Two parameters are used to fit the data: C_1 and C_2. C_1 is proportional to the cross-link density, while the meaning of C_2 is less clear. The first parts of the curves are well fitted by the Mooney and Rivlin (MR) equation, but as soon as the material starts to crystallise the curves becomes convex and the MR equation is no longer valid. However, as the Young's modulus E' corresponds to the initial slope is not a problem. From **equation 7**, for the small deformations ($\lambda = 1 + \varepsilon$), the stress is estimated as following with $\varepsilon \rightarrow 0$:

Equation 5.8. $$\sigma \sim 6(C_1 + C_2)\,\varepsilon$$

Thus the Young's modulus, *E*, is calculated according to equation:

Equation 5.9. $$E \sim 6(C_1 + C_2)$$

Table 5.5. Parameters of Mooney-Rivlin fits and calculated Young's moduli

PI-BE-V1	C_1	C_2	E
Initial	0.14	0.15	1.7
Recycled x1	0.15	0.10	1.5
Recycled x2	0.11	0.14	1.5
Recycled x3	0.06	0.15	1.3
Recycled x4	0.03	0.15	1.1

5.7.3 Syntheses of azides

5.7.3.1 Synthesis of **BE-N₃-1** and **Bis-BE-N₃-1**
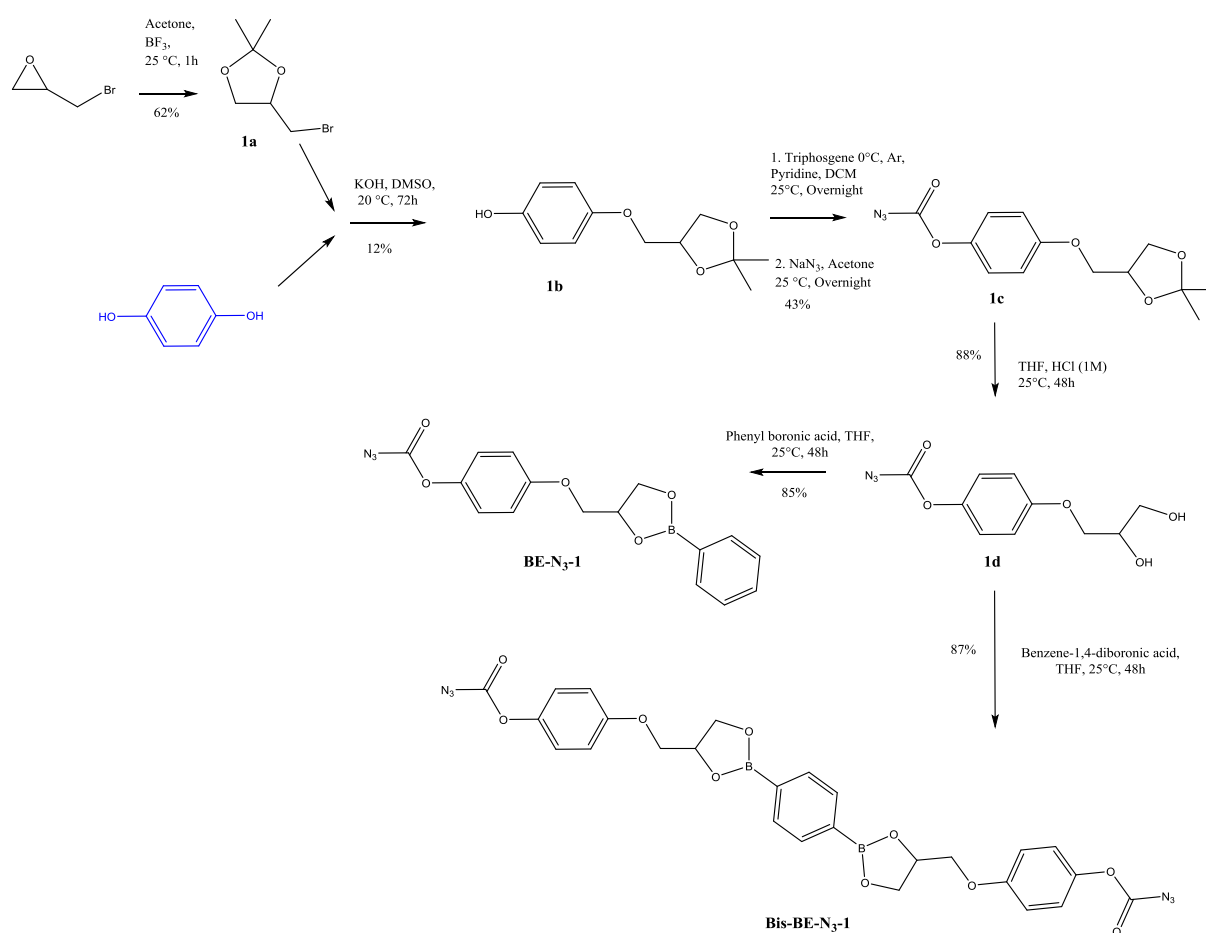
Scheme 5.14. Synthesis of **BE-N₃-1** and **Bis-BE-N₃-1** from hydroquinone, a mono azidoformate dioxaborolane and a bis-azidoformate dioxaborolane, respectively.

Synthesis of compound **1a**: 10 drops of boron trifluoride etherate were added dropwise to acetone (50 mL). Then, epibromohydrine (20.0 g, 146 mmol) was added dropwise to the mixture at room temperature. The reaction was stirred for 15 h at room temperature. The liquid product was distilled under vacuum. Compound **1a** was obtained as a colourless liquid (23.0 g, 82 %).

^{1}H NMR (CDCl$_3$, 400 MHz): δ (ppm) 4.33 (m, 1H), 4.11 (ddd, 1H, J = 8.7 Hz, J = 6.1 Hz, J = 0.6 Hz), 3.85 (dd, 1H, J = 8.7 Hz, J = 5.1 Hz), 3.40 (ddd, 1H, J = 10.0 Hz, J = 4.7 Hz, J = 0.6 Hz), 3.29 (dd, 1H, J = 10.0 Hz, J = 8.1 Hz), 1.42 (s, 3H), 1.33 (s, 3H).

Synthesis of compound **1b**: To a solution of hydroquinone (11.9 g, 108 mmol, 3.0 eq.) in DMSO (150 mL) was added KOH (40.3 g, 718 mmol, 20.0 eq.) in suspension. Then, compound **1a** (7.00 g, 35.9 mmol, 1.0 eq.) was added dropwise at room temperature. After 3 days at room temperature, the mixture was quenched with ammonium bicarbonate. Water was added and the organic compound was extracted with chloroform, washed with water and dried over MgSO$_4$. The solvent was removed and the product was purified by column chromatography using chloroform and then Et$_2$O as eluent. Compound **1b** was obtained as a colourless liquid (0.94 g, 12%).

^{1}H NMR (DMSO-d_6, 400 MHz): δ (ppm) 8.91 (s, 1H), 6.76 (m, 2H), 6.66 (m, 2H), 4.34 (m, 1H), 4.06 (dd, 1H, J = 8.3 Hz, J = 6.6 Hz), 3.87 (m, 2H), 3.71 (dd, 1H, J = 8.3 Hz, J = 6.3 Hz), 1.34 (s, 3H), 1.29 (s, 3H).

^{13}C NMR (DMSO-d$_6$, 100 MHz): δ (ppm) 151.28, 151.07, 115.60, 115.31, 108.63, 73.72, 69.16, 65.75, 26.53, 25.31.

Synthesis of compound **1c**: To a solution of triphosgene (0.50 g, 1.69 mmol, 0.36 eq.), in dichloromethane (5 mL) at 0°C, was added dropwise a solution of compound **1b** (1.06 g, 4.72 mmol, 1eq.) in DCM (2.5 mL). Then, pyridine (0.37 g, 4.70 mmol, 1 eq.) in DCM (2.5 mL) was added dropwise at 0°C. The mixture was allowed to warm up to room temperature and stirred at room temperature for 20 h. The reaction was monitored by TLC. The solvent was removed and the product re-dissolved in acetone (10 mL) was added dropwise to a solution of sodium azide (0.46 g, 7.12 mmol, 1.5 eq.) in water (5 mL) at 0°C. The mixture was allowed to

warm up to room temperature and stirred at room temperature for 16 h. The organic compound was extracted with ethyl acetate, washed with water and dried over MgSO$_4$. The solvent was removed and the product was purified by column chromatography using Et$_2$O as eluent. Compound **2c** was obtained as a colourless liquid (0.60 g, 43%).

^{1}H NMR (CDCl$_3$, 400 MHz): δ (ppm) 7.08 (m, 2H), 6.91 (m, 2H), 4.47 (m, 1H), 4.16 (dd, 1H, J = 8.5 Hz, J = 6.4 Hz), 4.04 (dd, 1H, J = 9.4 Hz, J = 5.4 Hz), 3.92 (dd, 1H, J = 9.4 Hz, J = 5.8 Hz), 3.89 (dd, 1H, J = 8.5Hz, J = 5.8 Hz), 1.46 (s, 3H), 1.40 (s, 3H).

^{13}C NMR (CDCl$_3$, 100 MHz): δ (ppm) 156.74, 156.59, 144.47, 121.77, 115.23, 109.81, 73.88, 69.22, 66.73, 26.75, 25.31.

Synthesis of compound **1d**: compound **1c** (0.250 g, 0.85 mmol) was solubilized in THF (10 mL) at room temperature. Then, an aqueous solution of HCl (10 mL, 1M) was added dropwise. The mixture was stirred 48 hours at room temperature. The organic compound was extracted with dichloromethane and dried over MgSO$_4$. The solvent was removed. Compound **1d** was obtained as a white powder (0.190 g, 88%).

^{1}H NMR (DMSO-d_6, 400 MHz): δ (ppm) 7.18 (m, 2H), 6.98 (m, 2H), 4.95 (d, 1H, J = 5.1 Hz), 4.66 (t, 1H, J = 5.7Hz), 4.00 (dd, 1H, J = 9.8 Hz, J = 4.1 Hz), 3.86 (dd, 1H, J = 9.8 Hz, J = 6.1 Hz), 3.79 (m, 1H), 3.44 (t, 2H, J = 5.7 Hz).

^{13}C NMR (DMSO-d_6, 100 MHz): δ (ppm) 156.85, 155.91, 143.67, 122.00, 115.04, 69.94, 69.79, 62.54, 39.43.

Synthesis of compound **BE-N$_3$-1:** compound **1d** (0.51 g, 2.01 mmol, 1eq.) was dissolved in THF (5 mL), phenylboronic acid (0.257 g, 2.11 mmol, 1.05 eq.) was added followed by water (0.5 mL). The mixture was stirred 20 minutes then MgSO$_4$ was added (728 mg, 3eq.). The mixture was stirred overnight at room temperature. Then, the mixture was filtrated and the solvent was removed. Compound **BE-N$_3$-1** was obtained as a colourless viscous solid (0.58 g, 85%).

^{1}H NMR (CDCl$_3$, 400 MHz): δ (ppm) 7.84 (m, 2H), 7.50 (m, 1H), 7.40 (m, 2H), 7.09 (m,2H), 6.93 (m, 2H), 4.93 (m, 1H), 4.52 (dd, 1H, J = 9.2 Hz, J = 8.1 Hz), 4.32 (dd, 1H, J = 9.2 Hz, J = 6.3 Hz), 4.15 (dd, 1H, J = 9.8 Hz, J = 4.6 Hz), 4.09 (dd, 1H, J = 9.8 Hz, J = 5.2 Hz).

^{13}C NMR (CDCl$_3$, 100 MHz): δ (ppm) 156.68, 156.57, 144.58, 134.88, 131.62, 127.95, 127.83, 121.82, 115.36, 75.22, 70.00, 68.24.

Synthesis of compound **Bis-BE-N$_3$-1**: compound **1d** (0.75 g, 2.96 mmol, 2eq.) was dissolved in THF (20 mL), 1,4-phenylenediboronic acid (245 mg, 1.48 mmol, 1.0 eq.) was added followed by water (0.5 mL). The mixture was stirred 20 minutes then MgSO$_4$ was added (360 mg, 3eq.). The mixture was stirred overnight at room temperature. Then, the mixture was filtered and the solvent was removed. Compound **Bis-BE-N$_3$-1** was obtained as a white powder (0.88 g, 99%).

^{1}H NMR (CDCl$_3$, 400 MHz): δ (ppm) 7.84 (s, 4H), 7.08 (m, 4H), 6.92 (m, 4H), 4.93 (m, 2H), 4.54 (t$_{app}$, 2H), 4.33 (dd, 2H, $J = 9.2$ Hz, $J = 6.4$ Hz), 4.18-4.08 (m, 4H)

5.7.3.2 Synthesis of **BE-N$_3$-2** and **Bis-BE-N$_3$-2**
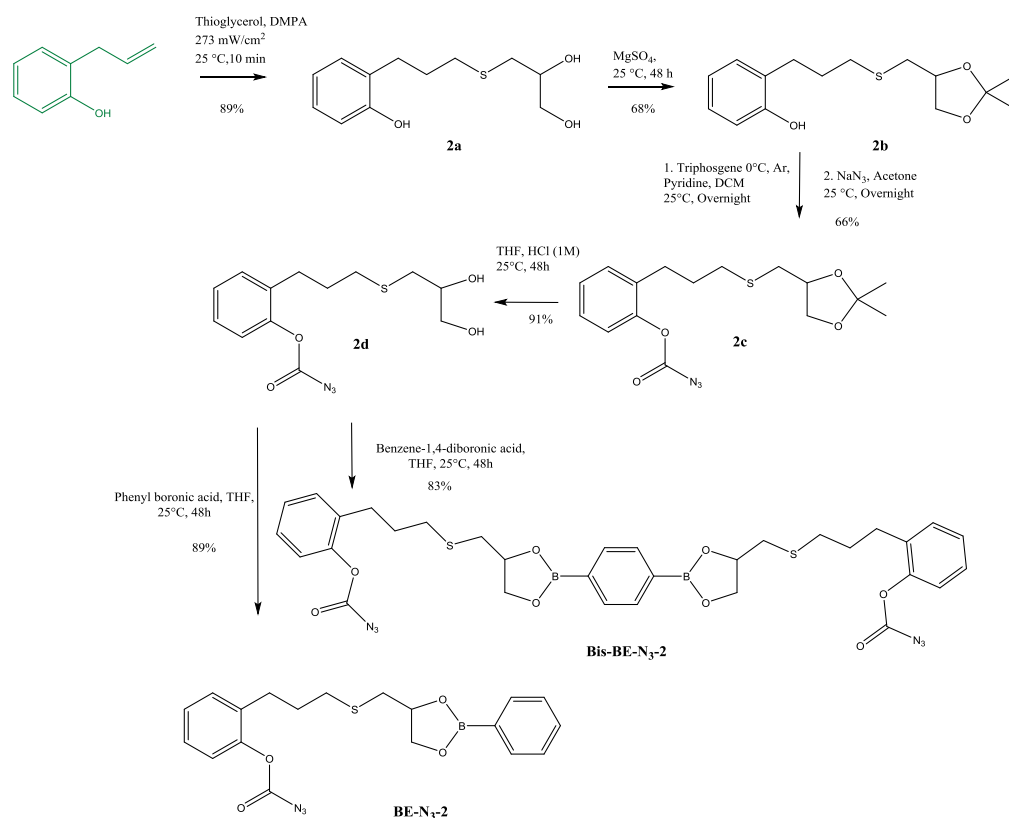
Scheme 5.15. Synthesis of **BE-N$_3$-2** and **Bis-BE-N$_3$-**2 from 2-allylphenol, a mono azidoformate dioxaborolane and a bis-azidoformate dioxaborolane, respectively.

Synthesis of compound **2a**: 2-allylphenol (20.0 g, 149 mmol, 1 eq) was mixed with thioglycerol (16.1 g, 149 mmol, 1 eq) and DMPA (0.38 g, 1.5 mmol, 0.01 eq). The mixture was irradiated with mercury lamp (light intensity 272 mW cm^{-2}) for 10 min at room temperature. After the irradiation, the mixture was dissolved in ethyl acetate (300 mL) then washed three times (1 × 100 mL and 2 × 50 mL) with a saturated NaCl solution to remove the unreacted thioglycerol. Then product was obtained by removing the solvent under reduced pressure and further dried under vacuum overnight at room temperature to yield a colourless viscous oil (36.0 g, 89%).

^{1}H NMR (DMSO, 400 MHz): δ (ppm) 1.76 (q, J = 7.5 Hz, 2H), 2.41-2.63 (m, 6H), 3.36 (m, 2H), 3.53 (sxt, J = 5.6 Hz, 1H), 4.55 (t, J = 5.7 Hz, 1H), 4.74 (d, J = 5.2 Hz, 1H), 6.70 (td, J = 7.9 Hz and J = 1.2 Hz, 1H), 6.77 (dd, J = 6.9 Hz and J = 1.1 Hz, 1H), 6.96-7.04 (m, 2H), 9.23 (s, 1H).

^{13}C NMR (DMSO, 100 MHz): δ (ppm) 155.01, 129.71, 127.54, 126.76, 118.76, 114.80, 71.31, 64.50, 35.19, 31.78, 29.34, 28.83.

Synthesis of compound **2b**: Compound **2a** (36.0 g, 149 mmol, 1 eq.) was dissolved in 200 mL acetone at room temperature. APTS (2.56 g, 14.9 mmol, 0.1 eq.) and then MgSO$_4$ (53.7 g, 445 mmol, 3 eq) were added. After overnight stirring at room temperature, the reaction was quenched with NaHCO$_3$, the solid was filtered off and acetone evaporated. The product was dissolved in 150 mL Et$_2$O, washed three times with water (3 × 50 mL), dried over MgSO$_4$ and filtered. Et$_2$O was evaporated under reduce pressure and then under vacuum 1h.To remove the remaining allylphenol, the product was distilled at 120 °C under reduced pressure. To remove the unreacted molecule **2,** the product was purified by column chromatography (SiO$_2$) with Et$_2$O as an eluent. The product was obtained as colourless liquid (28.6 g, 68 %).

^{1}H NMR (DMSO, 400 MHz): δ (ppm) 1.25 (s, 3H), 1.31 (s, 3H), 1.76 (q, J = 7.4 Hz, 2H), 2.53-2.71 (m, 6H), 3.59 (dd, J = 6.5 Hz, J = 8.2 Hz, 1H), 4.02 (dd, J = 6.1 Hz, J = 8.2 Hz, 1H), 4.16 (q, J = 6.3 Hz, 1H), 6.69 (td, J = 8.0 Hz, J= 1.2 Hz, 1H), 6.76 (dd, J = 9.1 Hz and J = 1.1 Hz, 1H), 6.96-7.04 (m, 2H), 9.24 (s, 1H).

<superscript>13</superscript>C NMR (DMSO, 100 MHz): δ (ppm) 25.6, 26.8, 28.8, 29.3, 31.5, 34.3, 68.2, 75.3, 108.6, 114.9, 118.8, 126.9, 129.8, 155.1

Synthesis of compound **2c**: Triphosgene (5.43 g, 18 mmol, 0.36 eq) was dissolved in 40 mL anhydrous dichloromethane under argon. To the latter solution, was added dropwise at 0 °C compound **2b** (14.4 g, 51 mmol, 1 eq) dissolved in 20 mL anhydrous dichloromethane then pyridine (4.02 g, 51 mmol, 1 eq) dissolved in 20 mL anhydrous dichloromethane. After 15 min, the reaction was left at room temperature overnight. The solvent was evaporated. The resulting product was dissolved in 80 mL acetone and added dropwise at 20 °C to a solution of NaN$_3$ (water/acetone : 20mL/20mL). After stirring 24h at room temperature acetone was evaporated and the product extracted with Et$_2$O (500 mL), washed with water (3 × 75 mL), washed 3 times with a 1M NaOH solution, dried with MgSO$_4$ and the solvent was evaporated. The compound **2c** was obtained as a colourless liquid (11.8 g, 66%).

^{1}H NMR (CDCl$_3$, 400 MHz): δ (ppm) 1.25 (s, 3H), 1.31 (s, 3H), 1.76 (q, J = 7.4 Hz, 2H), 2.53-2.71 (m, 6H), 3.59 (dd, J = 6.5 Hz, J = 8.2 Hz, 1H), 4.02 (dd, J = 6.1 Hz, J = 8.2 Hz, 1H), 4.16 (q, J = 6.3 Hz, 1H), 7.23-7.40 (m, 4H).

^{13}C NMR (CDCl$_3$, 100 MHz): δ (ppm) 155.69, 148.48, 133.04, 130.40, 127.39, 126.84, 121.93, 108.48, 75.16, 68.04, 34.08, 31.08, 29.46, 27.97, 26.64, 25.43.

Synthesis of compound **2d**: Compound **2c** (11.8 g, 34 mmol, 1 eq) was dissolved in 80 mL of THF. 80 mL of 1M HCl was added and the solution was let stirring 48h at 25 °C. The reaction was quenched with NaHCO$_3$ (6.72 g, 80 mmol). The product was extracted with dichloromethane (3 × 80 mL), washed with water (1 × 80 mL), dried with MgSO$_4$ and concentrated under reduce pressure and further dried under vacuum at 50 °C. Compound **2d** was obtained as a colourless viscous liquid (9.52 g, 91%).

^{1}H NMR (DMSO, 400 MHz): δ (ppm) 1.76 (m, 2H), 2.42-2.65 (m, 6H), 3.35 (m, 2H), 3.54 (m, 1H), 4.56 (t, J = 5.5 Hz, 1H), 4.74 (d, J = 5.1 Hz, 1H), 7.23-7.36 (m, 4H).

^{13}C NMR (DMSO, 100 MHz): δ (ppm) 28.1, 29.6, 31.5, 35.2, 64.6, 71.4, 122.0, 126.9, 127.4, 130.5, 133.2, 148.6, 155.8

Synthesis of compound **BE-N₃-2**: Compound **2d** (9.52 g, 31 mmol, 1 eq) was dissolved in 150 mL of THF, phenylboronic acid (3.73 g, 31 mmol, 1 eq) was added with $MgSO_4$ (11.04 g, 92 mmol, 3 eq) and the solution was let stirring overnight at 25 °C. The solution was filtered, the solvent evaporated under reduce pressure and the product dried under vacuum at 50 °C overnight Compound **BE-N₃-2** was obtained as a yellowish viscous liquid (10.80 g, 89%).

^{1}H NMR (CDCl₃, 400 MHz): δ (ppm) 1.84-1.97 (m, 2H), 2.63-2.92 (m, 6H), 4.15 (m, 1H), 4.49 (m, 1H), 4.76 (m, 1H), 7.10-7.30 (m, 4H), 7.39 (m, 2H), 7.49 (m, 1H), 7.62 (m, 2H).

^{13}C NMR (CDCl₃, 100 MHz): δ (ppm) 156.40, 148.84, 134.82, 132.94, 131.55, 130.52, 127.83, 127.49, 126.92, 121.69, 76.86, 70.56, 37.09, 32.28, 29.69, 28.71.

Synthesis of compound **Bis-BE-N₃-2**: Compound **2d** (2.21 g, 7.10 mmol, 2eq.) was dissolved in THF (50 mL), 1,4-phenylenediboronic acid (588 mg, 3.55 mmol, 1.0 eq.) was added followed by water (0.5 mL). The mixture was stirred 20 minutes then $MgSO_4$ was added (428 mg, 3 eq.). The mixture was stirred overnight at room temperature. Then, the mixture was filtered and the solvent was removed. Compound **Bis-BE-N₃-2** was obtained as a yellowish viscous solid (2.10 g, 83%).

^{1}H NMR (CDCl₃, 400 MHz): δ (ppm) 7.73 (s, 4H), 7.20-7.00 (m, 8H), 4.68 (m, 2H), 4.41 (dd, 2H, J = 9.2 Hz, J = 7.9 Hz), 4.07 (dd, 2H, J = 9.2 Hz, J = 6.6 Hz), 2.82 (dd, 2H, J = 13.7 Hz, J = 5.0 Hz), 2.70-2.50 (m, 10H), 1.81 (m, 4H).

^{13}C NMR (CDCl₃, 100 MHz): δ (ppm) 156.34, 148.84, 134.07, 132.91, 130.53, 127.50, 126.93, 121.70, 76.91, 70.62, 37.08, 32.27, 29.69, 28.71.

5.7.3.3 Synthesis of **BE-N₃-3** and **Bis-BE-N₃-3**
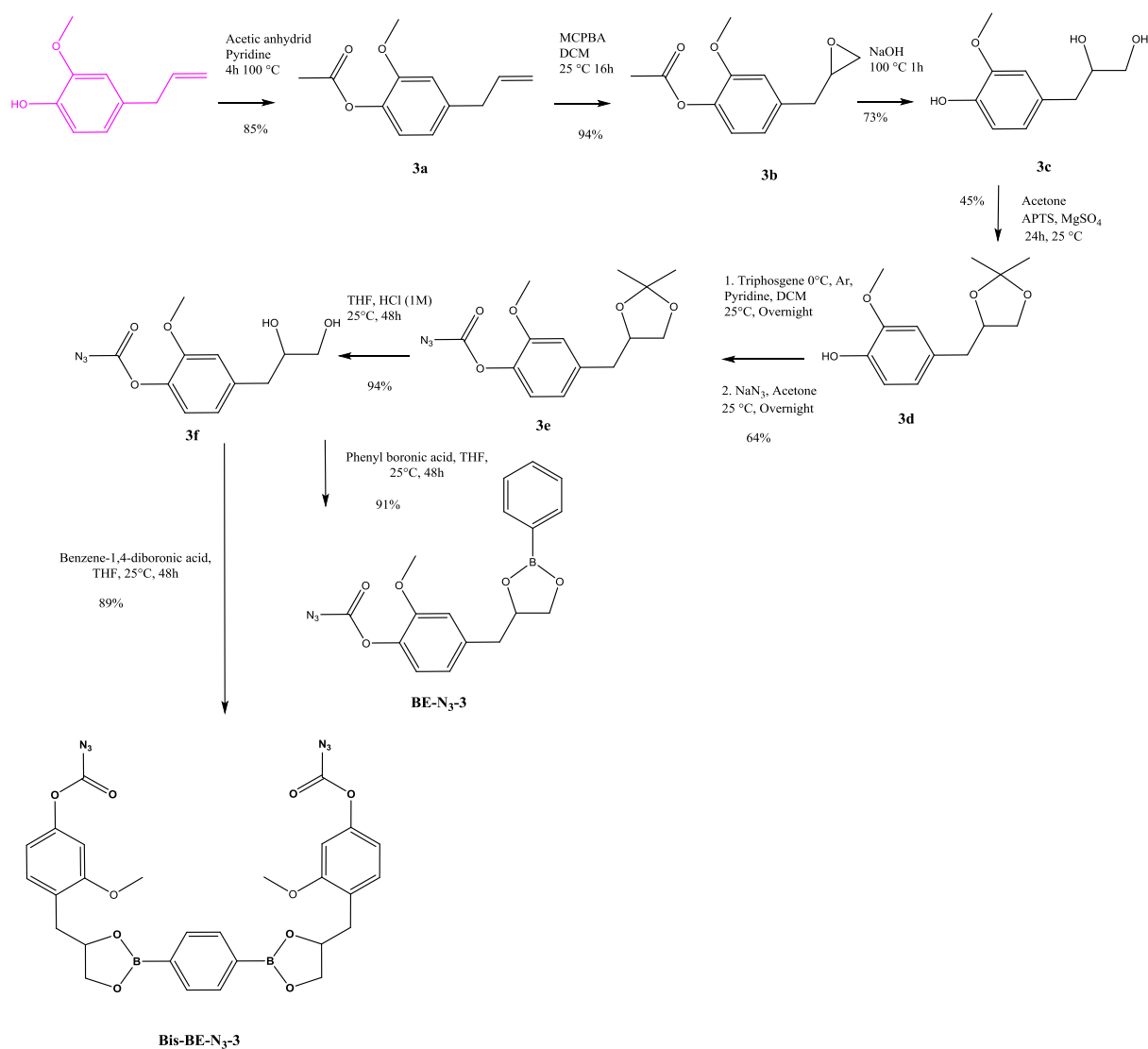
Scheme 5.16. Synthesis of **BE-N₃-3** and **Bis-BE-N₃-3** from eugenol, a mono azidoformate dioxaborolane and a bis-azidoformate dioxaborolane, respectively.

Synthesis of compound **3a**: Eugenol (15.0 g, 91 mmol, 1 eq.), acetic anhydride (70.0 g, 685 mmol, 7.5 eq.) and pyridine (88 mL, 1.10 mol, 12 eq.) were heated at 100 °C for 4 h. The mixture was cooled to room temperature, diluted with ice water and acidified. The organic compound was extracted with chloroform, washed with a solution of hydrochloric acid in water, dried over $MgSO_4$ and concentrated. Compound **3a** was obtained as an orange oil (16.0 g, 85%).

^{1}H NMR (CDCl$_3$, 400 MHz): δ (ppm) 2.31 (s, 3H), 3.38 (d, J = 6.7 Hz, 2H), 3.82 (s, 3H),), 5.00-5.18 (m, 2H), 5.90-6.02 (m, 1H), 6.73-6.82 (m, 2H), 6.95 (d, J = 7.9 Hz, 1H).).

^{13}C NMR (CDCl$_3$, 100 MHz): δ (ppm) 169.4, 151.0, 139.1, 138.1, 137.2, 122.6, 120.8, 116.3, 112.8, 55.9, 40.2, 20.8.

Synthesis of compound **3b**: Compound **3a** (18.8 g, 91 mmol, 1 eq.) and *m*CPBA (24.3 g, 101 mmol, 72 %, 1.11 eq.) were dissolved in dichloromethane (190 mL) and stirred 26h at 25 °C. The white powder was filtered and washed with dichloromethane. The filtrate was washed with a 10 wt% solution of Na$_2$S$_2$O$_5$ in water (3 ×) then with saturated NaHCO$_3$ (2 ×) and saturated NaCl (1 ×), dried over MgSO$_4$ and concentrated. Compound **3b** was obtained as an orange oil (19.12 g, 94%).

^{1}H NMR (CDCl$_3$, 400 MHz): δ (ppm) 2.31 (s, 3H), 2.55 (m, 1H), 2.78-2.96 (m, 3H), 3.15 (m, 1H), 3.83 (s, 3H), 6.80-6.89 (m, 2H), 6.97 (d, J = 8.0 Hz, 1H).

^{13}C NMR (CDCl$_3$, 100 MHz): δ (ppm) 169.3, 151.1, 138.6, 136.4, 122.8, 121.2, 113.3, 56.0, 52.4, 47.0, 38.8, 20.8.

Synthesis of compound **3c**: Compound **3b** (15.3 g, 69 mmol, 1 eq.) was added dropwise to a solution of sodium hydroxide (27.5 g, 689 mmol, 10 eq., 2.75 mol/L) at 100 °C and the mixture was stirred for 1 hour. The mixture was cooled to room temperature and diluted with ice water and acidified to pH 1. The organic compound was extracted with ethyl acetate (4 × 200 ml), washed with water (1 × 200 ml), dried over MgSO$_4$ and concentrated under reduced pressure and then under vacuum at 70°C for 2h. Compound **3c** was obtained as an orange oil (8.60 g, 63%).

^{1}H NMR (DMSO, 400 MHz): δ (ppm) 2.40-2.43 (m, 1H), 2.61-2.64 (m, 1H), 3.26 (m, 2H), 3.57 (m, 1H), 3.73 (s, 3H), 4.47 (m, 2H), 6.57 (d, J = 8.0 Hz, 1H), 6.64 (d, J = 8.0 Hz, 1H), 6.76 (s, 1H), 8.76 (s, 1H).

^{13}C NMR (DMSO, 100 MHz): δ (ppm) 147.04, 144.42, 130.29, 121.41, 114.99, 113.44, 72.64, 65.19, 55.44.

Synthesis of compound **3d**: Compound **3c** (5.50 g, 28 mmol, 1 eq.) was dissolved in acetone (130 mL) at room temperature. Then *p*-TSA (0.48 g, 2.8 mmol, 0.1 eq.) and $MgSO_4$ (10.0 g, 83 mmol, 3 eq) were added slowly and the mixture was stirred at room temperature for 24h. $NaHCO_3$ (0.70 g, 8.3 mmol, 0.3 eq) was added and stirring was continued for 30 min at room temperature. The solid was filtered off and acetone evaporated. The slurry was dissolved in Et_2O (150 mL), washed with water (3 × 100 mL), dried with $MgSO_4$, filtered and concentrated. The product was purified by column chromatography (SiO_2) with Et_2O and obtained as a viscous oil (3.08 g, 47 %).

^{1}H NMR ($CDCl_3$, 400 MHz): δ (ppm) 1.25 (s, 1H), 1.32 (s, 1H), 2.60-2.65 (m, 1H), 2.74-2.79 (m, 1H), 3.53 (m, 1H), 3.74 (s, 3H), 3.87 (m, 1H), 4.22 (q, J = 6.5, 1H), 6.60 (d, J = 8.0 Hz, 1H), 6.66 (d, J = 8.0 Hz, 1H), 6.79 (s, 1H), 8.73 (s, 1H).

^{13}C NMR ($CDCl_3$, 100 MHz): δ (ppm) 146.38, 144.26, 129.32, 121.78, 114.32, 111.69, 109.08, 76.82, 68.86, 55.83, 39.66, 27.00, 25.69.

Synthesis of compound **3e**: Triphosgene (1.38 g, 4.7 mmol, 0.36 eq) was dissolved in 20 mL of anhydrous dichloromethane under argon. To the latter solution, was added dropwise at 0 °C compound **3d** (3.08 g, 12.9 mmol, 1 eq) dissolved in 10 mL anhydrous dichloromethane then pyridine (1.02 g, 12.9 mmol, 1 eq) dissolved in 10 mL anhydrous dichloromethane. After 15 min, the reaction was left at room temperature overnight. The solvent was evaporated. The resulting product was dissolved in 40 mL acetone and added dropwise at 20 °C to a solution of NaN_3 (water/acetone : 20mL/20mL). After stirring 24h at room temperature, the acetone was evaporated and the product extracted with Et_2O (250 mL), washed with water, dried with $MgSO_4$ and the solvent evaporated. Compound **3e** was obtained as an orange liquid (2.72 g, 69%).

^{1}H NMR (DMSO, 400 MHz): δ (ppm) 7.02 (d, *J* = 8 Hz, 1H), 6.86 (d, *J* = 1.6 Hz, 1H), 7.02 (d, *J* = 8 Hz, *J* = 8 Hz, 1H), 4.32 (m, 1H), 4.00 (dd, *J* = 8.1 Hz, *J* = 5.9 Hz, 1H), 3.85 (s, 3H), 3.63 (dd, *J* = 8.0 Hz, *J* = 7.0 Hz, 1H), 2.96 (dd, *J* = 13.8 Hz, *J* = 6.4 Hz, 1H), 2.78 (dd, *J* = 13.8 Hz, *J* = 6.4 Hz, 1H), 1.43 (s, 3H), 1.35 (s, 3H).

^{13}C NMR (DMSO, 100 MHz): δ (ppm) 155.86, 150.66, 138.19, 137.55, 122.01, 121.23, 113.57, 109.23, 76.34, 68.84, 55.89, 39.92, 26.99, 25.65.

Synthesis of compound **3f**: Compound **3e** (2.72 g, 8.9 mmol, 1 eq) was dissolved in 40 mL of THF, 40 mL of 1M HCl was added and the solution was let stirring 48h at 25 °C. The reaction was quenched with $NaHCO_3$ (3.36 g, 40 mmol). The product was extracted with dichloromethane, washed with water, dried with $MgSO_4$ and concentrated under reduce pressure and further dried under vacuum at room temperature. Compound **3f** was obtained as an orange liquid (2.29 g, 97%).

^{1}H NMR (DMSO, 400 MHz): δ (ppm) 2.55 (m, 1H), 2.77 (m, 1H), 3.29 (m, 2H), 3.66 (m, 1H), 3.79 (s, 3H), 4.61 (m, 2H).

^{13}C NMR (DMSO, 100 MHz): δ (ppm) 155.5, 149.9, 139.9, 137.1, 121.4, 114.0, 72.3, 67.0, 65.4, 55.8, 25.2.

Synthesis of compound **BE-N₃-3**: Compound **3f** (2.29 g, 8.6 mmol, 1 eq) was dissolved in 40 mL of THF, phenylboronic acid (1.05 g, 8.6 mmol, 1 eq) was added with $MgSO_4$ (3.10 g, 25.8 mmol, 3 eq) and the solution was let stirring overnight at 25 °C. The solution was filtered and solvent evaporated under reduce pressure and furthered dried under vacuum at 50 °C overnight. Compound **BE-N₃-3** was obtained as an orange viscous liquid (2.81 g, 93%).

^{1}H NMR (CDCl₃, 400 MHz): δ (ppm) 2.89-2.93 (m, 1H), 3.03-3.09 (m, 1H), 3.80 (s, 3H), 4.07 (m, 1H), 4.41 (m, 1H), 4.82 (q, J = 6.8 Hz, 1H), 6.86 (m, 1H), 6.92 (m, 1H), 7.05 (m, 1H), 7.51 (m, 2H), 7.60 (m, 1H), 7.80 (m, 2H).

^{13}C NMR (CDCl₃, 100 MHz): δ (ppm) 42.0, 55.9, 70.4, 113.8, 121.5, 122.1, 127.9, 128.0, 131.6, 132.6, 134.8, 135.6

Synthesis of compound **Bis-BE-N₃-3**: Compound **3f** (1.60 g, 5.99 mmol, 2eq.) was dissolved in THF (50 mL), 1,4-phenylenediboronic acid (0.50 g, 2.99 mmol, 1.0 eq.) was added followed by water (0.5 mL). The mixture was stirred 20 minutes then $MgSO_4$ was added (3 eq.). The mixture was stirred overnight at room temperature. Then, the mixture was filtered and the solvent was removed. Compound **Bis-BE-N₃-3** was obtained as an orange viscous solid (1.59 g, 84%).

¹H NMR (THF-d$_8$, 400 MHz): δ (ppm) 2.89-2.93 (m, 1H), 3.03-3.09 (m, 1H), 3.78 (s, 3H), 4.05 (m, 1H), 4.36 (m, 1H), 4.83 (q, J = 6.8 Hz, 1H), 6.88 (m, 1H), 7.04 (m, 2H), 7.76 (m, 2H).

¹³C NMR (THF-d$_8$, 100 MHz): δ (ppm) 42.6, 56.1, 71.3, 78.9, 114.7, 122.1, 122.7, 134.0, 138.1, 139.6

5.7.4 Others
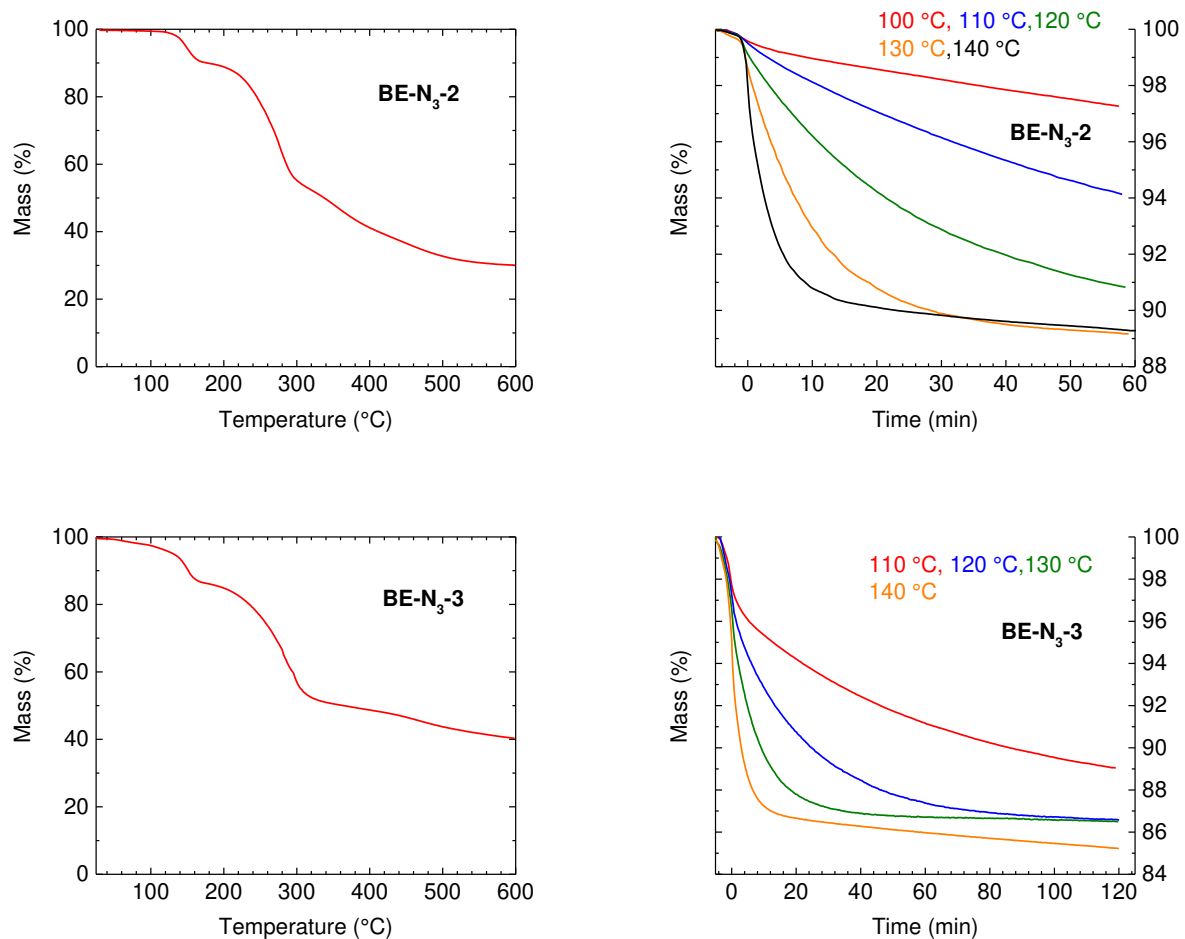
Figure 5.21. Top: TGA of **BE-N$_3$-2**. Bottom: TGA of **BE-N$_3$-3.** Left: Analysis from 25 to 600 °C at 20 °C/min. Right: Isothermal analysis at 100, 110, 120, 130 or 140 °C.

5.8 References

(1) Worrell, B. T.; Malik, J. A.; Fokin, V. V. Direct Evidence of a Dinuclear Copper Intermediate in Cu(I)-Catalyzed Azide-Alkyne Cycloadditions. *Science* **2013**, *340* (6131), 457–460. https://doi.org/10.1126/science.1229506.

(2) Saal, K.-A.; Richter, F.; Rehling, P.; Rizzoli, S. O. Combined Use of Unnatural Amino Acids Enables Dual-Color Super-Resolution Imaging of Proteins via Click Chemistry. *ACS Nano* **2018**, *12* (12), 12247–12254. https://doi.org/10.1021/acsnano.8b06047.

(3) Breslow, D. S. 10 - Industrial Applications. In *Azides and Nitrenes*; Scriven, E. F. V., Ed.; Academic Press, 1984; pp 491–521. https://doi.org/10.1016/B978-0-12-633480-7.50014-6.

(4) Balci, M. Acyl Azides: Versatile Compounds in the Synthesis of Various Heterocycles-. *Synthesis* **2018**, *50* (7), 1373–1401. https://doi.org/10.1055/s-0036-1589527.

(5) Huang, D.; Yan, G. Recent Advances in Reactions of Azides. *Adv. Synth. Catal.* **2017**, *359* (10), 1600–1619. https://doi.org/10.1002/adsc.201700103.

(6) Hyatt, I. F. D.; Meza-Aviña, M. E.; Croatt, M. P. Alkynes and Azides: Not Just for Click Reactions. *Synlett* **2012**, *23* (20), 2869–2874. https://doi.org/10.1055/s-0032-1317545.

(7) Jia, J.; Baker, G. L. Cross-Linking of Poly[1-(Trimethylsilyl)-1-Propyne] Membranes Using Bis(Aryl Azides). *J. Polym. Sci. Part B Polym. Phys.* **1998**, *36* (6), 959–968. https://doi.org/10.1002/(SICI)1099-0488(19980430)36:6<959::AID-POLB3>3.0.CO;2-B.

(8) Gangolphe, L.; Déjean, S.; Bethry, A.; Hunger, S.; Pinese, C.; Garric, X.; Bossard, F.; Nottelet, B. Degradable Multi(Aryl Azide) Star Copolymer as Universal Photo-Cross-linker for Elastomeric Scaffolds. *Mater. Today Chem.* **2019**, *12*, 209–221. https://doi.org/10.1016/j.mtchem.2018.12.008.

(9) Wentrup, C. Carbenes and Nitrenes: Recent Developments in Fundamental Chemistry. *Angew. Chem. Int. Ed.* **2018**, *57* (36), 11508–11521. https://doi.org/10.1002/anie.201804863.

(10) Lwowski, W.; Maricich, T. J. Carbethoxynitrene by α-Elimination. Reactions with Hydrocarbons1,2. *J. Am. Chem. Soc.* **1965**, *87* (16), 3630–3637. https://doi.org/10.1021/ja01094a018.

(11) Lwowski, Walter.; Maricich, T. J. Carbethoxynitrene. Selectivity of the C-H Insertion. *J. Am. Chem. Soc.* **1964**, *86* (15), 3164–3165. https://doi.org/10.1021/ja01069a047.

(12) Lwowski, W.; McConaghy, J. S. Carbethoxynitrene. Control of the Stereospecificity of an Addition to Olefins. *J. Am. Chem. Soc.* **1965**, *87* (23), 5490–5491. https://doi.org/10.1021/ja00951a044.

(13) Lwowski, W.; Woerner, F. P. Carbethoxynitrene. Control of Chemical Reactivity. *J. Am. Chem. Soc.* **1965**, *87* (23), 5491–5492. https://doi.org/10.1021/ja00951a045.

(14) Smolinsky, G.; Wasserman, E.; Yager, W. A. The E.P.R. of Ground State Triplet Nitrenes. *J. Am. Chem. Soc.* **1962**, *84* (16), 3220–3221. https://doi.org/10.1021/ja00875a060.

(15) Arenas, J. F.; Marcos, J. I.; Otero, J. C.; Tocón, I. L.; Soto, J. Nitrenes as Intermediates in the Thermal Decomposition of Aliphatic Azides. *Int. J. Quantum Chem.* **2001**, *84* (2), 241–248. https://doi.org/10.1002/qua.1326.

(16) Kyba, E. P. 1 - Alkyl Azides and Nitrenes. In *Azides and Nitrenes*; Scriven, E. F. V., Ed.; Academic Press, 1984; pp 1–34. https://doi.org/10.1016/B978-0-12-633480-7.50005-5.

(17) Smolinsky, G.; Pryde, C. A. Vinyl Azide Chemistry. Thermally Induced Reactions. *J. Org. Chem.* **1968**, *33* (6), 2411–2416. https://doi.org/10.1021/jo01270a053.

(18) Carlson, A. S.; Topczewski, J. J. Allylic Azides: Synthesis, Reactivity, and the Winstein Rearrangement. *Org. Biomol. Chem.* **2019**, *17* (18), 4406–4429. https://doi.org/10.1039/C8OB03178A.

(19) Horner, L.; Spietschka, E.; Gross, A. The Course of Rearrangement of Diazoketones. *Ann Chem* **1951**, *573*, 17–30.

(20) Gritsan, N. P. Properties of Carbonyl Nitrenes and Related Acyl Nitrenes. In *Nitrenes and Nitrenium Ions*; John Wiley & Sons, Ltd, 2013; pp 481–548. https://doi.org/10.1002/9781118560907.ch12.

(21) Wentrup, C.; Bornemann, H. The Curtius Rearrangement of Acyl Azides Revisited – Formation of Cyanate (R–O–CN). *Eur. J. Org. Chem.* **2005**, *2005* (21), 4521–4524. https://doi.org/10.1002/ejoc.200500545.

(22) Ghosh, A. K.; Sarkar, A.; Brindisi, M. The Curtius Rearrangement: Mechanistic Insight and Recent Applications in Natural Product Syntheses. *Org. Biomol. Chem.* **2018**, *16* (12), 2006–2027. https://doi.org/10.1039/C8OB00138C.

(23) Lwowski, W.; Tisue, G. T. The Photodecomposition of Pivaloyl Azide. *J. Am. Chem. Soc.* **1965**, *87* (17), 4022–4023. https://doi.org/10.1021/ja01095a069.

(24) Cotter, R. J.; Beach, W. F. Thermolysis of Azidoformates in Aromatic Compounds. A Synthesis of 1H-Azepin-1-Yl Carboxylates. *J. Org. Chem.* **1964**, *29* (3), 751–754. https://doi.org/10.1021/jo01026a502.

(25) Sloan, M. F.; Prosser, T. J.; Newburg, N. R.; Breslow, D. S. The Relative Reactivities of Azidoformates and Sulfonyl Azides with Certain Hydrocarbons. *Tetrahedron Lett.* **1964**, *5* (40), 2945–2949. https://doi.org/10.1016/0040-4039(64)83067-7.

(26) Lwowski, W.; Mattingly, T. W. The Photodecomposition of Ethyl Azidoformate. *Tetrahedron Lett.* **1962**, *3* (7), 277–280. https://doi.org/10.1016/S0040-4039(00)70866-5.

(27) Lwowski, W.; Mattingly, T. W. The Decomposition of Ethyl Azidoformate in Cyclohexene and in Cyclohexane1. *J. Am. Chem. Soc.* **1965**, *87* (9), 1947–1958. https://doi.org/10.1021/ja01087a019.

(28) Hafner, K.; Kaiser, W.; Puttner, R. Zur Stereoselektivität Der Addition Der Alkoxycarbonyl-Nitrene an Olefine. *Tetrahedron Lett.* **1964**, *5* (52), 3953–3956. https://doi.org/10.1016/S0040-4039(01)89347-3.

(29) McConaghy, J. S.; Lwowski, Walter. Singlet and Triplet Nitrenes. II. Carbethoxynitrene Generated from Ethyl Azidoformate. *J. Am. Chem. Soc.* **1967**, *89* (17), 4450–4456. https://doi.org/10.1021/ja00993a037.

(30) Wan, H.; Xu, J.; Liu, Q.; Li, H.; Lu, Y.; Abe, M.; Zeng, X. Contrasting Photolytic and Thermal Decomposition of Phenyl Azidoformate: The Curtius Rearrangement Versus Intramolecular C–H Amination. *J. Phys. Chem. A* **2017**, *121* (45), 8604–8613. https://doi.org/10.1021/acs.jpca.7b07969.

(31) Li, H.; Wu, Z.; Li, D.; Wan, H.; Xu, J.; Abe, M.; Zeng, X. Direct Observation of Methoxycarbonylnitrene. *Chem. Commun.* **2017**, *53* (35), 4783–4786. https://doi.org/10.1039/C7CC01926B.

(32) Lieber, Eugene.; Rao, C. N. R.; Chao, T. S.; Hoffman, C. W. W. Infrared Spectra of Organic Azides. *Anal. Chem.* **1957**, *29* (6), 916–918. https://doi.org/10.1021/ac60126a016.

(33) Smith, M. K.; Northrop, B. H. Vibrational Properties of Boroxine Anhydride and Boronate Ester Materials: Model Systems for the Diagnostic Characterization of Covalent Organic Frameworks. *Chem. Mater.* **2014**, *26* (12), 3781–3795. https://doi.org/10.1021/cm5013679.

(34) Hall, H. K.; Zbinden, R. Infrared Spectra and Strain in Cyclic Carbonyl Compounds. *J. Am. Chem. Soc.* **1958**, *80* (23), 6428–6432. https://doi.org/10.1021/ja01556a063.

(35) Spell, H. L. Infrared Spectra of N-Substituted Aziridine Compounds. *Anal. Chem.* **1967**, *39* (2), 185–193. https://doi.org/10.1021/ac60246a009.

(36) White, J. L.; Wang, Y.; Isayev, A. I.; Nakajima, N.; Weissert, F. C.; Min, K. Modelling of Shear Viscosity Behavior and Extrusion through Dies for Rubber Compounds. *Rubber Chem. Technol.* **1987**, *60* (2), 337–360. https://doi.org/10.5254/1.3536134.

(37) Zelentsov, S. V.; Kormil'tseva, E. B.; Zhezlov, A. B. Effect of Additives Containing a Heavy Atom on the Yield of Photooxidation Products of Arylazides. *High Energy Chem.* **2002**, *36* (2), 94–97. https://doi.org/10.1023/A:1014611012709.

(38) Treloar, L. R. G. The Elasticity of a Network of Long-Chain Molecules—II. *Trans. Faraday Soc.* **1943**, *39* (0), 241–246. https://doi.org/10.1039/TF9433900241.

General Conclusion

General Conclusion

In this work, elastomers were transformed into vitrimers using dioxaborolane and dioxaborinane dynamic covalent links. The two most produced elastomers, polybutadiene and polyisoprene, were converted into vitrimers using different grafting chemistries.

Pendant dioxaborolanes were grafted onto high vinyl content polybutadiene using the thiol-ene chemistry. The grafting occurred within one hour in solution to give the targeted functionalised polymer in high yields (superior to 80%). A bis-thiol dioxaborolane was synthesised to generate polybutadiene vitrimers. Gel formation was observed during the cross-linking. The networks were dried and shaped in order to test their dynamic and cross-linked nature. All the vitrimer materials were compared to conventionally cross-linked polybutadienes, which were used as references. Vitrimers exhibited a well-defined rubbery plateau which increases as the cross-linking density is increased. The glass transition was significantly impacted by the latter; it shifted to higher temperatures as the number of cross-links per chain increased. As the molecular weight of the polybutadiene precursor was low (3900 Da, *i.e.* below the molar mass between entanglement), a compromise had to be found between the formation of a highly insoluble network (many cross-links per chain) and a T_g below room temperature (low polymer grafting and cross-linking density). Although vitrimers are chemically cross-linked networks, they could completely relax stresses and thus flow at processing temperatures. Viscosities and characteristic relaxation times were found to range from 10^8 to 10^{11} Pa.s. Interestingly, the activation energy of the viscous flow was showed to depend on the cross-linking density. The more cross-linked was the vitrimer, the higher was its activation energy. This reveals that the viscoelastic behaviour of vitrimers is not only dependant on the dynamics of the exchange reaction, but also on the functionality and topology of the network. Recycling steps, by compression moulding at 150 °C, combined with tensile testing proved the reprocessability of the prepared vitrimers. Stresses and elongations at break, and Young's moduli were rather constant after three recycling steps, even if the values were low due to the unentangled nature of the polybutadiene precursor. The dynamic nature of the cross-links was confirmed by the selective cleavage of the boronic esters bonds. In the presence of an excess of free diols, the vitrimer gels completely dissolved within less than five minutes. SEC analysis showed that neither the molar mass nor the dispersity of the polybutadiene chains were affected by the reprocessing/testing cycles.

Surprisingly, even if the vitrimers with at least 4 cross-links per chain showed high insoluble fractions (superior to 78%) after 24 hours in THF, they became totally soluble after long immersion times. This dissolution time depends on several parameters, such as the cross-linking density, the nature of the solvent, the dynamic of exchange of the covalent bonds, the polymer concentration, etc. To better characterise the influence of these different parameters on the dissolution of vitrimers, further work needs to be performed. The vitrimers could creep at room temperature due to their molecular structure and composition, as well as the dynamic of exchange of the dioxaborolane cross-links under these conditions. As this behaviour represents a significant limitation for numerous potential applications, a dual network with both dynamic and static cross-links was designed. The amount of the latter was high enough to form a percolated network. Nevertheless, the material could be recycled without losing its mechanical properties and the creep resistance of dual networks was improved as compared to that of vitrimers.

Model studies were conducted on dioxaborolane (5-membered ring boronic esters) and dioxaborinane (6-membered ring boronic esters) compounds. Highly pure dioxaborinanes were synthesised and used to conduct model studies. The water stability of different boronic esters was studied by calculating the association and dissociation equilibrium constants via ^{1}H-NMR spectroscopy. It was shown that the more substituted is the boronic ester, the higher is the hydrolytic stability. Dioxaborinanes were found to be more than five times less sensitive to hydrolysis than their five-membered rings counterparts. Then, the exchange between two dioxaborinanes was investigated. The importance of water was highlighted by using atmospheric and protective conditions. Boronic ester transesterification of 5- and 6-membered compounds was studied in solution under argon. The reaction was more than four times faster with dioxaborolanes than with dioxaborinanes. It was found that the speed of the exchange depends on the nature of the boronic ester ring size and substitution degree), while it is not significantly impacted by the nature of the free diol, (1,2- or 1,3-diol). Switching from an unsubstituted to a highly substituted dioxaborinane drastically slowed down the transesterification reaction and resulted in non-equimolar amounts of products, owing to differences of stabilities between substituted and unsubstituted boronic esters. When two pure dioxaborinanes were mixed in bulk under protective atmosphere, the four products of the exchange reaction were observed by GC analysis. No traces of diols or boronic acids could be detected by ^{1}H-NMR spectroscopy. However, two mechanisms may explain this apparent metathesis reaction; a direct exchange between dioxaborinanes, or an indirect route through

successive transesterifications with undetected traces of diols. A frequency factor of 83 L.mol^{-1}s^{-1} and an activation energy of 61 kJ.mol^{-1} were calculated for the exchange reaction in bulk. The same reaction was performed in a highly concentrated dodecane solution (1M), which was used both as an internal standard and to simulate the elastomeric matrix. The exchange was slowed down and the activation energy was lower (39 kJ.mol^{-1}). Thus the exchange reaction was strongly dependent on the polarity of the medium and/or on the concentration of the considered species.

An attempt to incorporate dioxaborinane functions into the same polybutadiene matrix was performed. First, mono and bis thiol-dioxaborinanes were synthesised to dynamically cross-link the elastomer. Grafting yields of the former compounds were lower than those of the corresponding dioxaborolanes, which may be due to the lower solubility of the 6-membered species in the cross-linking solution. Surprisingly, when the divalent cross-linker was used, no gel formed during the reaction. A cross-linked network formed after drying only, yielding a non-transparent material. The dioxaborinane cross-linker contained an ester function, which may have induced macro phase separation in the apolar polybutadiene matrix. Nevertheless, the solvent resistance of the vitrimer was increased compared to dioxaborolane based vitrimers; at a fixed time the insoluble fraction was higher for dioxaborinane than for dioxaborolane based vitrimers. ^{1}H-NMR analysis revealed that the cross-linker was partially hydrolysed, but in proportions insufficient to explain such high soluble fractions after long immersion times. However, the hydrolysis of the dioxaborinanes generated diols, which allowed the transesterification to occur. As this reaction is significantly faster than the exchange between two dioxaborinanes, the polymer chains could rearrange more quickly their topology, potentially leading to the formation of loops which would decrease the cross-linking density of the network. This rearrangement could explain the full dissolution of these vitrimers after long immersion times. This phenomenon needs to be further investigated, *e.g.* by analysing the soluble fractions via light scattering and NMR for example, in order to characterize the nature, size and topology of the soluble objects. Polybutadiene vitrimers incorporating dioxaborinane cross-links were found to age at room temperature. Indeed, a stiffening of the materials was observed after seven days of rest at ambient temperature. DMA confirmed these results with the apparition of a second plateau, ranging from 25 to 50 °C, observable before the rubbery plateau, which ranged from 50 to 200 °C. This regime completely disappeared after the reprocessing at 150 °C. DSC analysis revealed that a part of the cross-linker crystallised during the ageing at room temperature. This result indicates that

the bis-thiol dioxaborinane tends to form clusters in the polymer matrix. The presence of an additional polar ester group in the dioxaborinane cross-linker, as compared to the dioxaborolane cross-linker, may explain this phase separation. The vitrimer without ageing, was reprocessed multiple times by compression moulding. The mechanical properties, such as stress and strain at break, were not altered, proving the recyclability of the material under the tested conditions. These key properties were observed to be lower than for the dioxaborolane vitrimer due to the lower grafting efficiency of the dioxaborinane cross-linker. To avoid the phase separation and to improve the grafting yields, another compound should be synthesised containing a thiol and a dioxaborolane function but without ester or other polar groups.

In order to cross-link industrially relevant elastomers, a high molar mass low vinyl content polybutadiene was considered. Regardless of the experimental conditions, the grafting could not exceed 10%, indicating that thiol-ene chemistry in solution is not a solution of choice for the efficient chemical modification of such polymers.

We also investigated the possibility to transform high molar mass polyisoprene into a vitrimer. The functionalisation was attempted by using nitrene chemistry. To this aim, three azidoformate compounds containing a dioxaborolane function were designed and synthesised with different overall yields, 3.9%, 29% or 14%. Among them, two were able to graft onto polyisoprene in bulk through reactive extrusion. Two strategies were considered to obtain vitrimer networks. The first one used a bis-azide, allowing the formation of a network in a single step. The obtained network could relax stresses, be cleaved by an excess of diols and possessed relevant elongation and stress at break. However, the reprocessing at 150 °C resulted in a network with decreased mechanical properties. The second approach relied on the functionalisation of polyisoprene with pendant dioxaborolanes. Then, the divalent complementary dioxaborolane cross-linker was added in extrusion to the functional polymer. The vitrimer did not dissolve after 24 hours in THF, unlike the thermoplastic precursor, while diolysis led to the full dissolution of the network. Nevertheless, the creep resistance of the vitrimer was low, limiting its potential for numerous industrial applications. The presence of free mono dioxaborinanes, coupled to the low grafting density, is likely responsible for this poor mechanical behaviour. To form a polyisoprene vitrimer by reactive processing, another grafting chemistry should probably be considered to increase the grafting efficiency.

Résumé

Résumé

Le domaine des caoutchoucs fait face à deux enjeux majeurs, l'augmentation continue de la demande d'une part et l'impossibilité de recycler ces matériaux en fin de vie d'autre part. La première engendre une pression croissante sur les ressources en caoutchoucs, pétrolifères ou naturelles (*Hevea brasiliensis*), tandis que la seconde pose la question de la valorisation de ces composés en fin de vie, considérés comme déchet à l'heure actuelle.

Face à ces deux défis, une partie de la solution consiste à allonger la durée de vie des caoutchoucs en améliorant leur recyclabilité. Pour se faire, ces matériaux doivent pouvoir être remis en forme en fin de vie, ou le polymère initial doit pouvoir être récupéré en gardant les mêmes caractéristiques qu'avant sa réticulation.

La réticulation actuelle, au soufre ou aux peroxydes, empêche leur remise en forme car les liaisons formées étant statiques, les chaines de polymères ne peuvent réarranger leur topologie même à haute température. De plus, ces liaisons, notamment C-S, ne peuvent être cassées sélectivement pour dé-réticuler ces matériaux, ce qui entraîne une diminution drastique de la masse molaire du précurseur linéaire et conduit à une importante baisse des propriétés mécaniques du matériau recyclé. C'est pourquoi les pneus usagés ne sont pas recyclés en pneus neufs mais transformés en matériaux aux performances mécaniques moindres, tels les remblais, murs de soutènement, bassins de rétention, terrains de jeux pour enfants, etc.

Au lieu de créer un caoutchouc totalement différent, l'objectif de cette thèse est de changer la méthode de réticulation. Partant des caoutchoucs utilisés aujourd'hui, principalement le polyisoprène, le polybutadiène et ses copolymères, ceux-ci sont réticulés par des liaisons covalentes dynamiques qui s'échangent via un mécanisme de type associatif. Ces liaisons permettent la remise en forme du matériau à haute température tout en gardant le nombre de points de réticulation constant. Il s'agit alors d'un vitrimère, une nouvelle classe de matériaux qui se comportent comme des réseaux élastiques sous une température caractéristique, les échanges étant très lents, alors qu'au-dessus de cette température, ils peuvent relaxer les contraintes via les réactions d'échange, et donc couler et être remis en forme.

Réussir à transformer ces polydiènes en vitrimères demande de trouver deux chimies différentes qui n'interfèrent pas entre elles. L'une est la chimie d'échange, dont la vitesse doit être élevée aux températures de remise en forme (aux alentours de 150 °C) et très faible à la température d'utilisation, pour que le caoutchouc ne s'écoule pas dans ces conditions. Par

270

conséquent, l'énergie d'activation de la réaction d'échange se doit d'être élevée. En outre, cette chimie d'échange doit être inerte vis-à-vis de la matrice élastomérique, et posséder une bonne stabilité thermique. L'autre chimie concerne la chimie de greffage du réticulant dynamique sur le caoutchouc. Parmi les caractéristiques requises nous pouvons citer sa rapidité, un haut rendement et sa sélectivité. Ainsi, cette chimie ne doit pas engendrer de réactions secondaires qui pourraient créer des points de réticulation statiques et donc empêcher le recyclage, ou couper les chaines polymères et ainsi détériorer les propriétés du matériau.
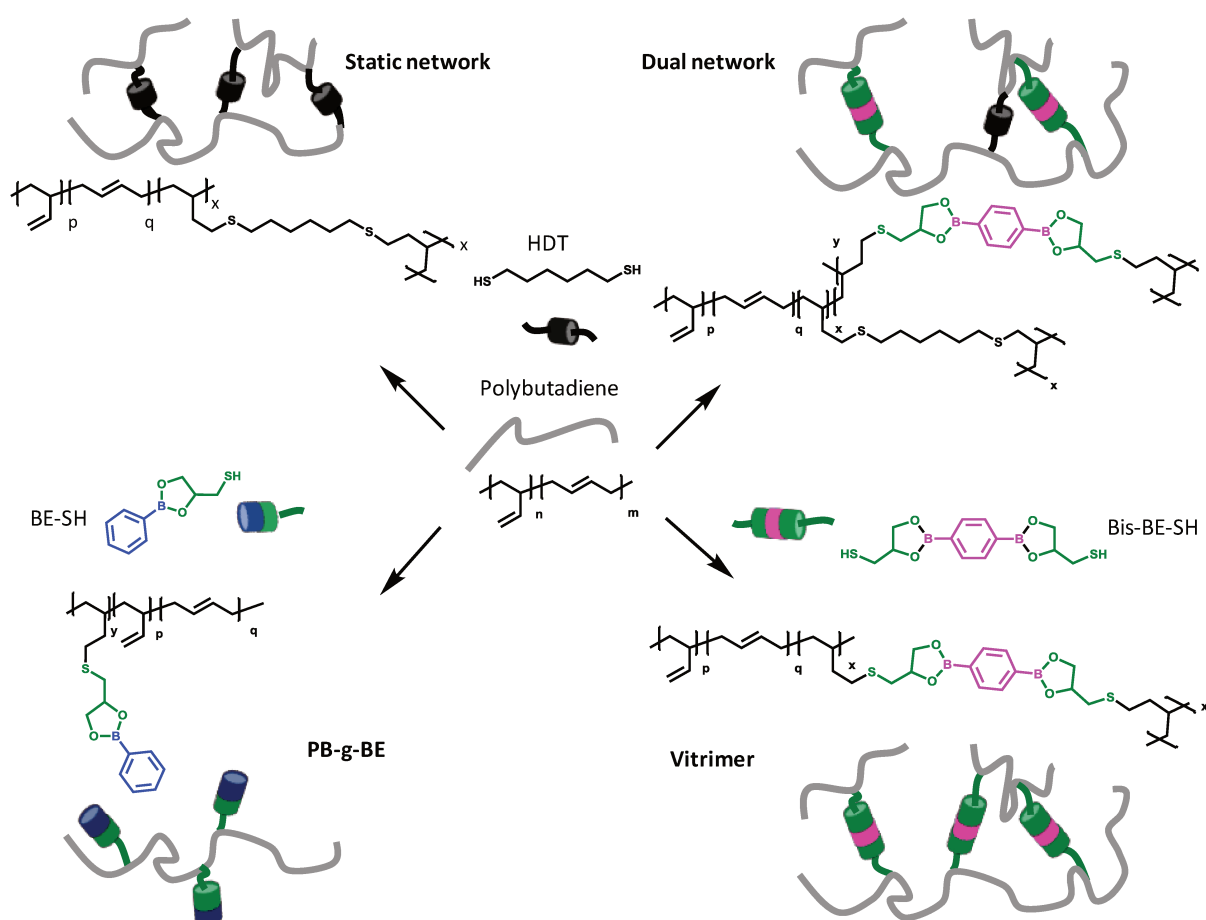

Figure 1. Synthèse du: polybutadiène greffé avec des dioxaborolanes (en bas à gauche), polybutadiène vitrimère (en bas à droite), réseau polybutadiène mixte (en haut à droite) et statique (en haut à droite).

Le chapitre 1 présente dans un premier temps une revue bibliographique des interactions réversibles implémentées dans les élastomères, en consacrant une attention spécifique aux liaisons covalentes dynamiques, notamment celles qui s'échangent par un mécanisme associatif. Dans un second temps, différentes chimies de greffages des caoutchoucs sont détaillées.

Dans le chapitre deux, la chimie thiol-ène a été sélectionnée pour le greffage sur le polybutadiène, car elle remplit les critères mentionnés ci-dessus vis-à-vis des fonctions vinyliques. Pour la réaction d'échange, c'est la métathèse des dioxaborolanes (esters boroniques constitués d'un cycle à 5 atomes) qui a été choisie compte tenu de sa rapidité à haute température et de la stabilité de ces espèces envers les autres groupes fonctionnels, bien que son énergie d'activation soit faible (16 kJ/mol). Un réticulant combinant ces deux chimies a alors été synthétisé (**Figure 1, Bis-BE-SH**). La réticulation a été réalisée en solution à 100 °C par greffage radicalaire pour obtenir un réseau vitrimère. La densité de réticulation a pu être facilement modifiée en changeant la quantité de réticulant introduite, mais jusqu'à une certaine limite. En effet, l'incorporation de groupements phényle-dioxaborolanes, ainsi que la réticulation elle-même, font augmenter fortement la transition vitreuse du matériau. Les vitrimères obtenus sont insolubles après 24 heures dans le THF et le toluène. Néanmoins, si l'expérience de gonflement se prolonge, alors ces systèmes se dissolvent à cause de la faible masse molaire du polybutadiène utilisé, du petit nombre de réticulant par chaîne et de la dynamique d'échange des dioxaborolanes dans ces conditions. Ces résultats montrent que les tests de solubilité ne sont pas nécessairement pertinents pour déterminer la densité de réticulation d'un vitrimère. En effet, malgré leur solubilisation, ces matériaux possèdent tous un plateau caoutchoutique, comme le prouvent les résultats d'analyse mécanique dynamique, ce qui confirme leur caractère réticulé. Ces vitrimères peuvent relaxer entièrement les contraintes et leur viscosité peut être ajustée jusqu'à deux ordres de grandeur par simple modification de la quantité de réticulant introduite. Il a été prouvé que l'énergie d'activation de l'écoulement visqueux de ces systèmes dépend de la structure moléculaire du réseau. La température de transition caractéristique d'un vitrimère, T_v, peut alors variée de plus de 120 °C. Ceci montre que les propriétés d'écoulement du matériau sont fortement reliées à la dynamique d'échange intrinsèque des réticulants ainsi qu'à la mobilité et l'accessibilité des liaisons échangeables. Ces paramètres peuvent être modifiés en jouant sur la densité de réticulation, la topologie et la fonctionnalité du réseau vitrimère.

Il est apparu que certains réseaux fluent à température ambiante, ce qui limite fortement leur potentiel applicatif. Pour réduire ce fluage tout en conservant la recyclabilité, des réseaux mixtes comportant à la fois des points de réticulation dynamiques et statiques ont été synthétisés (**Figure 1**). Dans certaines conditions, il est alors possible d'améliorer la résistance au fluage tout en maintenant la recyclabilité de l'élastomère. De plus, ces réseaux

mixtes possèdent une adhésion forte entre eux, comme les vitrimères, mais qui n'existe pas pour les réseaux purement statiques.

Néanmoins, la présence de points de réticulation statiques rend quand même le recyclage plus difficile. De plus, les polymères linéaires initiaux ne peuvent pas être récupérés, contrairement aux vitrimères. Dans l'optique d'augmenter la résistance au fluage des élastomères vitrimères, une étude cinétique des réactions d'échange entre dioxaborolanes, dioxaborinanes et diols a été menée dans le chapitre trois. Les constantes d'association et de dissociation de la réaction de condensation entre diols 1,2- ou 1,3- et acides phénylboroniques ont été mesurées par résonance magnétique nucléaire (NMR) du proton. Les dioxaborinanes, des esters boroniques cycliques constitués de 6 atomes, possèdent une résistance à l'hydrolyse 10 à 100 fois plus importante que leurs homologues cycliques à 5 atomes, les dioxaborolanes. De plus, les dioxaborinanes se forment quantitativement même en présence d'importantes quantités d'eau. Une nouvelle réaction d'échange a été développée et étudiée, celle entre deux dioxaborinanes. Différentes conditions ont été testées et ont montré que la présence d'humidité atmosphérique changeait radicalement la cinétique d'échange. Les traces d'eau produisent des diols, par hydrolyse des esters boroniques. Les premiers pouvant alors réagir avec les deniers par transestérification. Cette réaction est beaucoup plus rapide que l'échange entre deux esters boroniques, mais plus lente quand elle implique des dioxaborinanes à la place des dioxaborolanes. Aucun échange entre deux dioxaborinanes n'a pu être observé lorsque la réaction est conduite dans le THF à 100 mM sous atmosphère protectrice. Cependant, un échange entre dioxaborinanes a pu être détecté dans le dodécane à haute concentration, ainsi qu'en masse (**Figure 2**).
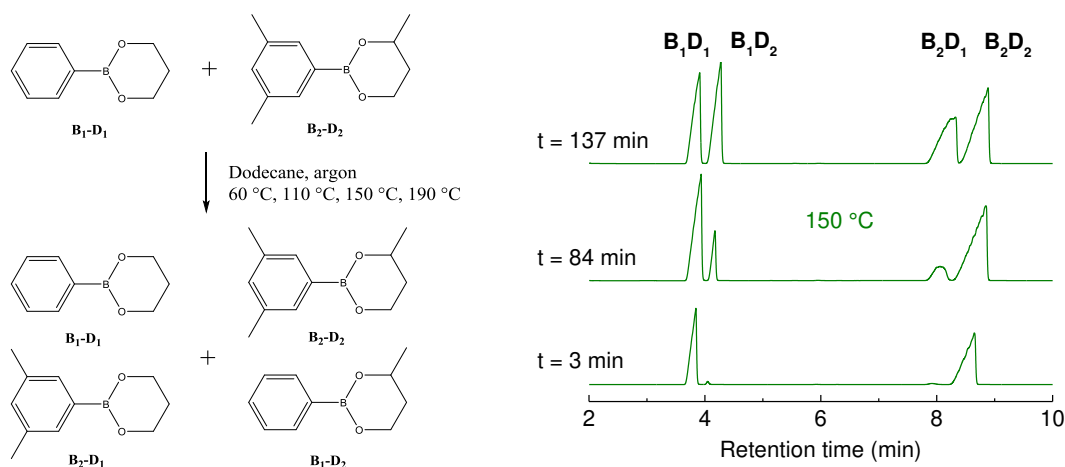

Figure 2. Côté gauche: Schéma de la métathèse des dioxaborinanes B_1D_1 et B_2D_2 en solution concentrée à différentes températures sous atmosphère protectrice. Côté droit: Suivi cinétique de la réaction par chromatographie en phase gazeuse à 150 °C.

Des expériences réalisées à différentes températures ont permis de calculer les énergies d'activation en solution dans le dodécane et en masse, respectivement 39.1 kJ/mol et 61.6 kJ/mol. Cette dernière est trois fois plus élevée que l'énergie d'activation de la métathèse des dioxaborolanes (15.9 kJ/mol) et sa constante cinétique à 60 °C lui est inférieure de plusieurs ordres de grandeurs. Ces résultats montrent que la réaction d'échange des dioxaborinanes est extrêmement lente à température ambiante, ce qui pourrait empêcher le réseau de se réarranger et donc le polymère de fluer, tandis qu'à haute température (150-190°C) la réaction est environ 1000 fois plus rapide, ce qui pourrait permettre un réarrangement rapide de la topologie du réseau et donc une mise en forme facile.

Le chapitre quatre propose d'introduire les dioxaborinanes dans la matrice polybutadiène. Pour se faire, deux molécules ont été synthétisées; l'une comporte une fonction thiol et une fonction dioxaborinane, tandis que l'autre possède deux fonctions thiol et deux fonctions dioxaborinane. La première a permis de quantifier le greffage, avec des rendements compris entre 65 et 77%. La seconde a été utilisée pour réticuler le polybutadiène de façon dynamique et donc synthétiser un vitrimère. Ce réseau possède une résistance au solvant accrue par rapport à son homologue réticulé par les dioxaborolanes, même si la majeure partie de ce réseau peut se dissoudre après une immersion prolongée dans le THF. La présence de diols et d'eau n'a pas été détectée en quantités suffisantes pour expliquer la dissolution importante du vitrimère (**Figure 3**). Néanmoins, ces molécules accélèrent la réaction d'échange entre dioxaborinanes par transestérification. Par conséquent, le réseau peut réarranger plus rapidement sa topologie qu'en l'absence de diols, ce qui conduit à sa dissolution, probablement par formation de boucles et par hydrolyse partielle.
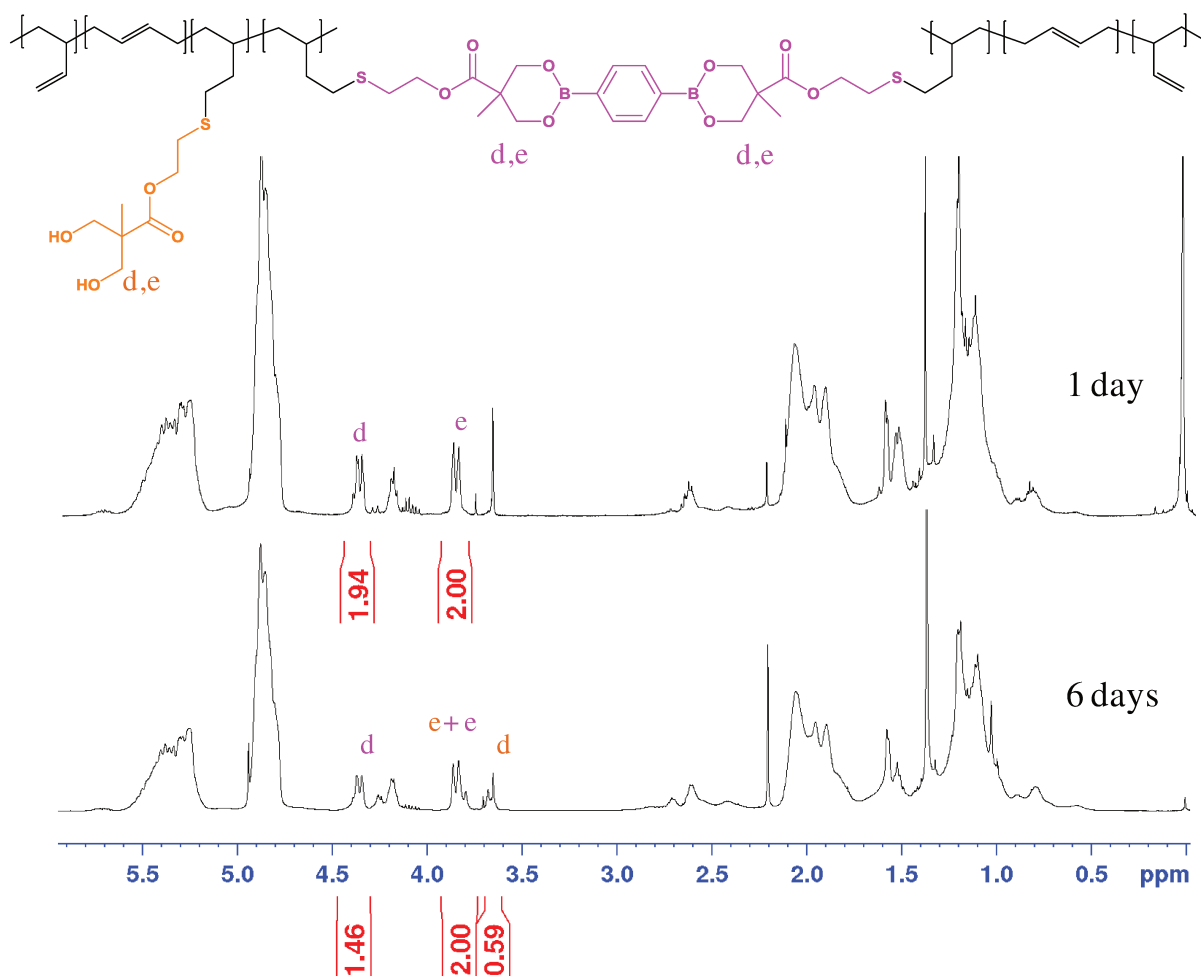
Figure 3. Spectres RMN du proton dans CDCl₃ des fractions solubles du vitrimère dioxaborinane après 1 jour et 6 jours dans le THF.

Le réarrangement des chaînes de polymères et son lien avec l'hydrolyse du réseau doivent être étudiés plus en détails. Le matériau flue à température ambiante ce qui peut s'expliquer par le taux de greffage plus faible que celui de son homologue dioxaborolane. En outre, ce système tend à former des agrégats qui conduisent à l'apparition d'une phase cristalline. Pour empêcher ce phénomène, un dioxaborinane moins polaire pourrait être utilisé. Cependant, les tests de traction ont montré que le vitrimère est bien recyclable plusieurs fois, même si ses propriétés mécaniques sont inférieures à celles du vitrimère dioxaborolane.

La fonctionnalisation d'un polybutadiène de haute masse molaire et comportant un faible taux de fonctions vinyliques a également été entreprise, mais tous les conditions testées ont conduit à des rendements de greffage inférieurs à 8%. Par conséquent, la chimie thiol-ène en solution ne semble pas adaptée à ce type d'élastomère. D'autres conditions de greffage, telles que l'extrusion réactive ou une autre chimie doivent être développées pour transformer les polydiènes disponibles commercialement en vitrimères.

Le chapitre 5 propose d'utiliser la chimie des nitrènes pour fonctionnaliser un polyisoprène comportant 98% de motifs de répétition cis-1,4. Six dioxaborolanes comportant une ou deux fonctions azotures ont été conçus et synthétisés à partir de trois molécules ; l'hydroquinone, le 2-allylphénol et l'eugénol. Le greffage du mono azoture issu de l'hydroquinone a été réalisé par extrusion réactive avec des rendements de 50% environ. La présence d'oxygène ne modifie pas le greffage mais fait chuter la masse molaire du polyisoprène. Des vitrimères ont été produits selon deux stratégies différentes. La première approche consiste à utiliser un azoture difonctionnel pour fonctionnaliser et réticuler le polymère en une seule étape. Le matériau obtenu comporte une haute fraction insoluble après 24 heures d'immersion dans le THF, tandis qu'il se solubilise entièrement en présence d'un excès de diols. Le système peut relaxer une grande partie des contraintes à hautes températures mais ne peut être recyclé, ses propriétés mécaniques diminuant à chaque cycle de traction - compression moulage. En outre, cet azoture a conduit à l'apparition d'une séparation de phase. C'est pourquoi il a été remplacé par un azoture issu du 2-allylphénol et comportant trois atomes de carbones supplémentaires, facilitant ainsi sa dispersion homogène dans la matrice élastomérique apolaire. Mais ce composé, même avec une seule fonction azoture, réticule le polymère de façon statique. Un autre azoture, fait à partir d'eugénol, a alors été synthétisé et utilisé. Le composé mono azoture possède un meilleur taux de greffage que celui à base d'hydroquinone, néanmoins le réticulant issu de l'eugénol provoque également la réticulation statique du polyisoprène.

Par conséquent, une seconde approche a été envisagée pour transformer le polydiène en vitrimère (**Schéma 1**). Le polyisoprène a d'abord été fonctionnalisé avec des dioxaborolanes pendants à l'aide du mono azoture eugénol, suivi par la réticulation grâce à un bis-dioxaborolane qui ne possède pas de fonction azoture. Ce dernier est en effet le complémentaire des esters boroniques pendants, il peut donc réticuler les chaînes par la réaction d'échange. Un matériau réticulé a été obtenu de cette façon. Sa température de transition vitreuse n'a été que peu modifiée par rapport au polyisoprène de départ. Son réseau tridimensionnel est stable vis-à-vis de la température et du solvant. Ce système est facilement re-façonnable mais ses propriétés mécaniques sont inférieures à celles des caoutchoucs réticulés conventionnellement, notamment sa résistance au fluage à température ambiante. La présence d'un trop grand nombre d'esters boroniques libres au sein du matériau est une des raisons de ce réarrangement trop rapide à cette température de service.
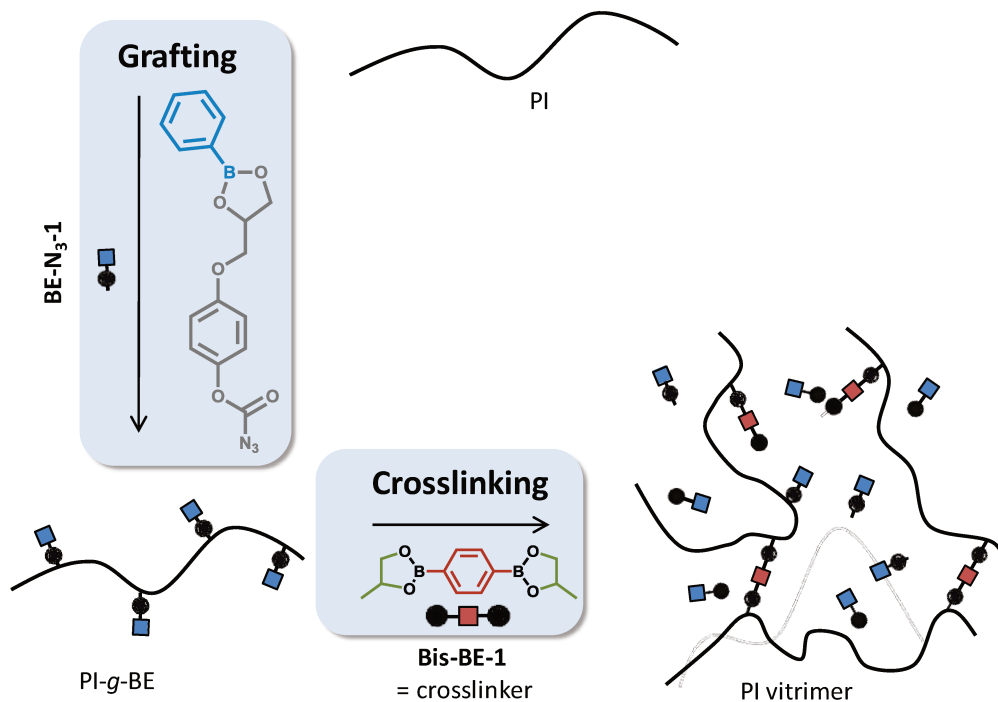
Schéma 1. Seconde stratégie utilisée pour réticuler le polyisoprène. Celui est fonctionnalisé par des dioxaborolanes pendant puis réticulé par l'addition d'un bis-dioxaborolane.

Dans cette thèse, des polydiènes commerciaux, le polybutadiène et le polyisoprène, de basses et hautes masses molaires ont pu être transformés en vitrimères en couplant la chimie thiol-ène ou la chimie des nitrènes pour le greffage, à la chimie d'échange des esters boroniques. Des études cinétiques ont été entreprises sur des composés esters boroniques modèles. En particulier, les constantes de vitesse, les facteurs de fréquence ainsi que les énergies d'activation de la métathèse des dioxaborinanes ont été déterminés dans différents environnements. Des agents de réticulation comportant des fonctions dioxaborolanes ou dioxaborinanes (pour l'échange) ainsi que des fonctions thiols ou azotures (pour le greffage) ont été synthétisés puis utilisés pour créer des réseaux vitrimères. Ces systèmes sont réticulés et possèdent un plateau caoutchoutique, mais peuvent être recyclés par compression moulage à haute température ou par dé-réticulation via diolyse.

RÉSUMÉ

Les caoutchoucs actuels étant réticulés par des liaisons covalentes statiques, ils ne peuvent être recyclés en fin d'utilisation. Avec pour objectif d'allonger le cycle de vie des caoutchoucs, une réticulation covalente dynamique a été utilisée pour développer des élastomères recyclables. Grâce à l'échange entre points de réticulation esters boroniques, introduits dans le polybutadiène via la chimie thiol-ène, ce dernier a pu être transformé en vitrimère. La comparaison avec des réseaux statiques a permis de mettre en évidence la recyclabilité du réseau sans détecter de réactions parasites durant la remise en forme. Cependant, la dynamique d'échange entre dioxaborolanes étant trop rapide à température ambiante, le vitrimère polybutadiène flue dans les conditions d'utilisation. Pour limiter le fluage, des réseaux mixtes, comprenant à la fois des points de réticulation statiques et dynamiques, ont été synthétisés. Toutefois, l'aptitude au recyclage des réseaux s'en est retrouvée altérée. Souhaitant une dynamique ralentie à température ambiante mais rapide à haute température, une nouvelle réaction d'échange entre dioxaborinanes a été étudiée. Les constantes de vitesse et l'énergie d'activation de la réaction ont été mesurées. Des points de réticulation dioxaborinanes ont ensuite été introduits dans la matrice polybutadiène. Dans l'optique d'élargir le spectre des élastomères transformables en vitrimères, une nouvelle chimie de greffage a également été testée, la chimie des azotures. De nouvelles molécules, portant une fonction azoture et une fonction ester boronique ont été synthétisées puis greffées sur du polyisoprène.

MOTS CLÉS

Vitrimères, Elastomères, Recyclage, Chimie Covalente Dynamique, Greffage

ABSTRACT

Rubbers are usually cross-linked through static covalent bonds. Consequently, they cannot be reshaped after their synthesis. With the aim to extend the shelf life of elastomers, dynamic covalent chemistry was used to cross-link elastomers and develop recyclable rubbers. Thanks to the associative exchange reaction between boronic ester cross-links, incorporated into polybutadiene via thiol-ene chemistry, this elastomer was transformed into a vitrimer. The comparison with static networks showed the ability of the vitrimer to be recycled efficiently without detecting any side reactions during the synthesis nor the recycling process. As the exchange between dioxaborolanes is already occurring at room temperature, the polybutadiene vitrimer crept at service temperature. To avoid creep, dual networks, with both static and dynamic cross-links, were synthesised but their recyclability was decreased as compared to vitrimers. Aiming to slow down the exchange at room temperature while keeping its high rate at high temperatures, a new exchange reaction between dioxaborinanes was studied. Key parameters such as the rate constant and the activation energy were measured. Dioxaborinane based cross-links were incorporated into polybutadienes. In order to widen the range of recyclables elastomers, another grafting chemistry was tested, the nitrene chemistry. New molecules, bearing an azide and a boronic ester were synthesized and then introduced into polyisoprene.

KEYWORDS

Vitrimers, Elastomers, Recycling, Dynamic Covalent Chemistry, Grafting